

DOE/NASA/0038-80/2  
NASA CR-159727  
HI #79188

---

# **ACTIVE HEAT EXCHANGE SYSTEM DEVELOPMENT FOR LATENT HEAT THERMAL ENERGY STORAGE**

R. T. LeFrois and A. K. Mathur  
Technology Strategy Center  
Honeywell Inc.

**April 1980**

Prepared for  
**NATIONAL AERONAUTICS AND SPACE ADMINISTRATION**  
Lewis Research Center  
Under Contract DEN 3-38

for  
**U.S. DEPARTMENT OF ENERGY**  
**Conservation and Solar Energy**  
**Division of Energy Storage Systems**

#### NOTICE

This report was prepared to document work sponsored by the United States Government. Neither the United States nor its agent, the United States Department of Energy, nor any Federal employees, nor any of their contractors, subcontractors or their employees, makes any warranty, express or implied, or assumes any legal liability or responsibility for the accuracy, completeness, or usefulness of any information, apparatus, product or process disclosed, or represents that its use would not infringe privately owned rights.

DOE/NASA/0038-80/2

NASA CR-159727

HI 79188

ACTIVE HEAT EXCHANGE  
SYSTEM DEVELOPMENT FOR  
LATENT HEAT THERMAL ENERGY STORAGE

R. T. LeFrois and A. K. Mathur  
Technology Strategy Center  
Honeywell Incorporated  
2600 Ridgway Parkway  
Minneapolis, Minnesota 55413

April 1980

Prepared for  
National Aeronautics and Space Administration  
Lewis Research Center  
Cleveland, Ohio 44135  
Under Contract DEN 3-38

for

U. S. DEPARTMENT OF ENERGY  
Conservation and Solar Energy  
Division of Energy Storage Systems  
Washington, D. C. 20545  
Under Interagency Agreement EC-77-A-31-1034

## TABLE OF CONTENTS

	<u>Page</u>
SECTION 1.0 SUMMARY	1-1
SECTION 2.0 INTRODUCTION	2-1
SECTION 3.0 CONCEPTS SELECTION REVIEW	3-1
3.1 GENERAL SYSTEM APPLICATIONS AND REQUIREMENTS	3-1
3.2 STORAGE MEDIA SELECTION	3-2
3.2.1 TES System Cost Evaluation for Salt Screening	3-2
3.2.2 Salt Screening	3-9
3.3 SELECTION OF HEAT EXCHANGE CONCEPTS	3-19
3.3.1 Survey of Heat Exchange Concepts	3-19
3.3.2 Candidate Concepts for Evaluation	3-21
3.3.3 Evaluation Criteria	3-22
3.3.4 Performance and Cost Evaluation	3-24
3.4 SELECTED CONCEPTS	3-42
3.5 SELECTED EXPERIMENTS	3-43
SECTION 4.0 CONCEPTS MECHANIZATION AND EXPERIMENTS DESIGN	4-1
4.1 REFLUX BOILER CONCEPT MECHANIZATION	4-1
4.1.1 System Description	4-1
4.1.2 Methods of Fabrication	4-3
4.1.3 Scalability	4-5
4.1.4 Technical Issues	4-5
4.2 REFLUX BOILER EXPERIMENT	4-7

## TABLE OF CONTENTS (continued)

	<u>Page</u>
4.2.1 Modeling	4-7
4.2.2 Experimental Mechanization	4-7
4.2.3 Major Components	4-10
4.3 SHELL AND TUBE FLOWBY HEAT EXCHANGE CONCEPT MECHANIZATION	4-54
4.3.1 System Description	4-54
4.3.2 Technical Issues	4-57
4.4 SHELL AND TUBE FLOWBY HEAT EXCHANGER EXPERIMENT	4-58
4.4.1 Modeling	4-58
4.4.2 Experiment Mechanization	4-59
SECTION 5.0 EXPERIMENTS TESTS, RESULTS AND DISCUSSION	5-1
5.1 TEST RESULTS AND DISCUSSION--REFLUX BOILER	5-1
5.2 TEST RESULTS AND DISCUSSION--SHELL AND TUBE FLOWBY	5-15
SECTION 6.0 RECOMMENDATIONS	6-1
6.1 SELECTED TES APPLICATION EVALUATION	6-1
6.2 FOLLOW-ON TES PROGRAM PLAN CONCEPT	6-1
6.2.1 Reflux Boiler Concept	6-1
6.3 COATED TUBE AND SHELL FLOWBY CONCEPT	6-2
APPENDIX A COATED TUBE DATA	A-1
APPENDIX B PROPERTIES OF MOLTEN NITRATES AT HIGH PRESSURES	B-1

## TABLE OF CONTENTS (concluded)

---

	<u>Page</u>
APPENDIX C    REFLUX BOILER MODULE DRAWING LIST	C-1
APPENDIX D    INSTRUMENTATION	D-1

## LIST OF FIGURES

<u>Figure</u>		<u>Page</u>
1-1	Shell and Coated Tube Flowby Heat Exchange Concept	1-2
1-2	Direct Contact Heat Exchange Concept	1-3
1-3	Phase Diagram for Selected Phase Change Media	1-5
3-1	Temperature and Pressure Regime of Conventional Turbomachinery	3-3
3-2	Power System Cycles	3-4
3-3	Standard Steam Cycles	3-5
3-4	Latent Heat/Active Heat Exchange Storage Cost Trends	3-7
3-5	Phase Change TES System Cost Curve	3-8
3-6	Salt Selection Methodology Flowchart	3-10
3-7	Salt Cost Versus Heat of Fusion--TES System Cost Parameter	3-13
3-8	Close-up View of Bottom of Vaporizer Module Showing Total Scraper	3-28
3-9	Shell and Tube Exchanger with Deposit-Resistant Tubes	3-30
3-10	Jet Impingement Salt Removal	3-32
3-11	Self-Pressurizing Reflux Boiler	3-36
3-12	Continuous Salt Flow Reflux Boiler	3-38
3-13	Continuous Salt Flow Reflux Boiler with Hydraulic Head Recovery	3-39
4-1	Continuous Salt Flow Reflux Boiler with Hydraulic Head Recovery	4-2
4-2	Continuous Salt Flow Reflux Boiler with Hydraulic Head Recovery	4-4

## LIST OF FIGURES (continued)

<u>Figures</u>		<u>Page</u>
4-3	Reflux Boiler Functional Schematic	4-8
4-4	Salt Storage Test Facility Mechanical Layout	4-11
4-5	Salt Storage Test Facility Electrical Layout	4-12
4-6	Side View of Reflux Boiler Showing Filler Tank Air Heater and Condenser Receiver in Foreground	4-13
4-7	Front View of Reflux Boiler Showing Hand Valves with Filler Tank at Left	4-14
4-8	Back View of the Reflux Boiler Showing Condenser Above the Boiler Tank on the Right. Water Heater is Lower Center Tank	4-15
4-9	Reflux Boiler Module (Guard Heater Panels Removed)	4-16
4-10	Reflux Boiler Shell	4-17
4-11	Heads for Reflux Boiler	4-18
4-12	Reflux Boiler with Head Being Welded in Place	4-19
4-13	Air Preheater	4-20
4-14	Water Preheater	4-21
4-15	Condenser Unit in Welding Fixture	4-22
4-16	Unit Installed at Test Facility with Test Cell Enclosure Partly Completed - Side View	4-23
4-17	Unit Installed at Test Facility with Test Cell Enclosure Partly Completed - Front View	4-24
4-18	Test Cell and Mechanical Work Nearing Completion	4-25
4-19	Reflux Boiler Control and Instrument Panel	4-26
4-20	Reflux Boiler Module Installation	4-27



## LIST OF FIGURES (continued)

<u>Figures</u>		<u>Page</u>
4-21	Molten Salt Fluid Level Sensor	4-29
4-22	Location and Function of Probes Installed Along Top of the Boiler	4-30
4-23	Location and Function of Probes Installed on the Transfer Tank	4-31
4-24	Level Sensor Display Unit and Audio High-level Alarm Unit Schematic	4-31
4-25	Reflux Boiler Enclosure Panels--Guard Heater Arrangement and Valves	4-32
4-26	Reflux Boiler Aluminum Panel with Guard Heaters	4-33
4-27	Arrangement of Guard Heaters	4-34
4-28	Power Control Panel No. 1	4-36
4-29	Power Control Panel No. 2	4-37
4-30	High-pressure Water Pumping Unit	4-38
4-31	High-pressure Water Pumping Unit Components	4-38
4-32	Gaseous Nitrogen System Schematic	4-39
4-33	External Tubular Heater Bands	4-40
4-34	Salt Storage Tank	4-40
4-35	Installation of Submerged Centrifugal-Type Pump in Tank	4-43
4-36	Installation of Submerged Centrifugal-Type Pump in Tank	4-44
4-37	Screen Used to Separate Solids from Returning Salt Slurry and to Prevent Solids From Being Pumped Out of the Tank	4-45

## LIST OF FIGURES (concluded)

<u>Figure</u>		<u>Page</u>
5-14	Flowby Experiment - Run 3, Salt Coefficient Versus $\Delta T$	5-22
5-15	Flowby Experiment - Run 4, Salt Coefficient Versus $\Delta T$	5-23
5-16	Flowby Experiment - Run 4, Heat Rate Versus $\Delta T$	5-23

## LIST OF TABLES

---

<u>Table</u>		<u>Page</u>
1-1	Economic and Technical Evaluation of Heat Exchange Concepts	1-6
3-1	Properties of Selected TES Inorganic Salts	3-11
3-2	Selected Major Components--System Cost	3-16
3-3	Salt System Selection	3-17
3-4	Performance and Cost Evaluation of Candidate Heat Exchanger Concepts	3-25
4-1	Reflux Boiler Technical Issues	4-6
4-2	Ratings of Salt Storage Tank Range Heaters	4-42
4-3	Active Heat Exchanger Instrumentation	4-51
4-4	Shell and Tube Exchanger Technical Issues	4-58

## SECTION 1.0

## SUMMARY

This final report documents the results of Contract DEN 3-38, Active Heat Exchanger System Development for Latent Heat Thermal Energy Storage Systems.

The project was sponsored by the U.S. Department of Energy/Division of Energy Storage Systems and managed by the National Aeronautics and Space Administration/Lewis Research Center. The overall project consisted of five tasks to select, design, fabricate, test and evaluate candidate active heat exchanger modules for future applications to solar and conventional utility power plants.

Alternative mechanizations of active heat exchange concepts were analyzed for use with heat of fusion Phase Change Materials (PCMs) in the temperature range of 250° to 350°C. Twenty-six heat exchange concepts were reviewed, and eight were selected for detailed assessment. Two candidates were selected for small-scale experimentation: a coated tube and shell heat exchanger and a direct contact reflux boiler.

A dilute eutectic mixture of sodium nitrate and sodium hydroxide was selected as the PCM from over 50 candidate inorganic salt mixtures. Based on a salt screening process, eight major component salts were selected initially for further evaluation. Using an economic assessment program coupling the candidate salt mixtures and heat exchange concepts,  $\text{NaNO}_3$ ,  $\text{NaNO}_2$ , and  $\text{NaOH}$  appeared to be the most attractive major components in the temperature range of 250° to 350°C. The minor components, selected in similar fashion, were  $\text{NaOH}$ ,  $\text{NaOH}$ , and  $\text{NaNO}_3$ , respectively.

Sketches of the two active heat exchange concepts selected for test are shown in Figures 1-1 and 1-2.

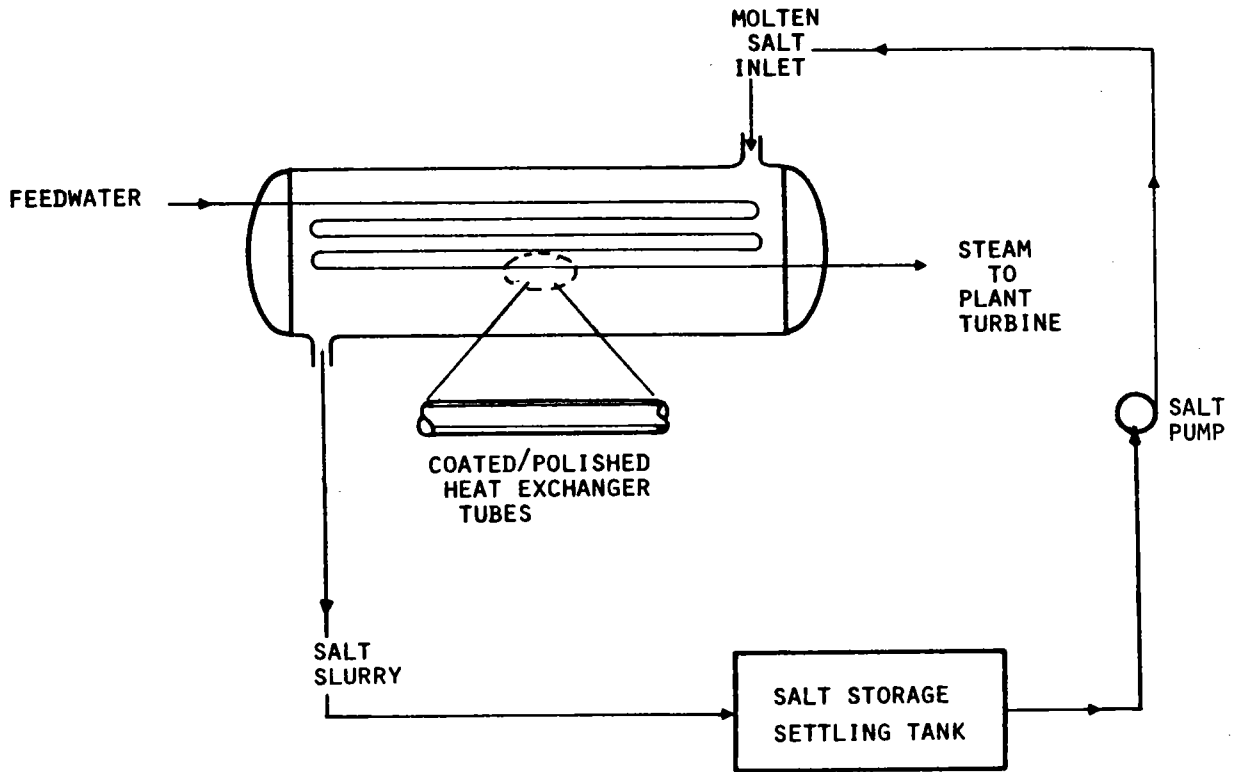


Figure 1-1. Shell and Coated Tube Flowby Heat Exchange Concept

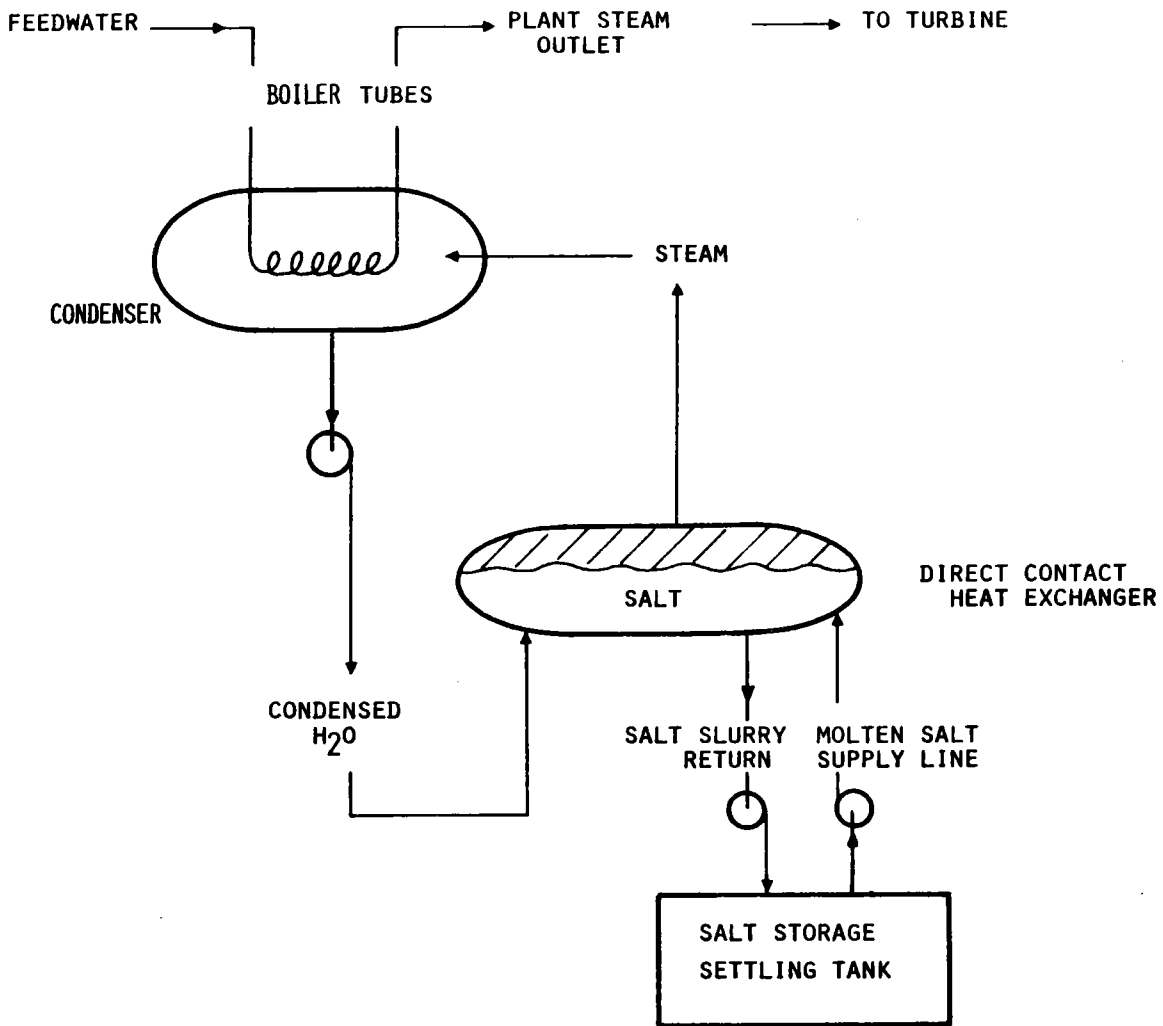


Figure 1-2. Direct Contact Heat Exchange Concept

Table 1-1. Economic and Technical Evaluation of Heat Exchange Concepts

EVALUATION PARAMETER  HEAT EXTRACTION CONCEPT		(A) RATE-RELATED COSTS	(B) CAPACITY-RELATED COSTS	(C) NORMALIZED TOTAL CAPITAL COSTS	(D) NORMALIZED TOTAL CAPITAL COSTS (W/O BOP)	(E) TECHNICAL STATUS	(F) EXPECTED OPERATING COSTS	(G) EXPECTED MAINTENANCE COSTS
		\$/kW <sub>(t)</sub>	\$/kWh <sub>(t)</sub>	DIMENSION-LESS	DIMENSION-LESS	FT I NT	HIGH NORM. LOW	HIGH NORM. LOW
1	INTERNAL SURFACE SCRAPER	201	13	1.72	2.2	FT	H	H
2	EXTERNAL SURFACE SCRAPER	55	16	0.90	0.84	I	H	H
3	SHELL AND COATED TUBE FLOWBY	45	13	0.77	0.62	NT	L	N
4	JET IMPINGEMENT	47	15	0.78	0.63	FT	N	H
5	REFLUX BOILER { SELF PRESSURIZING CONTINUOUS SALT FLOW OPEN SYSTEM	50	13	0.80	0.66	FT	L	H
6		46	13	0.77	0.62	I	N	N
7		46	13	0.75	0.59	FT	N	L
8	TUMBLING ABRASIVE	58	13	0.85	0.74	FT	H	H
9	PASSIVE TUBE INTENSIVE (REF)	94	27	1.00	1.00	NT	N	L

FT = FAR TERM (5-10 YEARS)  
 I = INTERMEDIATE (3-5 YEARS)  
 NT = NEAR TERM (2-3 YEARS)  
 H = HIGH  
 N = NORMAL  
 L = LOW

BOP = BALANCE OF PLANT (OTHER THAN TANKAGE, HEAT EXCHANGE, MANIFOLD AND SALT COSTS)

of expected operating and maintenance costs for the respective concepts. This enables total life-cycle costs to be brought into perspective. As a result of this evaluation, the shell and coated tube (3) and reflux boiler (6) emerged as the most attractive heat exchange concepts from among those studied.

A number of technical issues and questions regarding feasibility were addressed for each concept to establish the requirements for the experiments. The ability to model and scale each concept was reviewed to ensure that a 10 kW(t) discharge rate and a 10 kW(t)-hour capacity was adequate. These aspects of the

program are discussed in Section 4.0 along with a description of the experimental setup, the hardware, and instrumentation. Supporting PCM data, and experiment design and instrumentation details, are contained in Appendices C and D.

The experimental results are discussed in Section 5.0. The results from the Direct Contact Reflux Boiler experiment indicate that heat rates of 14.5 kW(t) were achieved at a boiler pressure of 5.5 MPa. Severe degradation of the PCM occurred, however, when in contact with water. The PCM underwent hydrolysis, forming sodium hydroxide and nitric acid. This was compounded by an irreversible chemical reaction of nitric acid with the container walls forming iron oxides in aqueous solution. As a result, only 60 percent of the design steam pressure (9.3 MPa or 1350 psig) was achieved. These results, along with the testing program, are described in more detail in Subsection 5.1.

The results of tests using the Shell and Coated Tube Flowby module were equally disappointing. Although qualitative "dip" tests seemed to indicate that several coatings might alleviate the problem of salt freezing on discharge tube surfaces, tests using an electroless nickel coating in the Coated Tube Flowby experiment confirmed that salt adhesion still had a deleterious effect on heat transfer--to an extent which did not warrant further consideration. Other coatings such as chrome or Teflon were not tested in the Coated Tube Flowby experiment because of schedular and financial constraints.

It is recommended that experimentation continue to assess: (1) other selected materials for use with the Direct Contact Reflux Boiler concept; and (2) the antistick properties of the other candidate coatings (i.e., chrome, Teflon and Ryton). These and other recommendations are discussed in Section 6.0.



## SECTION 2.0

## INTRODUCTION

High Temperature Thermal Energy Storage (HT/TES) can provide large-scale conservation of irreplaceable petroleum and natural gas resources. This in part can be achieved in load leveling applications for conventional electric plants and in thermal storage applications for solar thermal power plants.

Studies and analyses on the usefulness of HT/TES systems (NASA CR-159577) seem to indicate that the economic viability is marginal, at best, with today's technology. The capacity and power related capital costs for storage must be lowered significantly before the economic leverage will shift in favor of its use.

A promising candidate for thermal energy storage at high temperatures is the utilization of the heat of fusion of molten salts. Many salts are attractive because of their relatively high weight and volumetric heat storage capabilities, their abundance in nature and as a result of industrial processes, and their low cost per unit storage capability. By utilizing the heat of fusion (liquid-solid transition) of various salts, large amounts of thermal energy can be stored and subsequently released at a relatively constant temperature.

One problem, however, is inherent to systems that utilize the heat of fusion of molten salts by a passive heat exchange process (e.g., heat exchange tubes immersed in a static salt bath). The accumulation of salt deposits on discharge tube surfaces imposes a large heat exchanger surface area requirement. This component can be the major cost item of the system.

To minimize a potentially large capital investment in required heat exchangers, alternate heat exchange concepts have been proposed to enhance energy removal from a TES module by actively inhibiting or removing the formation of salt

depositions on the discharge tube surfaces. One such concept, developed by Honeywell in competition for the 10 MW(e) solar pilot plant, used mechanical scrapers to remove the formation of a sodium nitrate salt mixture as it froze on external vaporizer tube surfaces (TID-27775).

The intent of this investigation was to extend the technological development of active heat exchange systems for potential application to conventional high-pressure steam utilities and to advanced solar thermal energy conversion systems. Utilization of an HT/TES module to provide boiling for a steam power cycle was emphasized. Therefore active heat exchange concepts considered for this function were to be capable of accomplishing boiling in the temperature range of 250 to 350<sup>o</sup>C, which corresponds to a wide steam pressure range of about 400 to 1650 N/cm<sup>2</sup> (580 to 2400 psia).

The approach was to evaluate advanced active heat exchange concepts relative to a passive tube-intensive design, identify the critical issues, select the most likely candidates, experimentally address the outstanding issues, recommend the most promising concept for continued development, and identify areas requiring further research and technology.

## SECTION 3.0

## CONCEPTS SELECTION REVIEW

## 3.1 GENERAL SYSTEM APPLICATIONS AND REQUIREMENTS

Thermal Energy Storage (TES) is important for efficient use of energy resources. Advanced storage technologies can improve the operation and economics of electric power systems by storing excess off-peak energy for later use in meeting peak demands.

In electric utilities, baseload is the round-the-clock load that is met with the most fuel-efficient equipment. As the daily load increases, the utility incrementally brings the next most efficient equipment on-line. For the near term (ref. 1), energy storage can effectively increase the use of existing baseload equipment. In the longer term, energy storage can increase the percentage of baseload capacity. Thus, there is an economic incentive for utilities to use baseload plants to meet the peaking loads now met by less fuel-efficient equipment.

Energy storage is a practical necessity for solar-thermal generation of electric power. It is necessary for plant stability and control issues related to high-frequency solar transients. Two techniques (ref. 2) can be used to maintain the reliability of the grid with a large solar plant on the line. In the first technique, the solar plant is backed up with a conventional plant that is pressed into service as needed after available instantaneous solar power has been supplied to the grid. The second technique controls the delivery of power to the grid so that the collected energy can be stored when it is available and not needed to meet grid demand. This stored energy becomes available for electric generation when the demand is high and direct insolation is not available.

For these applications, the specific operating conditions and machinery typically used in power plants needs to be considered. The operational regime of conventional turbomachinery is shown in Figure 3-1. In Figure 3-2, operating conditions for current and advanced solar power plants and for utility systems are shown on a steam enthalpy diagram. Here, the turbine pressures are shown with corresponding entry flow temperatures. Notice that most of the steam power plants operate within a band of 4.1 MPa to 16.5 MPa (600 psia to 2400 psia); the saturation temperatures corresponding to these pressures are between 250° and 350°C.

Heat from storage can be used to boil water and provide high-temperature steam to the plant. To provide steam at 250° to 350°C, heat should be stored at a temperature greater than the desired steam temperature. With an assumed temperature drop of 18C°, the useful temperature range for storage media is from 268° to 368°C. Salts with melting points up to 400°C were thus considered in media selection.

Media for various steam turbine cycles are shown in Figure 3-3. A temperature difference of at least 18C° each was allowed for heat transfer from charge steam to salt and from salt to discharge steam. Only standard steam turbine cycles were considered.

## 3.2 STORAGE MEDIA SELECTION

### 3.2.1 TES System Cost Evaluation For Salt Screening

TES system cost is an important economic parameter in determining the usefulness of storage to utility and solar plants.

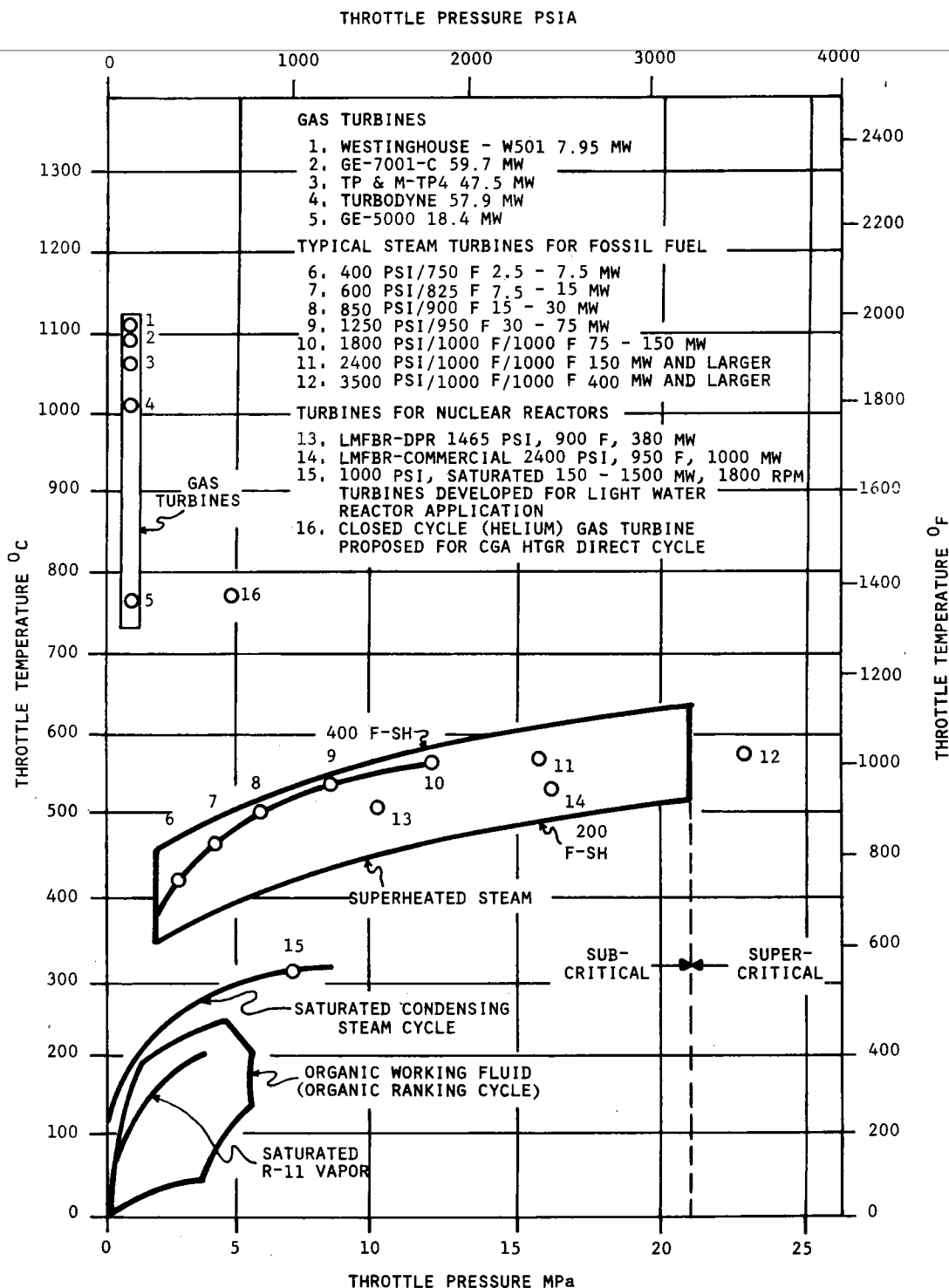


Figure 3-1. Temperature and Pressure Regime of Conventional Turbomachinery

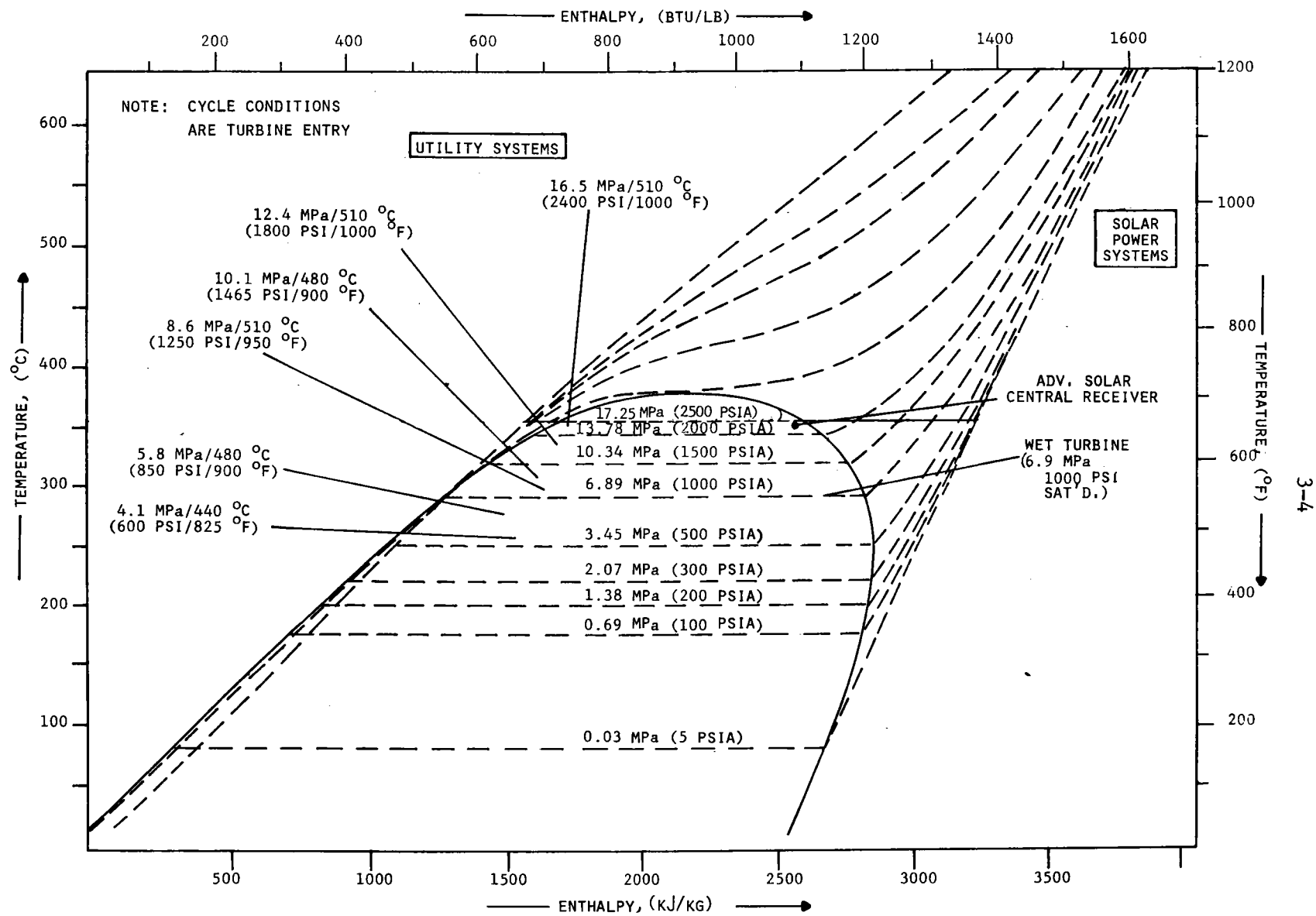


Figure 3-2. Power System Cycles

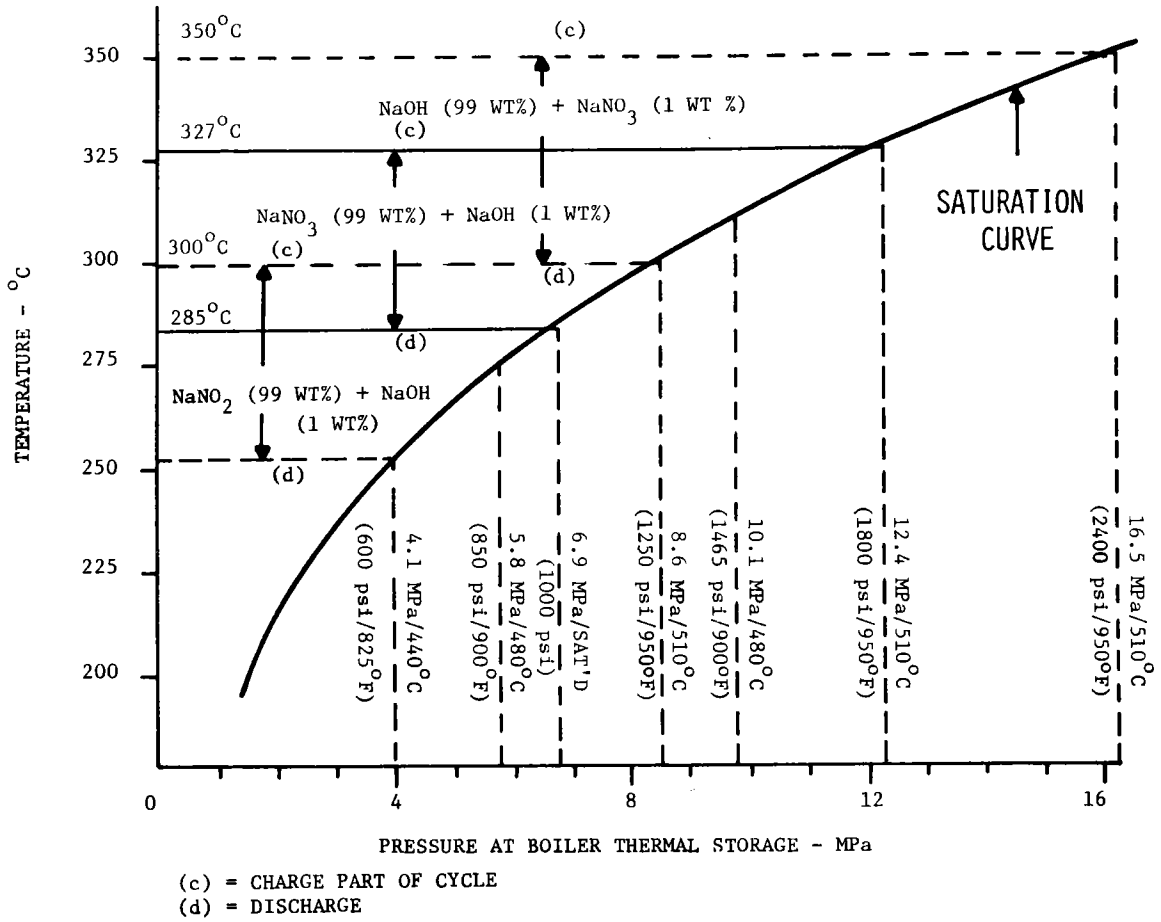


Figure 3-3. Standard Steam Cycles

Honeywell developed a model to compare the capital costs of candidate TES systems. The model was based on build and detailed cost estimates for latent heat systems for the Solar Pilot Plant program. Figure 3-4 shows a logarithmic plot of storage installed cost as a function of storage capacity based on small-scale, SRE, and pilot plant experience. The costs in the figure are the actual accrued costs. The figure shows that TES costs follow the exponential relationship. The cost exponent of the slope of the curve in Figure 3-4 was determined to be -0.34. This cost exponent was used for scaling storage system costs for salt systems. The model is described in ref. 4.

TES system costs include the costs of the storage medium, containment, heat exchangers, circulation equipment for working fluid and storage medium, instrumentation and control, storage-medium handling and support equipment, foundation and site preparation. For latent heat systems, the energy density of the salt, which includes its heat of fusion, will determine system size. Storage in high-energy-density salts will have smaller containment, smaller lengths of piping, reductions in valves, controls, instrumentation, salt-handling equipment, foundation and site preparation (like emergency containment for salt in event of leakage, etc.). Therefore, the salt cost (in  $\$/\text{kWh}(t)$  or  $\$/10^6\text{Btu}$ ), determined from the specific salt cost and energy density, should not be used as the sole indication of system cost for screening salts. This would be especially true with low-capacity storage systems, where the balance of plant cost rather than salt cost is significant and where a high-heat-of-fusion salt would be more economical. Details on the preparation of the cost curves are contained in Appendix A of NASA-CR-159479. From this analysis, a plot was obtained of salt cost versus salt heat of fusion using system costs as parameters. The curves shown in Figure 3-5 can be used to estimate TES system costs once specific salt cost and heats of fusion are known. The curves are used in the following subsection on screening salts.



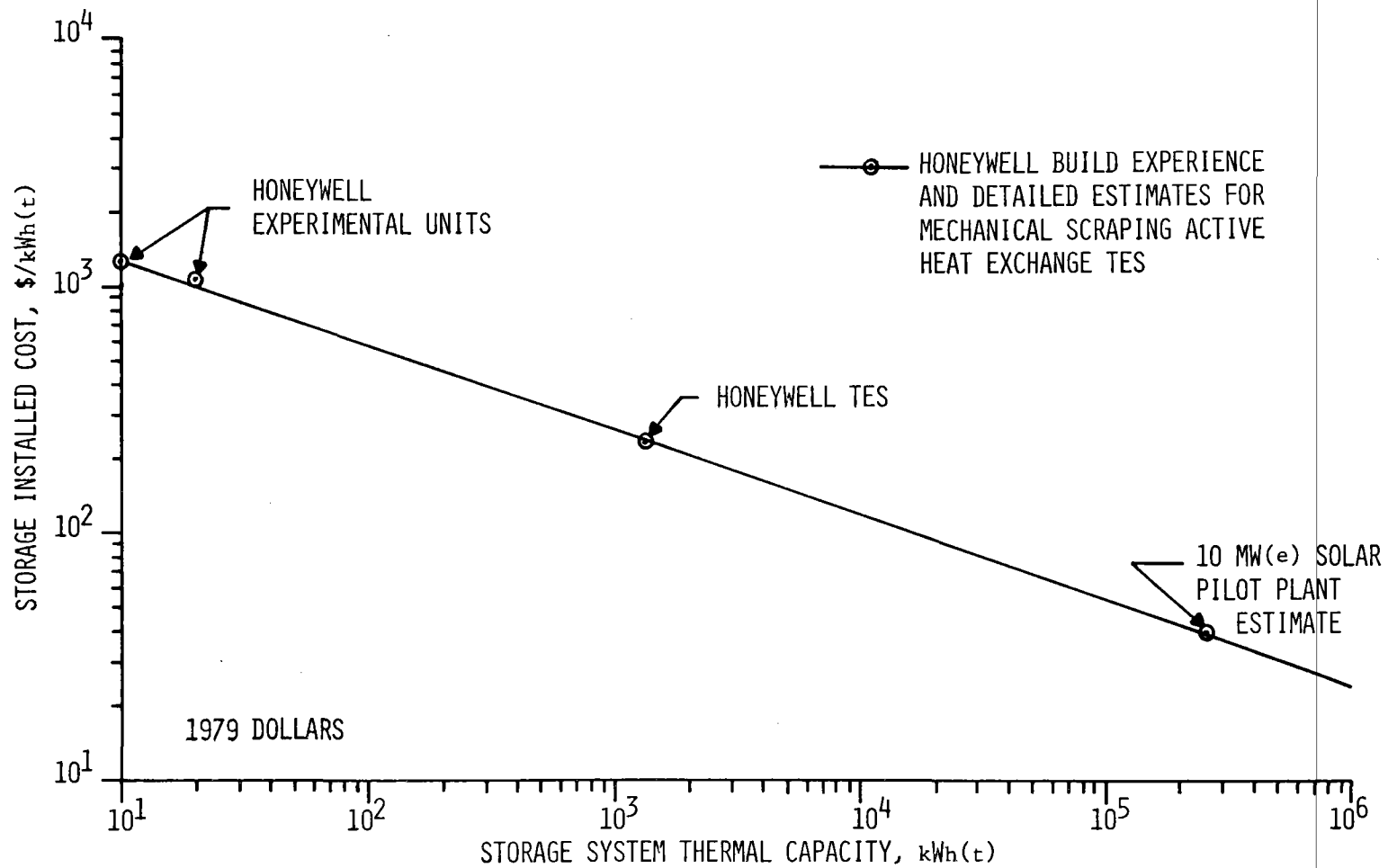


Figure 3-4. Latent Heat/Active Heat Exchange Storage Cost Trends

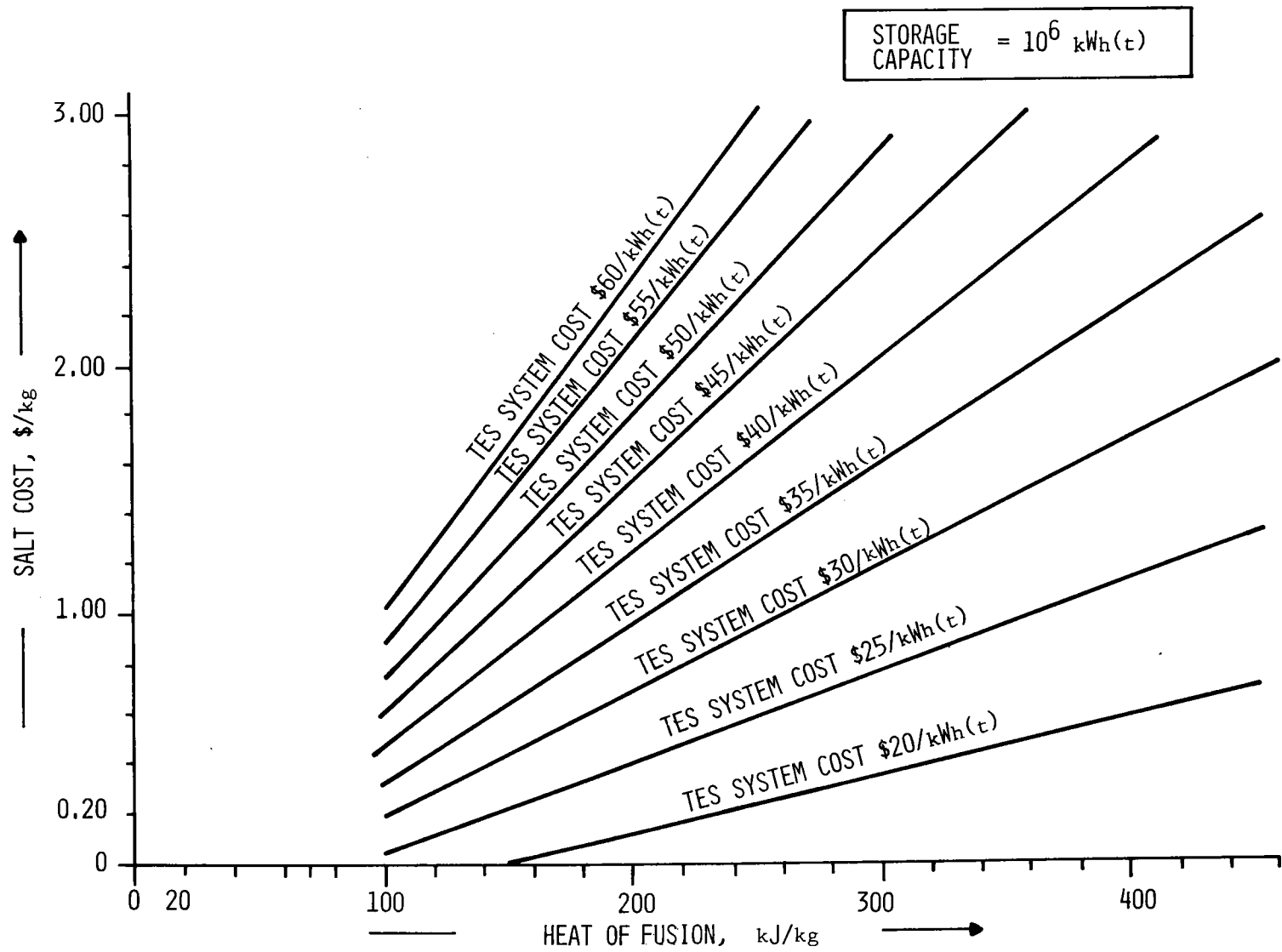


Figure 3-5. Phase Change TES System Cost Curve

### 3.2.2 Salt Screening

A systematic technical and economic evaluation was conducted of about 200 salt mixtures with melting temperatures between 250<sup>o</sup> and 400<sup>o</sup>C. Figure 3-6 shows a flowchart of the salt selection methodology. A list of salts and salt eutectics with melting temperatures between 250<sup>o</sup>C and 350<sup>o</sup>C is given in Appendix C, Tables C-1 and C-2. The salt selection was made after screening on the basis of the criteria described in the next paragraphs.

Nonavailability and Hazardous Properties--Salts of uncommon metals were eliminated because of high costs and unavailability in large quantities. Salts belonging to certain groups like amides, cyanides, and chlorates were eliminated because of their high toxicity and high volatility. Table 3-1 lists seven single salts and 45 binary and ternary eutectic salts, that were selected for further screening, with their salt costs and heat of fusion.

Salt Thermal Properties and System Costs--Important salt properties are salt energy density, thermal conductivity, and corrosivity. An earlier section explained the importance of salt energy density on system cost. Salt thermal conductivity affects the heat exchanger costs. In general, heat exchanger costs are inversely proportional to  $\sqrt{h_f \cdot k_s \Delta T}$ , where  $h_f$  is salt energy density,  $k_s$  is thermal conductivity, and  $\Delta T$  is heat transfer temperature difference. Corrosion properties of salt affect the costs of containment, handling, and heat exchangers.

The salt costs and heats of fusion given in Table 3-1 for the seven single salts and 45 eutectics are plotted on Figure 3-7, the system cost plot obtained from the cost model (Figure 3-5). The numbers on the graph refer to those in Table 3-1. TES system installed costs increase as you go from the lower right to the upper left corner of this figure.

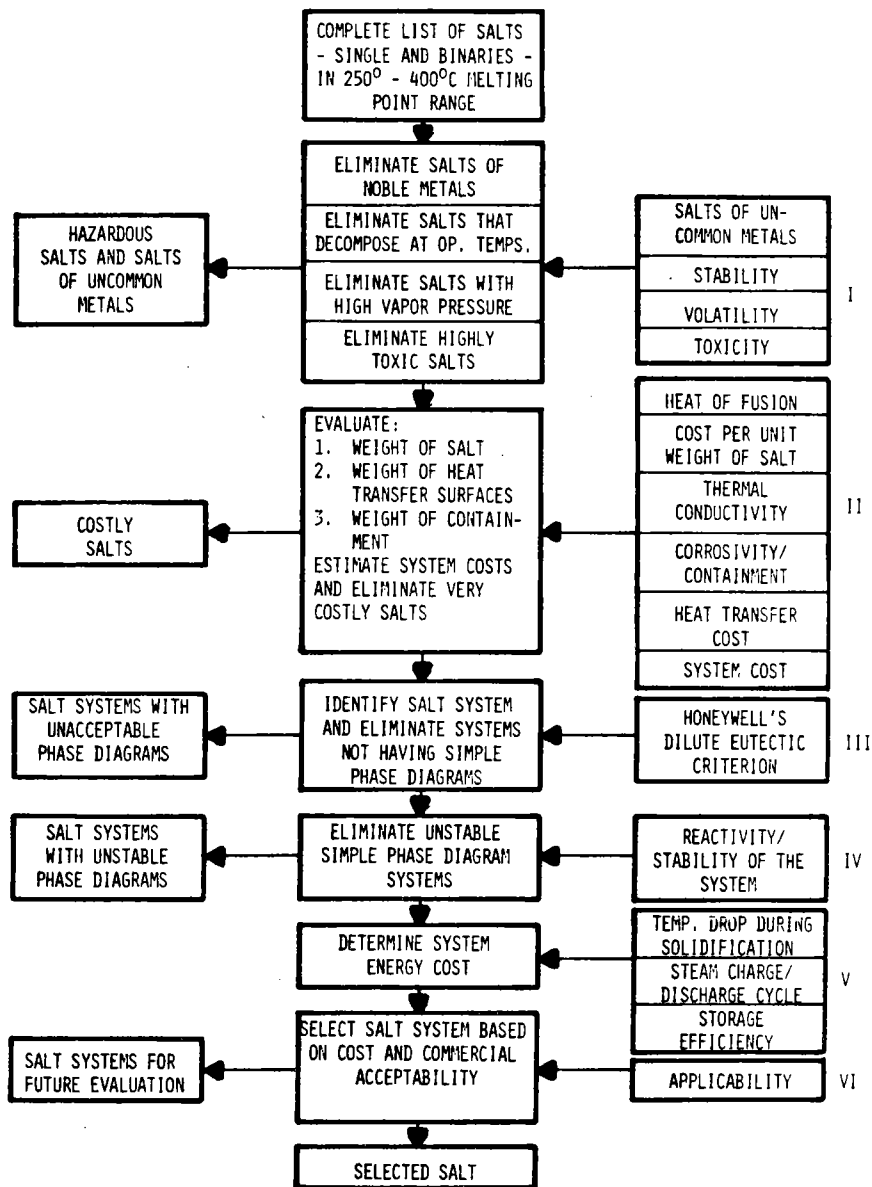


Figure 3-6. Salt Selection Methodology Flowchart

Table 3-1. Properties of Selected TES Inorganic Salts

SALT (A-B-C)	T <sub>f</sub> °C	MOLE % (A-B)	WT % (A-B)	DENSITY AT M. Pt. kg/m <sup>3</sup>	H <sub>f</sub> kJ/kg	H <sub>f</sub> MJ/m <sup>3</sup>	\$/kg*	\$/kWh(ε)
1. LiNO <sub>3</sub>	254	-	-	1776	372 (344)**	663	3.51	33.90
2. NaNO <sub>2</sub>	282	-	-	1808	212	383	0.53	9.00
3. ZnCl <sub>2</sub>	283	-	-	2384	150	354	3.06	74.12
4. NaNO <sub>3</sub>	310	-	-	1920	174	335	0.18	3.65
5. NaOH	318	-	-	1776	158	281	0.33	7.50
6. NaOH	318 *** (299)***	-	-	1776	316	563	0.33	3.75
7. KNO <sub>3</sub>	337	-	-	1872	116	218	0.33	10.25
8. KOH	360	-	-	1728	167	290	0.55	11.85
9. NaNO <sub>3</sub> -NaOH	246 (250)***	70	83	1926	182 (167)**	352 (317)	0.19	3.80
10. LiNO <sub>3</sub> -Li <sub>2</sub> SO <sub>4</sub>	250	98	97	1797	190	342	2.76	52.20
11. LiNO <sub>3</sub> -Li <sub>2</sub> CO <sub>3</sub>	250	98	95	1784	192	342	2.73	51.30
12. Ba(NO <sub>2</sub> ) <sub>2</sub> -LiNO <sub>3</sub>	252	2.8	10	1901	181	387	2.51	49.90
13. NaBr-NaOH	260	22.3	42.5	2018	247	500	0.79	21.60
14. LiOH-LiCl	262	63	49	1725	423	730	2.95	25.20
15. Na <sub>2</sub> CO <sub>3</sub> -Na <sub>2</sub> O-NaOH	263	6.5-7.4	15-10	1878	314	591	NA	-
16. Ca(NO <sub>3</sub> ) <sub>2</sub> -LiCl	265	40.9	73	1866	177	330	1.06	21.50
17. Ba(NO <sub>2</sub> ) <sub>2</sub> -KNO <sub>2</sub>	265	95	98	3186	88	283	NA	-
18. LiBr-LiOH	275	55	81.6	2538	235	597	6.13	94.00
19. KCl-LiCl-LiOH	280	11.5-45	22.6-50	1710	364	624	3.65	36.05
20. Ca(NO <sub>3</sub> ) <sub>2</sub> -NaCl-NaNO <sub>3</sub>	280	5.8-7.9	16.3-5	2090	154	323	0.16	3.80
21. NaCl-NaNO <sub>2</sub>	281	1.1	1	1813	202	367	0.43	7.65
22. NaCl-Na <sub>2</sub> CO <sub>3</sub> -NaOH	282	7.8-6.4	10-14.9	1876	316	594	0.26	2.90
23. KCl-LiCl-LiOH	283	1.5-36.5	3.6-49.1	1701	444	756	2.86	23.20
24. Na <sub>2</sub> CO <sub>3</sub> -NaOH	283	7.2	12	1872	340	636	0.29	3.10
25. Ba(NO <sub>3</sub> ) <sub>2</sub> -NaNO <sub>2</sub>	284	15.2	40.4	1904	154	489	0.27	24.70
26. KNO <sub>3</sub> -NaNO <sub>2</sub>	285	45.2	49.8	1851	152	281	0.41	9.75

\* CHEMICAL MARKETING REPORTER (1975) PRICE LIST.

\*\* EXPERIMENTAL VALUES.

\*\*\* TRANSITION TEMPERATURE.

Table 3-1. Properties of Selected TES Inorganic Salts (Concluded)

SALT (A-B-C)	T <sub>F</sub> <sup>o</sup> C	MOLE % (A-B)	WT % (A-B)	DENSITY AT M. PT. kg/m <sup>3</sup>	H <sub>F</sub> kJ/kg	H <sub>F</sub> MJ/m <sup>3</sup>	\$/kg *	\$/kWh (τ)
27. NaCl-NaNO <sub>3</sub> -Na <sub>2</sub> SO <sub>4</sub>	287	8.4-86.3	5.7-85.5	1956	176	345	2.15	3.50
28. LiOH-LiCl	290	63	49	1664	432	719	2.96	24.70
29. KNO <sub>3</sub> -Ba(NO <sub>3</sub> ) <sub>2</sub>	290	87	72	2277	124	282	0.26	7.70
30. NaCl-NaNO <sub>3</sub>	284	6.4	5	1906	171	327	2.15	3.35
31. LiOH-LiCl	297	50	36	1827	460	841	3.07	24.05
32. LiBr-KBr	310	68	60.8	2597	151	392	4.84	95.65
33. KOH-LiOH	314	60	77.8	1773	341	605	0.91	9.65
34. KCl-KNO <sub>3</sub>	320	6	4.5	1890	150	284	0.37	9.00
35. KNO <sub>3</sub> -K <sub>2</sub> CO <sub>3</sub>	320	98	97.3	1890	147	277	0.39	9.55
36. KNO <sub>3</sub> -K <sub>2</sub> SO <sub>4</sub>	330	98	96.6	1880	149	281	0.39	9.40
37. BaCl <sub>2</sub> -KCl-LiCl	337	6.4-39.4	20.2-44.8	2080	241	502	1.22	18.30
38. KCl-LiCl-CaCl <sub>2</sub>	340	45-45	52.8-29.9	1763	262	462	0.98	13.50
39. KBr-KCl-KNO <sub>3</sub>	342	10-10	4.7-7.3	1920	140	269	0.42	10.90
40. KCl-LiCl-NaCl	346	24-43	32.4-32.8	1720	281	483	1.15	14.70
41. LiCl-KCl	355	58	44	1704	282	481	1.41	17.95
42. KBr-KCl-LiCl-LiBr	357	21.3-37.7	34.4-38-20	1880	214	403	1.54	29.30
43. NaF-NaOH	360	10	10.5	1819	396	720	0.36	3.30
44. NaCl-NaOH	370	20	26.8	1744	370	645	0.28	2.70
45. K <sub>2</sub> CO <sub>3</sub> -Li <sub>2</sub> CO <sub>3</sub> -LiOH	422	16.4-26.4	40-35	1966	352	693	1.40	14.35
46. FeCl <sub>2</sub> -NaCl	374	44	63	-	224	-	NA	-
47. FeCl <sub>2</sub> -KCl	380	52.2	65	-	203	-	NA	-
48. KCl-LiCl-NaCl	384	30-15	41.2-42.7	1690	303	513	1.48	17.60
49. K <sub>2</sub> CO <sub>3</sub> -Li <sub>2</sub> CO <sub>3</sub> -Na <sub>2</sub> CO <sub>3</sub>	394	25-43.5	34.5-32.5	2085	252 (276)**	527 (581)**	0.73	10.45
50. KCl-MgCl <sub>2</sub> -NaCl	396	22-51	20.4-60	1764	261	461	0.19	9.35
51. BaCl <sub>2</sub> -Ca(NO <sub>3</sub> ) <sub>2</sub>	402	41.7	47.6	2734	140	382	0.18	4.60
52. Ba(NO <sub>3</sub> ) <sub>2</sub> -NaCl	408	62	88	2848	122	347	0.30	23.80

\* CHEMICAL MARKETING REPORTER (1975) PRICE LIST.

\*\* EXPERIMENTAL VALUES.

\*\*\* TRANSITION TEMPERATURE.

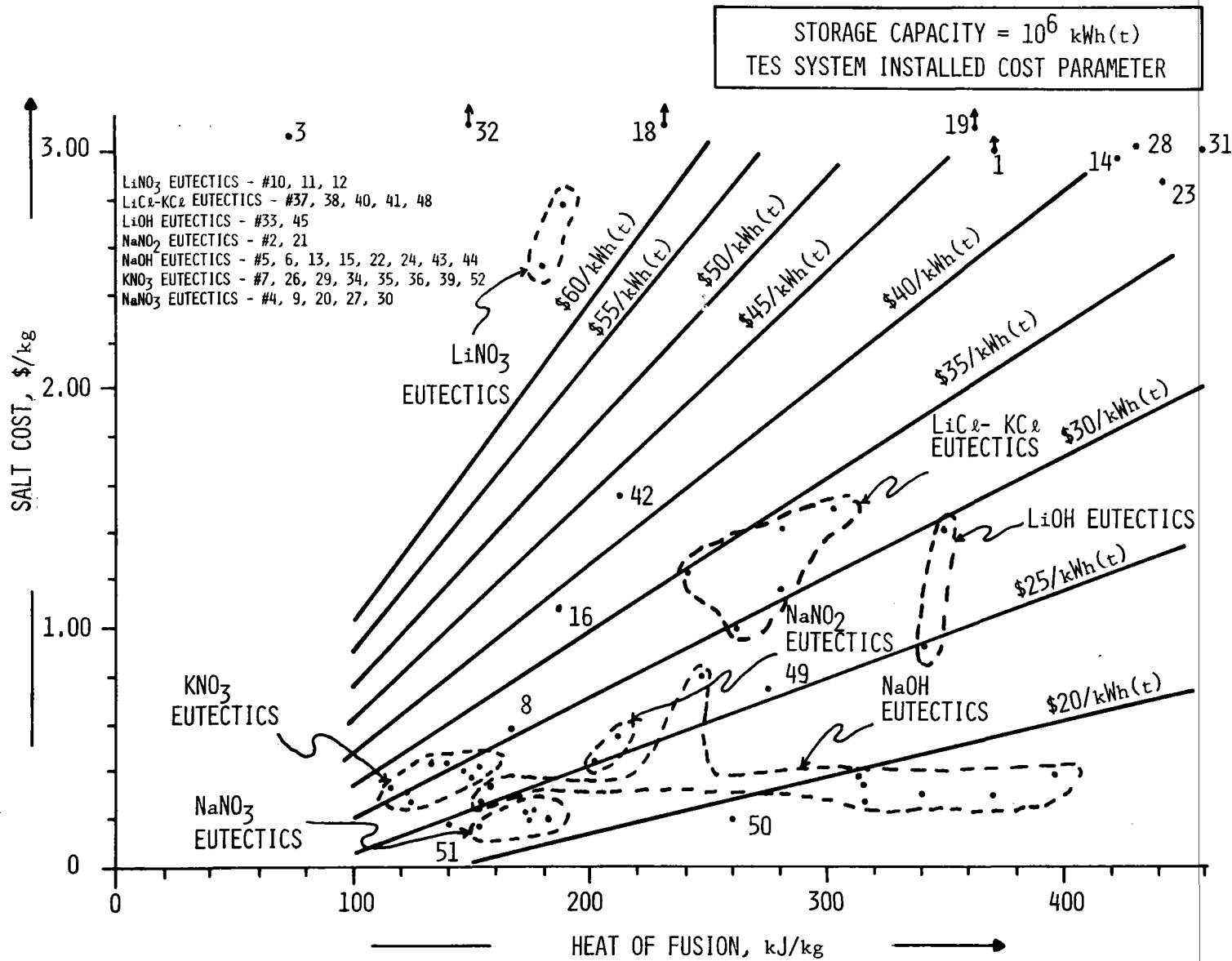


Figure 3-7. Salt Cost versus Heat of Fusion--TES System Cost Parameter

Although a few salts ( $\text{LiNO}_3$  and  $\text{ZnCl}_2$ , for example) demonstrated high system costs, none are eliminated at this stage of the screening; all salts remain under consideration until the end of the screening process when cost considerations are crucial. For now, the cost criteria merely undertone other considerations.

Dilute Eutectic Criterion--Through experimental and analytical work, Honeywell has demonstrated that solidification characteristics of the molten salt mixture are important selection criteria. By referring to the right-hand portion of Figure 1-3, it can be seen that with a 99/1 nitrate-to-hydroxide composition ratio a wide temperature range can be achieved. The wider the range the greater is the heat transfer potential. As long as the outside tube wall temperature carrying the coolant is above the solidus temperature a hard freeze on the tube will not occur. The hard freeze would reduce the heat transfer drastically. Meanwhile, the temperature drop that is required in the medium for a given amount of solidification is small. These characteristics would also maintain a two-phase slush in the crystallizing material, making heat transfer to the melt and pumping the material more efficient. Such crystallization characteristics can be achieved by adding another component (salt or salt mixture) that, together with the primary salt, forms a simple eutectic system. A simple eutectic system is one that does not form any significant solid solutions between the single salt melting point and the eutectic point for the system. The minor component is added in small quantities (about one weight percent), hence the term dilute eutectic system. For example, a 99wt%  $\text{NaNO}_3$  + 1wt%  $\text{NaOH}$  mixture melting at  $303^\circ\text{C}$  is a dilute eutectic system of a  $\text{NaNO}_3$  -  $\text{NaOH}$  simple eutectic system (eutectic point  $272^\circ\text{C}$ , eutectic composition 83%  $\text{NaNO}_3$  and 17%  $\text{NaOH}$ ). For this system it would take approximately 95-percent solidification before the eutectic composition is reached. The solid in this simple eutectic system is pure  $\text{NaNO}_3$ , and there is always a liquid in equilibrium with this solid.



The next step in salt screening was based on the dilute eutectic criterion; here, the purpose was to find simple eutectic phase diagrams for the 52 salts listed. Table 3-2 gives the system costs of the seven salts. (Notice that the information contained in this table is a subset of that in Table 3-1, reprinted here for convenience.) The  $\text{ZnCl}_2$  system was eliminated because of very high system cost. The melting point of  $\text{LiNO}_3$  is  $254^\circ\text{C}$  and is too close to the limit of the range of interest. For other salts, the steam charge and discharge cycles are listed in the comments column. The charge cycle refers to steam conditions of a standard steam turbine cycle required for charging storage. The heat charged is the heat of condensation of steam. The condensation temperature is assumed to be about  $18$  to  $20^\circ\text{C}$  over the salt temperature in determining charge condition. Similarly, discharge cycle refers to the steam conditions of a standard steam turbine cycle obtained when storage is discharged. The heat transferred from storage is used to vaporize water. A  $\Delta T$  of about  $18$  to  $20^\circ\text{C}$  is allowed for heat transfer in determining the standard discharge cycle.

Final Media Selection--At this stage, the list of salts was reduced to the eutectic systems of  $\text{NaNO}_3$ ,  $\text{NaNO}_2$ , and  $\text{NaOH}$ . Table 3-3 lists eutectic systems of these salts. In selecting the minor component, several factors must be considered.

- Reactivity
- Supercooling
- Temperature drop
- Stability
- Safety
- Cost and availability

The minor component should not react with the major component. In the  $\text{NaOH} - \text{Na}_2\text{CO}_3$  system,  $\text{Na}_2\text{CO}_3$  reacts with moisture to give off  $\text{CO}_2$ , and  $\text{NaOH}$  absorbs moisture. Supercooling is a common phenomenon and it is a serious problem

Table 3-2. Selected Major Components--System Cost

SALT #	MAJOR COMPONENT (99 wt%)	MELTING POINT (°C)	HEAT OF FUSION (kJ/kg)	SALT COST (\$/kg)	TES SYSTEM COST (\$/kWh(t))	COMMENTS
1	LiNO <sub>3</sub>	254	372	3.51 (2.51)	49 39	MELTING POINT TOO CLOSE TO LIMIT OF RANGE OF INTEREST--ELIMINATE
2	NaNO <sub>2</sub>	282	212	0.53	26	FITS 8.6 MPa CHARGE/4.1 MPa DISCHARGE (1250/600 PSI)
3	ZnCl <sub>2</sub>	283	150	3.06	75	VERY HIGH SYSTEM COST - ELIMINATE
4	NaNO <sub>3</sub>	310	174	0.17	22	FITS 12.4 MPa CHARGE AND 6.9 MPa DISCHARGE CYCLE (1800/1000 PSI)
5	NaOH	318	158	0.33	26	FITS 16.5 MPa CHARGE/12.4 MPa DISCHARGE CYCLE (2400/1800 PSI)
6	NaOH	318	158	0.33	19	IF SYSTEM COULD BE DESIGNED TO UTILIZE THE HEAT OF TRANSITION
7	KNO <sub>3</sub>	337	116	0.33	30	FITS 22 MPa CHARGE/--DISCHARGE CYCLE (3200 PSI)
8	KOH	360	167	0.55	29	FITS SUPERCRITICAL CYCLE

Table 3-3. Salt System Selection

Major Component (Melting point)	Minor Component ( lwt%)	Eutectic Melting Point (°C)	Temperature drop for 60% Solidification (°C)	Comments	Selected System	Recommended System
NaNO <sub>3</sub> (310°C)	NaOH	243	6	Has performed very well supercools; forms vitreous solid Has a larger temp drop and is no better than NaOH.KOH is more corrosive. Hazardous minor component. Very costly minor component. LiNO <sub>3</sub> is hygroscopic; could be an alternate candidate.	NaNO <sub>3</sub> (99wt%) + NaOH (1wt%)	NaNO <sub>3</sub> (99wt%) + NaOH (1wt%) we have all the data available on this sytem and will be an excellent candidate for heat exchanger evaluation.
	Ca(NO <sub>3</sub> ) <sub>2</sub>	232	2			
	KOH	222	10			
	NH <sub>4</sub> NO <sub>3</sub>	121	4			
	TlNO <sub>3</sub>	162	1			
NaNO <sub>2</sub> (282°C)	LiNO <sub>3</sub>	196	4	A possible candidate for lower cycle selection	NaNO <sub>2</sub> (99wt%) + NaOH (1wt%)	The NaNO <sub>2</sub> system will require salt characterization studies and is therefore not recommended for application at this time.
	NaOH	232	7			
NaOH (318°C)	Na <sub>2</sub> CO <sub>3</sub>	283	2	Reacts to give CO <sub>2</sub> Eutectic temp too close Possible candidates. NaNO <sub>3</sub> & NaNO <sub>2</sub> are believed to have a passivating effect for corrosion.	NaOH (99wt%) + NaNO <sub>3</sub> (1wt%)	NaOH system will need a corrosion inhibitor*. It's selection is therefore conditional.
	Na <sub>2</sub> SO <sub>4</sub>	293	3			
	NaBr	265	2			
	NaI	215	2			
	NaNO <sub>3</sub>	258	3			
	NaNO <sub>2</sub>	238	4			

\*Comstock and Wescott have a patented corrosion inhibitor for this system.

with phase-change materials in passive systems. The amount of supercooling is generally less for large samples. The  $\text{NaNO}_3 - \text{Ca}(\text{NO}_3)_2$  system is known to supercool and forms a glassy solid. The freezing temperature of the eutectic system (generally) decreases with solidification. The freezing temperature drop for a given amount of solidification should be as small as possible for efficient operation. Table 3-3 lists the calculated temperature drop for the eutectic system. The system should be stable.  $\text{NaNO}_2$  decomposes at temperatures greater than  $450^\circ\text{C}$ . Furthermore, the system should maintain thermal and physical properties over the life of the storage system. The component should be safe.

$\text{NH}_4\text{NO}_3$  is a hazardous salt, and  $\text{TlNO}_3$  is very toxic and should be avoided even in minute quantities. Cost of the minor component is generally unimportant; however, 1 weight percent of  $\text{TlNO}_3$  added to  $\text{NaNO}_3$  increases the salt mixture cost about twofold.

Table 3-3 also lists the reasons for selecting the candidate salt media. The recommended salt system is 99 weight percent  $\text{NaNO}_3$  with 1 weight percent  $\text{NaOH}$ . The recommended system, in addition to meeting all the criteria discussed, has performed well with the mechanical scraper concept developed for the 10 MW(e) Pilot Plant Storage Subsystem. Most of the data required for advanced active heat exchange evaluation is available for this system.

The use of  $\text{NaOH}$  as the major component was considered based on its apparent cost advantage, especially when the heat of transition is included. However, due to its pervasive caustic effects on human tissue and material, the need for closed system operation and the uncertainty of being able to recover the heats of fusion and transition effectively, it was not selected.

### 3.3 SELECTION OF HEAT EXCHANGE CONCEPTS

#### 3.3.1 Survey of Heat Exchange Concepts

A candidate heat exchange concept applicable to latent heat thermal storage units must be capable of transferring heat from a source into the frozen media causing it to melt. Likewise, the concept must be capable of transferring the thermal energy stored in the medium to a sink while the medium undergoes a solidification process. In both cases, the concept should permit relatively high heat transfer rates while undergoing the phase changes.

A survey of heat transfer and chemical processing literature was made to determine the equipment used industrially and the chemical and physical processes exploited in extracting the latent heat of fusion from a melt. An investigation of crystallization processes (ref. 5, 6, and 7) was performed to determine if existing industrial methods might be directly applicable to or provide new ideas for latent heat storage design. The types of crystallization methods used industrially are listed below.

- Crystallization through cooling
- Crystallization through evaporation
- Salting out with a common ion or second solvent that reduces the solubility of the crystallizing substance
- Crystallization involving chemical reaction

The processing literature is limited in coverage of heat exchanger crystallizers, as this approach has often been disregarded in favor of alternatives. The major design and operating problem of a cooling crystallizer is crystal deposits on the heat exchanger tubes. Once this takes place, the accumulation

can increase rapidly, and not only does the heat transfer from the molten salt decrease dramatically, but the solids are not in a mobile form for pumping. Following is a list of different methods used in the past and innovative ideas put forth by Honeywell engineers to overcome the solid film problem.

- Mechanical Solids-Removing Techniques:

- Agitation
- Vibration
- Ultrasonics
- Internal surface scrapers
- External surface scrapers
- Flexing surfaces
- Tumbling solids
- Fluidized beds

- Hydraulic Techniques:

- Flow variations
- Fluid pulsing
- Jet impingement
- Sprayed surface exchanger
- Freeze-remelt

- Techniques Involving Physical Properties of the Salt:

- Crystal volume change
- Crystal weakening additive
- Conductivity-enhancing additives
- Magnetic susceptibility
- Electrostatic separation
- Finishing and coating of heat exchanger surfaces
- Delayed nucleation and supercooling

- Other Concepts:

- Direct contact heat exchange
- Shot tower latent heat of fusion concept
- Prilling tower crystallization
- Liquid metals salt system
- Immiscible salts
- Encapsulation (passive system)
- Distributed tube exchanger (passive system)

### 3.3.2 Candidate Concepts for Evaluation

From the survey, Honeywell selected the following concepts as candidates for further evaluation.

- Internal Surface Scraper
  - External Surface Scraper
  - Shell and Tube Flowby
  - Jet Impingement
  - Reflux Boiler/Self-pressurizing
  - Reflux Boiler/Continuous Salt Flow
  - Reflux Boiler/Continuous Salt Flow with Hydraulic Head Recovery
  - Tumbling abrasive
- } Direct Contact  
Heat Transfer

These concepts embody the most conventional and promising heat transfer processes. The passive tube-intensive system was chosen as a reference system against which cost comparisons could be made.

### 3.3.3 Evaluation Criteria

To get an idea of the total system cost implications of the basic concepts chosen, it was necessary to make a preliminary system layout and to estimate costs of all major components for each of the systems. The following conditions provided the basis for all cost estimates:

- Storage medium has the properties of  $\text{NaNO}_3$  plus 1 percent NaOH.
- The latent heat storage module will supply saturated steam at 6.9 MPa/300°C (1000 psi/574°F).
- The heat rate would be 1000 MW(t) ( $3.41 \times 10^9$  Btu/hr) for 6 hours.
- All systems would be charged by steam-condensing coils in the storage tanks (except in the tube-intensive system where the same tubes perform both charge and discharge functions).

The performance and costs of the eight heat exchange concepts were compared in Table 3-4. The comparison criteria were broken into five major groups:

- Performance Parameters
- Operational Criteria
- Subjective Evaluation Criteria
- Materials Required
- System Costs



Performance parameters are those heat-transfer-related quantities that are necessary to size the various systems and that indicate the extent of possible system size reductions attainable if the heat transfer coefficient is improved. With water vaporizing inside of a 2.5 cm outside diameter, 13-gauge carbon steel tube, the overall heat transfer coefficient will be less than  $6000 \text{ Wm}^2\text{-}^\circ\text{K}$  due to thermal resistance of the tube wall and the water film coefficient. Salt film coefficients and any fouling resistance will further reduce this value.

Operational criteria are control and maintenance parameters that may influence the overall complexity of the systems. Some of the critical control items are discussed, along with the numbers of individual units that may contribute to maintenance and/or control complexity.

Subjective evaluation criteria are parameters that are strictly engineering judgment. It would be difficult to place a dollar figure on these quantities, but they must be considered in the selection and overall evaluation of the system.

Materials required are weight estimates of major components of the thermal storage system. These estimates were made by calculating sizes and weights of the necessary fluid-handling and storage components, while considering the various code requirements and good engineering practices in designing systems.

System costs in 1979 dollars were broken down into costs of each of the major components and finally into capacity- and rate-related costs. The final, bottom-line figure is the estimated cost for the total system capable of providing 100 MW(t) for a 6-hour period. These cost estimates were based upon data obtained by quotations developed under the Solar Pilot Plant program and scaled using appropriate scaling laws for each of the components. The passive tube-intensive system was chosen as a reference to which cost comparisons could be made.

### 3.3.4 Performance and Cost Evaluation

The following paragraphs discuss each of the concepts chosen. Table 3-4 outlines their performance based on the criteria described. Notice that for most systems, the balance of plant cost, which includes all auxiliary components, is a large percentage of the total system cost.

Internal Surface Scrapers--Mechanical blades may be mounted on a rotating shaft to remove material freezing on the inner walls of the heat exchanger. The mechanically induced turbulence in the equipment makes it possible to handle highly viscous liquids and slurries while maintaining moderately high transfer coefficients.

The internal surface scraper was envisioned as either an Armstrong or Votator commercially available scraped-surface heat exchanger. This device has a long record of successful commercial use and does not need major design changes to be adapted to thermal storage applications. The device can be disassembled readily to service the scraper blades.

The system layout assumes that the heat exchangers would be centrally located between the storage tanks and that the salt would be pumped to the exchangers and back to storage. Here, the salt slurry would separate, and the rich liquid would be recycled back through the exchanger. A 75-percent heat recovery factor was used as bases for the designs.

The heat transfer coefficient was estimated as  $2271 \text{ Wm}^{-2}\text{-}^\circ\text{K}$  based on Votator literature data. For a 1000 MW(t) heat rate and  $18^\circ\text{C}$  heat transfer,  $\Delta T$ , the heat transfer surface required is  $2.44 \times 10^4 \text{ m}^2$ . The largest commonly manufactured Votator unit made was listed as  $4.65 \text{ m}^2$  ( $50 \text{ ft}^2$ ) of surface, 0.25 m (10 inches) diameter, and 6.1 m (20 ft) in length. Therefore, this requires about 5300 units.

Table 3-4. Performance and Cost Evaluation of Candidate Heat Exchanger Concepts

CRITERIA		UNITS	1	2	3	4
			INTERNAL SURFACE SCRAPER	EXTERNAL SURFACE SCRAPER	SHELL AND TUBE FLOW-BY	JET IMPINGEMENT
PERFORMANCE	HEAT TRANSFER COEFF.	$W.m^{-2} K^{-1}$	2271	2868	2260	2084
	TEMPERATURE DROP	K	18	18	18	18
OPERATION	HEAT TRANSFER RATE	$W.m^{-2}$	40878	51624	40680	37512
	AUXILIARY POWER	$kW(e) \times 10^{-3}$	25.2	25.2	8.4	9.0
	PERCENT OUTPUT (a)		8.4	8.4	2.8	3.0
	CONTROL REQUIREMENTS	TYPE	FREEZE-UP	FREEZE-UP	TEMP. BAL.	TEMP. BAL.
	MAINTENANCE	FREQUENCY	SHARPENING	WEAR	MINIMUM	MINIMUM
SUBJECTIVE EVALUATION PARAMETERS	SYSTEM SIZE	m	0.25m x 6.1m	35m x 2.4m	1.5m x 12.2m	3m x 3m x 5.5m
	SCALABILITY	# OF UNITS	5300	54	10	10
MATERIALS REQUIRED	TECHNOLOGICAL DEV.		BAD	BAD	GOOD	GOOD
	COMPATIBILITY WITH STEAM CYCLE		GOOD	PHOTOTYPE	GOOD	CONCEPT
	INSTITUTIONAL BARRIERS		FAIR	GOOD	GOOD	GOOD
COSTS	SAFETY		NONE	NONE	NONE	NONE
	HEAT EXCHANGERS		TUBE ABRASION	TUBE ABRASION	TUBE EROSION	TUBE EROSION
	SURFACES	$kg \times 10^{-6}$	--	1.40	0.42	0.83
	CONTAINMENT	"	--	NONE	0.09	0.05
	MANIFOLDING	"	0.27	0.27	0.20	0.20
	TANKAGE	"	3.7	7.6	3.7	3.7
COSTS	STORAGE MEDIA		166	166	166	166
	HEAT EXCHANGERS	\$/kWh(t)	27.50	3.13	1.52	1.90
	MANIFOLDS	"	0.33	0.33	0.25	0.25
	TANKAGE	"	2.14	4.20	2.14	2.14
	MEDIA @ 0.1 \$/LB	"	6.10	6.10	6.10	6.10
	BALANCE OF PLANT	"	10.8	10.8	10.8	10.8
	RATE RELATED COST	\$/kW	201	54.9	44.7	47.0
	CAPACITY RELATED COST	\$/kWh(t)	13.4	15.5	13.4	15.4
	SYSTEM COST	\$/kWh(t)	46.9	24.6	20.9	21.2
	SYSTEM TOTAL COST	$\$ \times 10^{-6}$	281	147	125	127
	RELATIVE COST		1.72	0.90	0.77	0.78
	REL. COST LESS BALANCE OF PLANT		2.2	0.84	0.62	0.63

Table 3-4. Performance and Cost Evaluation of Candidate Heat Exchanger Concepts (Concluded)

CRITERIA		5	6	7	8	9
		SELF PRESSURIZING REFLUX BOILER	CONTINUOUS SALT FLOW (c) REFLUX BOILER	OPEN SYSTEM REFLUX BOILER	TUMBLING ABRASIVE	PASSIVE TUBE INTENSIVE
PERFORMANCE	HEAT TRANSFER COEFF.	4656	--	--	568	55
	TEMPERATURE DROP	15	15	4	18	18
	HEAT TRANSFER RATE	69840	69840	--	10224	990
OPERATION	AUXILIARY POWER	9.0	9.0	9.0	9.0	1.5
	PERCENT OUTPUT (a)	3.0	3.0	3.0	3.0	0.5
	CONTROL REQUIREMENTS MAINTENANCE	SLURRY CONV. VALVE SEATS INFREQUENT	SLURRY CONC. MINIMUM INFREQUENT	SLURRY CONC. VALVE SEATS INFREQUENT	MINIMAL TUBE WEAR INFREQUENT	MINIMAL NONE INFREQUENT
SUBJECTIVE EVALUATION PARAMETERS	SYSTEM SIZE	2.1m x 12.2m	2.1m x 12.2m	2.1m x 12.2m	1.8m x 12.2m	35m x 12.2m
	SCALABILITY	24	8	16	117	6
	TECHNOLOGICAL DEV. COMPATIBILITY WITH STEAM CYCLE	GOOD	GOOD	GOOD	GOOD	GOOD
MATERIALS REQUIRED	INSTITUTIONAL BARRIERS SAFETY	CONCEPT	CONCEPT	CONCEPT	CONCEPT	SMALL SCALE
	HEAT EXCHANGERS SURFACES	GOOD	GOOD	GOOD	GOOD	GOOD
	CONTAINMENT	PR. VESSEL CODE ABMA CODE	PV. VESSEL CODE ABMA CODE	PR. VESSEL CODE ABMA CODE	NONE TUBE EROSION	NONE NONE
COSTS	TANKAGE	0.29	0.29	0	2.70	16.5
	STORAGE MEDIA	1.11	0.65	0.93	1.25	NONE
	HEAT EXCHANGERS	0.09	0.09	0.09	0.27	1.12
	MANIFOLDS	3.7	3.7	3.7	3.7	3.1
	TANKAGE	166	166	166	166	125
	MEDIA @ 0.1 \$/LB	2.58	1.84	1.92	3.60	8.63
	BALANCE OF PLANT	0.11	0.11	0.11	0.33	1.38
RATE RELATED COST	2.14	2.14	2.14	2.14	1.78	
CAPACITY RELATED COST	6.10	6.10	6.10	6.10	4.58	
SYSTEM COST	10.8	10.8	10.8	10.8	10.8	
SYSTEM TOTAL COST	50.2	45.5	46.0	57.7	94.1	
RELATIVE COST	13.4	13.4	13.4	13.4	11.5	
REL. COST LESS BALANCE OF PLANT	21.7	20.9	20.5(b)	23.0	27.2	
	0.80	0.77	0.75	0.85	1.00	
	0.66	0.62	0.59	0.74	1.00	

FOOTNOTE: (a) PERCENTAGE OF THERMAL OUTPUT USED TO GENERATE ELECTRICITY TO DRIVE AUXILIARIES  
(b) SYSTEM COSTS ADJUSTED FOR HIGHER EFFICIENCY ATTAINABLE AT HIGHER TEMPERATURE.  
(c) AT THIS LEVEL OF AN ESTIMATION, THE CONTINUOUS SALT FLOW REFLUX BOILER WITH AND WITHOUT HYDRAULIC HEAD RECOVERY ARE REPRESENTED BY THE SAME NUMBERS.  
(d) ALL ESTIMATES IN THIS TABLE HAVE BEEN SIZED TO A 1000 MW<sub>e</sub>, 6 HR. STORAGE UNIT OPERATING WITH 1000 PSI SATURATED STEAM.

A disadvantage in the use of these units is that the heat transfer surface area per unit weight and volume is relatively small. A second deficiency of these units is that high-pressure steam must be contained in a large-diameter annulus; this requires very thick-walled tubular construction and may require exotic expansion joints to accommodate differential expansion between inner and outer shells. This potential problem could be overcome with a shell and made-from-membrane wall structure formed into a cylinder, but this would require further development and would not overcome the low surface-to-volume ratio or improve the heat transfer coefficient. The system is basically not scalable, as larger single units decrease the surface-to-volume ratio; hence, large systems must contain large numbers of individual units manifolded together. Maintenance on large numbers of active scraper systems is potentially a major operational problem.

The cost estimate for this system of exchangers is based upon cost estimates for large number of systems from Votator, a Division of Chemtron. It is estimated to cost \$4305/m<sup>2</sup> surface.

The relatively high cost of individual units and the large number of them required places this system at a price disadvantage compared with other systems.

External Surface Scraper--Similar in function to the internal scrapers described, the external concept uses elliptical blades on the outside of the circular heat transfer tubes (see Figure 3-8). The scraper blades are held in place by a series of ribs forming an open cage structure that admits salt to the transfer tubes and permits frozen salt crystals to fall away. This concept has been mechanized in a storage subsystem research experiment under the Solar Pilot Plant Program (ref. 9).

The heat exchange system modeled in this concept was basically the external tube scraper designed by Honeywell under the Solar Pilot Plant program (ref. 10).

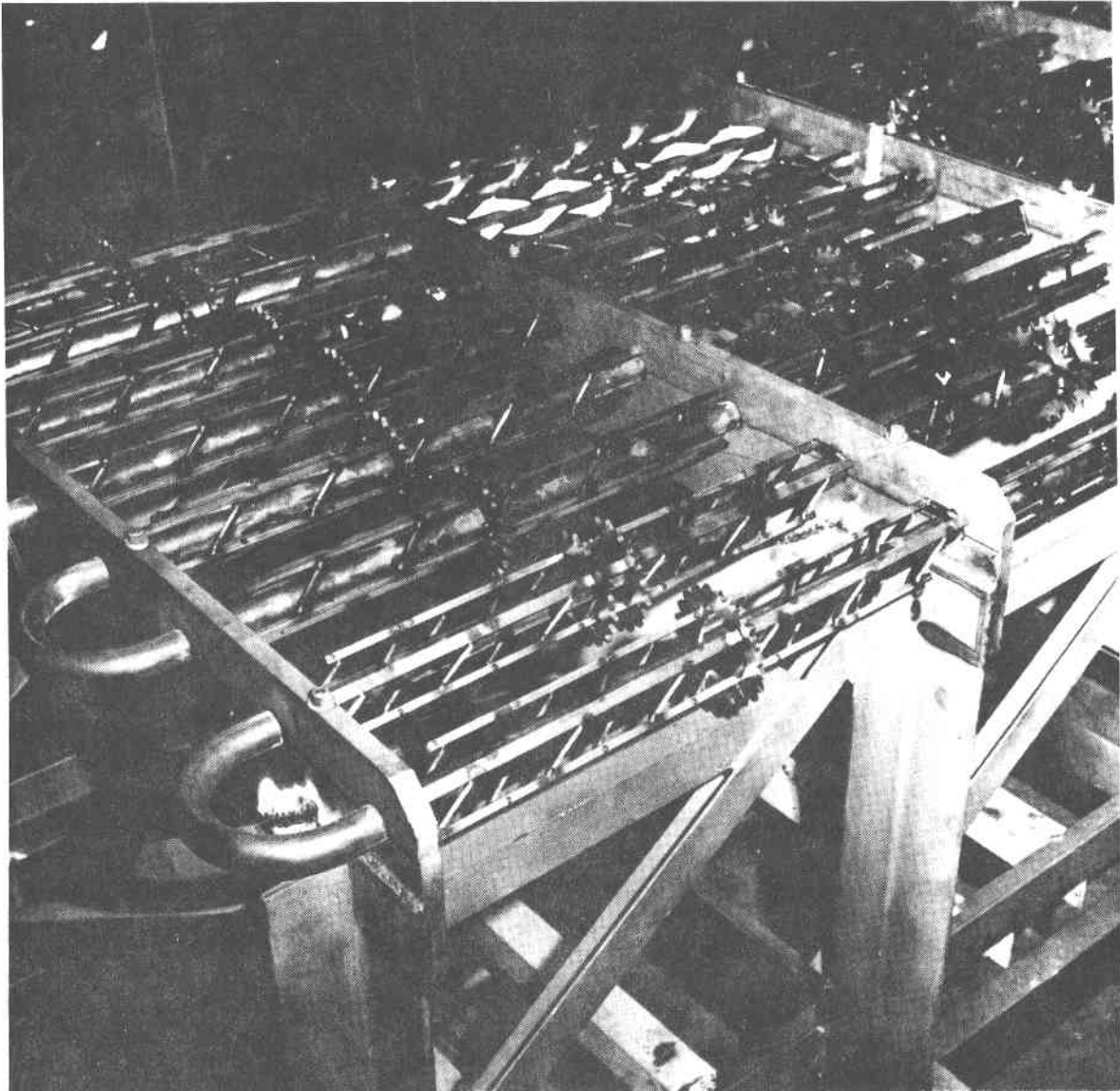


Figure 3-8. Close-up View of Bottom of Vaporizer Module Showing Total Scraper

The scraper modules are located in the top of the storage tanks, with a large tank top surface area required by the slow solid-salt settling rate. Improvement in the overall heat transfer rate compared with the internal scraper is obtained by the more favorable geometry and the thinner tube walls. Scraping power requirements were assumed to be similar.

For a 120-rpm scraper speed, with  $18^{\circ}\text{C}$   $\Delta T$  and  $7.62 \times 10^{-6}$  m (3 mil) scraper clearance, an overall coefficient of  $2867 \text{ Wm}^2\text{-}^{\circ}\text{K}$  was obtained. The results of the model correlated well with the experimental data in the Solar Pilot Plant program. The heat transfer surface required for 1000 MW(t) heat rate is  $1.94 \times 10^4 \text{ m}^2$ .

The solid salt scraped from heat exchanger tubes has to settle to the bottom of the tank. Due to the slow solid settling rate, a large tank top area is required. It was determined from the experiment that a heat rate of 20,500  $\text{W/m}^2$  of tank surface can be obtained. Therefore, the design required about 54 tanks, each 35 m in diameter by 2.4 m in height.

Cost estimates for the scraper units were based on fabrication cost of the modules made under the Solar Pilot Plant program, design changes to reduce the total weight, and an 85-percent learning curve for the increased quantity production. No salt manifolding was required, but tank costs increased due to the unfavorable surface-to-volume ratio required by having the exchanger in the tank. The total system cost estimate ranks this system close to the passive system, but maintenance and auxiliary power requirements were not included in the costs.

Scalability is poor because of the limited number of units that can be powered by a common drive and because the surface-to-volume ratio decreases as pipe size is increased. Heat transfer and high pressures tend to make 1-inch diameter tubing nearly optimal for the system.

Shell and Coated Tube Flowby--There are numerous applications in the chemical process industries where finishes and coatings are used to provide antistick and release properties for interfacing with the process medium. Any coating and/or finish for heat of fusion thermal storage applications should provide a smooth, thin, nonporous, nonreactive surface to discourage firm adherence of the freezing salt to the heat exchanger wall. The heat transfer should not be limited by this film. Surface morphology should minimize nucleation sites for the crystallizing medium. Any coating should be stable at the operating temperatures of the storage medium and should perform for an industrial lifetime. In addition, the coating should show promise of large-scale use at reasonable costs. This system was modeled assuming a shell-and-tube exchanger could be designed to function with a latent heat storage medium. Given the proper combinations of salt, tube coating or plating, flow velocities and temperature control, this system may function with minimal fouling (see Figure 3-9).

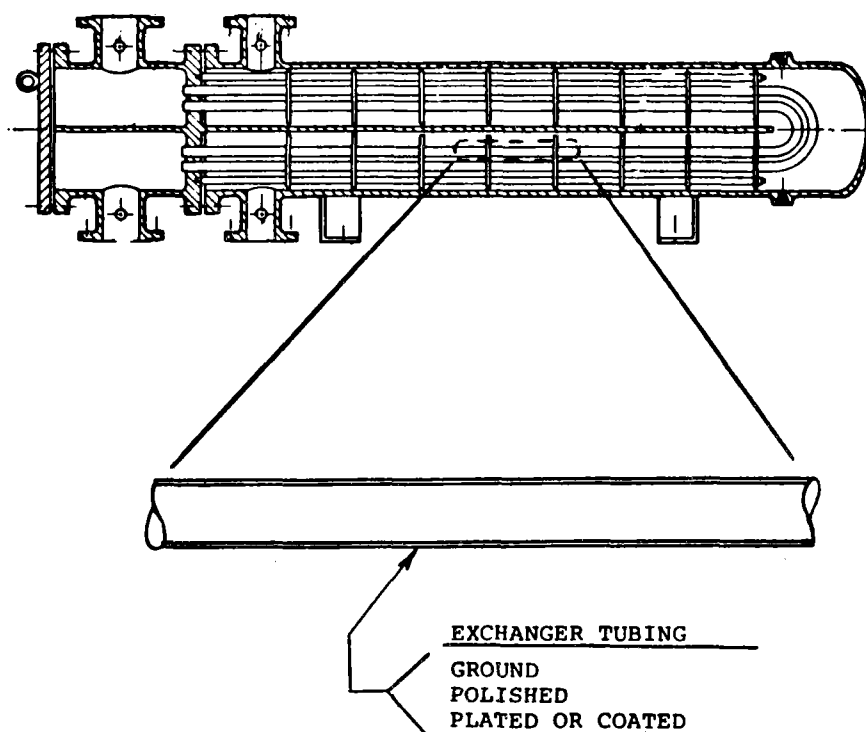


Figure 3-9. Shell and Tube Exchanger with Deposit-Resistant Tubes



The heat transfer coefficient for a shell and coated tube exchanger was estimated to be  $2260 \text{ Wm}^2\text{-}^\circ\text{K}$ . The shell-side or salt-side coefficient can be obtained by DeVore's method (ref. 11). A shell-side coefficient of  $4383 \text{ Wm}^2\text{-}^\circ\text{K}$  was used based on the manufacturer's (ref. 12) design coefficient for "Hitec storage" in a solar pilot plant. The design used a 0.6 m/s salt velocity. For a 1000 MW(t) heat rate, a  $2.46 \times 10^4 \text{ m}^2$  heat transfer surface is required.

Pumping power for the salt and for the water, assuming that a recirculating boiler concept is used, accounted for only a small percentage of the total power output. Besides initial cost, the main advantages of this system over scraped-surface exchangers are that shell and tube exchanger technology is very well developed, and that a few large exchangers can provide sufficient heat transfer area. Scalability is good, with presently manufactured shell and tube exchangers having surface areas from less than  $0.1 \text{ m}^2$  to over  $500 \text{ m}^2$  in one shell. Maintenance should be minimal, requiring only a periodic inspection for tube erosion.

In estimating the price of the exchangers, the estimate for the tube bundles was doubled to allow for grinding, polishing, and plating as necessary. A highly polished nickel plating on all tubes was assumed to be required. The exchanger accounts for only a small fraction of the total cost of the system. The balance of the plant is the largest single item and includes instrumentation, steel control valves, water treatment, preheaters, foundations, etc.

Jet Impingement--By using extremely high velocities in the flow of the melt past the heat exchange surfaces, accumulating solids may be transported away from the surface. In such a case, not only does the melt have a very short residence time at the surface, precluding freezing, but the forces of impingement of the liquid salt could be great enough to break off solids that may have been deposited previously. (See Figure 3-10.)

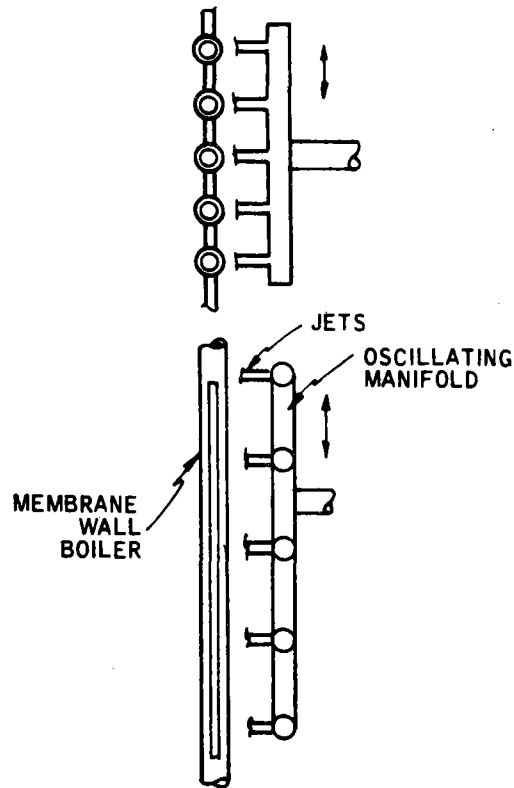


Figure 3-10. Jet Impingement Salt Removal

The jet impingement concept is one in which high-velocity jets of salt would be directed toward the heat exchange surface to aid in removing the solids buildup. This would be an option if the shell and tube flowby concept has marginal performance, or if flow velocities high enough to wipe the salt from the complete circumference of the tubes cannot be maintained.

The heat exchange surfaces are assumed to be formed from membrane wall material and are polished and coated to decrease salt adhesion. Membrane walls are a common heat transfer surface used in fossil-fired boilers. The idea is to apply developed, commercially available equipment and processes to salt storage. The salt pumping power requirements are not significantly different from a shell and tube design, as only 2 meters of salt head are required to obtain salt velocities greater than 5 m/s.

The heat transfer coefficient is lower due to both the buildup of layers of solids on the surface and the reduced conductance of the membrane walls as opposed to single tubes. For a membrane wall with a tube size of 0.025 m outside diameter by 0.019 m inside diameter (1 inch outside diameter by 0.75 inch inside diameter), a spacing of two diameters and 70-percent fin efficiency, an overall coefficient was assumed to be  $2975 \text{ Wm}^2\text{-}^\circ\text{K}$ . For 1000 MW(t),  $2.67 \times 10^4 \text{ m}^2$  of heat transfer surface was required. The quantity of metal in the heat exchangers is increased due to both the lower transfer coefficient and the increased weight of the membrane wall structure. In this case, the area per unit volume of exchanger is less than that of a shell and tube unit, requiring a much larger exchanger volume. These factors all lead to slightly higher system costs.

Reflux Boiler Heat Exchanger--The reflux boiler heat exchanger concept uses water as an intermediate fluid to transfer latent heat from the molten salt to a conventional heat exchanger, where the heat is imparted to the treated power plant water. Direct contact heat exchange between the water and salt provides good heat transfer and minimizes fouling of heat transfer surfaces by solid-salt deposits. Also, because the thermal energy does the salt pumping, this system offers the possibility of using pure eutectic compositions to minimize temperature degradation during discharge of storage. The disadvantages of the system are that all of the condensers and refluxing boilers require large, expensive high-pressure shells. Pressure cycling of the reflux boilers may pose a fatigue problem in thick-walled pressure vessels.

For reflux boilers there are two transfer coefficients. One is for direct contact of salt and water in the refluxing boiler, and the other is for condensation of steam on boiler tubes. For direct contact, a  $3^\circ\text{C}$  temperature drop was considered reasonable. Therefore, if  $18^\circ\text{C}$  is allowed overall, a  $15^\circ\text{C}$   $\Delta T$  is available for steam condensation. The condensation coefficient was assumed to be  $11,356 \text{ Wm}^2\text{-}^\circ\text{K}$  which gives an overall coefficient of  $4656 \text{ Wm}^2\text{-}^\circ\text{K}$ . A heat transfer surface of  $1.19 \times 10^4 \text{ m}^2$  is required for a heat transfer rate of 1000 MW(t).

The size of the refluxing boiler is based on steam velocity at the salt surface and the residence time of the salt. The required salt rate, assuming 75-percent solidification per cycle, is  $4 \text{ m}^3/\text{s}$  for 1000 MW(t) heat rate. The steam rate, calculated using steam properties, is  $12.5 \text{ m}^3/\text{s}$ . For 0.07 m/s (1/4 ft/s) steam velocity, the salt surface area required is  $20 \text{ m}^2$ . For a horizontal cylindrical tank,

$$A = L \times D \times N$$

$$V = \frac{N}{2} \frac{\pi D^2}{2} \frac{D}{2} + \frac{L}{2}$$

$$W = \pi D (L + D) \frac{t}{12} + \rho \times N$$

where

A = surface area

L = length of tank

D = diameter of tank

N = number of tanks

V = volume of salt in tank (1/2 filled)

W = weight of steel per tank

t = tank thickness =  $PD/2S$

$\rho$  = density of steel

Eight cylindrical tanks, 2.3 meters in diameter by 9 meters long give the required area with the salt residence time of 38 seconds per cycle. Twice the number of tanks are required if one set is filling while the other set is discharging. The total weight of steel required for the 16 tanks was estimated at about  $0.7 \times 10^6 \text{ kg}$ .

Self-Pressurizing System--Figure 3-11 is a schematic of a self-pressurizing reflux boiler heat transfer system. Liquid salt is allowed to flow into the reflux boiler because of head differences. After closing the supply valve, water injected into the molten salt flashes to steam quickly. This raises the system above the condensing pressure and opens the steam valve. Condensate from the shell and tube exchanger is continuously pumped through the salt until 60 to 75 percent of the latent heat is removed. At completion of the discharge, the steam valve and condensate return valve are closed to isolate the reflux boiler from the condenser. The pressure balancing valve is opened to relieve excess pressure, and the vented steam is used for feedwater heating at other points in the plant. When the pressure is sufficiently reduced, the salt return valve can be opened, and the remaining pressure can be used to push the slurry back to storage for settling and further separation. Recharging the reflux boiler with salt is then started by closing the return valve, venting the remaining pressure, and opening the salt supply valve.

All valves in the steam- and salt-handling system are pressure-compensated, large-bore pintle valves to minimize the external forces necessary for actuation and to facilitate short cycle times. Several reflux boilers may be coupled in parallel to one or more condensers to provide a continuous flow of steam to the condensers. In the design of the reflux boiler, it is advantageous to have a large salt surface area to minimize steam velocities leaving the surface and to reduce carryover. It is also necessary to minimize the ullage space to reduce the amount of steam blown down at the end of each discharge cycle. With the free ullage volume equal to 20 percent of the salt volume, assuming 60 percent salt solidification, more than 8 percent of the extracted energy would be blown down at the end of every cycle. With the free ullage space equal to 8 percent of the salt volume, less than 3 percent of the latent heat

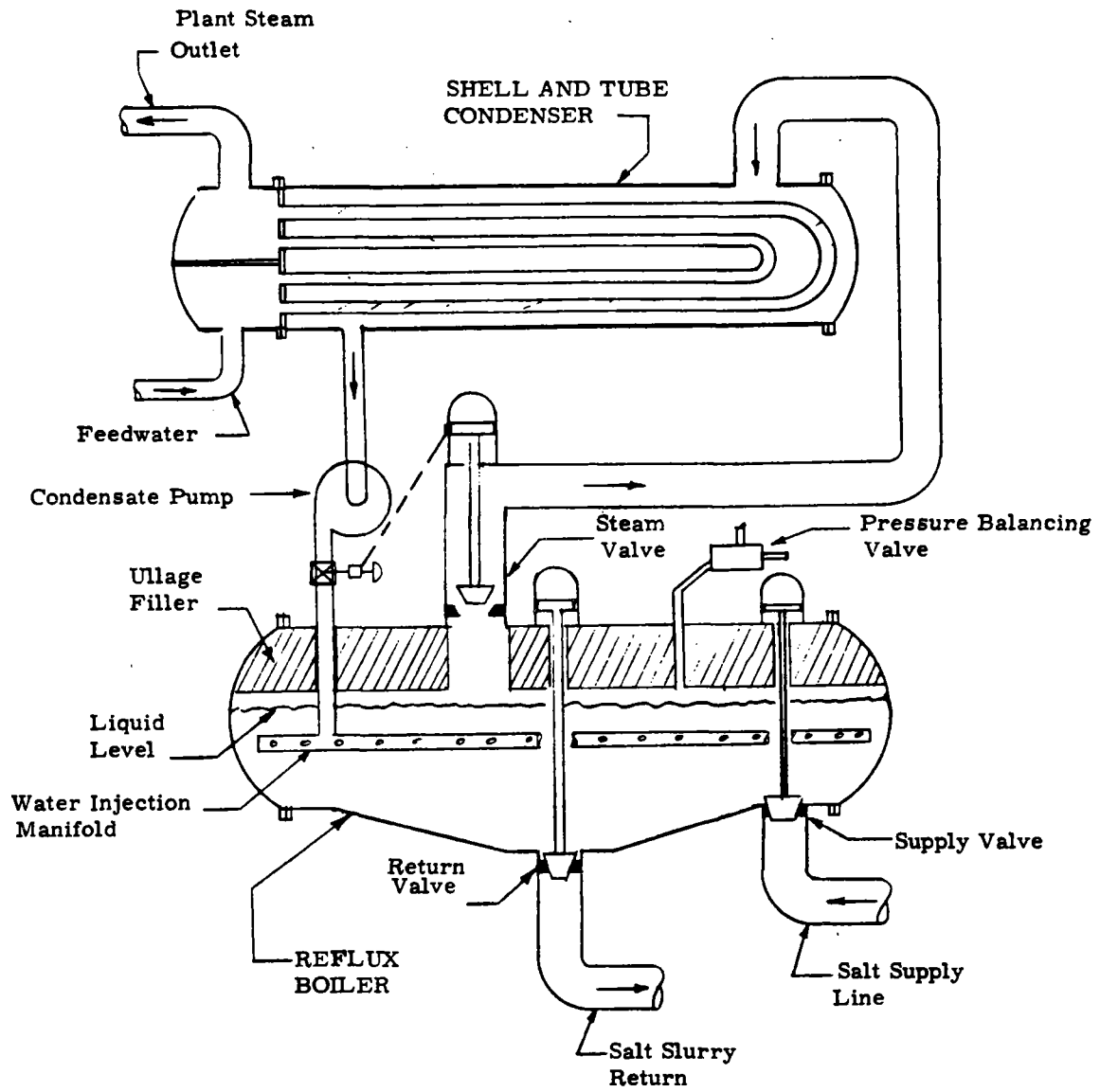


Figure 3-11. Self-Pressurizing Reflux Boiler

would be blown down. These low ratios would improve if the system temperature was lowered from the assumed 303°C saturation conditions.

Continuous Salt Flow Reflux Boiler--The reflux boiler can be used more effectively by operating on a continuous basis if a high-pressure source of salt is available. This has the advantages of reducing the number of reflux boilers required, reducing the high-pressure steam and salt valving requirements, and eliminating the flow surges in the salt supply and return lines. Figure 3-12 illustrates a system where the salt is pumped up to the working pressure, the latent heat is extracted, and the salt slurry is throttled back down to ambient pressure through an orifice and control valve. Assuming that a saturation temperature of 303°C must be reached, that 60 percent of the salt is solidified, and that the combined pump plus motor efficiency is 60 percent, then approximately 7.5 percent of the thermal output must be put back into the system as electric power to drive the pump. If the power plant efficiency is assumed to be 30 percent, the net decrease in electric power output is 25 percent. One characteristic of steam is that the pressure increases very rapidly with increasing temperature. For the pumped salt system, the pump work increases linearly with system pressure, but electric power generation efficiency increases with temperature. Therefore, this system would work more efficiently at lower pressures and temperatures and would become less inefficient at temperatures about 300°C.

To decrease the amount of pump work required to operate the continuous salt flow reflux boiler, a turbine may be used to recover the hydraulic head in the discharge slurry stream. The turbine is a pump run in reverse that can be directly coupled to the high-pressure pump. A system of this type is shown in Figure 3-13. Using the same pressures and slurry densities as in the previous systems and assuming an expander/turbine efficiency of 80 percent, the pumping power requirements can be cut to 4.1 percent of thermal output. Assuming an electric generation efficiency of 30 percent, the electric power required to drive the salt pumps is 14 percent of the total electric output.

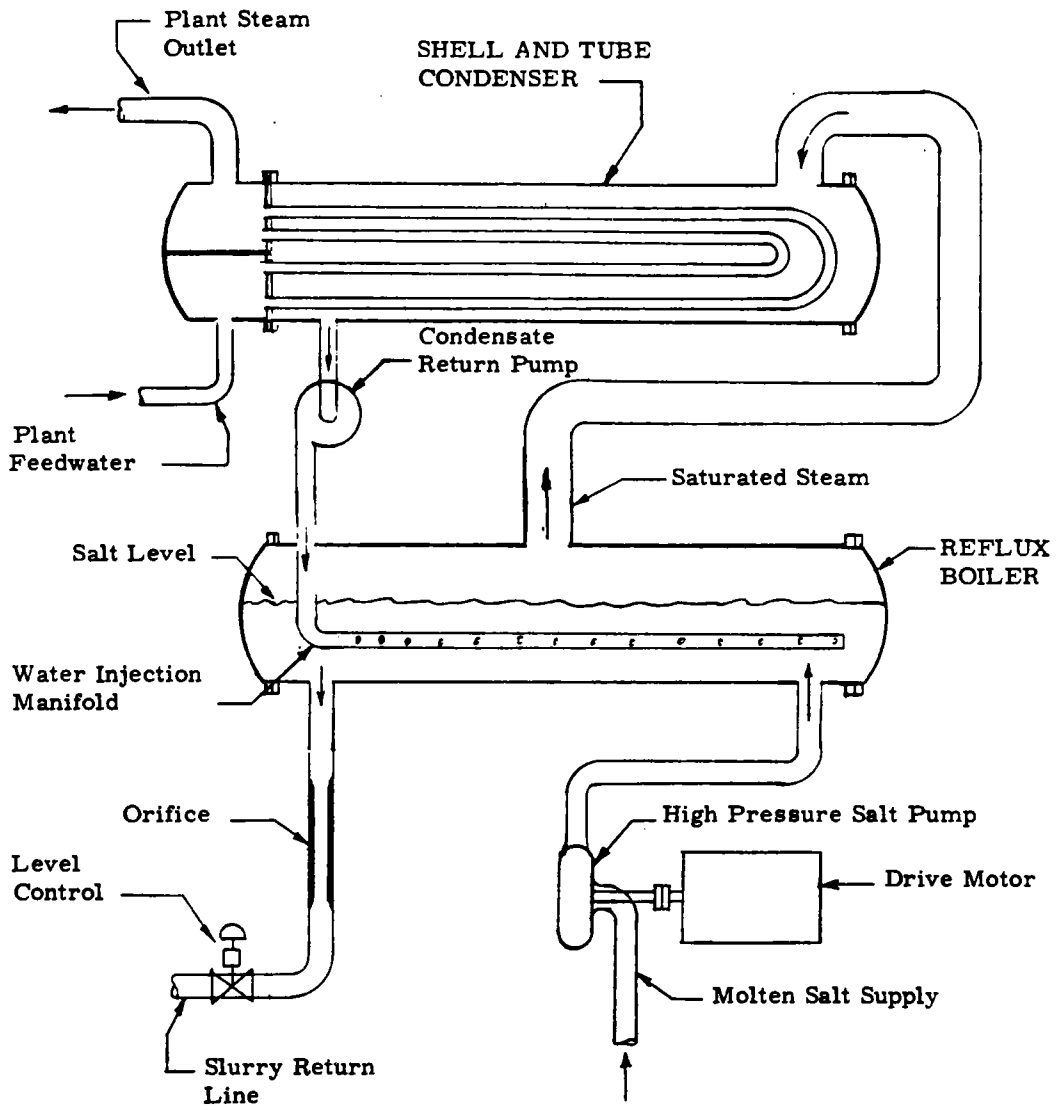


Figure 3-12. Continuous Salt Flow Reflux Boiler



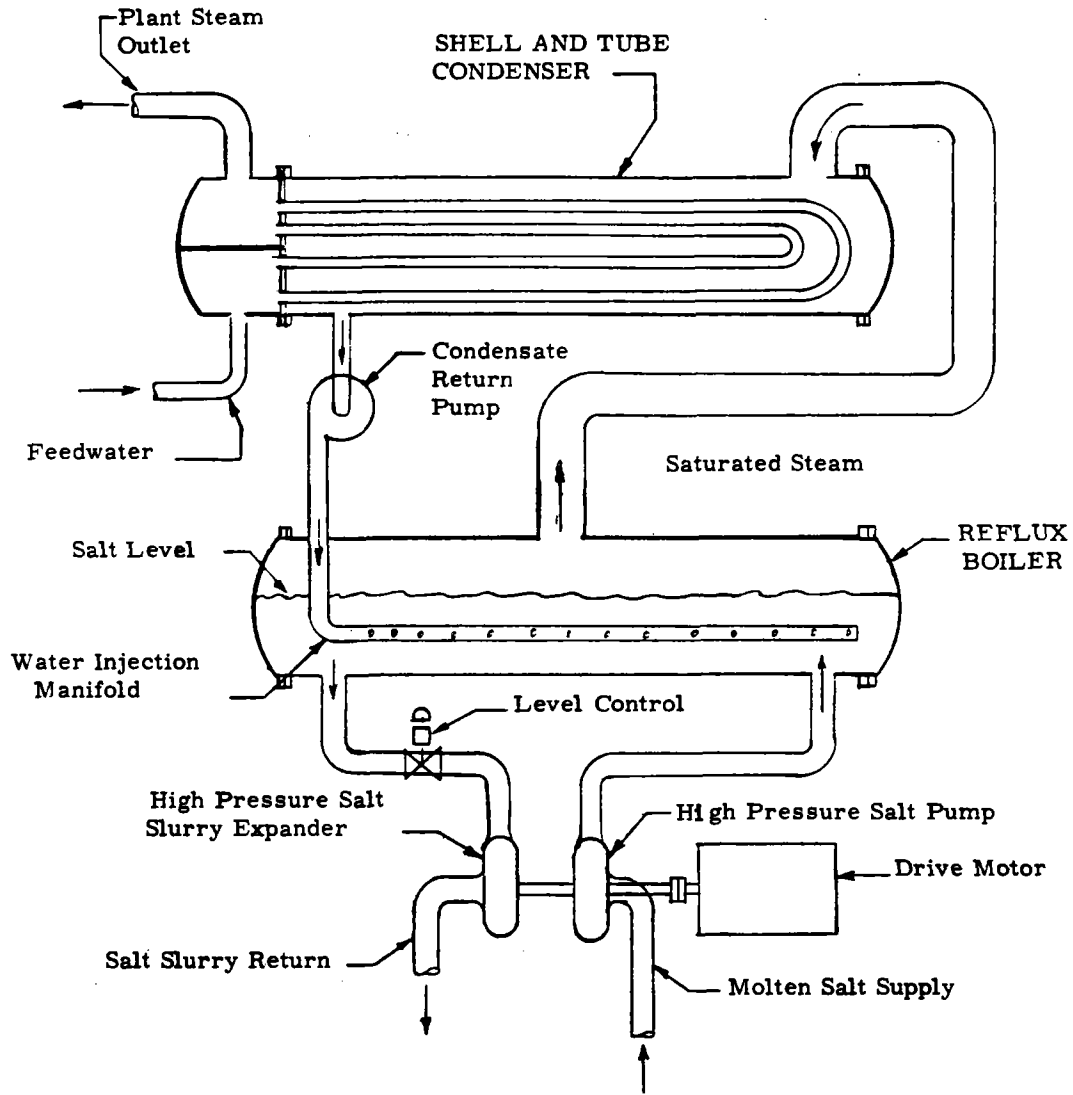


Figure 3-13. Continuous Salt Flow Reflux Boiler with Hydraulic Head Recovery

Reflux Boiler, Open Cycle--A basic assumption previously made was that steam passed through the turbine must be treated to the exacting standards of power plant feedwater; this need not always be true. Because heat from storage will generally be needed during peak plant hours (when all turbines may be operating at capacity), separate turbines may be necessary to handle the discharge steam from the storage system. If a larger thermal storage system has a turbine dedicated solely to it, the water-treatment standards may not be as exacting as that required for conventional boiler operation. Salt carryover might be sufficiently minimized by good steam separators and by acceptably clean and noncorrosive water obtained directly from the reflux boilers. This would eliminate approximately one-third of the high-pressure shells required and all of the condensing tube surfaces plus their associated temperature and pressure losses. Assuming the temperature could be increased by approximately 15°C by going to the open-cycle reflux boiler, the saturation pressure could be increased from 6.55 to 8.27 MPa (950 to 1200 psia) with an accompanying increase in thermal plant efficiency of approximately 3 percent.

The reduced cost of the heat exchanger and the slight improvement in cycle efficiency appear to make this system the most economical to build and operate.

Tumbling Solids--The effect of tumbling abrasive solids is considered an alternative to processes involving complex mechanical parts. Abrasive, inert solids can tumble through a high-velocity or turbulent flow and impinge upon the heat transfer walls with enough force to crack off pieces of solidified material.

This system consists of a U-tube heat exchanger tube bundle, around which is placed a drum carrying abrasives to the top of the bundle. As the drum is rotated, the abrasives rain down over the tubes and remove the salt from the tubes by impact and abrasion. The abrasive material probably would be steel shot. Shot size and rate of transport would be proportional to the strength of the salt-to-tube bond and the heat flux. This system would require greater

tube spacing than that of standard shell and tube exchangers to permit free passage of the shot and would have a lower heat transfer coefficient due to salt buildup on the lower surfaces of tubes where the shot would not be effective in removing the deposits.

Higher exchanger costs, lower heat transfer rates, and possible rapid erosion of the exchanger tubes makes this type of system less attractive than the shell and tube flowby or jet impingement systems.

Passive System (Reference System)--The modeled passive system assumed that enough 3/4-inch outside diameter tubes would be placed into a storage tank to provide 1000 MW(t) of energy for 6 hours, at the end of which time 100 percent of the salt would be converted to a solid. Calculations showed that the required tube spacing was on the order of 5.7 cm (2-1/2 inches). This requires a very large investment in tubes and creates a large manifolding and pressure-balancing problem. These costs are compensated by the ability of the system to recover 100 percent of the latent heat, thus reducing both tankage and medium requirements. Further savings are accrued by having the same in-tank exchanger perform both charging and discharging functions.

Disadvantages of the passive system include the tremendous manifolding problem from the number of pressure-tight tube-to-tube welds required and from flow balancing. Flow velocities through the tubing would be less than 0.3 m/s, thus creating very low pressure drops. Orifices would be required in most lines to provide both pressure differences and reasonably high velocities in the main steam lines. These problems, plus difficulties with large variations in heat rate, have not been considered in system prices.

### 3.4 SELECTED CONCEPTS

A comparative analysis of the active heat exchange systems indicates that the most economical systems are those that employ the most compact heat transfer surfaces. The compactness of the shell and coated tube heat exchanger and the high heat transfer rate associated with the direct contact reflux boiler concept are the two features that appear to be the most promising for large-scale implementation, i.e., 1000 MW(t) rate and 6-hour capacity.

The coated tube and shell system capitalizes on commercial availability of tube and shell heat exchangers and assumes successful development of a nonstick finish for the exchanger tubes. Studies and discussions with consultants have indicated that there is a good possibility of achieving major reductions in the adhesion strength of solid salts to the cold metal surfaces of the tubes. One technique suggested is polishing the heat transfer surfaces to minimize the mechanical bonding of the salt to the surface. Another technique involves the application of a thin coating of an amorphous material or a material with a crystalline structure different from, yet compatible with, the salt. This might reduce bonding strength of the microscopic scale.

In addition, the possibility of a bright nickel plating on heat exchanger tubes was investigated. The plating process and additives introduced into the plating material can have dramatic effects. Thus, a review of the plating material can have dramatic effects. Thus, a review of the plating and metal finishing literature was made to obtain information on the most effective means of obtaining clean, smooth nickel coatings. The most commonly added agents in nickel baths are those used for production of bright nickel deposits. Such brightening agents smooth surface imperfections on the exchanger tubes. Because imperfections are the points at which solid salt can adhere most readily, the smoothing introduced by brighteners may inhibit adhesion. Any such plating material must, of course, be chemically compatible with the salt media. One crucial consideration is how the salt crystal growth will affect the wear of the surface finish.

The second system selected for further study is the direct contact reflux boiler. Although two heat exchange processes are desired here (salt to water/steam and condensing steam on tubes), the individual thermal resistances are so low that their sum is less than the thermal resistance of most liquid-to-pipe-to-pipe-to-liquid exchange processes. Consequently, a high overall heat transfer coefficient can be continuously maintained. Furthermore, the system can be designed to operate without salt transfer pumps. This is accomplished by gravity filling the refluxing boiler and subsequently expelling the slurry with residual steam pressure.

Improved thermal efficiency through elimination of the heat exchangers can be achieved in a system where the heat transfer medium is the working fluid. The lifetime of this type of system is directly related to the content of salt remaining in the working fluid as it enters the turbine. The salt content can be minimized by good separator design.

### 3.5 SELECTED EXPERIMENTS

The first experimental module would test a series of flowby heat exchange processes where molten salt is pumped over specifically prepared heat exchanger tube surfaces. The purpose of the test was to determine the effects of various surface finishes and coatings, flow velocities, and temperature conditions on solid-salt buildup on heat exchanger tubes. It was intended that a small, easily modified apparatus be built to provide rapid qualitative assessment of these parameters and to provide heat transfer data. Should bulk flow of salt parallel or perpendicular to the tubes prove inadequate, jet impingement of the flow would be a possible alternative.

The second experimental module would test a scale model of the refluxing boiler. A small, high-pressure apparatus would be built to measure the heat transfer rates attainable, the proper point of injection of water into the

salt, and the dynamics of the vapor-salt heat transfer interface with special emphasis in the amount of salt carryover onto the condensing surfaces. Salt carryover would be measured by removing and analyzing small samples of the condensate. Another phenomenon of interest was the formation of solids in the melt as the heat is extracted. How well the solids settle and agglomerate and the ultimate slurry density attainable are important experimentally determined factors. Water carryover with the discharged salt and possible chemical decomposition are other facets of the total system that would be reviewed to determine salt and heat transfer fluid compatibility.

The mechanization of these concepts and the experimental designs are discussed in the following section.

## SECTION 4.0

## CONCEPTS MECHANIZATION AND EXPERIMENTS DESIGN

Two active heat exchange concepts applicable to large-scale, latent heat thermal storage systems were formulated and selected under Task IC of this contract. These two systems are described in sufficient detail to provide an understanding of the concepts and the technical issues that the experimental apparatus was designed to resolve.

The two concepts--the reflux boiler and shell and coated tube flowby--are first discussed from a large-scale systems point of view to establish the design rationale for the experimental configurations. This is followed by a description of experiments.

#### 4.1 REFLUX BOILER CONCEPT MECHANIZATION

##### 4.1.1 System Description

The reflux boiler concept of heat exchange is depicted in Figure 4-1. The molten salt thermal storage medium is pumped at high pressure into the pressure vessel, where water is injected into the salt. The water flashes to steam, which raises the pressure. The steam flows to a shell and tube condenser. Here the steam condenses and transfers its latent heat to boil the water flowing inside boiler tubes. This water can be delivered to a turbine. The condensate is collected and refluxed into the boiler to start the cycle over. Because the condenser and reflux boiler both operate at nearly the same pressure, the condensate pump need only supply enough head to overcome the salt hydrostatic head and the throttling necessary to achieve balanced flows through the injection nozzles.

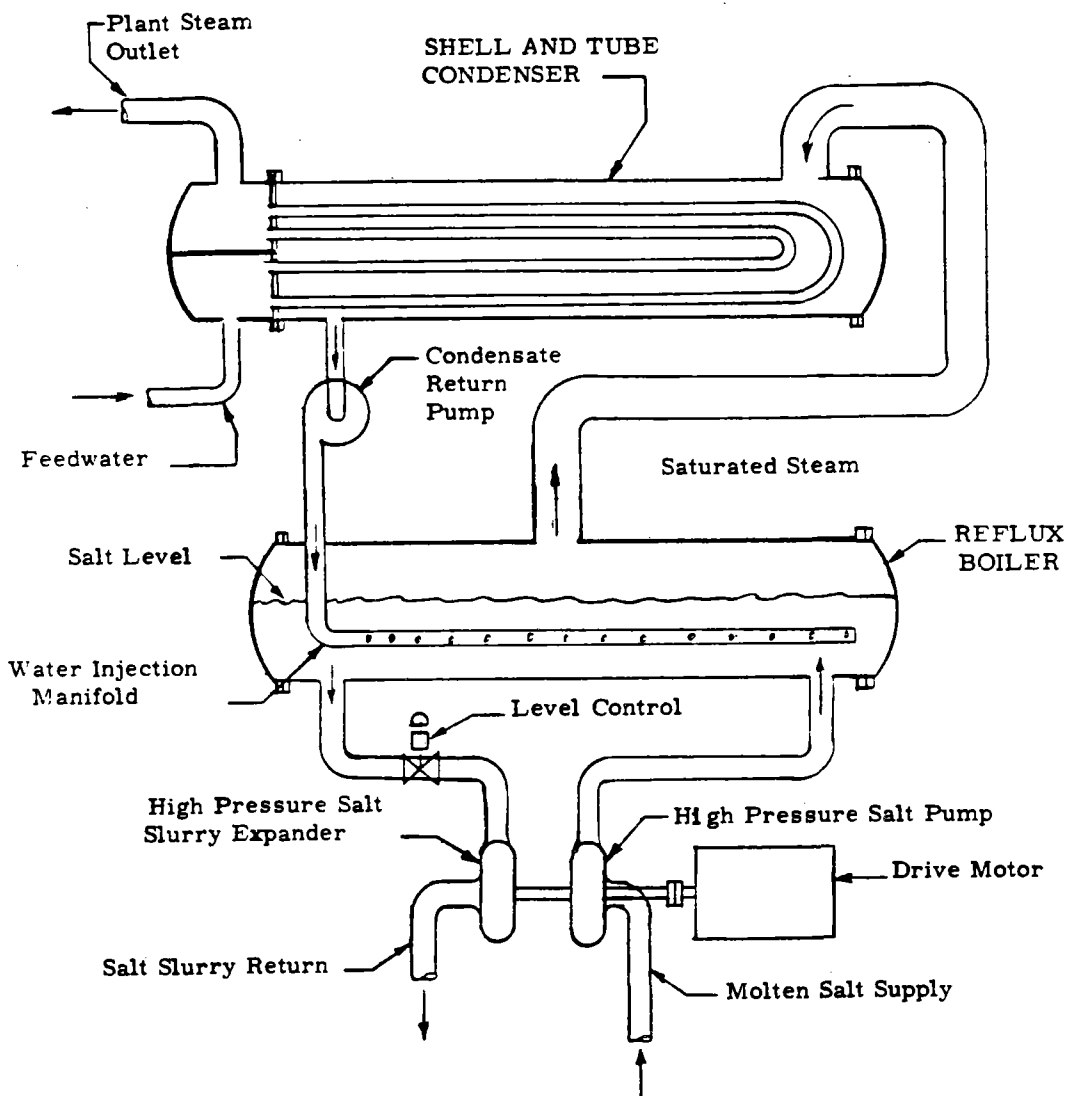


Figure 4-1. Continuous Salt Flow Reflux Boiler with Hydraulic Head Recovery



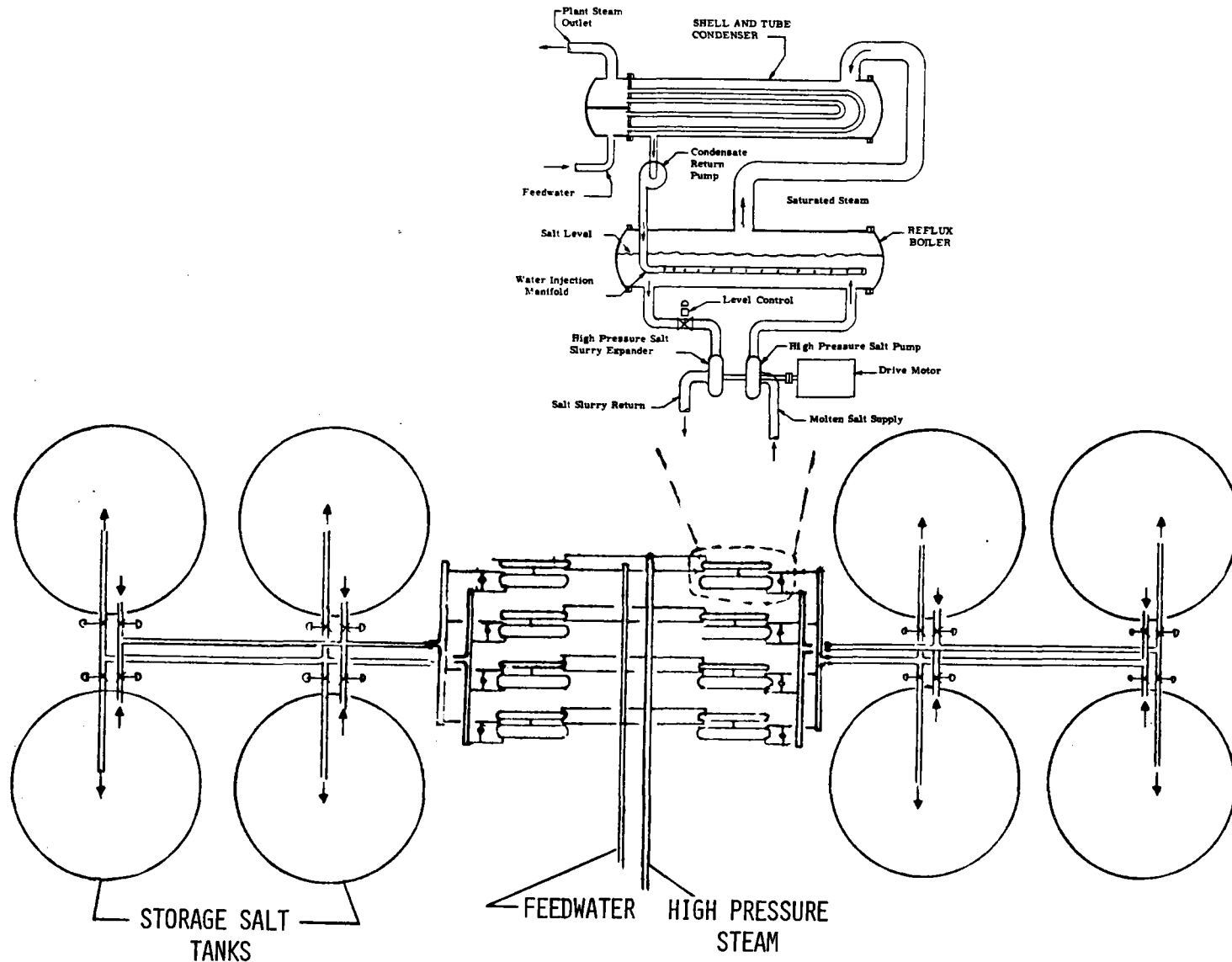
The salt slurry leaving the reflux boiler has a larger potential energy due to the high pressure. A hydraulic expander can be used to recover this energy by directly coupling the expander to the pump. For incompressible fluids, a well designed pump can be run in reverse to recover head. Salt level control in the reflux boiler will be maintained by modulating the slurry discharge stream.

A commercial size thermal storage system is shown schematically in Figure 4-2. This system was sized to deliver 1000 MW(t) for 6 hours using eight refluxing boilers and eight condenser units. Molten salt is pumped from the top of the storage tank through the reflux boilers, and the salt slurry is directed back into the bottom of the storage tanks. Settling, with increased separation of the liquid and solid phases, will occur in the storage tanks to increase the percentage of latent heat recoverable.

#### 4.1.2 Methods of Fabrication

The reflux boilers and condensers are envisioned as having conventional high-pressure tube and shell construction as used in the heat exchanger industry. Both the reflux boiler shells and the heat exchanger shells will see the same pressures and temperatures. The heat transfer capabilities of the boilers and condensers indicate that a good proportioning of demensions is that one reflux boiler supply steam to one condenser unit, all units being the same size. This will provide a price break by using greater numbers of identical components.

Condenser construction is standard shell with U-tubes construction with minor changes. The tube walls must be thicker than normal to withstand high external pressure should the plant steam pressure be low. The tube spacing may have to be increased slightly to provide adequate steam flow over the condensing surface to minimize the pressure and temperature drop.



4-4

Figure 4-2. Continuous Salt Flow Reflux Boiler with Hydraulic Head Recovery

Pump technology exhibited today in the high-pressure feedwater pumps in both conventional and nuclear power plants can be applied to high-pressure molten salt pumps. The abrasiveness of salt slurry is not known at this time, but pumps have been built that have hardened casings and impellers capable of providing long service in very abrasive environments.

#### 4.1.3 Scalability

The system may be scaled upwards by increasing the number of units or by increasing the size of units. Increasing the size of individual units will pose shipping problems due to size and weight limitations of the shell and tube exchangers currently sized at 2.1 meters in diameter by 12.2 meters in length (7 feet diameter by 40 feet in length). An on-site assembly of some type of modular construction such as prestressed, cast iron pressure vessels may shift the optimum size of individual units upwards.

Scaling the system size downward poses no problems until sizes are reached at which efficient high-pressure pumps are no longer practical. Staging of two or more pumps in series may extend the range of practical operation down to less than 10 MW(t). Design of systems below 1 MW(t) may require special, high-head, low-capacity salt pumps.

#### 4.1.4 Technical Issues

There are several technical issues that must be explored before a pilot plant with a full-scale system could be properly designed and operated. A listing of the major issues that the test program should resolve is provided in Table 4-1. These items will be discussed further in conjunction with the test results.

Table 4-1. Reflux Boiler Technical Issues

- What is the degree of compatibility of water and its vapor with a dilute eutectic mixture?
- What is the solubility of water in the salt and what is its influence on system operation?
- Is the salt or any particulate matter contained therein carried over to the condensing surface with the steam?
- If solids are carried over with the steam, do they form deposits that degrade performance?
- What are the steady-state processes at the water/steam and water/salt interface and how are they influenced by geometry, considering:
  - Water injection rate and location?
  - Direct contact heat transfer rates?
  - Liquid-vapor and melt-solid mass transport?
- What are the control issues involved during:
  - Operations?
  - Start-up?
  - Shutdown?
  - Load changes?
  - Non-operating?
- What are the transport dynamics of the salt slurry discharged from the reflux boiler and how are the dynamics influenced by geometry and slurry density?

## 4.2 REFLUX BOILER EXPERIMENT

### 4.2.1 Modeling

The experimental apparatus used to model the reflux boiler system for a 10-kWh(t) capacity and 10-kW(t) rate must resolve the technical issues yet circumvent the development of expensive, specialized equipment. This can be done by operating the model in a batch mode and using compressed gas to transfer the molten salt into the system. This eliminates the need for a high-pressure salt pump. In addition, the low-head, high-temperature pump necessary for feedwater refluxing is replaced by a low-temperature, high-pressure pump and water preheater.

### 4.2.2 Experimental Mechanization

The experimental apparatus, shown in the schematic of Figure 4-3, consists of a reflux boiler nearly filled with molten salt into which hot water is injected under high pressure. The molten salt gives up heat to boil the water. The steam bubbles to the surface of the salt and passes to the condenser, where it condenses on the cool condenser coils heating the secondary heat transfer fluid. For the experiment, the secondary fluid was a heat transfer oil, Mobiltherm 603. It provided close temperature control and high heat transfer rates without using a high-pressure recirculating water loop.

The water-steam cycle was operated open loop to provide an accurate means of measuring and controlling the water injection rate. This is achieved by measuring the rate of water uptake at the pump suction port. The condensate receiver provided a means of collecting and storing a nominal 15-minute flow of water, which can later be cooled and analyzed for salt content to estimate salt carryover. Further analysis of salt carryover can be made by disassembly of the shell and tube condenser at the end of a test run.

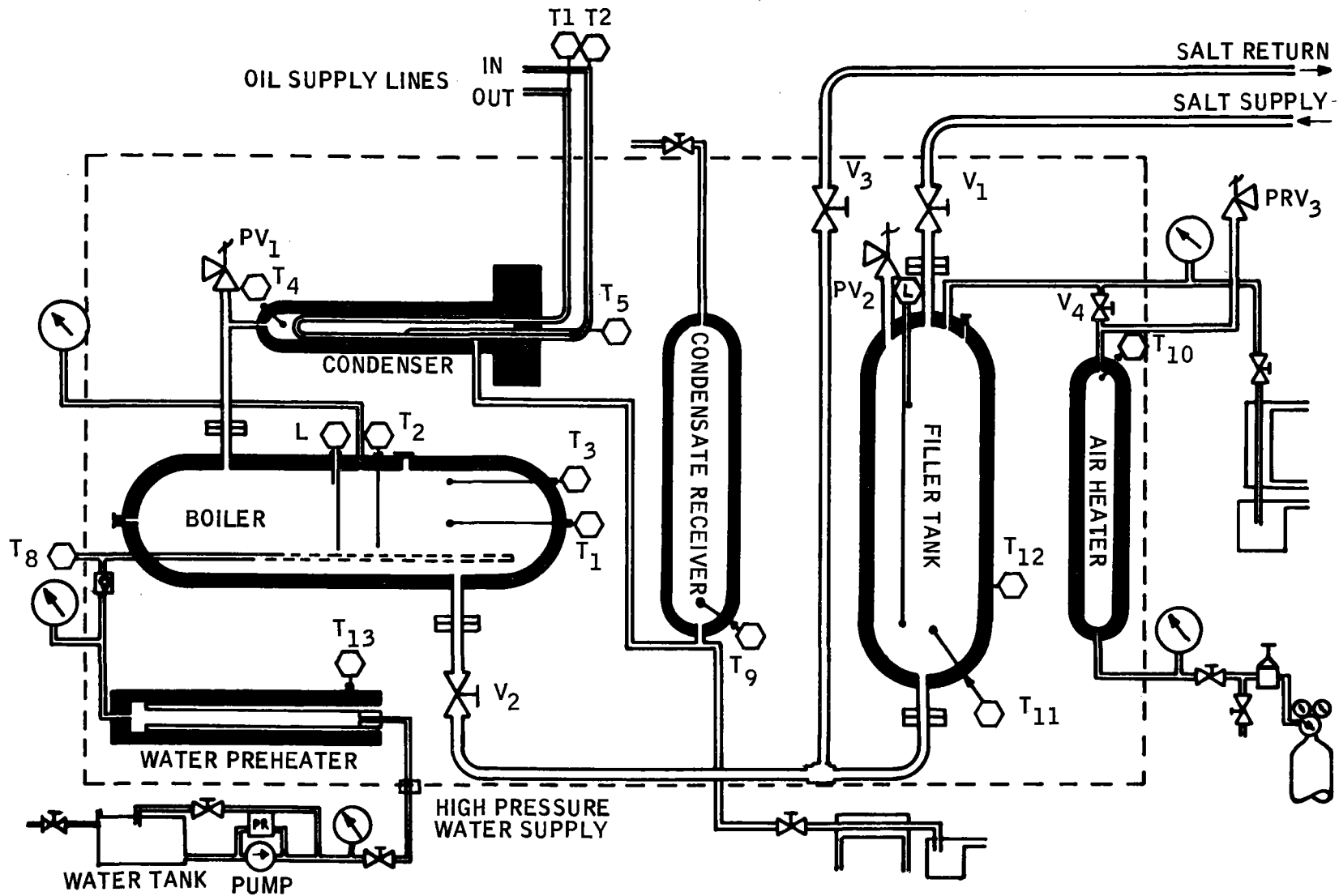


Figure 4-3. Reflux Boiler Functional Schematic

The filler tank provided a means of injecting and removing salt slurry from the reflux boiler while maintaining a high pressure within the reflux boiler. To charge the system, valves V2 and V3 are closed and valve V5 is opened to vent the filler tank to atmospheric pressure. Valve V1 is opened, and the charging tank is filled with molten salt to the desired level. After filling, valves V1 and V5 are closed, and high-pressure gas is used to increase the pressure in the filler tank to that of the reflux boiler. Valve V2 is then opened, allowing the salt to flow into the reflux boiler as the air pressure in the filler tank is increased. Conductivity sensors in the filler tank and the reflux boiler were used to indicate salt level.

A discharge cycle is initiated by adjusting the gas pressure in the fill-discharge tank to a pressure slightly lower than the reflux boiler pressure, and then opening valve 2. Air pressure bleed valve V5 is then opened to permit the salt to flow into the discharge tank. Valve V2 is then closed, and the pressure in the discharge tank is reduced to atmospheric pressure. Valve V5 is then closed, valve V3 opened, and valve V4 opened to allow high-pressure air to push the salt slurry back into the storage tank for settling or remelting. At this point the system is ready for recharging.

The advantages of this mechanization from a modeling standpoint are:

- No high-pressure pumping of salt is required.
- No throttling of a high-pressure salt or salt plus water is required.
- No valves in the salt lines must be opened or closed while high-pressure differentials exist across them.

The disadvantages include:

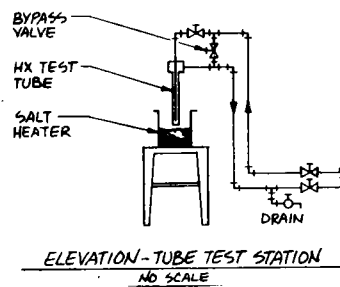
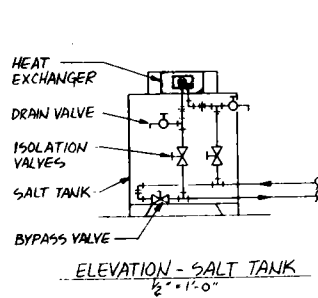
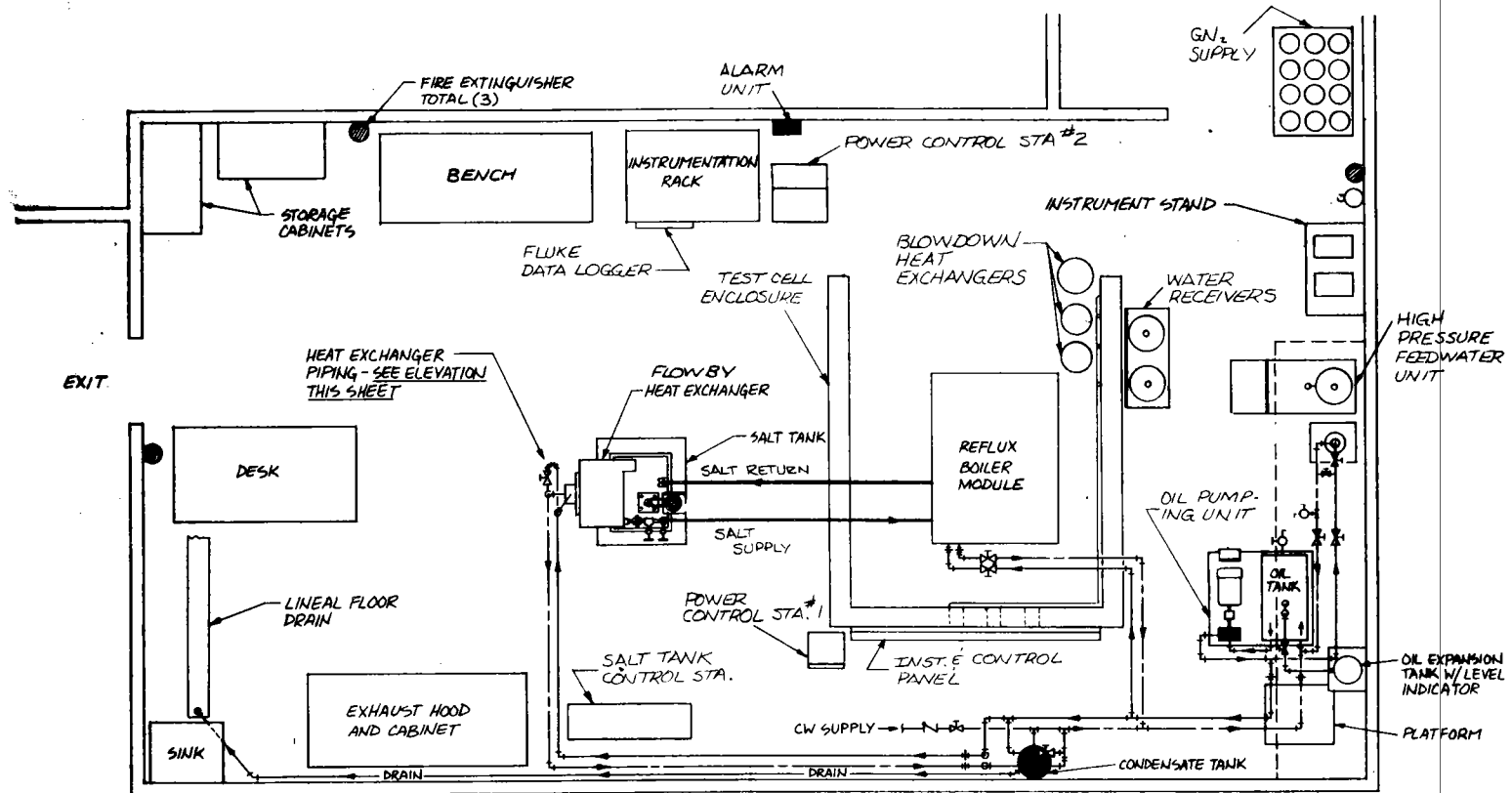
- Time-dependent operation.
- Stratification in the salt tank.

### 4.2.3 Major Components

The major components required for the experiments are depicted on the mechanical and electrical layout drawings shown in Figures 4-4 and 4-5, respectively. The salt storage tank, located in the center of the test facility, supplies molten salt to both the flowby heat exchange module and the reflux boiler module. The oil pumping unit located away from the salt tank supplies a heat transfer fluid to each experimental module. The instrumentation rack contains the common recording, data logging, and display equipment.

4.2.3.1 Reflux Boiler Module--The unit was built in accordance with the drawings contained in Appendix C. Figures 4-6 through 4-9 show the completed reflux boiler module at the manufacturer's facility. Various in-process manufacturing operations are depicted in Figures 4-10 through 4-15. The air preheater shown in Figure 4-13 is filled with taconite pellets. Figures 4-16 and 4-17 show the unit initially installed at the test facility and with the test cell enclosure partly completed. Figure 4-18 shows the test cell and most mechanical work completed. Figure 4-19(a) and (b) show left- and right-side views of the reflux boiler control and instrument panel. Four-foot valve extender rods from the reflux boiler module to the control panel allowed remote manual operation of the five primary flow valves. The salt level indicating system installed on the boiler and a portion of the heating control units are shown in Figure 4-20(a). Figure 4-20(b) shows the valve extender rods and the myriad of instrumentation wires and hydraulic and pneumatic lines. Figure 4-20(c) shows a portion of the electrical checkout under way.



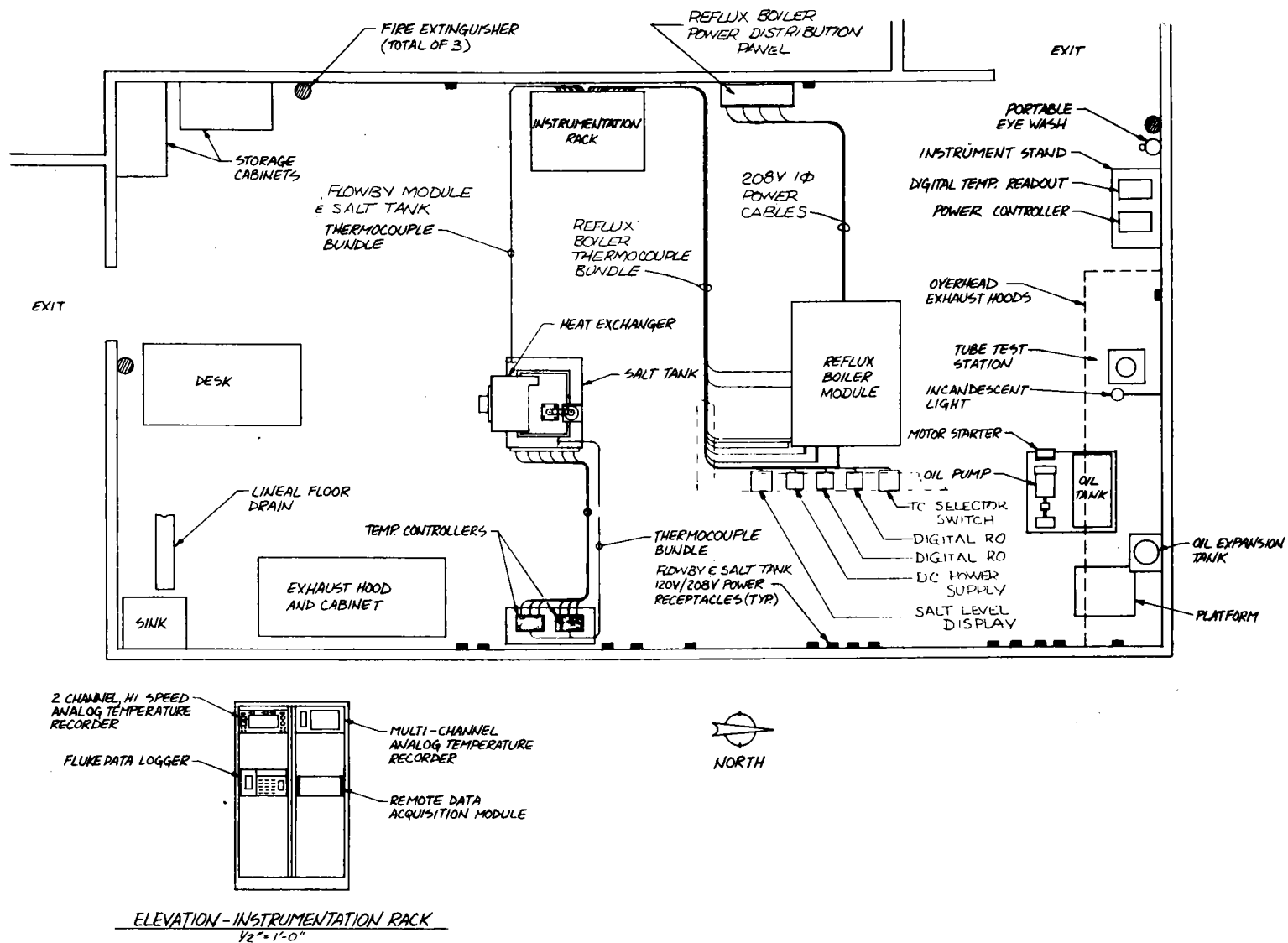


LIST OF SYMBOLS

	GATE VALVE		ELBOW
	DRAIN VALVE		TEE
	UNION		SUPPLY PIPING
	CHECK VALVE		RETURN PIPING



Figure 4-4. Salt Storage Test Facility Mechanical Layout



4-12

Figure 4-5. Salt Storage Test Facility Electrical Layout

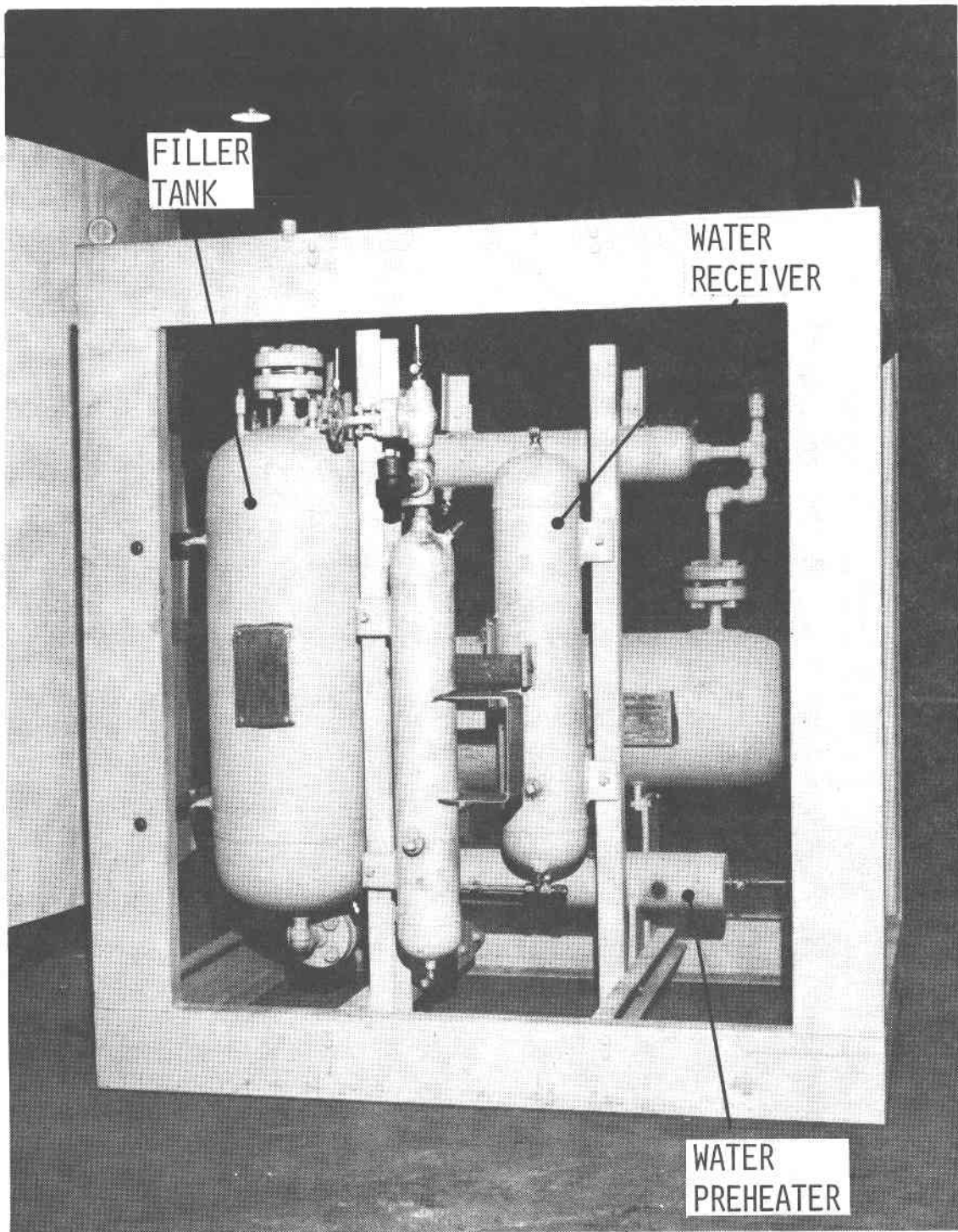


Figure 4-6. Side View of Reflux Boiler Showing Filler Tank Air Heater and Condenser Receiver in Foreground.

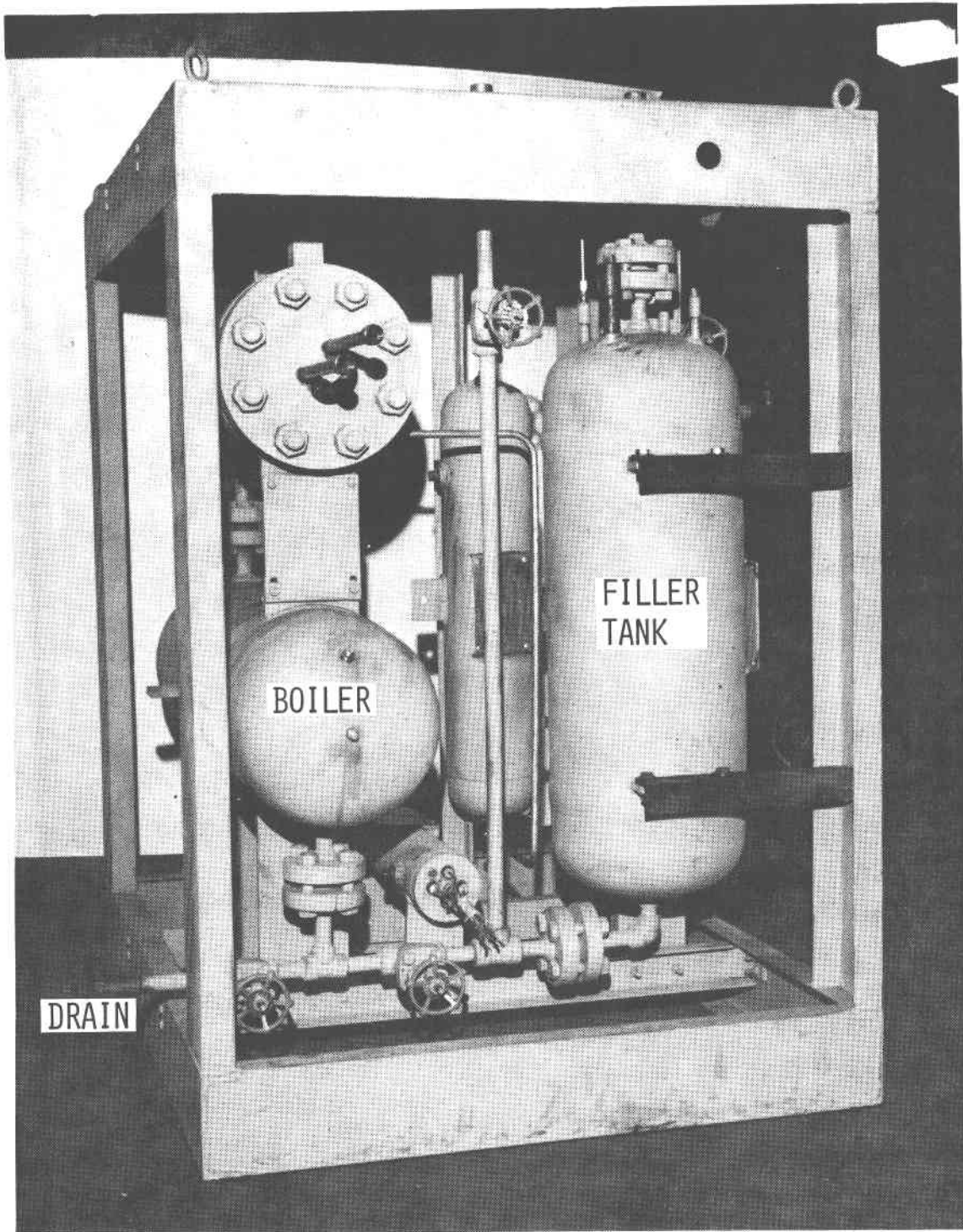


Figure 4-7. Front View of Reflux Boiler Showing Hand Valves with Filler Tank at Left

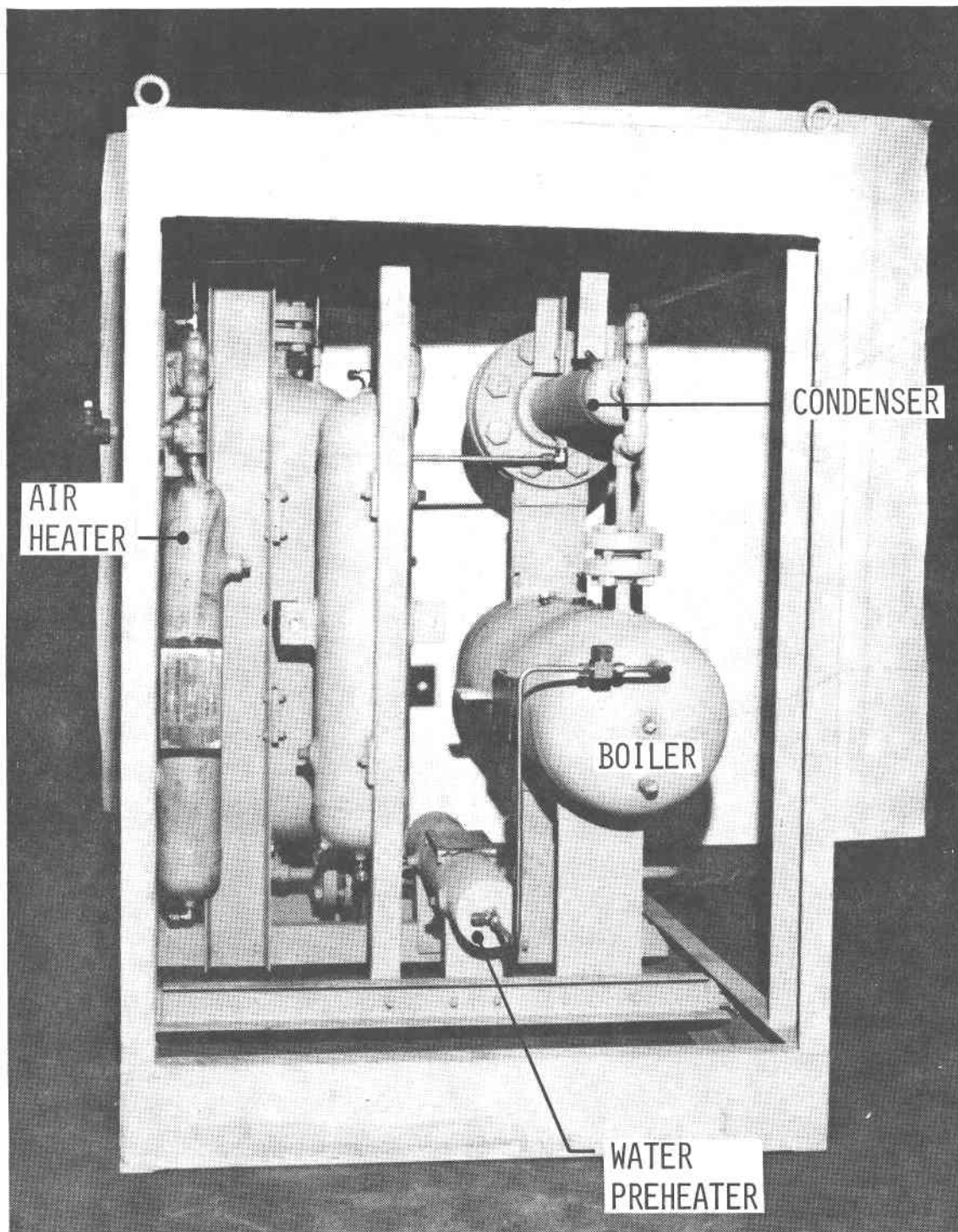


Figure 4-8. Back View of the Reflux Boiler Showing Condenser Above the Boiler Tank on the Right. Water Heater is Lower Center Tank.

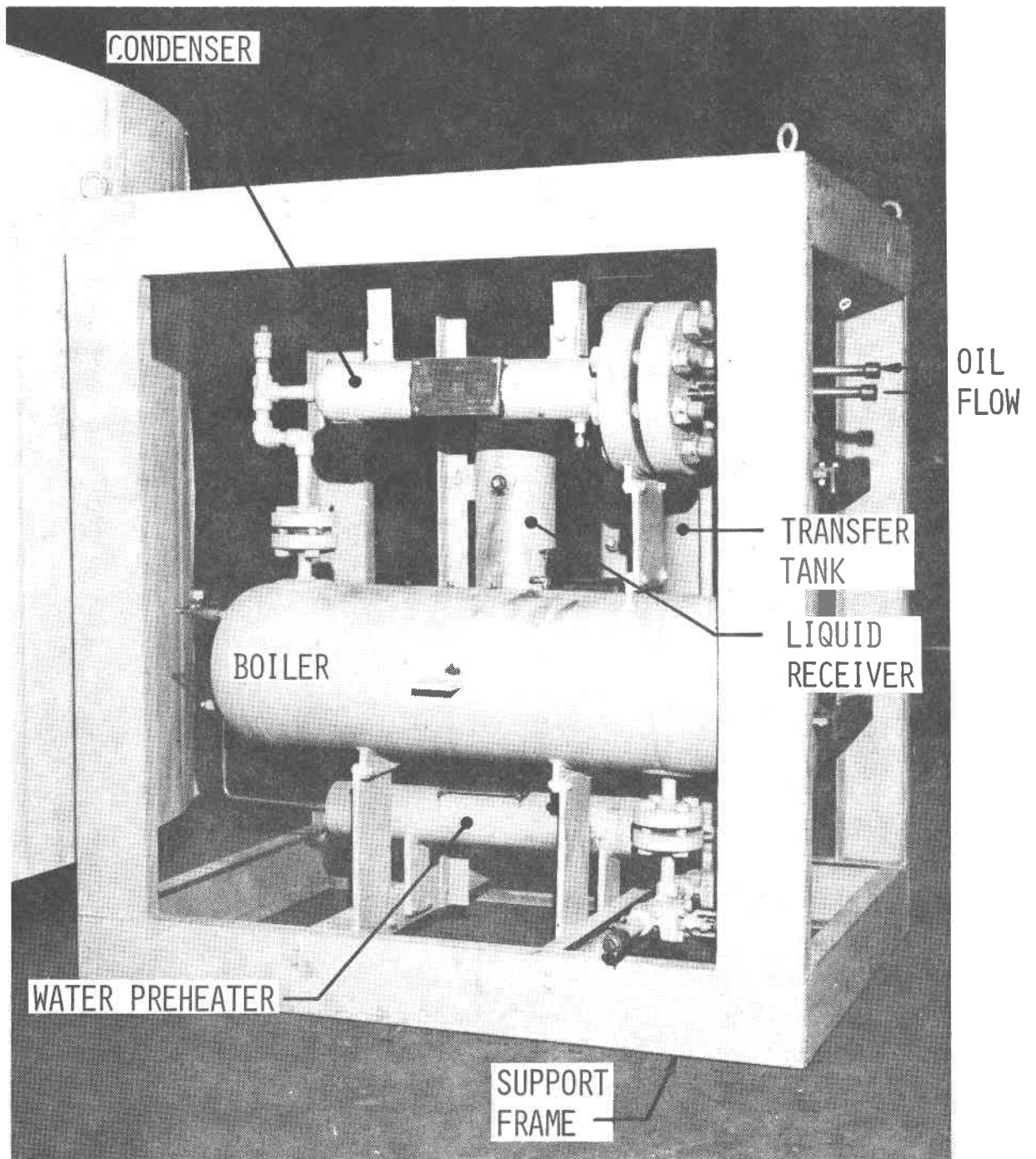


Figure 4-9. Reflux Boiler Module (Guard Heater Panels Removed)

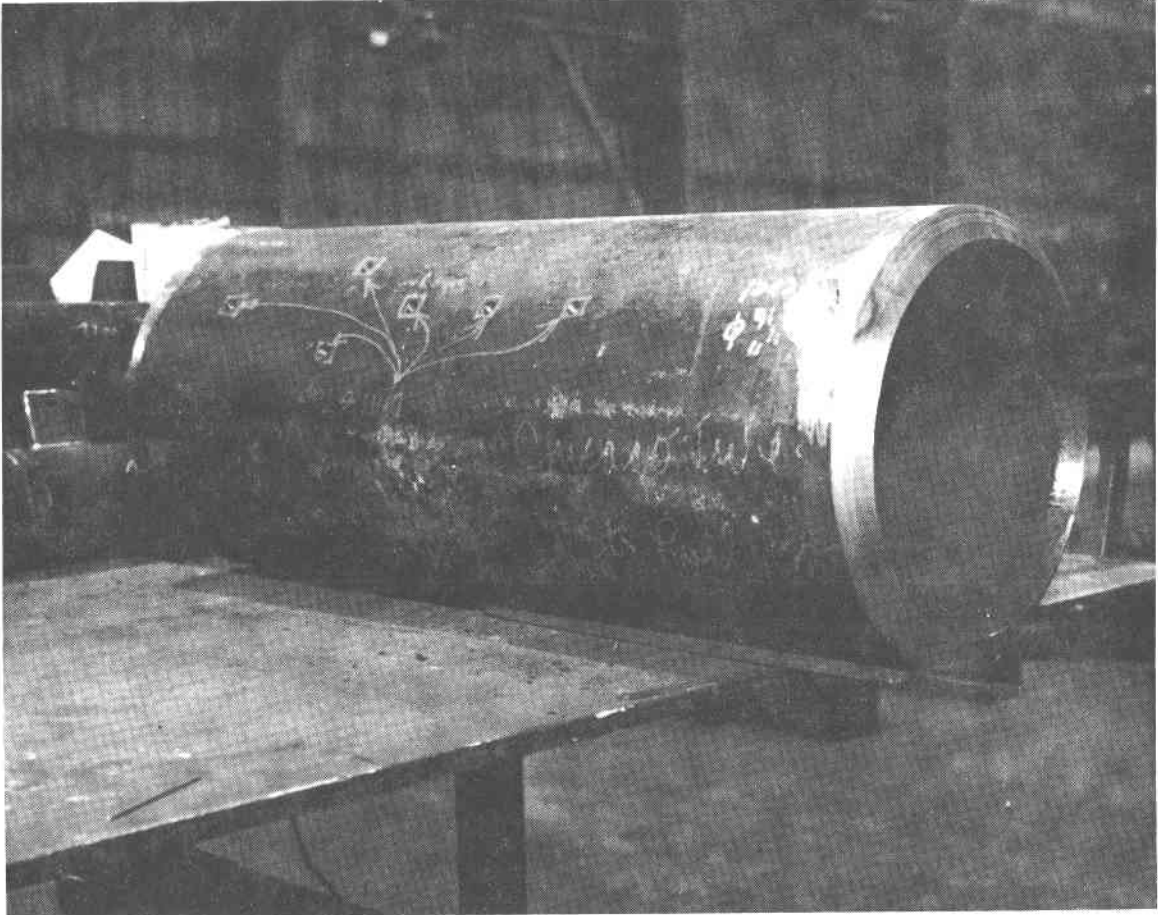


Figure 4-10. Reflux Boiler Shell

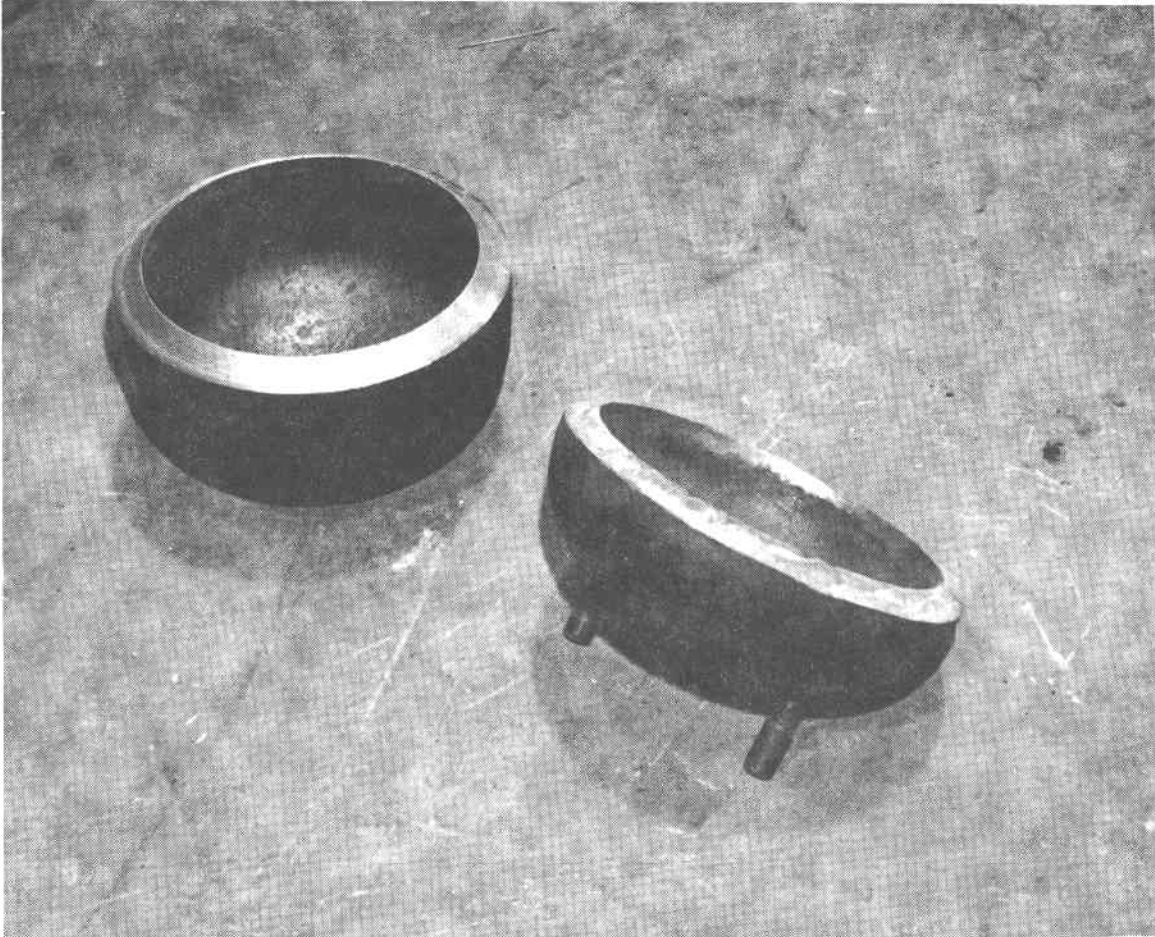


Figure 4-11. Heads for Reflux Boiler



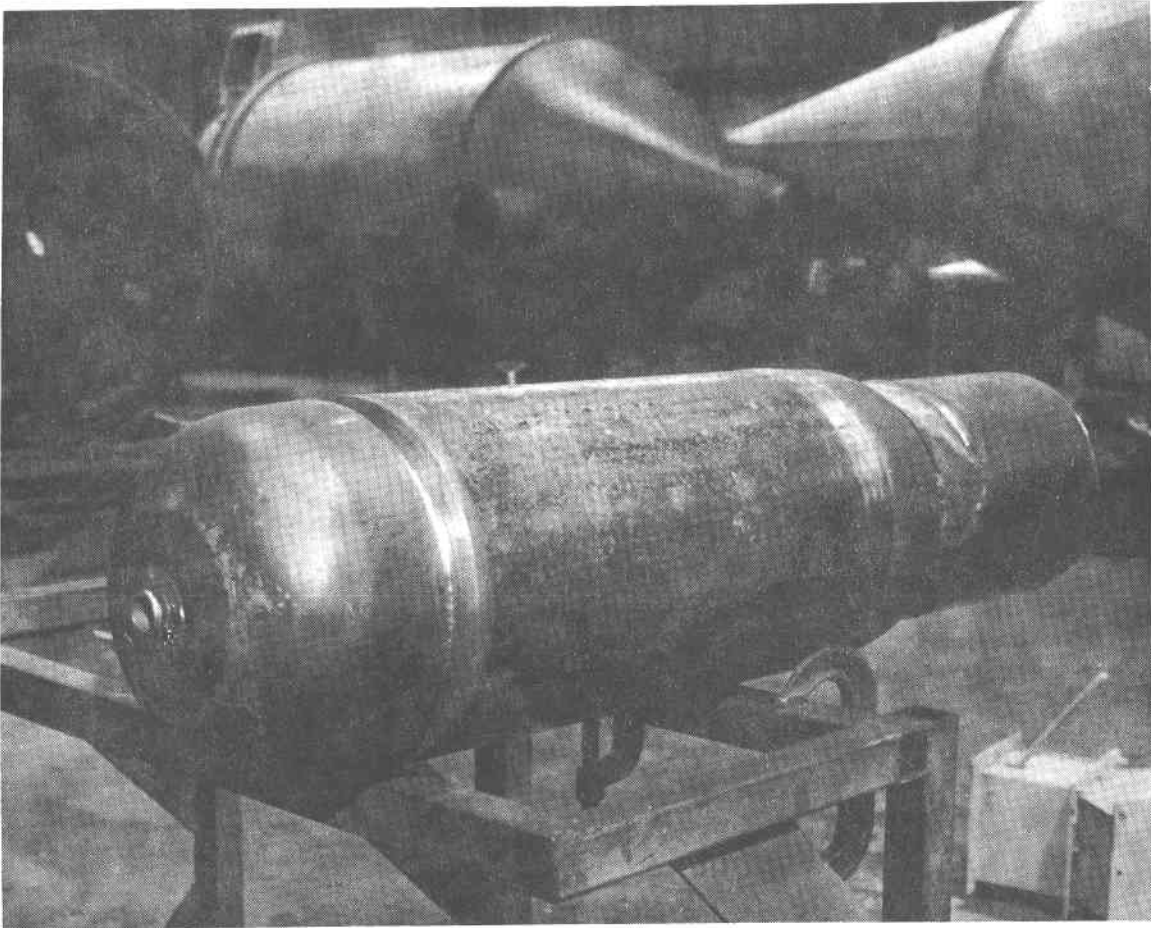
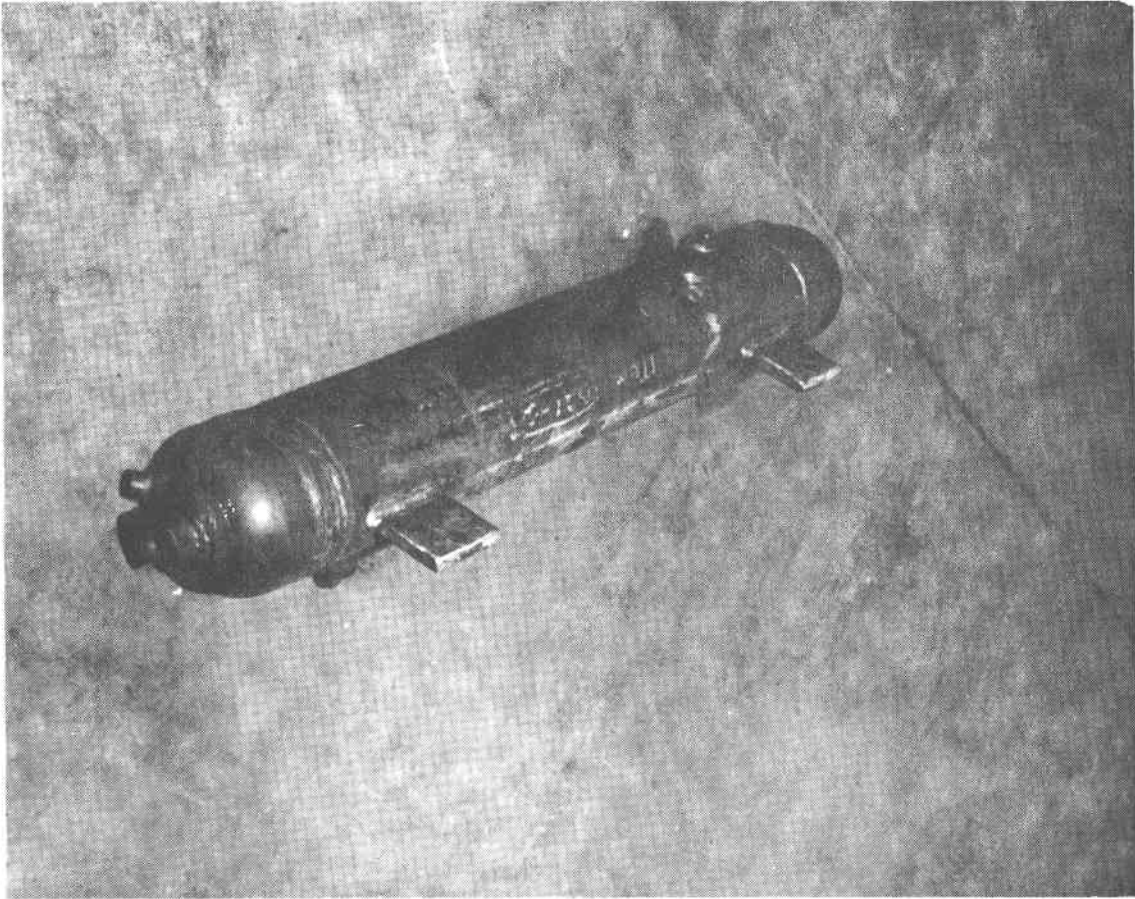
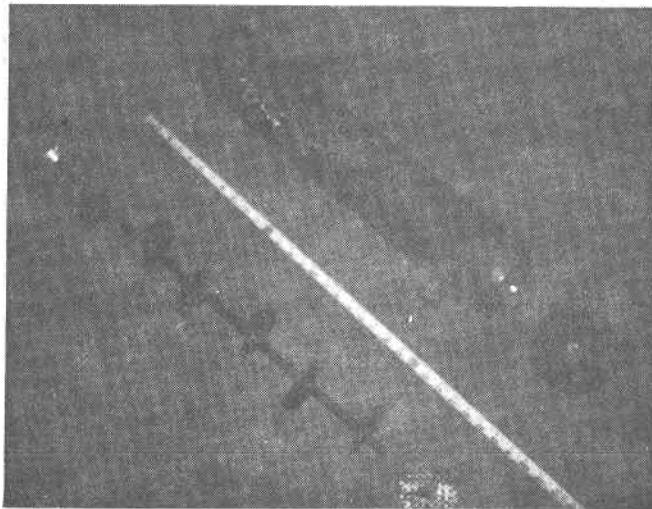


Figure 4-12. Reflux Boiler with Head Being Welded in Place

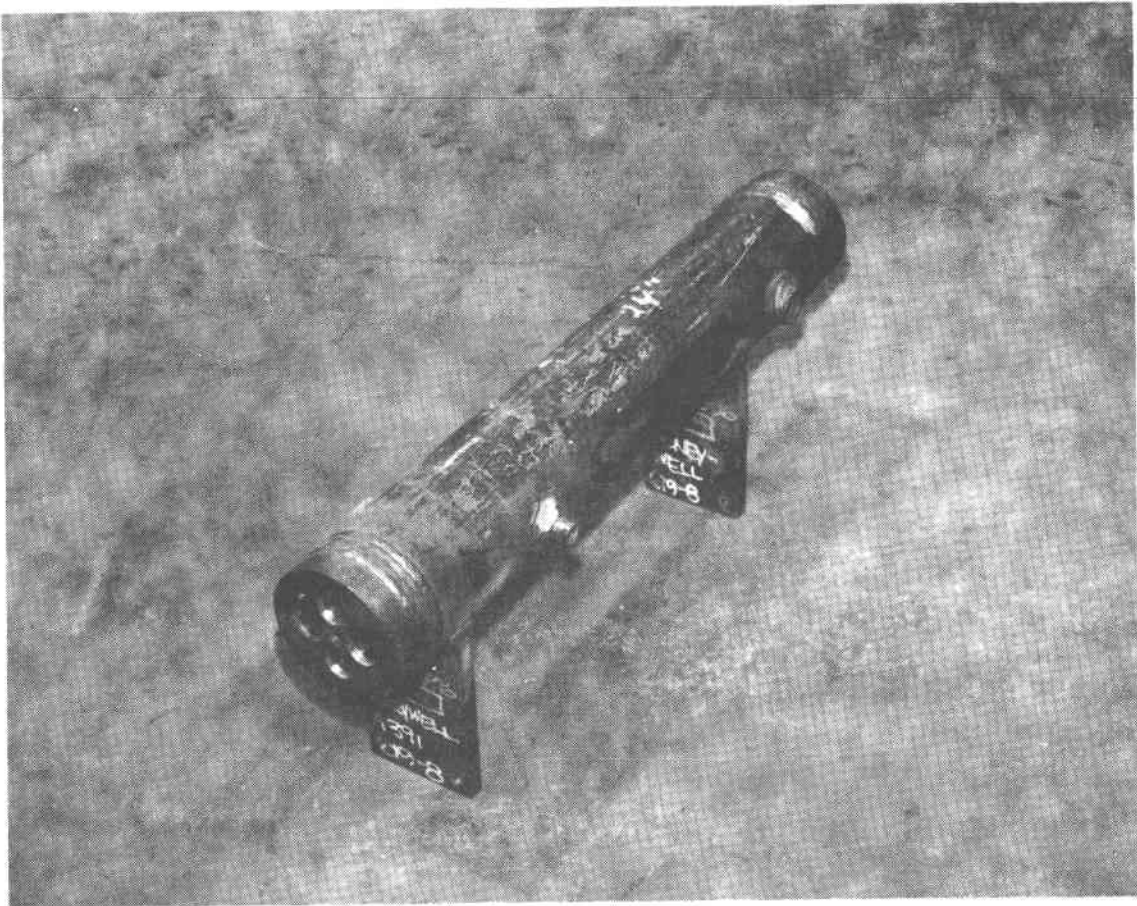


A. Assembled

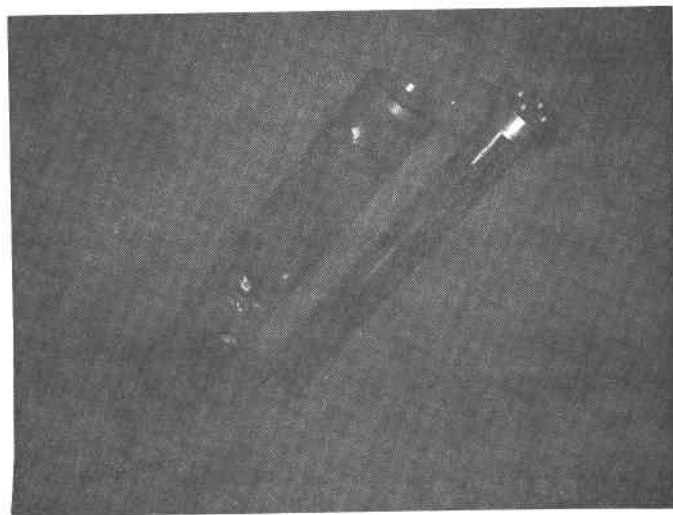


B. Pre-assembly

Figure 4-13. Air Preheater



A. Assembled



B. Pre-assembly

Figure 4-14. Water Preheater

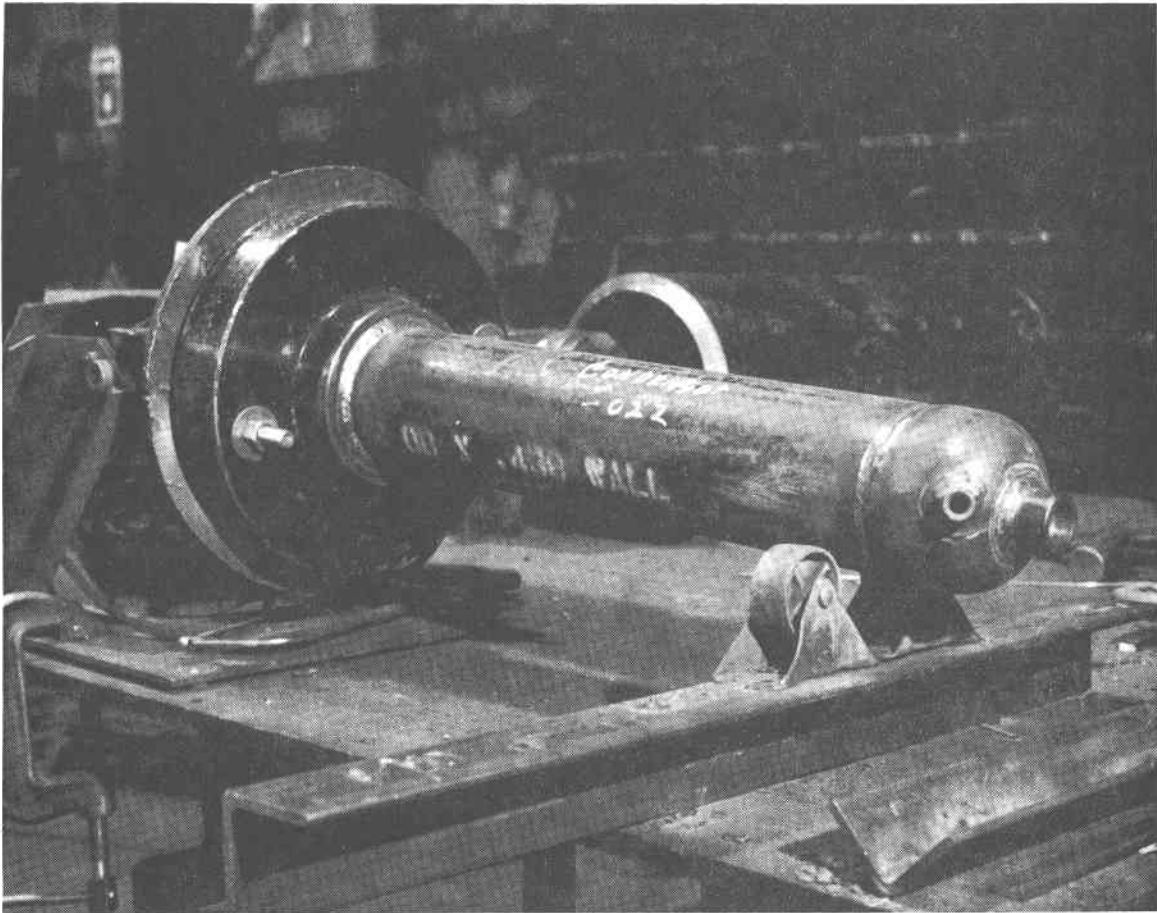


Figure 4-15. Condenser Unit in Welding Fixture

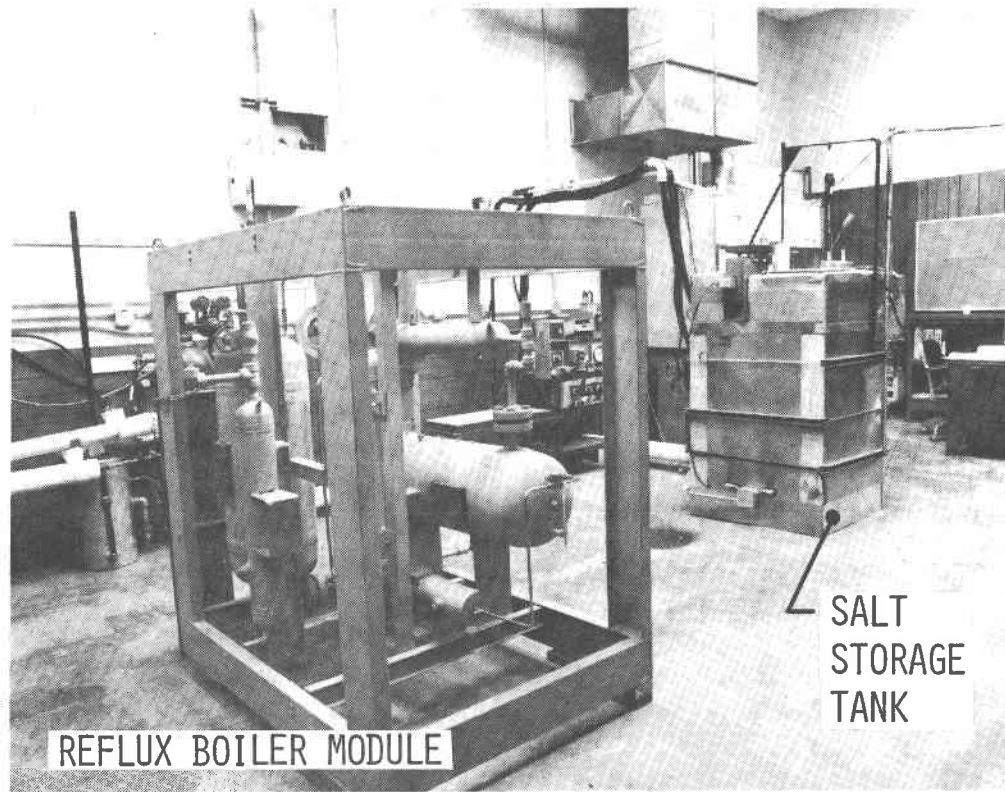


Figure 4-16. Unit Installed at Test Facility With Test Cell Enclosure Partly Completed - Side View

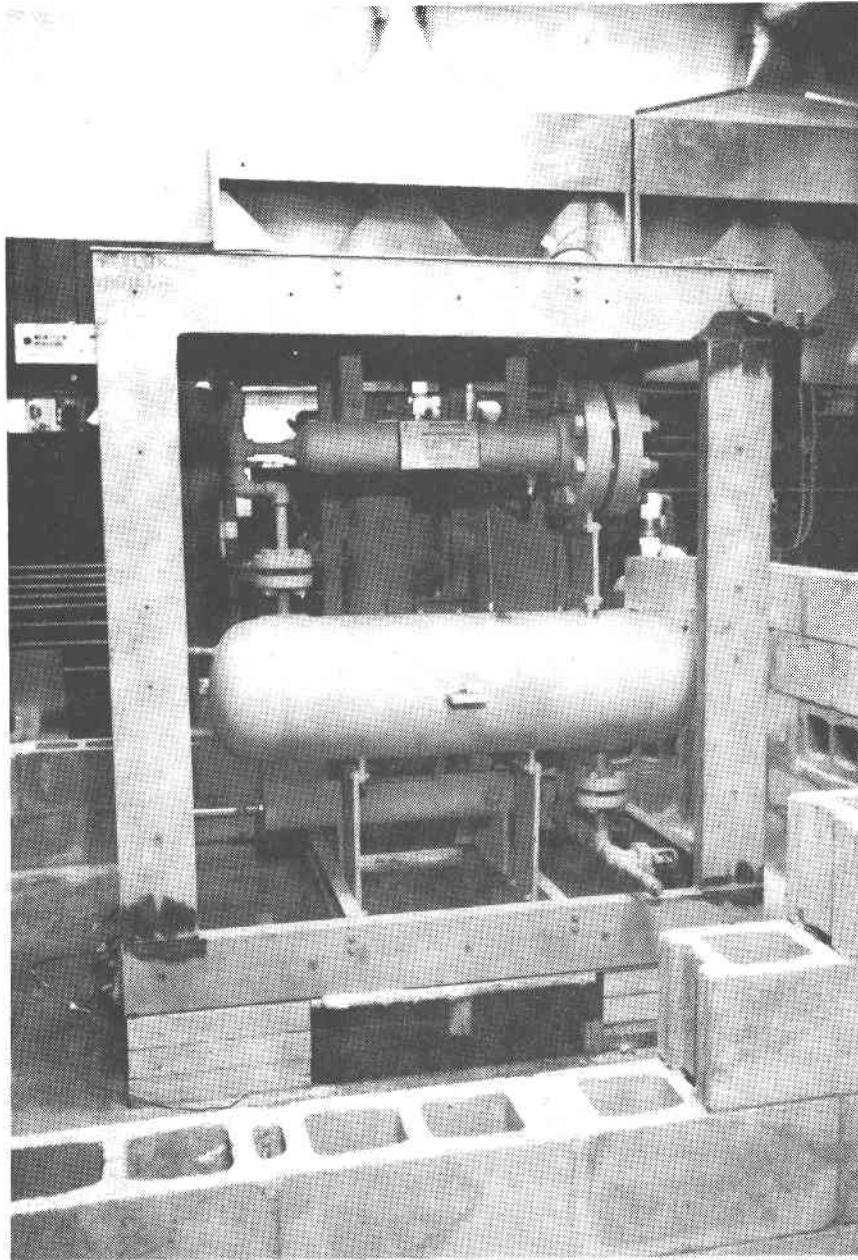


Figure 4-17. Unit Installed at Test Facility With Test Cell Enclosure Partly Completed - Front View

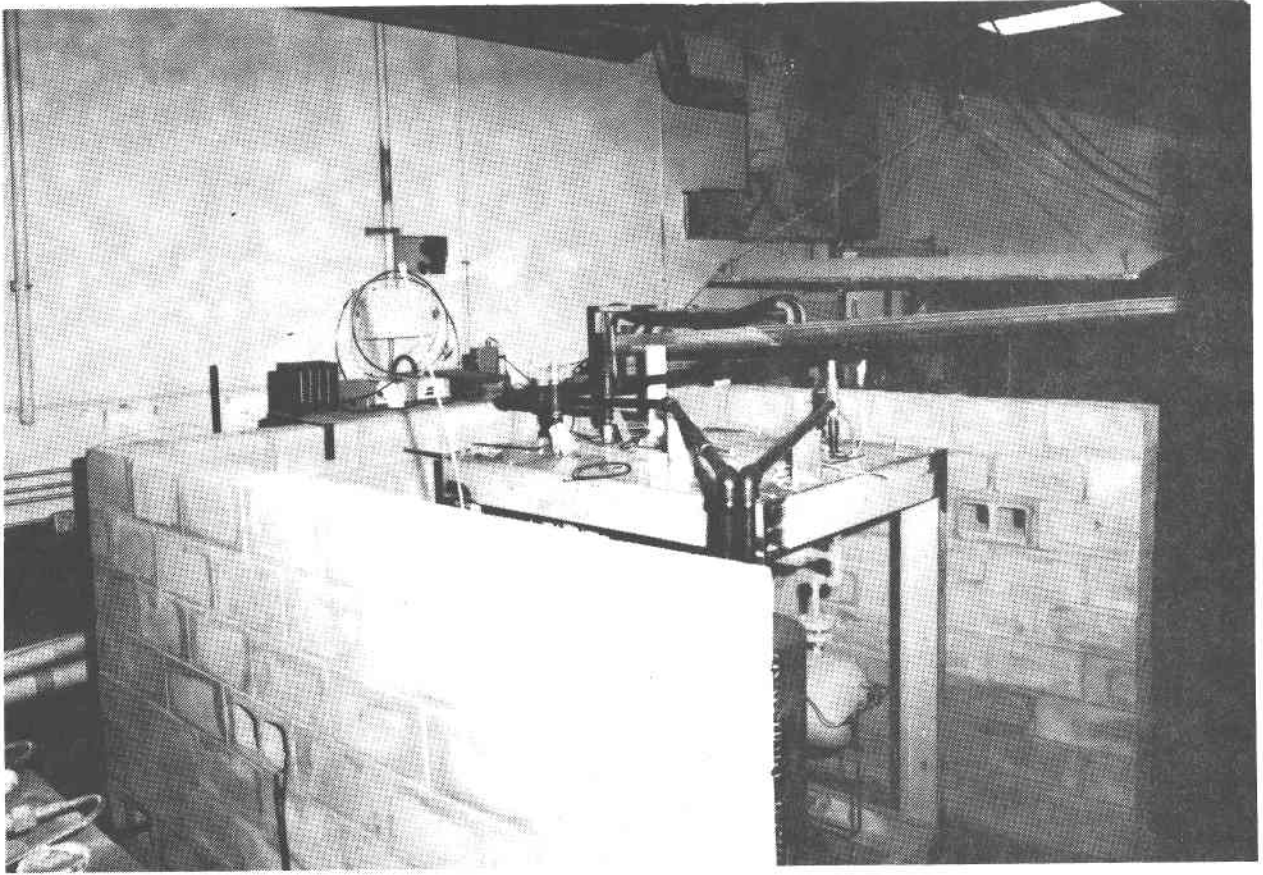
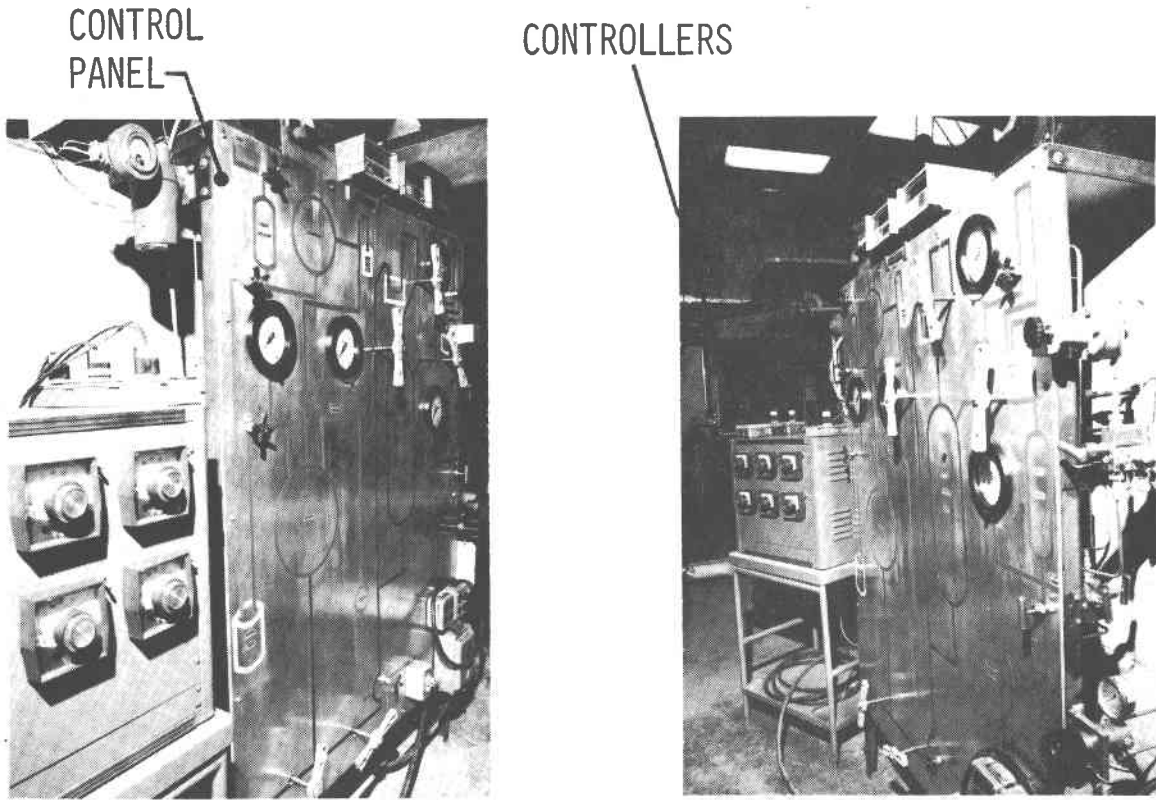


Figure 4-18. Test Cell and Mechanical Work Nearing Completion

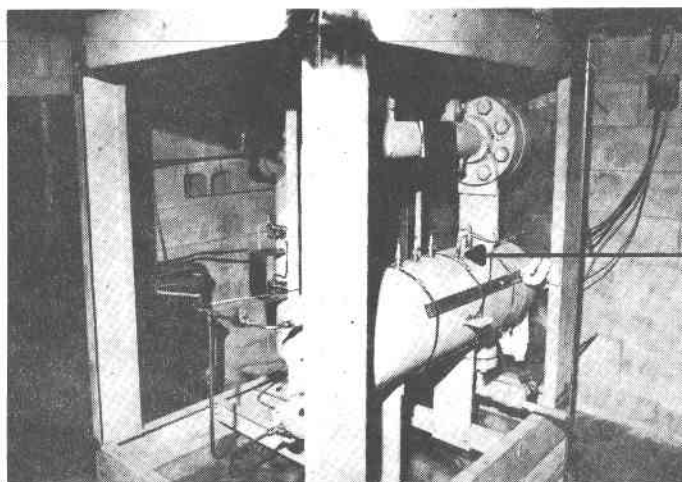


A. Left-side View

B. Right-side View

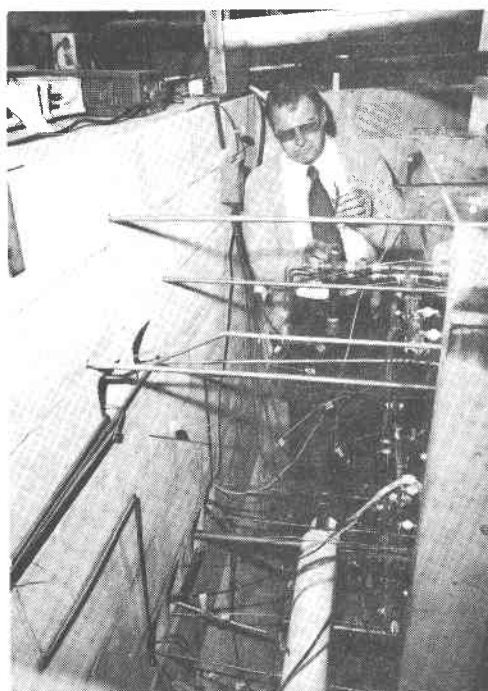
Figure 4-19. Reflux Boiler Control and Instrument Panel



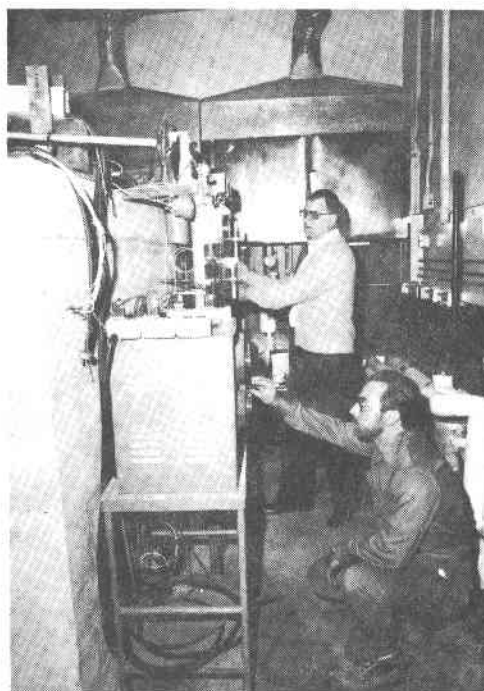


LEVEL  
SENSORS

A. Salt Level Indicating-System Installed on the Boiler



B. Valve Extender Rods,  
Instrumentation Wires, and  
Hydraulic and Pneumatic Lines



C. Reflux Boiler Electrical  
Checkout Under Way

Figure 4-20. Reflux Boiler Module Installation

Salt Level Display Unit--To obtain an accurate mass and energy balance, the salt level in the boiler must be known. This level must be measured under conditions of 13.8MPa, 315°C (2000 psig, 600°F). An electrical-conductivity-type probe was selected and a special connector was obtained to meet the temperature, pressure, and electrical isolation requirements. The connector with a probe is shown in Figure 4-21. The lower view shows the upper and lower ceramic sleeves of the connector with a boron nitride insert that flows under applied torque to seal and electrically isolate the probe from the tank. Four of these probes were installed along the top of the boiler as shown in Figure 4-22, and two were installed in the transfer tank as shown in Figure 4-23. The location of these probes was determined by accurately computing tank volume versus height. The resulting curves from these computations are given in Appendix E. A level sensor display unit was designed and constructed to indicate the salt level status. Figure 4-24 is a schematic of this unit and an audio high-level alarm unit.

Heat Loss and Power Control System--To control the rate of heat lost for experimental purposes, the reflux boiler is enclosed by six aluminum panels equipped with guard heaters installed as shown in Figure 4-25. A typical panel is shown in Figure 4-26. Ten centimeters (4 inches) of mineral wool insulation surround these panels. The guard heaters were specified to operate on 208 vac. The general arrangement of these heaters is as shown in Figure 4-27. Three set point controllers (G, H and I) are used to regulate the enclosure panel temperatures. Special adaptors allow for the two power levels as shown in the columns. Controller F (Figure 4-27) controls the electrical power to the gas heaters and the resulting temperature of the  $\text{GN}_2$  transfer supply. Controller E regulates the temperature of the salt supply and return lines to prevent freezing. Controllers A, B, C and D control the power to the water preheater based on the water temperature upon discharge. Separate thermocouples from the same TC well are supplied to each controller. Items 7, 8 and 10 are manually controlled based on periodic monitoring or as required. Controllers A through F are contained in power control panel No. 1

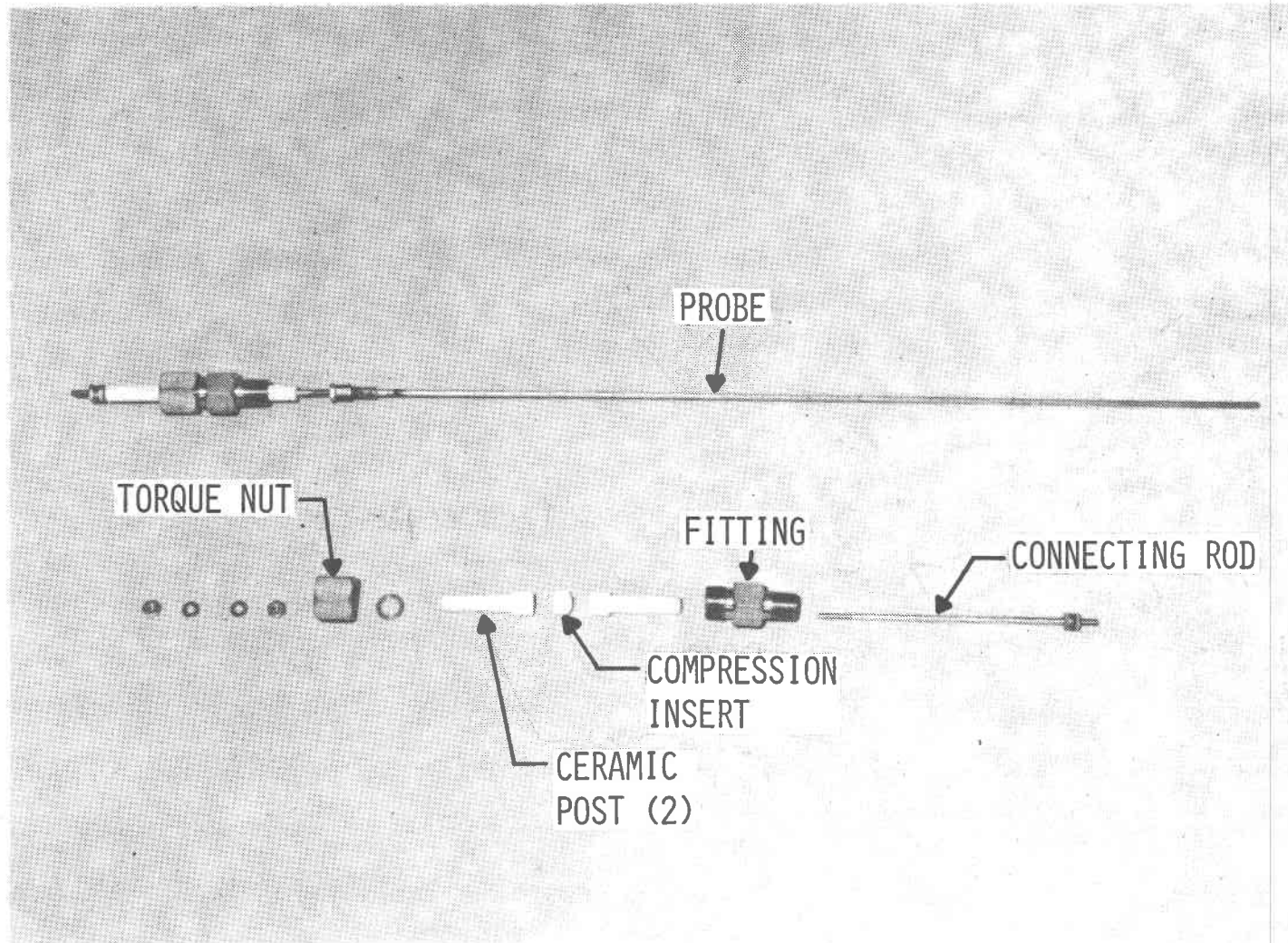
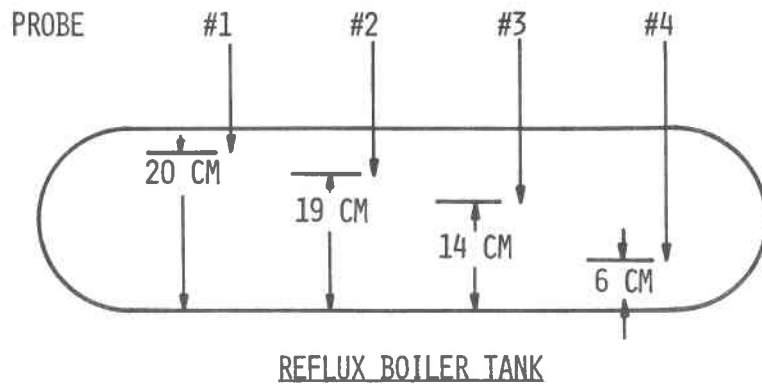
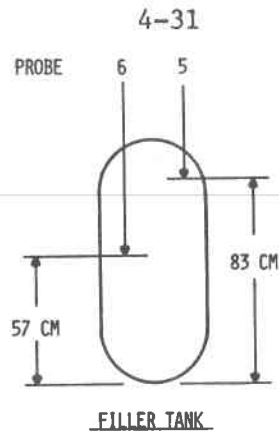


Figure 4-21. Molten Salt Fluid Level Sensor



<u>PROBE NO</u>	<u>INDICATION</u>	<u>FUNCTION</u>
1	75% FULL	INDICATES 86% OF MAXIMUM AREA AND 95% VOLUME OF THE FILLER TANK
2	71% FULL	INDICATES 60% SOLIDS GENERATION DURING EXTRACTION IF FILLED TO 75% AT START
3	50% FULL	INDICATES MAXIMUM AREA AND 64% OF VOLUME OF FILLER TANK
4	20% FULL	INDICATES 80% MAXIMUM AREA AND FILLING INITIATION

Figure 4-22. Location and Function of Probes Installed Along Top of the Boiler



PROBE NO	INDICATION	FUNCTION
5	95% FULL	MAXIMUM SALT FOR TRANSFER WITH 5% ULLAGE
6	64% FULL	INDICATES SALT LEVEL FOR 50% FILLING OF REFLUX BOILER AND AS FILLING INITIATION

Figure 4-23. Location and Function of Probes Installed on the Transfer Tank

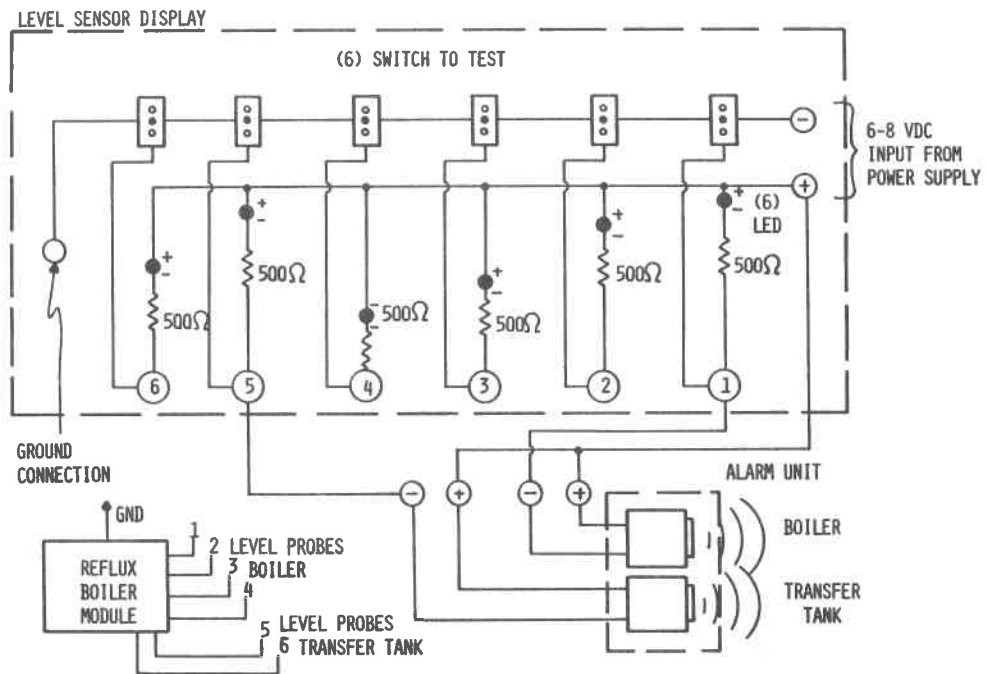


Figure 4-24. Level Sensor Display Unit and Audio High-level Alarm Unit Schematic

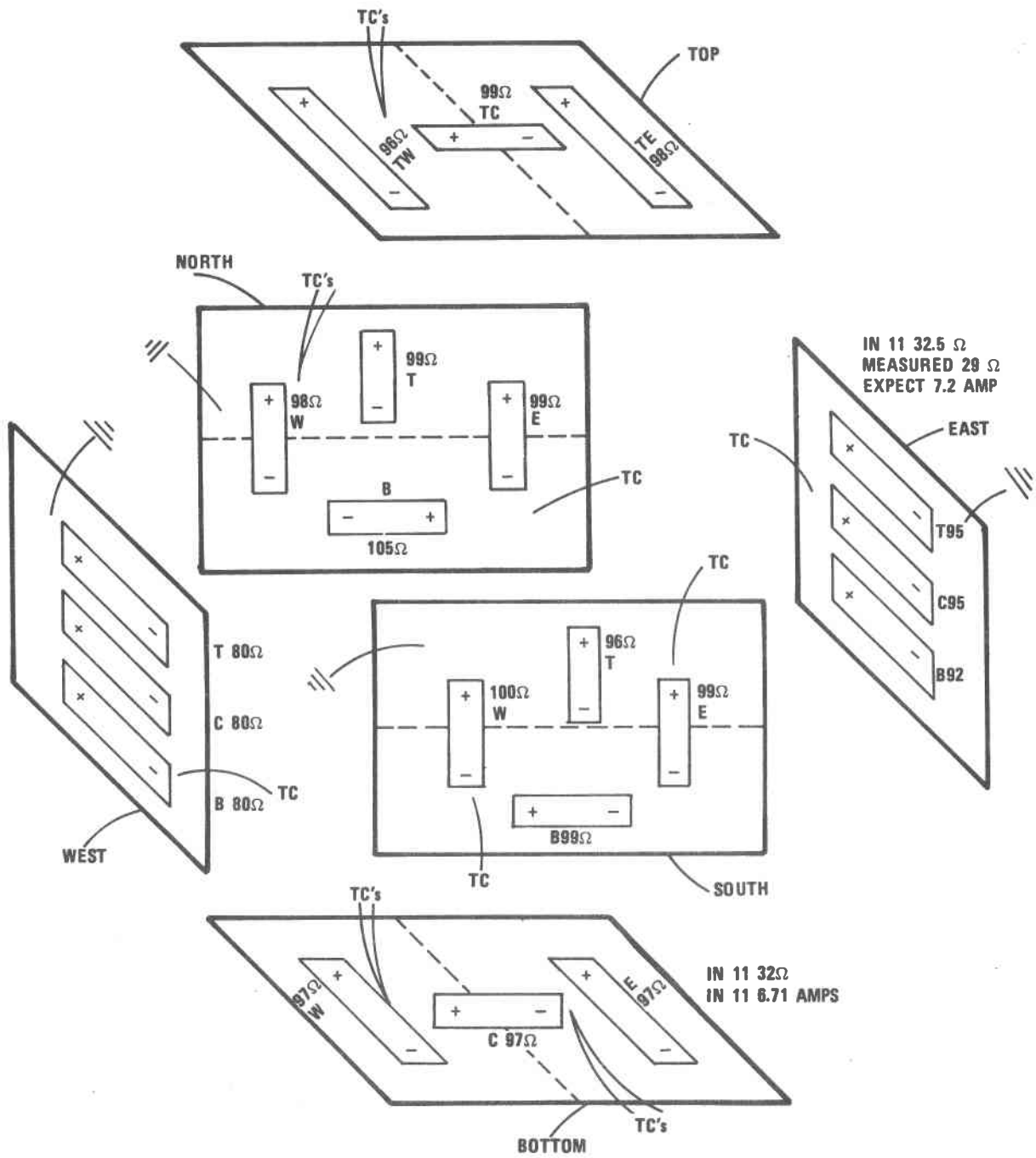


Figure 4-25. Reflux Boiler Enclosure Panels--Guard Heater Arrangement and Valves

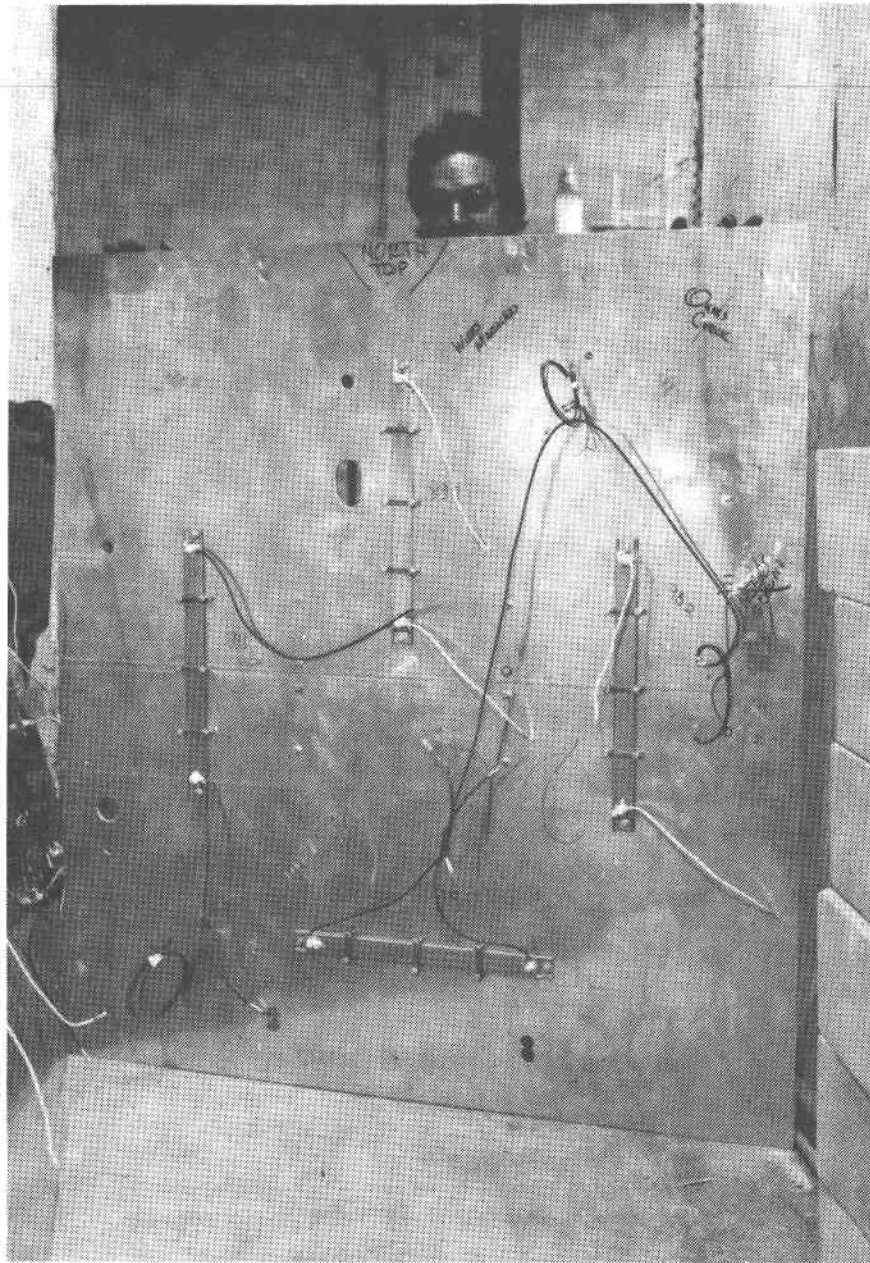


Figure 4-26. Reflux Boiler Aluminum Panel with Guard Heaters

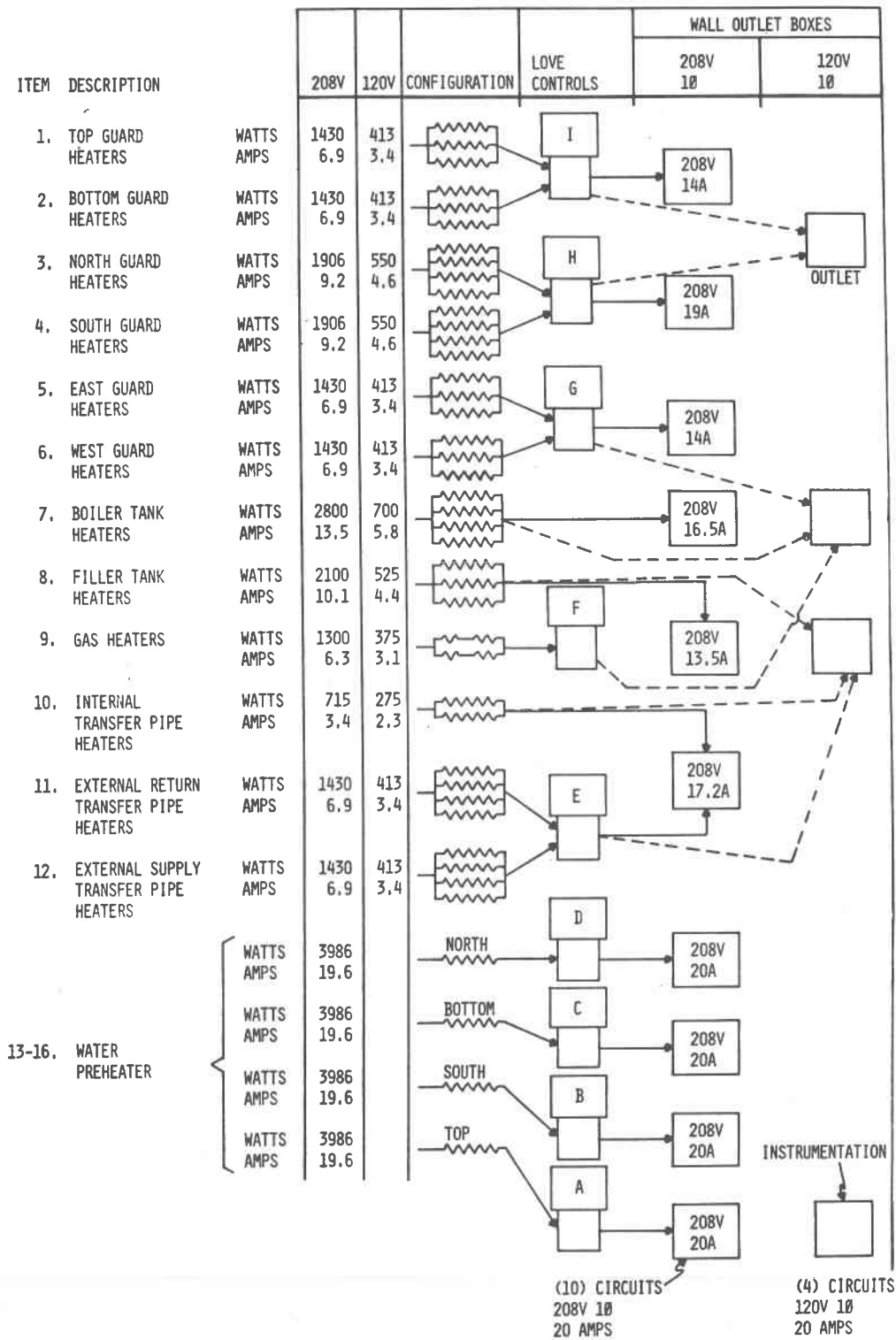


Figure 4-27. Arrangement of Guard Heaters



(Figure 4-28), and controllers G, H and I are housed in power control panel No. 2 (Figure 4-29). The circuit diagram for power control panel No. 1 is given in Appendix D.

4.2.3.2 High-pressure Water Pumping Unit--A high-pressure water pumping unit was designed and constructed as shown in Figure 4-30. It contains a water supply tank, a positive displacement pump with pulsation damper, and pressure regulator and flow control and bypass valves. This unit can supply 2.31/m (0.6 gpm) water at 428 MPa. To meet the heat rate requirements, approximately 0.61/m (0.15 gpm) must be delivered at 10.3 MPa. This unit supplies the high-pressure water to a preheater unit located within the reflux boiler module, where it is heated to saturation conditions for injection into the salt boiler. Figure 4-31 shows the basic components. The pump is of triplex, uniflow design with floating pistons. The water lubricates and cools the pistons. The motor is a 1.12 kW (1 1/2 HP) and requires 240 volt, 1 $\emptyset$ , 10 amp power. The water temperature must not exceed 71°C (160°F) during operation.

4.2.3.3 Gaseous Nitrogen System--To transfer salt to the boiler, gas pressure is used. The supply is obtained from a bank of "K" bottles manifolded together as shown in Figure 4-32. A high- and low-level pressure regulation capability is provided to effectively regulate pressures between 2000-100 and 0-100 psig. The regulated cool gas is supplied to the gas preheater, where it is heated to 315-330°C (600-650°F) before being admitted to the salt transfer tank. The gaseous nitrogen flows over taconite pellets, which are heated by external tubular heater bands. These heaters, shown in Figure 4-33, are rated for 750 watts (in a series configuration) at 240 volts.

4.2.3.4 Salt Storage Tank--The salt storage tank, shown in Figure 4-34, is of mild steel construction and measures 0.5 x 0.6 x 0.9 millimeters. Surrounding the tank are four heat loss control panels. These panels are equipped with guard heater thermocouples and 10 centimeters of fiberglass insulation. At the base, four range heaters are installed to provide the primary power for

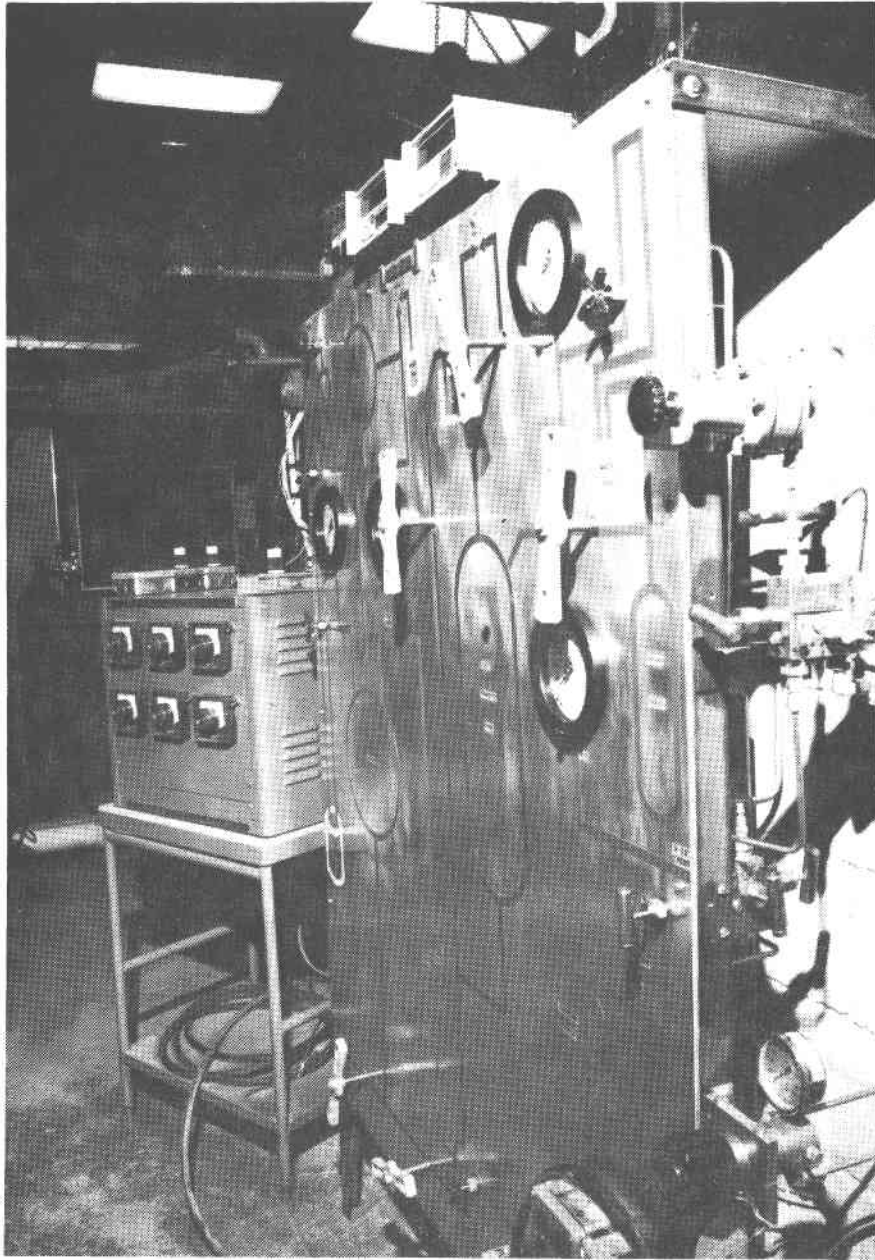


Figure 4-28. Power Control Panel No. 1

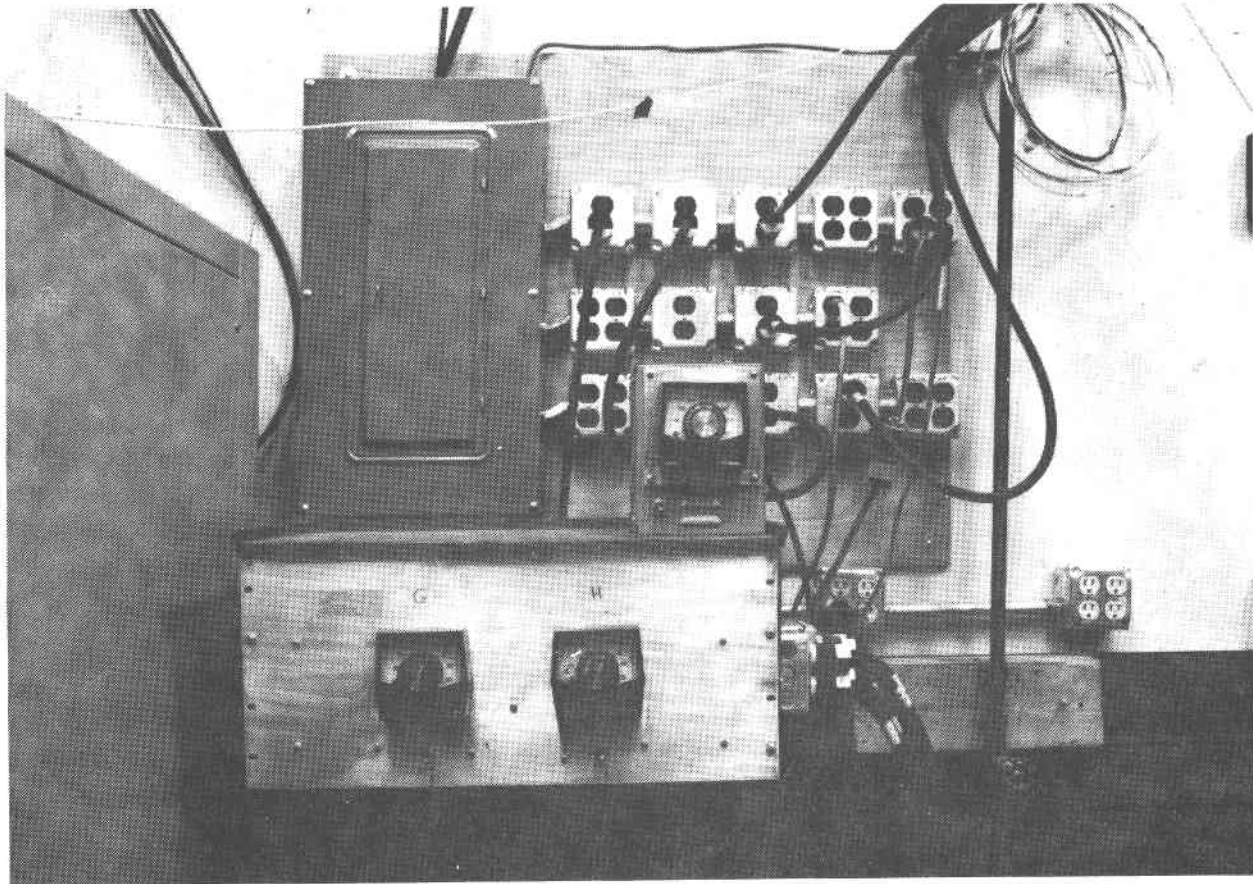


Figure 4-29. Power Control Panel No. 2

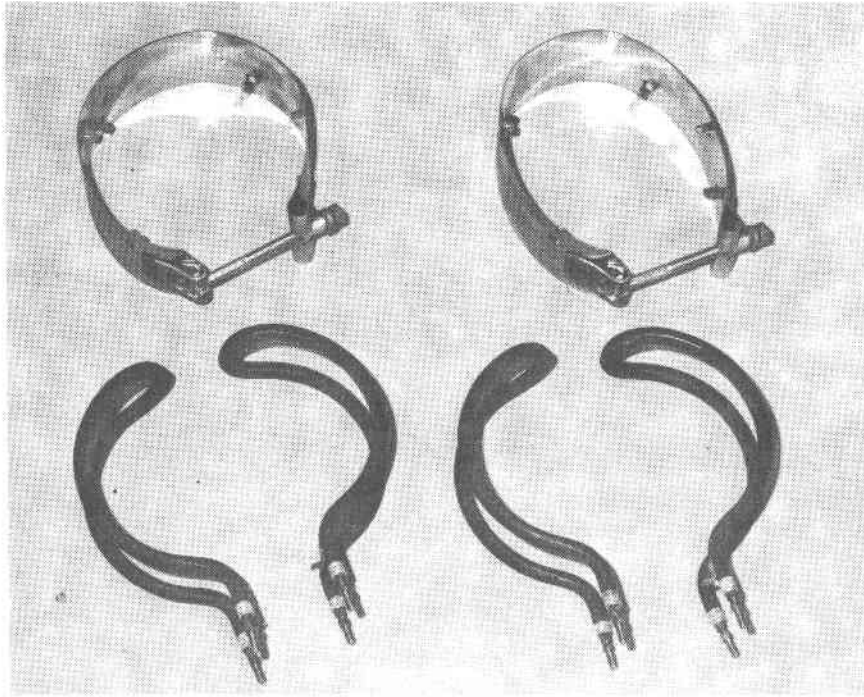


Figure 4-33. External Tubular Heater Bands

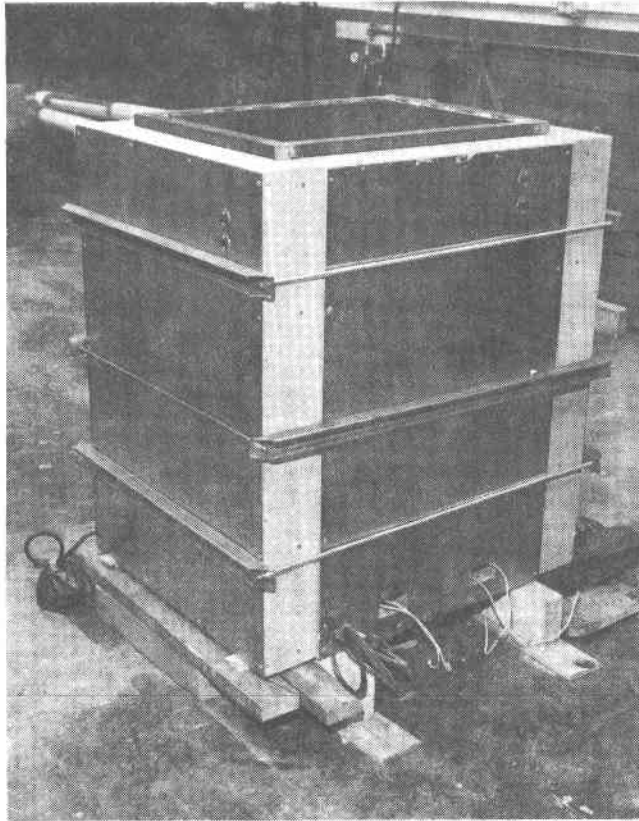


Figure 4-34. Salt Storage Tank

melting the salt. When filled with 454 kilograms of  $\text{NaNO}_3/\text{NaOH}$ , the tank has a stored thermal capacity of 22 kWh. The ratings of the heaters are given in Table 4-2. A special design, submerged centrifugal type pump is installed in the tank as shown in Figures 4-35 and 4-36. The pump shaft is cantilevered to eliminate the need for bearings being located in the molten salt. This pump is capable of delivering salt flows up to 1 l/s to either experiment.

A special screen was designed to separate the solids from the returning salt slurry and to prevent the solids from being pumped out of the tank. This screen, shown in Figure 4-37, is mounted on an inclined stand and placed into the tank. A splash guard is attached to the top to prevent salt solids from getting past the screen. Figure 4-38 shows the storage tank after the major mechanical work was completed. Figure 4-39 shows the storage tank during the instrumentation and electrical hookup to the controller station, and Figure 4-40 shows it in completed form with the flowby experiment installed and insulated. Notice the reflux boiler module in the background of Figure 4-40. A special thermocouple rake, shown to the right in Figure 4-36, was designed to measure the vertical temperature gradient in the salt tank with measurements every 15 centimeters.

Storage Electrical Power Distribution--The electrical power to the guard heaters is regulated by three set point controllers. Figure 4-41 is a schematic of the power distribution to the storage tank and flowby module guard heaters. The left-hand side of the diagram depicts the set point's power consumption, and the right-hand side shows the power controller and 208/120-volt distribution.

Instrumentation--Instrumentation parameters and locations are given in Figure 4-42 for the storage tank, flowby module, and oil flow loop. A mixture of type J and K thermocouples are used to accommodate instrument availability. Table 4-3 lists the instrumentation for both experiments. Details are contained in Appendix D.

Table 4-2. Ratings of Salt Storage Tank Range Heaters

QUANTITY	LOCATION	TYPE	RATING		ACTUAL	
			VOLTS	WATTS	VOLTS	WATTS
(4)	SALT TANK RANGE HEATERS	CHOMOLOX	240	1950	208	1465
(4)	SALT TANK GUARD HEATERS	MFG. AT HONEYWELL	120	400	120	400
(2)	BOTTOM GUARD HEATERS	CHROMOLOX STRIP	240	500	120	125
(2)	TOP GUARD HEATERS	FAST HEAT STRIP	208	700	120	233
(2)	FLOWBY HEAT EXCHANGER FRONT FACE HEATERS	CHROMOLOX STRIP	120	500	120	500
(2)	SIDE HEATERS	CHROMOLOX STRIP	120	250	120	250
(2)	TOP HEATERS	CHROMOLOX STRIP	120	1000	120	1000
(1)	TOP OF EXHAUST DUCT HEATER	CHROMOLOX STRIP	120	500	120	500
(2)	BOTTOM OF MODULE	CHROMOLOX STRIP	120	500	120	500
(6)	OIL FLOW LOOP TANK IMMERSION HEATER	CHROMOLOX IMMERSION	240	1500	208	1127

4.2.3.5 Hydraulic Pumping Unit--This unit was designed to provide a heat transfer fluid to either of the experiments. This unit is shown in Figure 4-43 and is shown schematically in Figure 4-44. This unit is capable of pumping 91 l/m (24 gpm) of Mobiltherm 603 oil at 2.8 mp (20 psig) and 315°C (600°F) for extended periods of time. Oil temperature is maintained by a set point controller. For rapid cooldown of the hot oil, a specially designed counterflow oil/water heat exchanger was built. The heat exchanger is capable of 11°C (20°F)/minute of oil cooldown. A cast iron centrifugal pump was modified to provide a seal-tight bearing and faceplate for 315°C (600°F) operation.

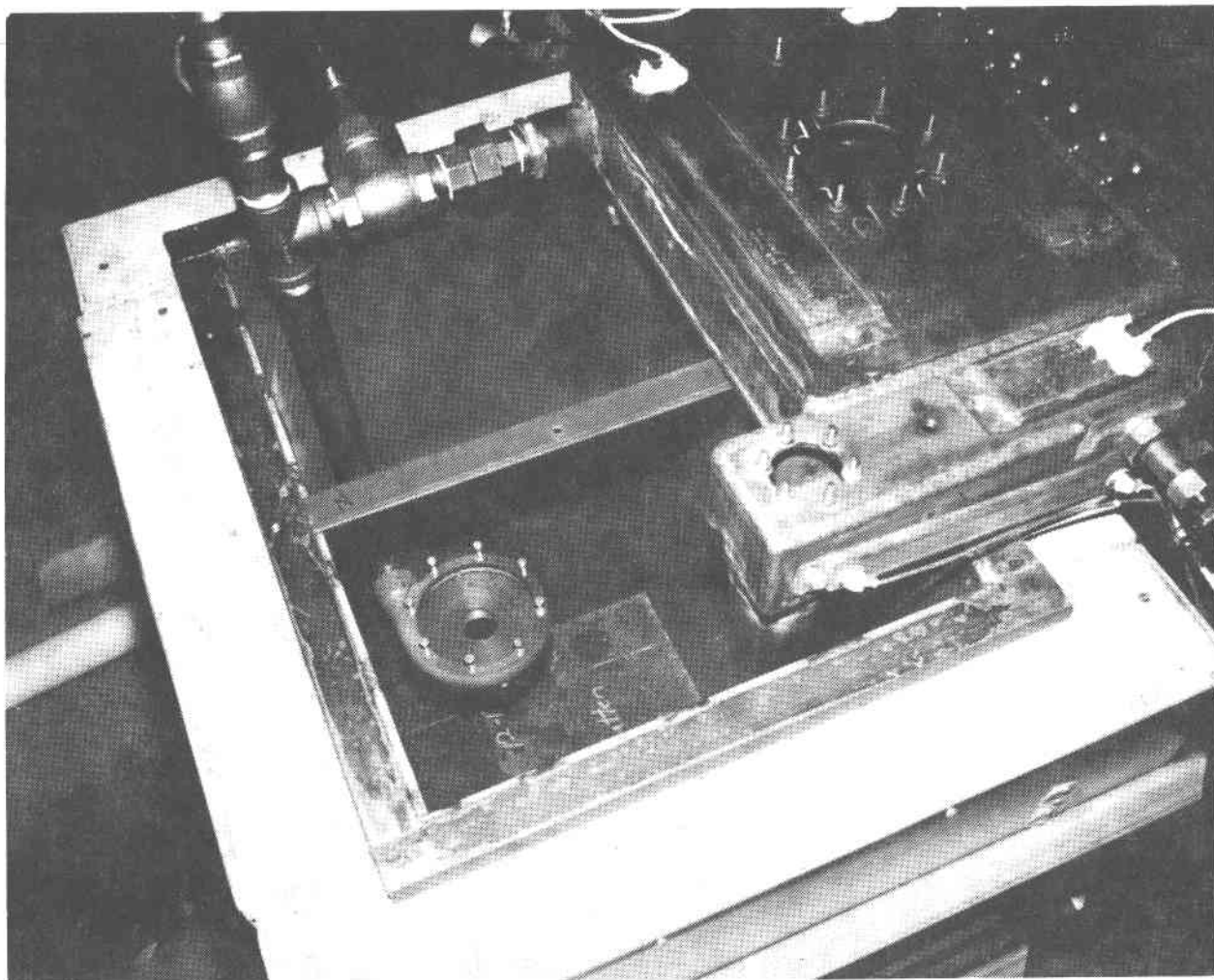


Figure 4-35. Installation of Submerged Centrifugal Type Pump in Tank

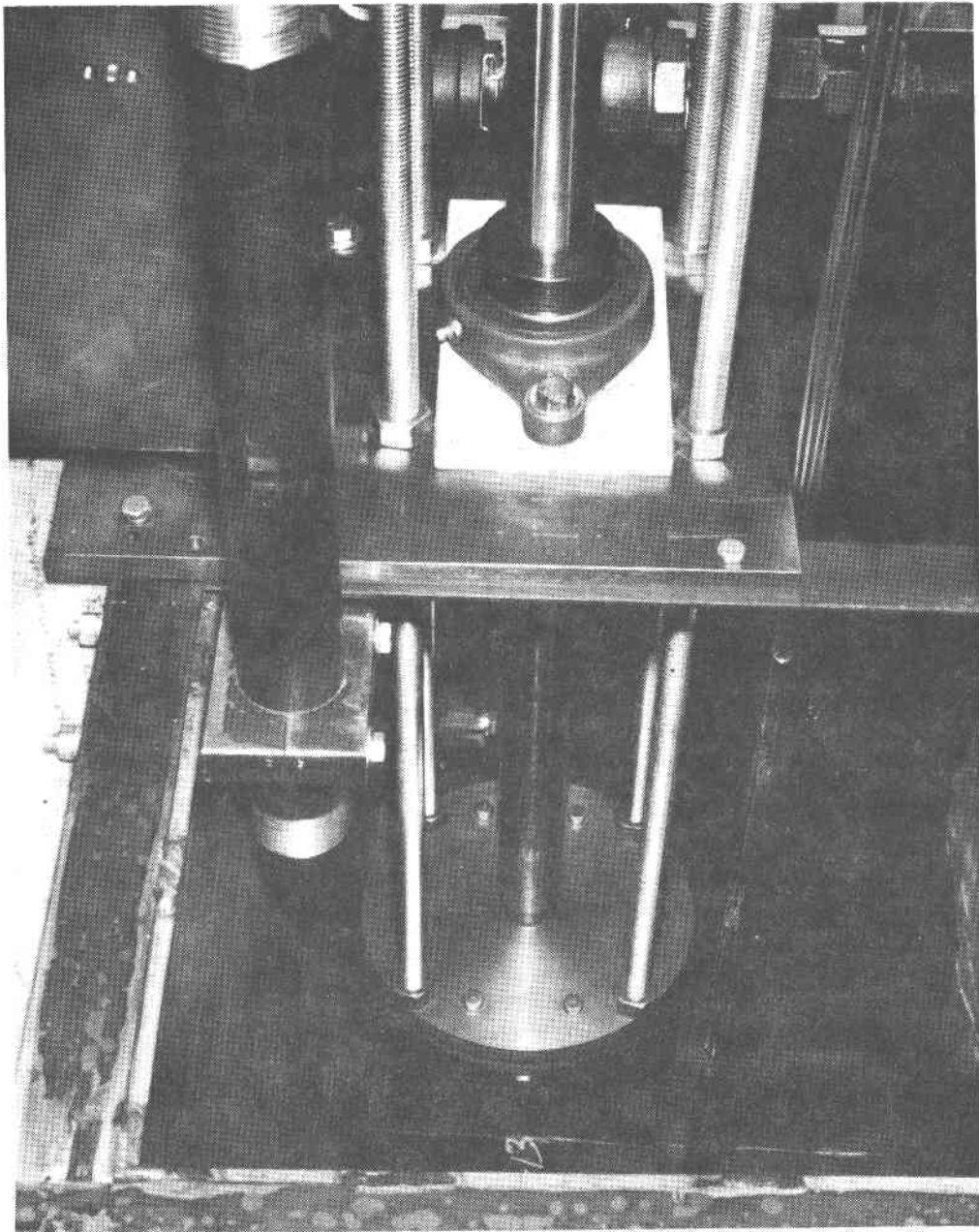


Figure 4-36. Installation of Submerged Centrifugal-Type Pump in Tank



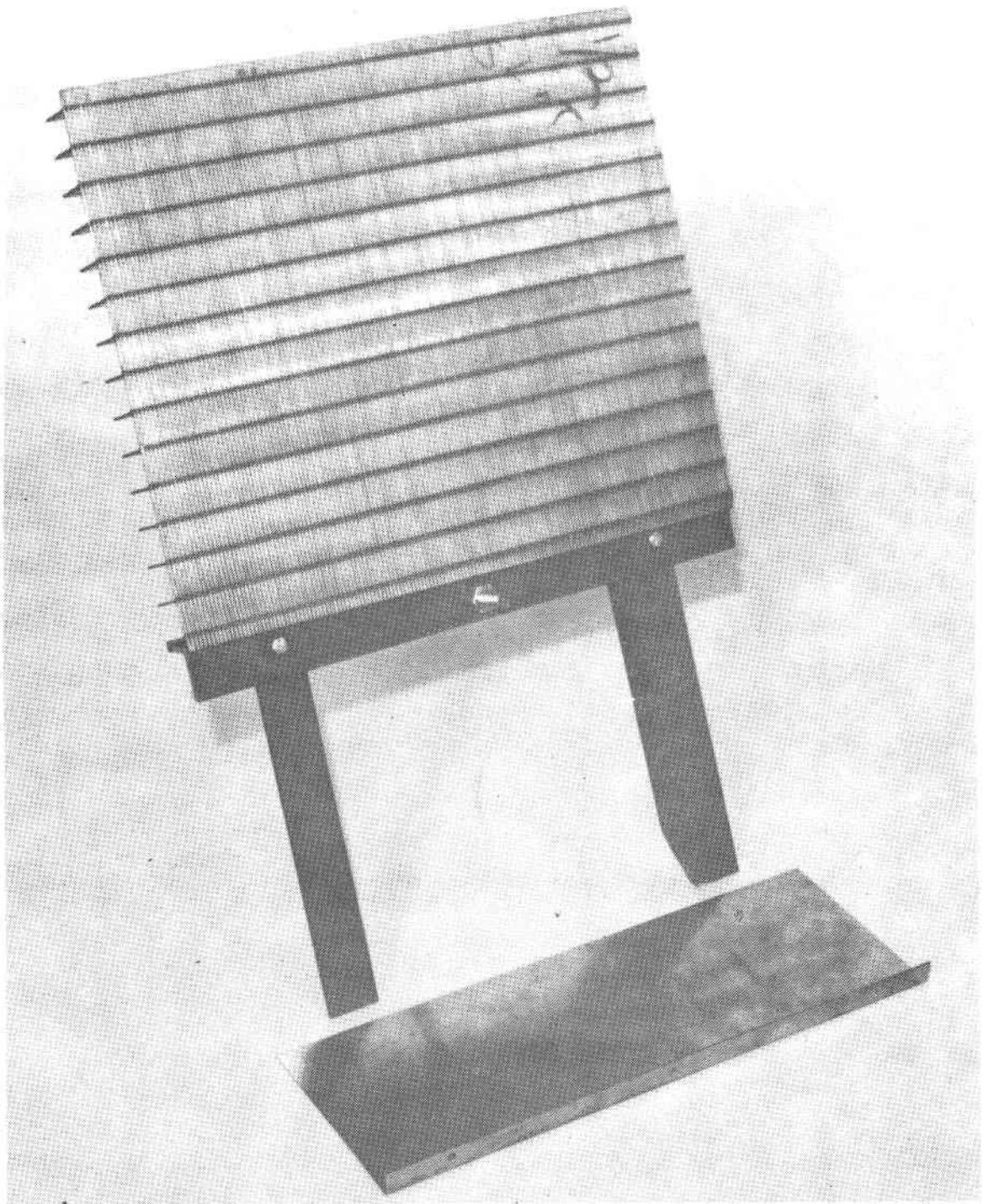


Figure 4-37. Screen Used to Separate Solids from Returning Salt Slurry and to Prevent Solids From Being Pumped Out of the Tank

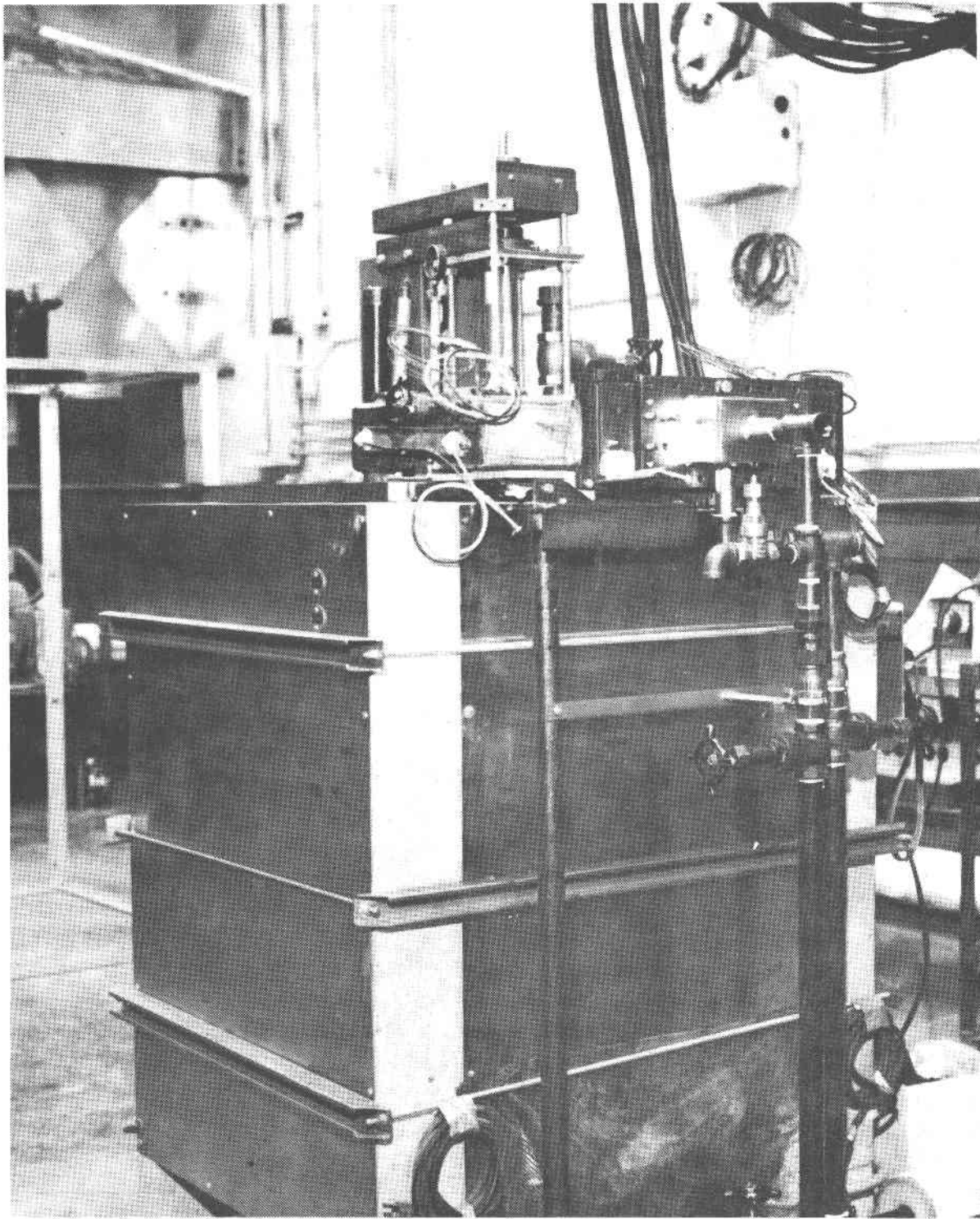


Figure 4-38. Completed Storage Tank

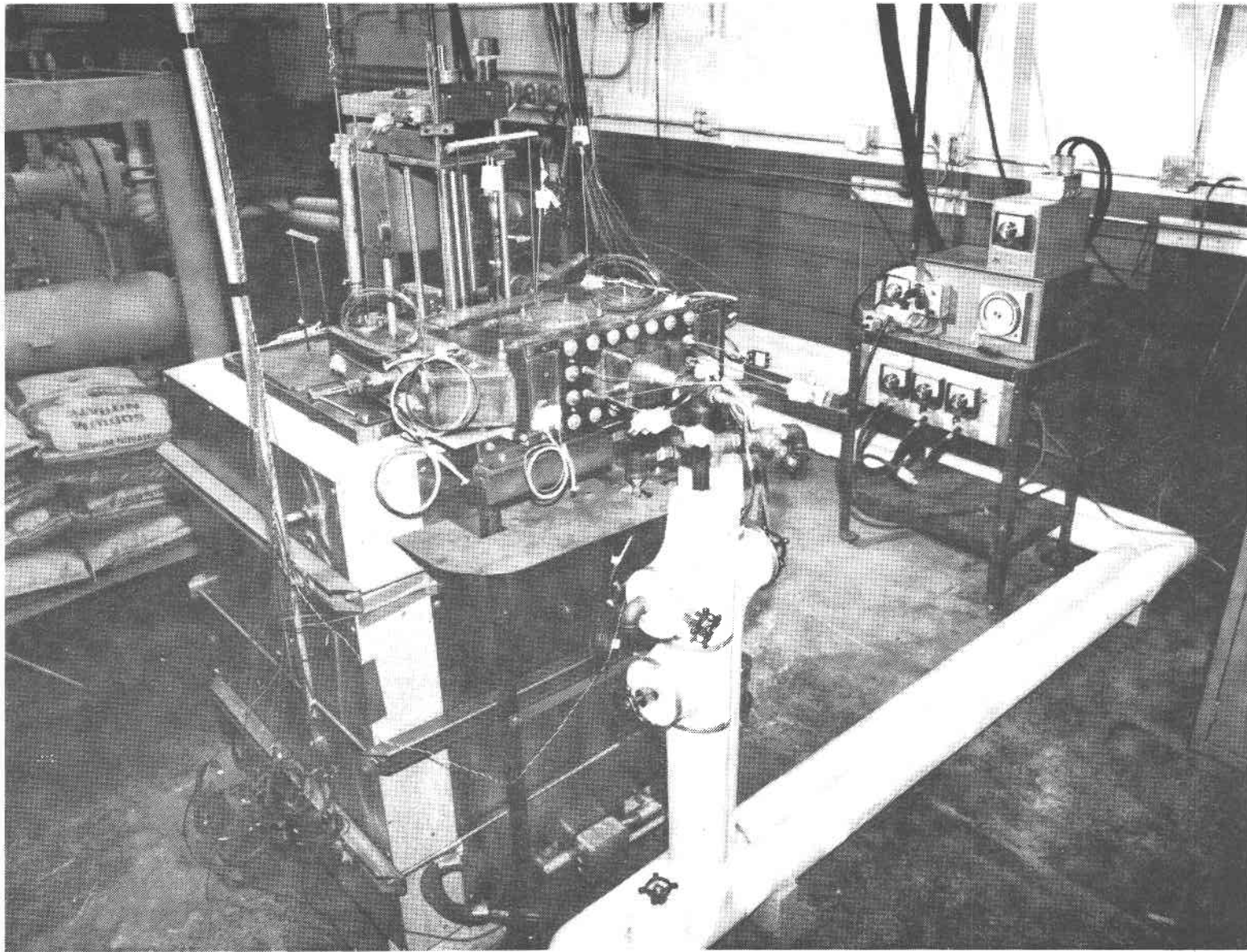


Figure 4-39. Storage Tank During the Instrumentation and Electrical Hookup to the Controller Station

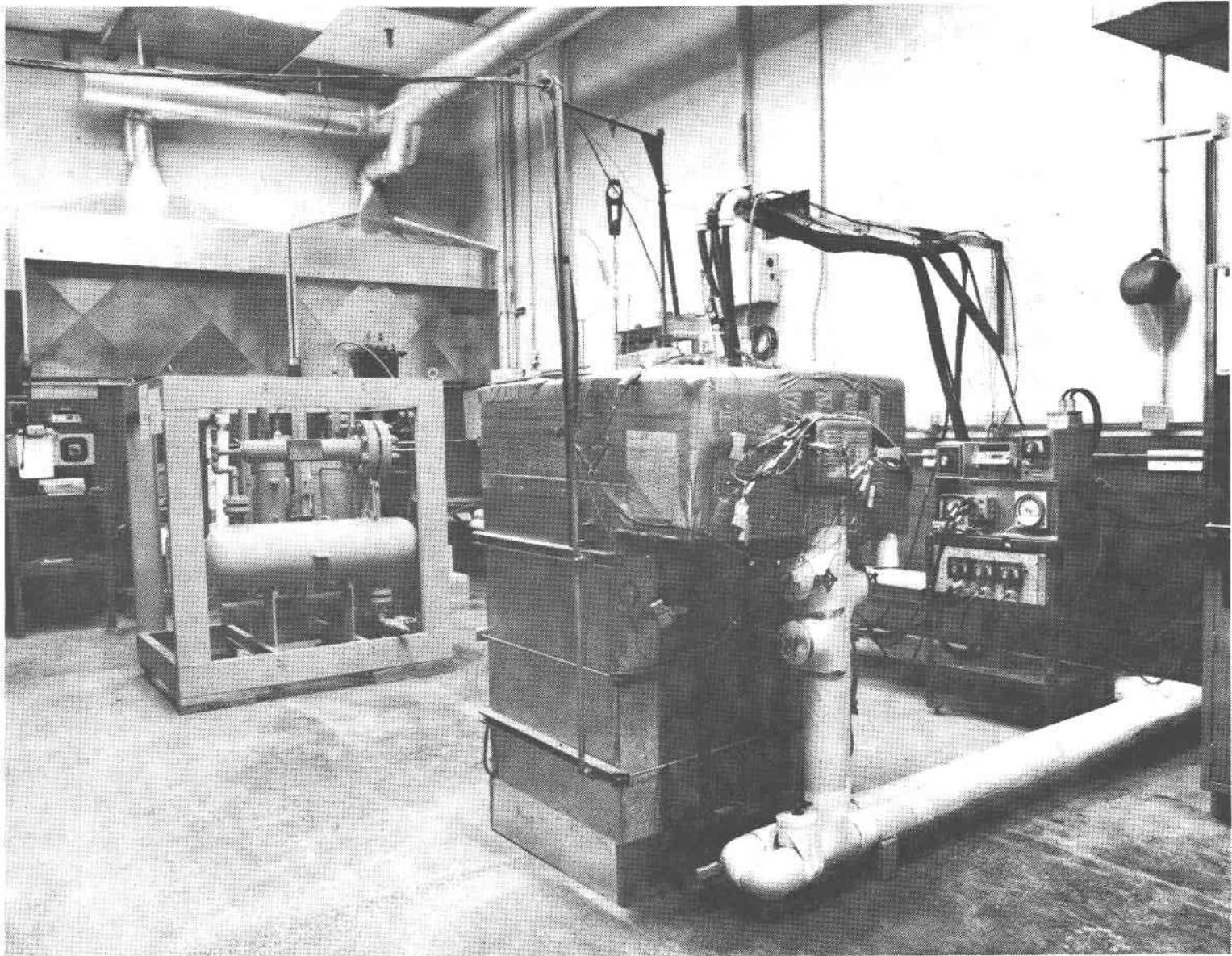


Figure 4-40. Storage Tank With the Flowby Experiment Installed and Insulated

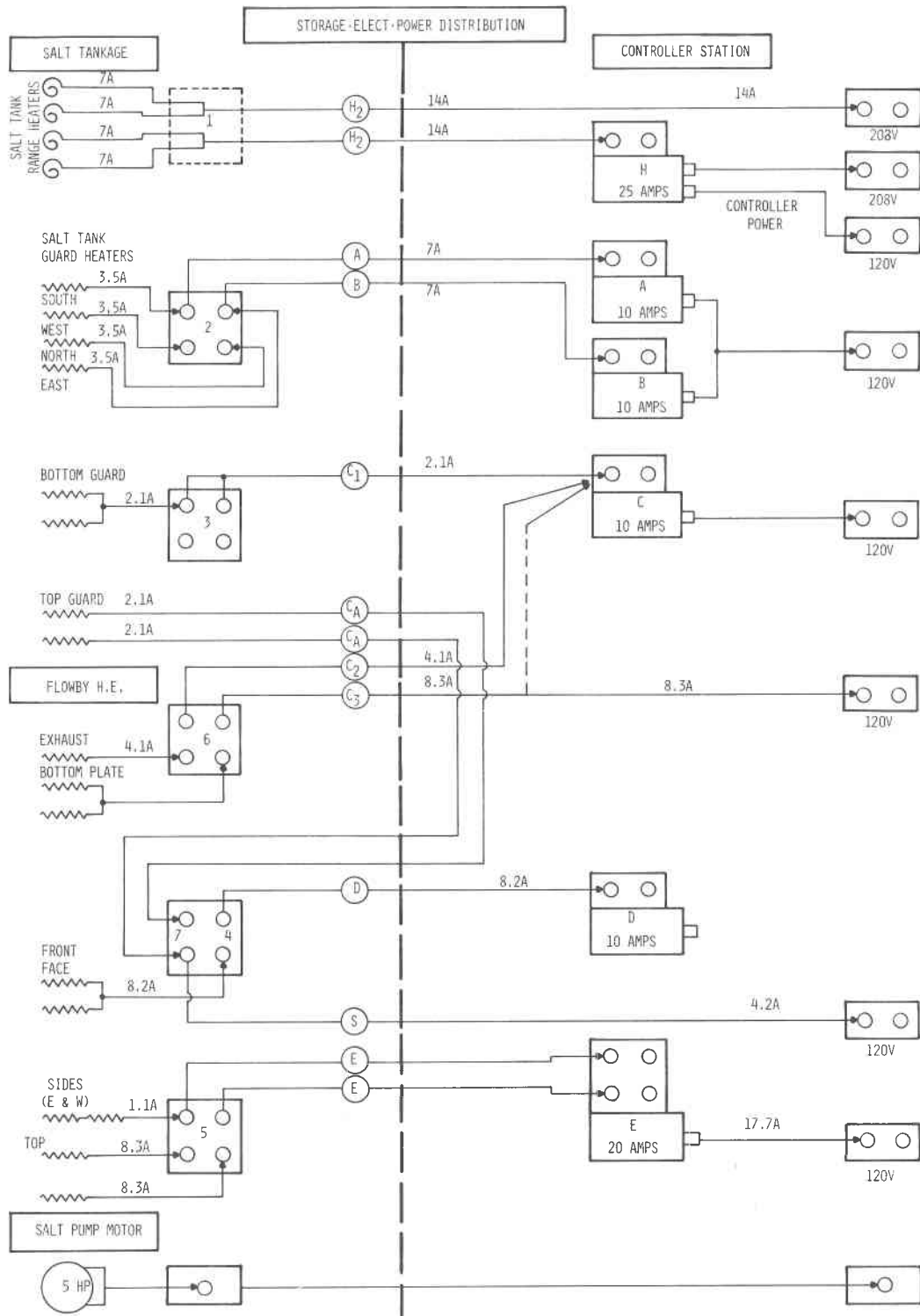


Figure 4-41. Schematic of the Power Distribution to the Storage Tank and Flowby Module Guard Heaters

WIRE NUMBER	CHANNEL NUMBER	INSTRUMENTATION IDENTIFICATION PARAMETERS AND TEMPERATURE PROBES	UNITS (MPA) (°C) (L/M)	TYPE OF T/C	QUANTITY	FITTINGS	T/C CONNECTOR MALE	T/C CONNECTOR FEMALE	TO DATA LOGGER	TO TEMPERATURE CONTROLLER	
33	(M) 25	NORTH HEATER	X	J	1			F			SALT TANK OUTSIDE
32	(M) 26	EAST HEATER	X	J	1			F		1	
	(M) 25	SOUTH HEATER	X	J	1			F			
	(M) 26	WEST HEATER	X	J	1			F		1	
30	27	BOTTOM HEATER (4) RANGE HEATERS (SEE M BELOW)	X	J&K	1		1	1	1	1	
29	28	EAST HEATER	X	J&K	1				1	1	FLOW MODULE BODY
39	29	SOUTH HEATER	X	J&K	1				1	1	
38	30	WEST SIDE HEATER	X	J&K	1				1	1	
45	31	BOTTOM HEATER	X	J&K	1				1	1	
28	32	TOP HEATER	X	J&K	1				1	1	
26	1	SALT TEMPERATURE - ENTER	X	K	1	1/8	1	1	1		FLOW MODULE HEAT EXCHANGER
43	2	SALT TEMPERATURE - LEAVE	X	K	1	1/8	1	1	1		
34	6	SALT TEMPERATURE PROXIMITY (EAST)	X	K	1	1/16	1	1	1		
37	8	SALT TEMPERATURE PROXIMITY (WEST)	X	K	1	1/16	1	1	1		
35	7	SKIN TEMPERATURE (EAST)	X		1	1/16	1	1	1		
36	9	SKIN TEMPERATURE (WEST)	X		1	1/16	1	1	1		
		FLOW METER PRESSURE (IN & OUT)	X	X	1						
			X		2						
1 THRU 5	11 THRU 15	SALT GRADIENT "RAKE"	X	K	5				5		INSIDE SALT TANK
41	16	SALT SCREEN TEMPERATURE	X	K	1		1	1	1		
	(M) 16	SALT TEMPERATURE (FOR HEATER CONTROL)	X	J&K	1		1	1		1	
31	17	TANK WALL TEMPERATURE	X	K	1		1	1	1		
27	4	FLOW (OIL)	X								OIL FLOW LOOP
42	5	TEMPERATURE (OIL) IN	X	K	1	1/8	1	1	X		
	5	TEMPERATURE (OIL) OUT	X	K	1	1/8	1	1	X		
	3	ΔT	M VOLTS	J	2	1/4			X		
	(M) 3	PRESSURE	X								
	(M) 3	OIL PUMP TEMPERATURE	X	J&K	1						
	(M) 3	OIL EXPANSION TANK (LEVEL)	X		1						
40	33	OIL BYPASS (AT SALT TANK)	X	K	1	1/8	1	1	X		
		OIL TEMPERATURE CONTROL (LOWBY)	X	J	1		1	1		X	

(M) TEMPERATURE MAY BE INDICATED FOR MONITORING.  
CHANNELS NOT ASSIGNED 0, 10, 18, 19, 20, 21, 22, 23, 24, 35

Figure 4-42. Instrumentation Parameters and Locations for the Storage Tank, Flowby Module, and Oil Flow Loop

Table 4-3. Active Heat Exchanger Instrumentation

ITEM	RECORDING CHANNEL	VALUE	INSTRUMENTATION ASSIGNMENT	
REFLUX BOILER MODULE	BOILER PRESSURE	53	23,45 MV *	
	OPEN	52	****, * OF	
	OPEN	51	****, * OF	
	TRANSFER TANK	50	103,6 OF T-11	
	RETURN PIPE	49	67,9 OF T-23	
	CONDENSER	48	95,8 OF T-22	
	BOILER FLANGE	47	140,6 OF T-20	
	GN <sub>2</sub> OUT	46	119,7 OF T-14	
	WATER PREHEATER	45	69,7 OF T-13	
	TRANSFER TANK	44	112,5 OF T-12	
	SALT RETURN	43	****, * OF T-17	
	SALT IN	42	****, * OF T-16	
	MODULE AMBIENT	41	67,4 OF T-24	
	CONDENSATE REC. SKIN	40	****, * OF T-10	
	CONDENSATE REC. IN	39	95,7 OF T-9	
	BOILER WATER IN	38	70,5 OF T-6	
	CONDENSER TUBE	37	109,1 OF T-5	
	CONDENSER	36	98,0 OF T-4	
	BOILER STEAM	35	140,9 OF T-2	
	BOILER SALT-MIDDLE	34	131,6 OF T-1	
	BOILER SALT-BOTTOM	33	127,5 OF T-3	
	OIL ΔT	32	0,21 MV	
	OIL OUT	31	68,5 OF T-8	
	OIL IN	30	68,2 OF T-7	
		SOUTH HEATER	29	476,6 OF
		EAST TOP HEATER	28	493,6 OF
		SALT PUMP	27	597,7 OF
		OPEN	26	****, * OF
		BOTTOM GUARD	25	469,4 OF
		WEST SIDE HEATER	24	482,0 OF
		BOTTOM HEATER	23	486,9 OF
		TOP HEATER	22	475,8 OF
		OIL BY-PASS	21	77,8 OF
		OIL-LOWER ΔT	20	348,3 OF
		OPEN	19	****, * OF
		OPEN	18	****, * OF
		TANK WALL	17	598,3 OF
		SALT SCREEN	16	599,4 OF
		TOP	15	597,6 OF
	STORAGE TANK RAKE		14	303,4 OF
			13	597,6 OF
			12	596,8 OF
		BOTTOM	11	596,1 OF
		AMBIENT	10	68,4 OF
		H. E. WEST SKIN	9	480,7 OF
	H. E. WEST PROX.	8	480,9 OF	
	H. E. EAST SKIN	7	71,2 OF	
	H. E. EAST PROX.	6	354,0 OF	
FLOW BY HEAT EXCHANGER	OIL OUT	5	456,1 OF	
	OIL IN	4	465,0 OF	
	OIL ΔT	3	13,283 MV	
	SALT OUT	2	480,4 OF	
	SALT IN	1	495,9 OF	

\* FAHRENHEIT SCALE WAS USED DUE TO CALIBRATION OF INSTRUMENTS

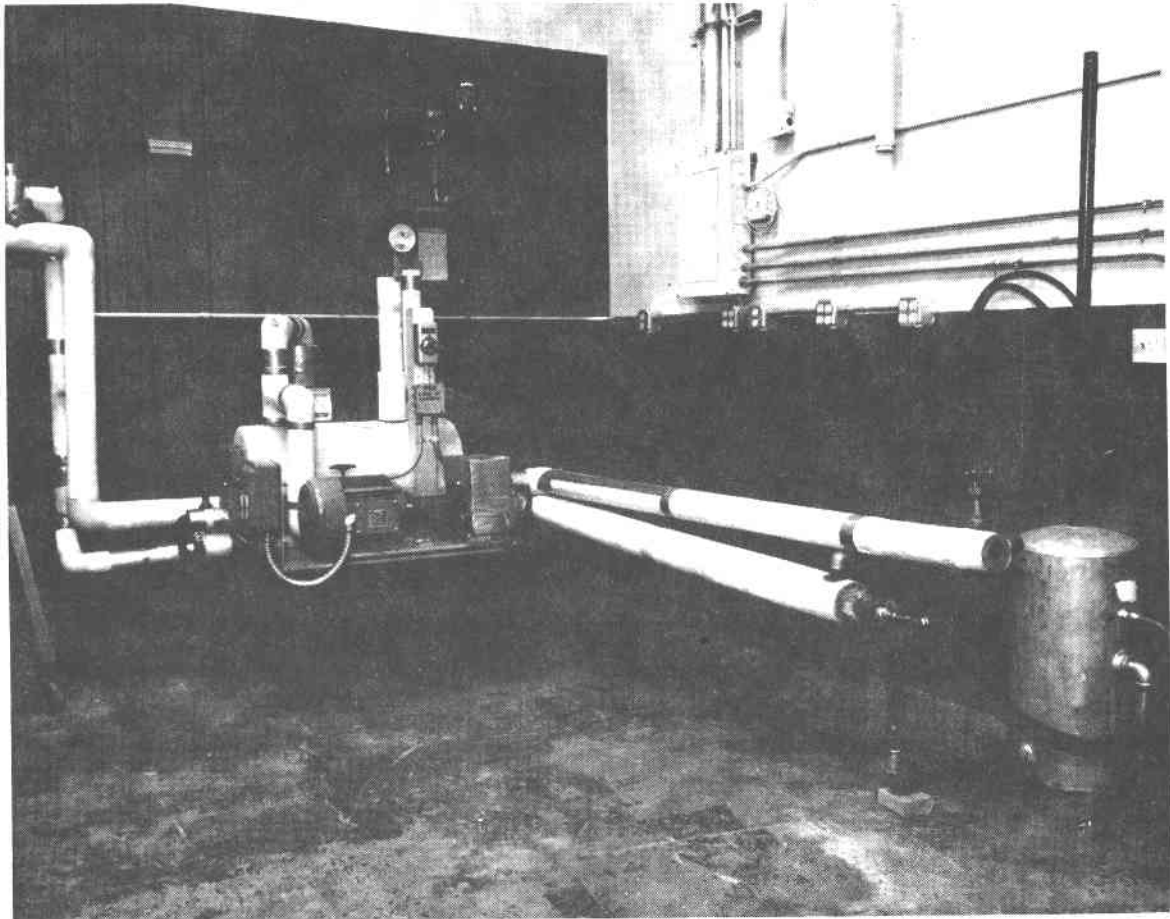


Figure 4-43. Hydraulic Pumping Unit



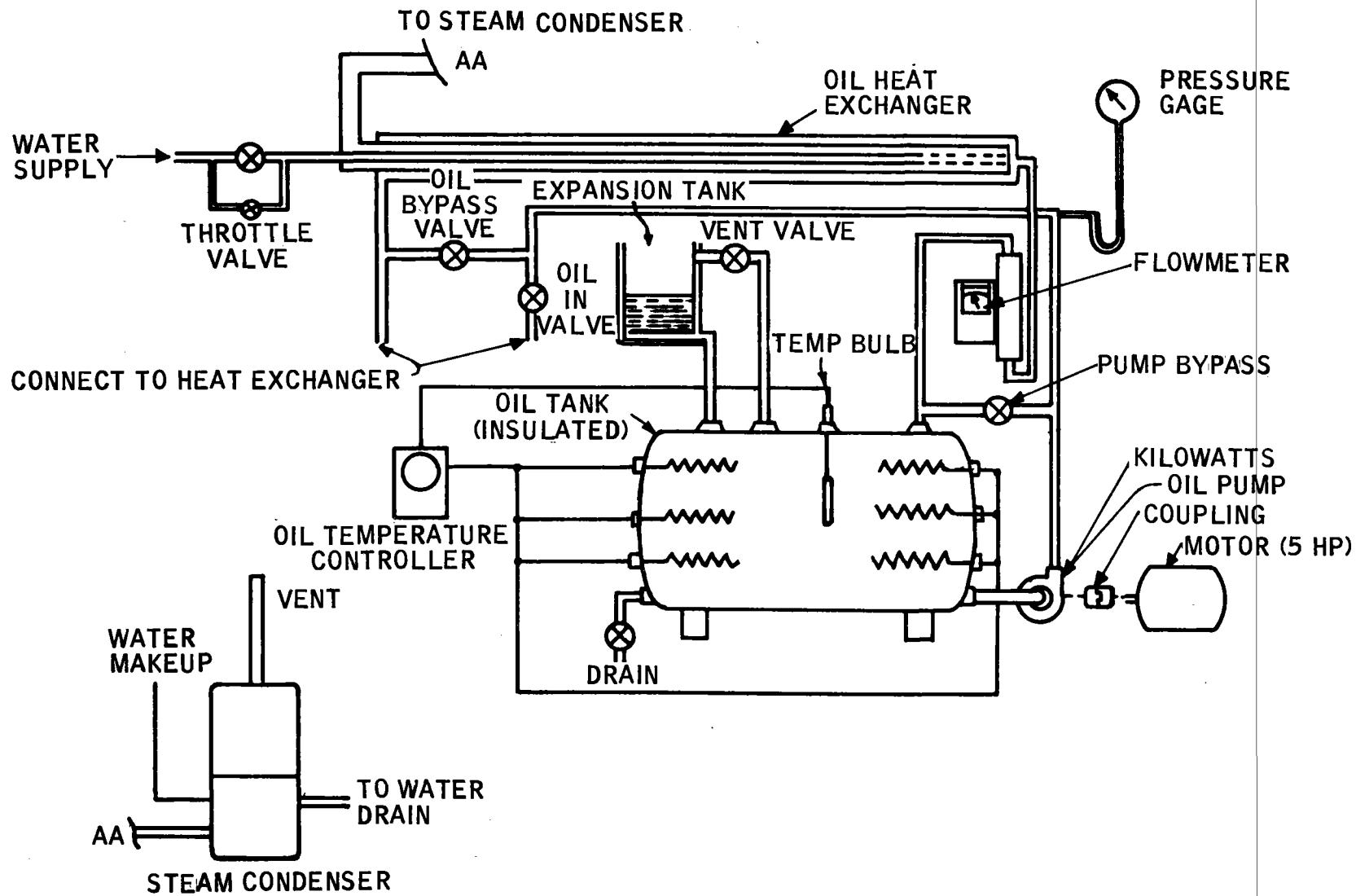


Figure 4-44. Oil Flow Loop

### 4.3 SHELL AND TUBE FLOWBY HEAT EXCHANGE CONCEPT MECHANIZATION

#### 4.3.1 System Description

The shell and tube heat exchange system for use with molten salts appears to be identical to any conventional shell and tube heat exchange system. The differences lie in the tube surface property and the heat storage medium. Available evidence indicated that the proper choice of tube surfaces, surface preparation, and medium selection would reduce the salt-to-tube bond strength to permit the solid salt to be removed by modest hydrodynamic forces.

Analysis of heat exchange concepts under Task I of this contract showed that the shell and tube exchanger system was the most cost-effective closed heat transfer system. Only the open-cycle reflux boiler, which can take advantage of a higher output temperature, shows possibilities of being more cost-effective. From the hardware development standpoint, the shell and tube heat exchanger technology is better developed and more widely used than any other industrial heat exchanger technology. The main questions to be resolved in its application to molten salt thermal storage are the suitable combinations of surfaces and medium, and the temperature, flow rate and heat rate range within which the system can be operated.

Figure 4-45 is a diagram of a typical counterflow heat exchanger with an enlarged section of tube broken out to illustrate the different surface conditions to be explored. Figure 4-46 is a schematic diagram of a 1000 MW(t) system with 6 hours of storage capacity using tube and shell heat exchangers to effect the removal of the heat of fusion from the molten salt medium thermal storage. For this system, it is expected that a slurry density of 20 to 30 percent will be readily transportable in the pipe lines. To achieve high latent heat recovery from storage, the slurry is returned

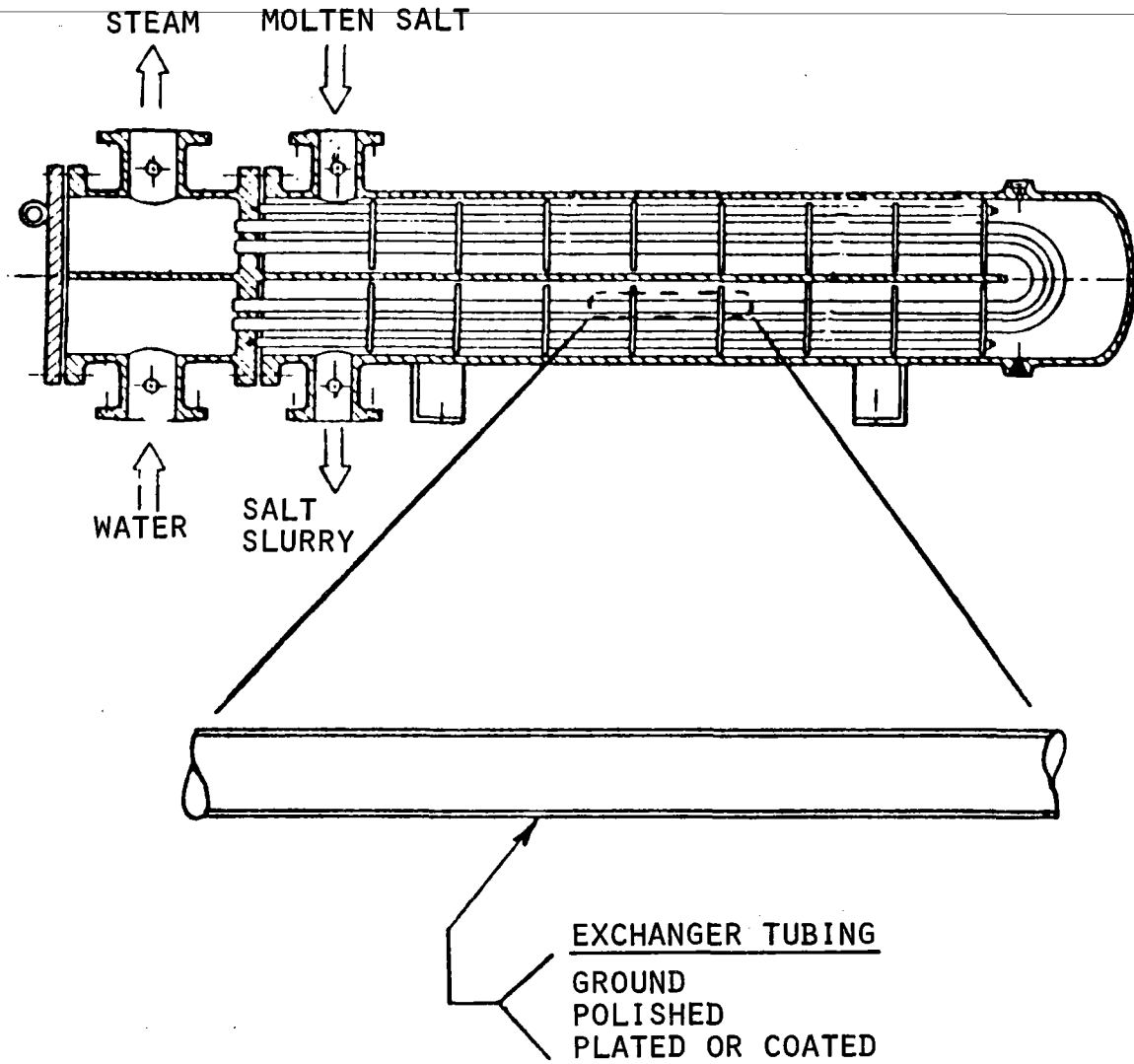
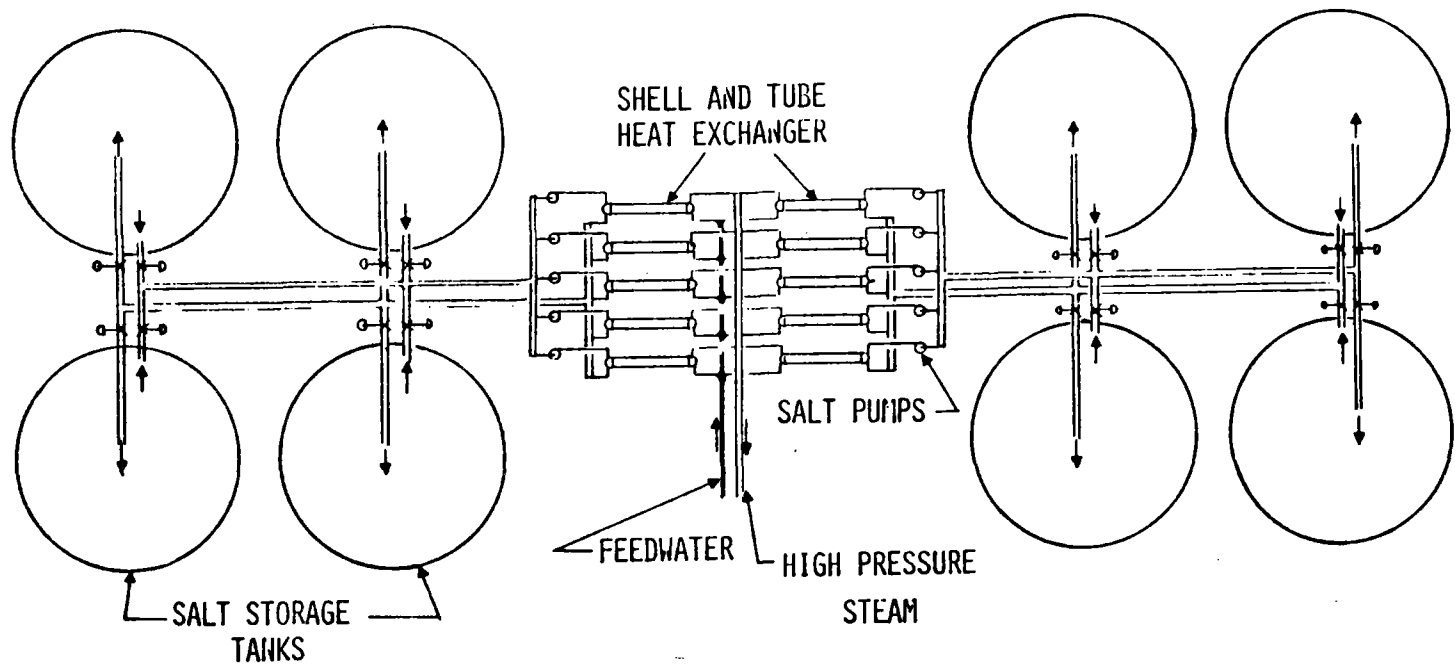


Figure 4-45. Coated Tube and Shell Heat Exchanger with Flowby



4-56

Figure 4-46. Tube and Shell Heat Exchange System

to storage where gravity separation is used, causing the solids to settle to the bottom of the tank. The less dense liquid rises to the top to be recirculated through the exchanger.

Scaling down the thermal storage system capacity to provide a high heat rate for a short duration may require settling augmentation. At a high heat rate with a small storage system, the gravity separation of the solid from the liquid may not occur rapidly enough to provide a high latent heat recovery factor. Separation of solid and liquid phases could be augmented by centrifugal separators.

System performance predictions made under Task I indicated that overall heat transfer coefficients of  $2260 \text{ Wm}^2\text{-}^\circ\text{K}$  would be attainable and that ten units, 1.5 millimeters in diameter by 12.2 millimeters in length, would be able to supply 1000 MW(t) with an  $18^\circ\text{K}$  temperature drop between the salt and the saturated steam.

Fabrication of the shell and tube exchanger would follow standard practices after the exchanger tubes receive the appropriate preparation and coating as will be determined by experiment.

Shell and tube exchangers are commonly made in a range of sizes having heat transfer areas from a fraction of a square meter to greater than a thousand square meters. The upper limit in size is usually determined by transportability rather than heat transfer considerations.

#### 4.3.2 Technical Issues

The technical issues that have to be considered when evaluating the feasibility of the shell and tube exchanger are few in number, but crucial to the success of the system. Table 4-4 lists these technical issues; they will be discussed further in conjunction with the test results.

Table 4-4. Shell and Tube Exchanger Technical Issues

- What conditions permit heat transfer without solids buildup on the heat exchanger tubes?
  - Salt to tube temperature differences?
  - Salt velocity?
  - Surface finish?
  - Surface coatings?
  
- What heat transfer rate can be sustained?
  
- Does slurry density effect heat transfer rate or salt buildup on the tubes?

#### 4.4 SHELL AND TUBE FLOWBY HEAT EXCHANGER EXPERIMENT

##### 4.4.1 Modeling

To model a heat exchanger, a differentiation must be made in the beginning between crucial parameters and those that can be scaled properly. For the purposes of determining if or how salt freezes to the tubes of a heat exchanger, it is important that the exchanger hydrodynamically approximate a full-size exchanger. A very common heat exchanger configuration uses outside diameter tubes spaced in a triangular pattern. This was chosen as the tube diameter and configuration to model.

In a large heat exchanger, as was considered for the large-scale system, the fluids in the course of a single pass through the exchanger will flow past several hundred rows of tubes as dictated by the tube sheets (baffles). It

becomes a monumental task to build a small heat exchanger model with hundreds of ranks of tubes, but the effect can be approximated by recirculating the flow repeatedly over the same tubes. This was the approach used for this experimental model.

Calculations indicated that approximately 1.2 percent of the salt would be solidified per pass through the experimental apparatus when flowing at 1.5 m/s and rejecting heat at the rate of 10 kW. Therefore, to achieve 20 to 30 percent solidification per pass, the salt must be recirculated 17 times before returning to the settling tank for separation.

A second effect that is of some importance in heat exchanger design is the hydrodynamic development of the flow field within the tube bundle. It is known that the heat transfer coefficients change significantly due to entry effects. To improve the approximation to fully developed flow, two rows of inactive tubes were inserted in the flow stream to develop the flow before it contacts the active heat exchange tubes and to reduce the number of piece parts that must be prepared when preparing new tube surfaces.

#### 4.4.2 Experiment Mechanization

The experiment, shown schematically in Figure 4-47, consists of an insulated mild steel tank that is heated externally with controllable guard heaters. A sump-type pump is mounted in the main storage tank such that the pump is always immersed in molten salt. A discharge line connects the salt pump to the flowby module. The module consists of a rectangular chamber with a tubular cross-flow heat exchanger, which extends across the test chamber.

The solid tubes are inactive; i.e., they do not transfer heat but are flow patterns. Fifteen tubes, 19 millimeters in diameter, are arranged to transmit

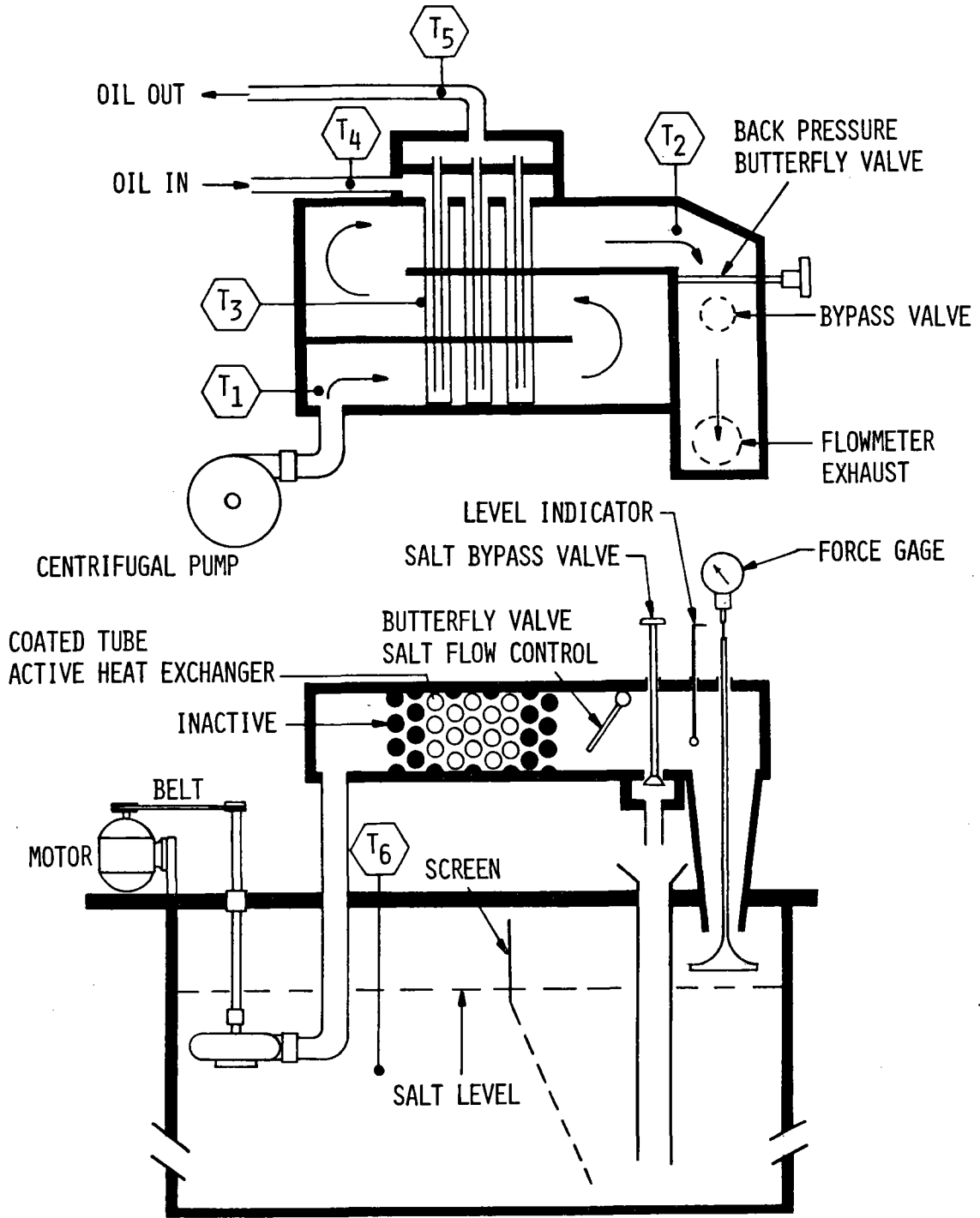


Figure 4-47. Flowby Heat Exchanger--General Schematic



heat and are shown by the plain tubes in Figure 4-47. These tubes are blanked off at the outboard ends and fed with cooling oil from a manifold through concentric internal tubes. Heated oil flows out through the outlet oil manifold.

The tube bundle is arranged with separator plates and, together with the oil manifolding, may be removed as a unit for servicing and changing of coated-tube elements. When the unit is inserted into the test chamber, salt flow, as shown by the arrows in Figure 4-47, passes through the tube bundle three times. Turning vanes maintain a proper flow pattern to simulate a large-tube bundle.

A discharge duct located above and at the outlet of the tube bundle and the salt stream channels the flow back to the tank. A butterfly valve regulates the back pressure and flow level in the channel. A force gauge attached to a contoured pintle measures changes in momentum of the salt slurry. By measuring the liquid height and by knowing the force, the salt slurry flow can be calculated. An electrical contact probe was planned to determine liquid levels in the flow meter. A small quantity of salt will be continually drained off the channel through a tube. This salt will flow into the main settling tank.

Figures 4-48 through 4-60 show the flowby module in various stages of construction and assembly. Figures 4-48 through 4-50 depict the elements that are assembled into the unit shown in Figure 4-51. The tube bundle shown in Figure 4-52 is next assembled into the shell shown in Figure 4-53. The resulting component is shown in Figure 4-54. Figure 4-55 shows the butterfly valve, return channel, and salt down comer. A cover, shown in Figures 4-56 and 4-57, and other auxiliary parts are assembled onto the shell to complete the flowby module. This module is attached to the salt tank as shown in Figure 4-58. Figure 4-59 is a picture of the flowby module after coating with 1-2 mil of electroless nickel plate. The module is then assembled into the awaiting shell, Figure 4-60.

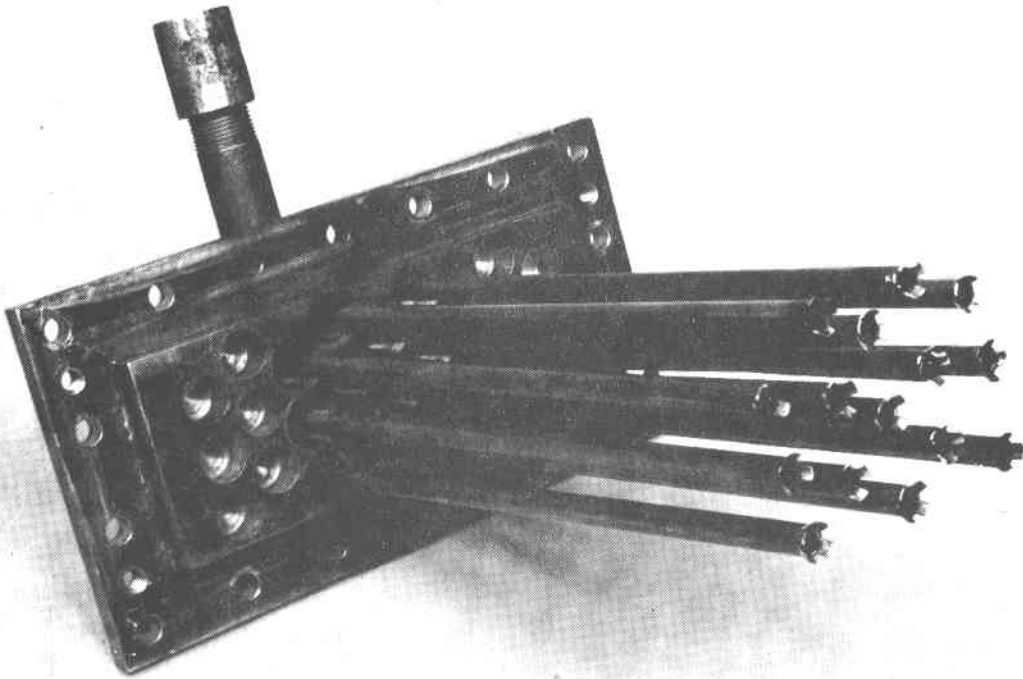


Figure 4-48. Flowby Module Tube Bundle with Inner Tubes Exposed

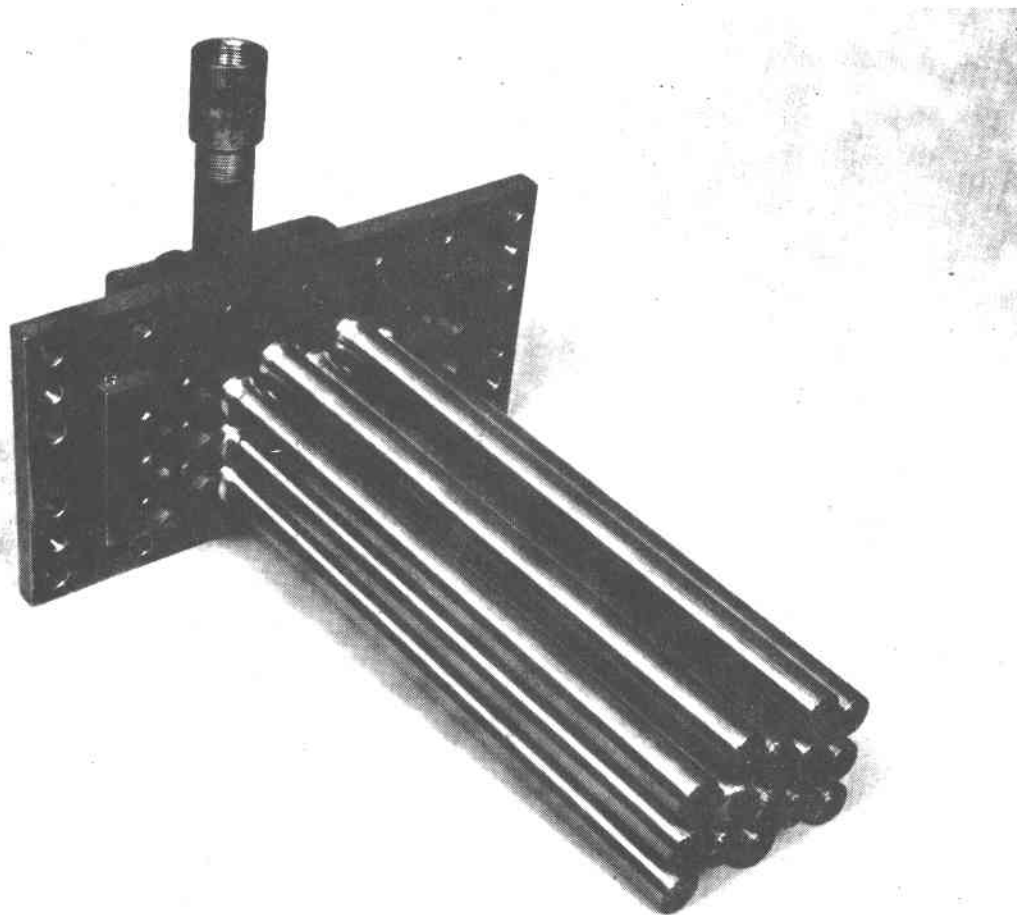


Figure 4-49. Flowby Module Tube Bundle with Active Tubes Installed

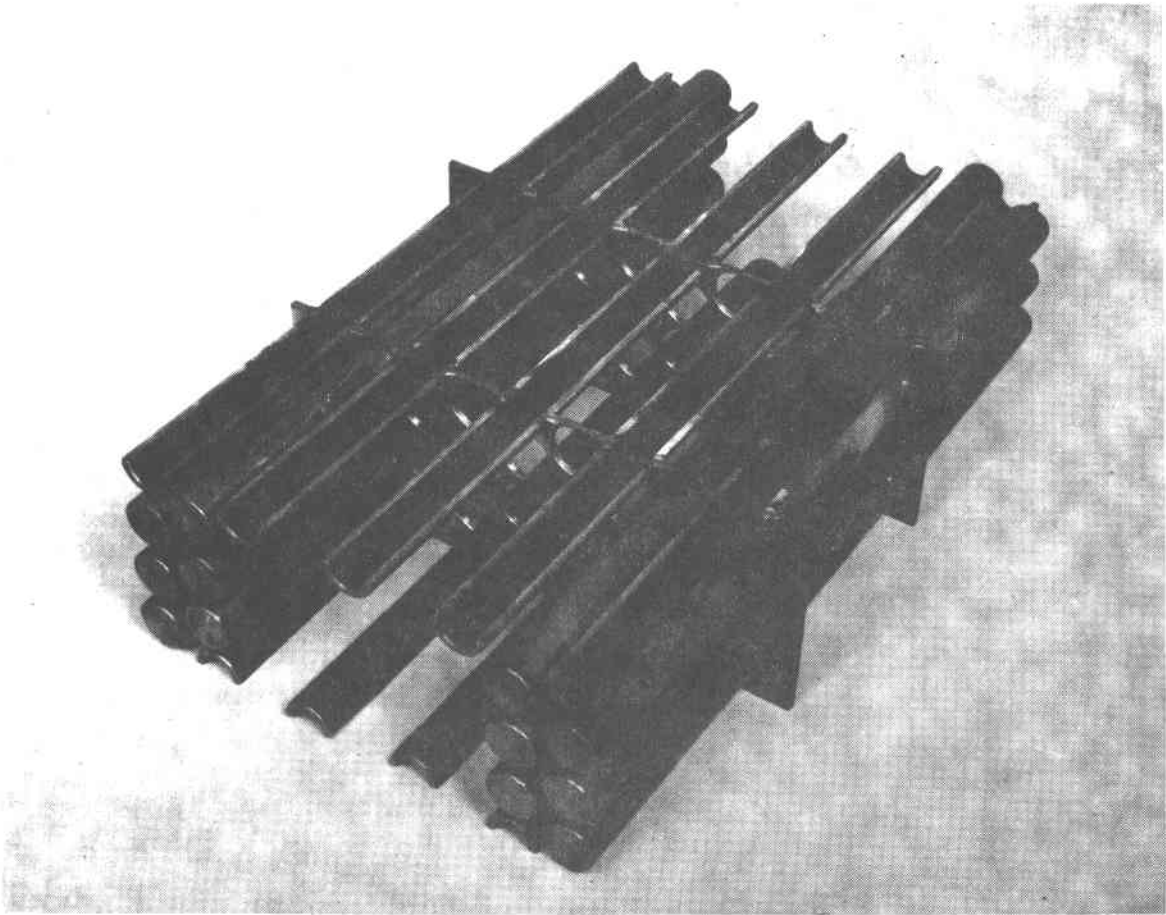


Figure 4-50. Flowby Module Tube Sheet with Inactive Tubes Installed

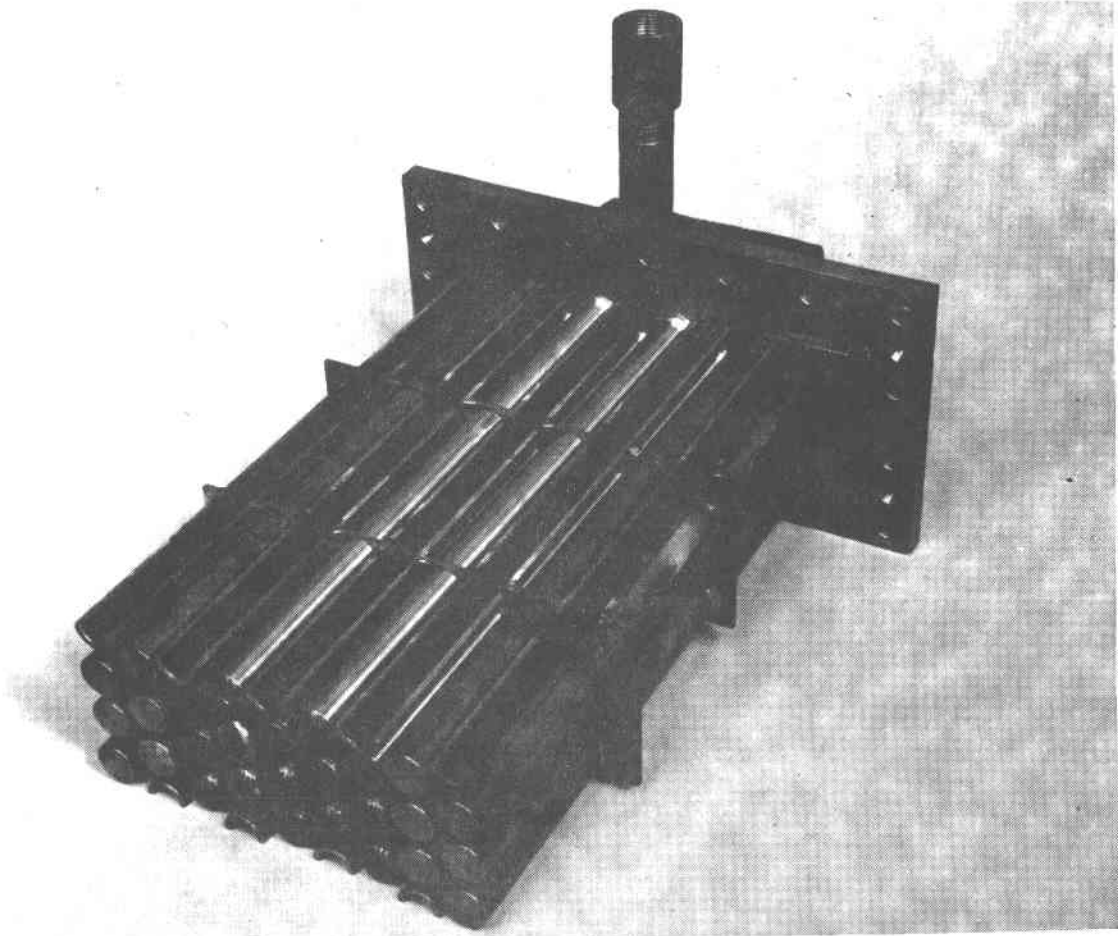


Figure 4-51. Flowby Module Tube Sheet Installed on Active Tube Assembly

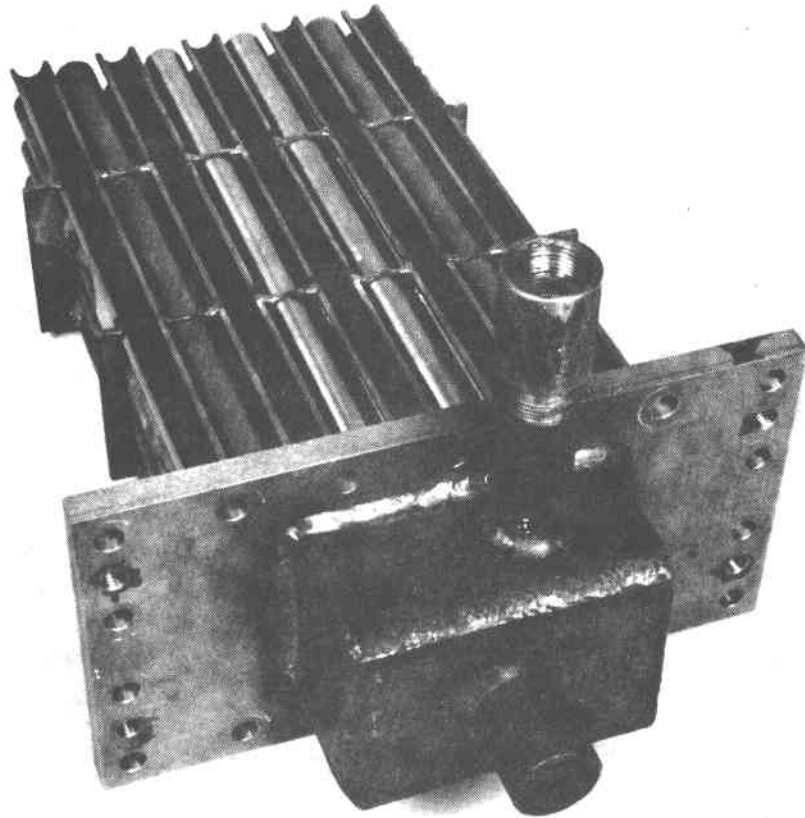


Figure 4-52. Tube Bundle from Manifold End

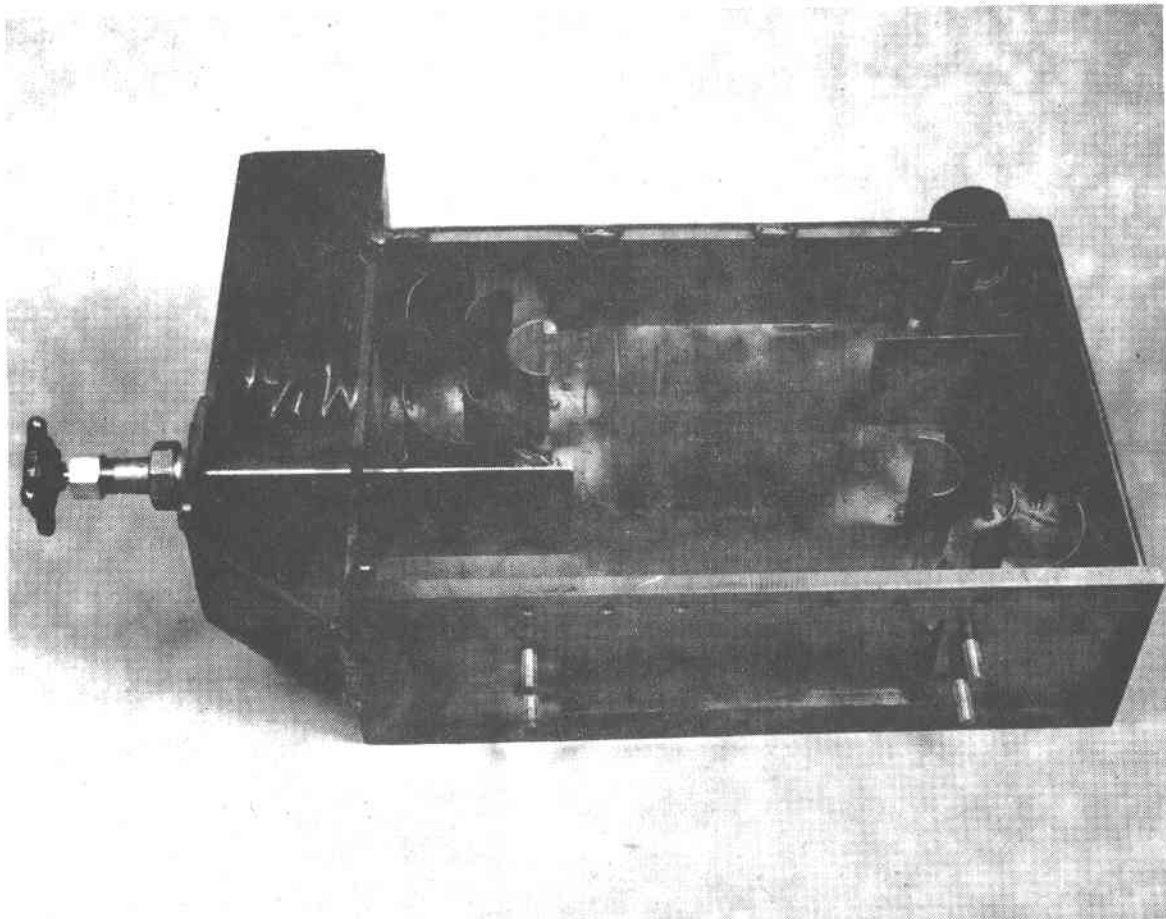


Figure 4-53. Flowby Module Heat Exchanger Shell with Cover Removed

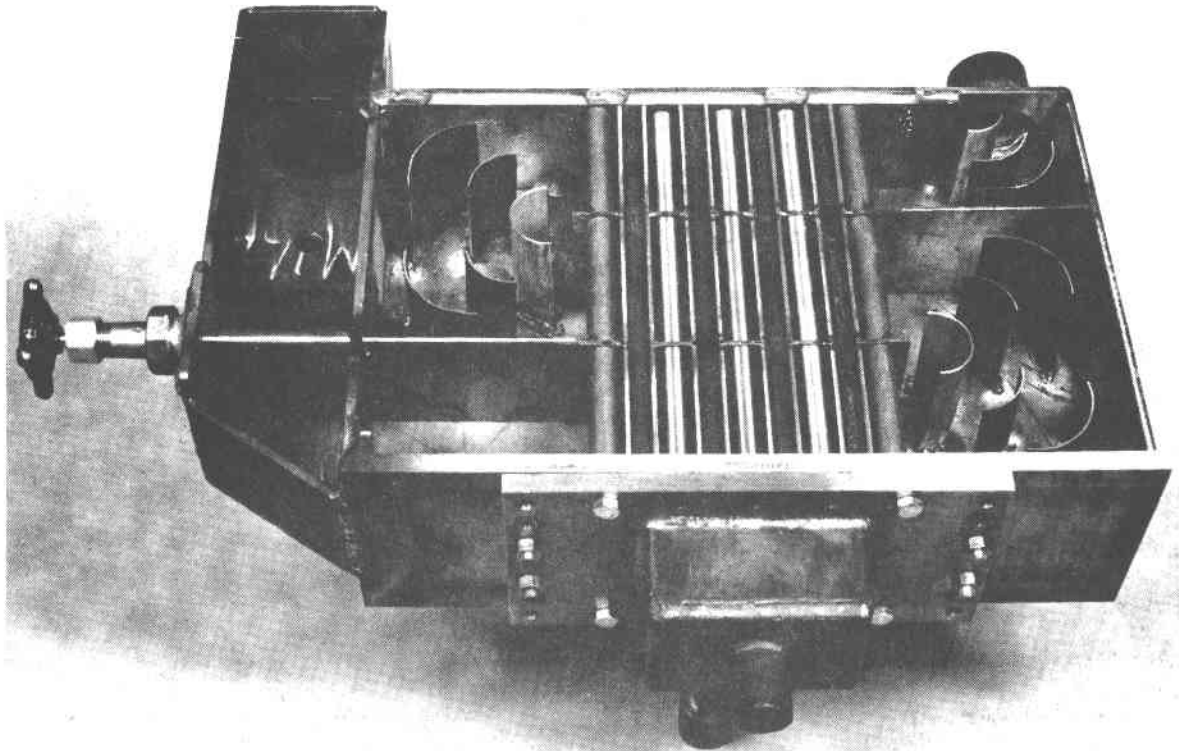


Figure 4-54. Heat Exchanger Shell with Tube Assembly Installed



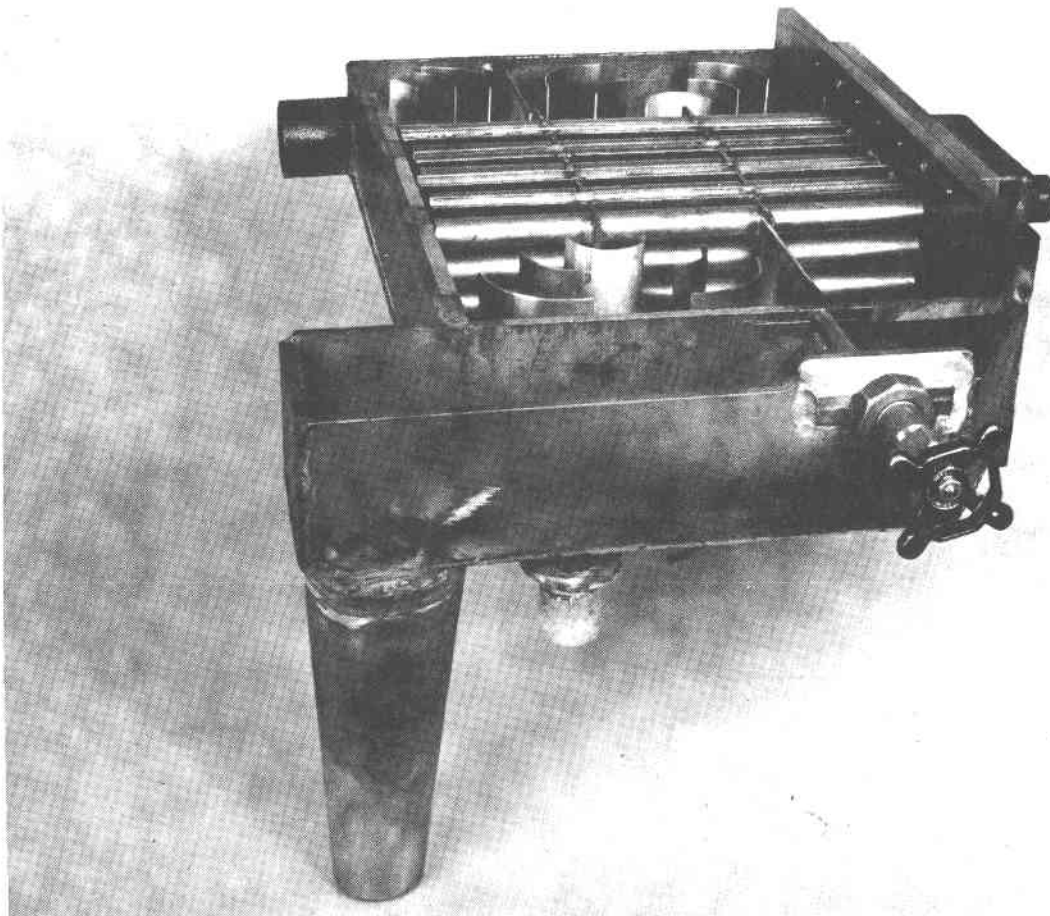


Figure 4-55. Side View of Flowby Heat Exchange Module

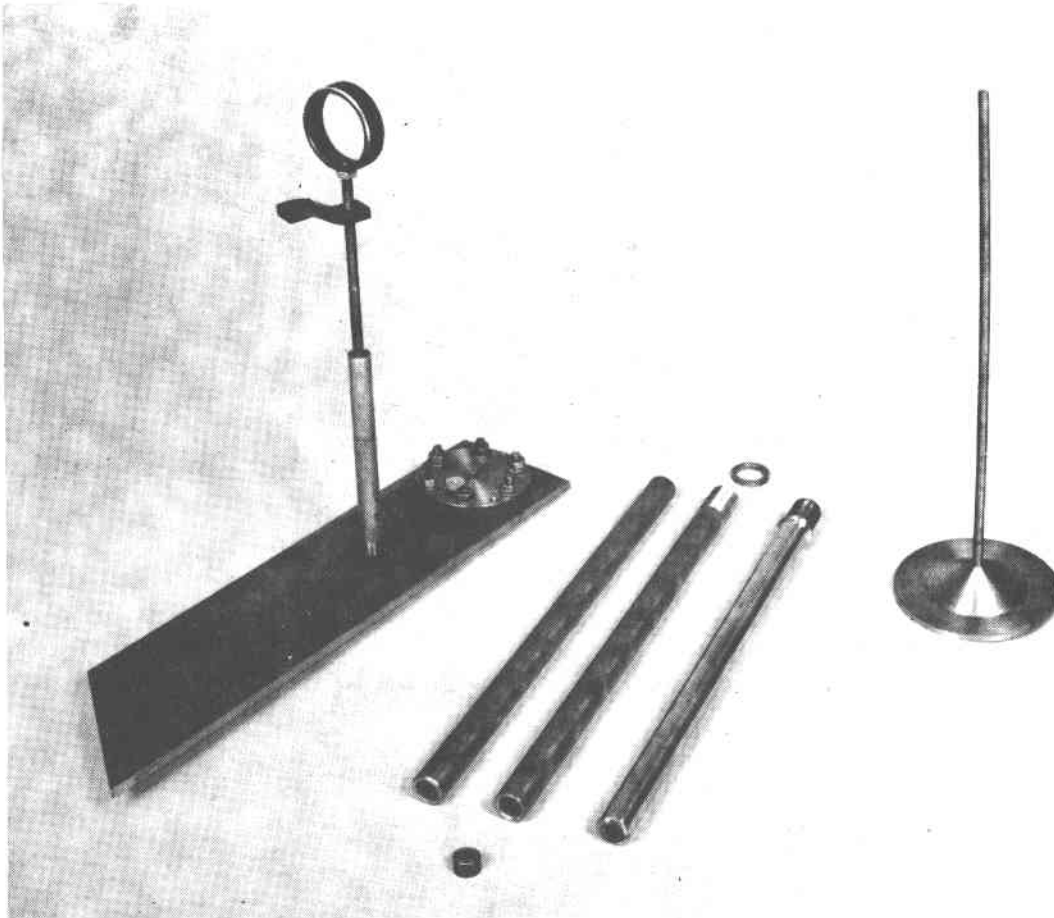


Figure 4-56. Auxiliary Parts of Flowby Module

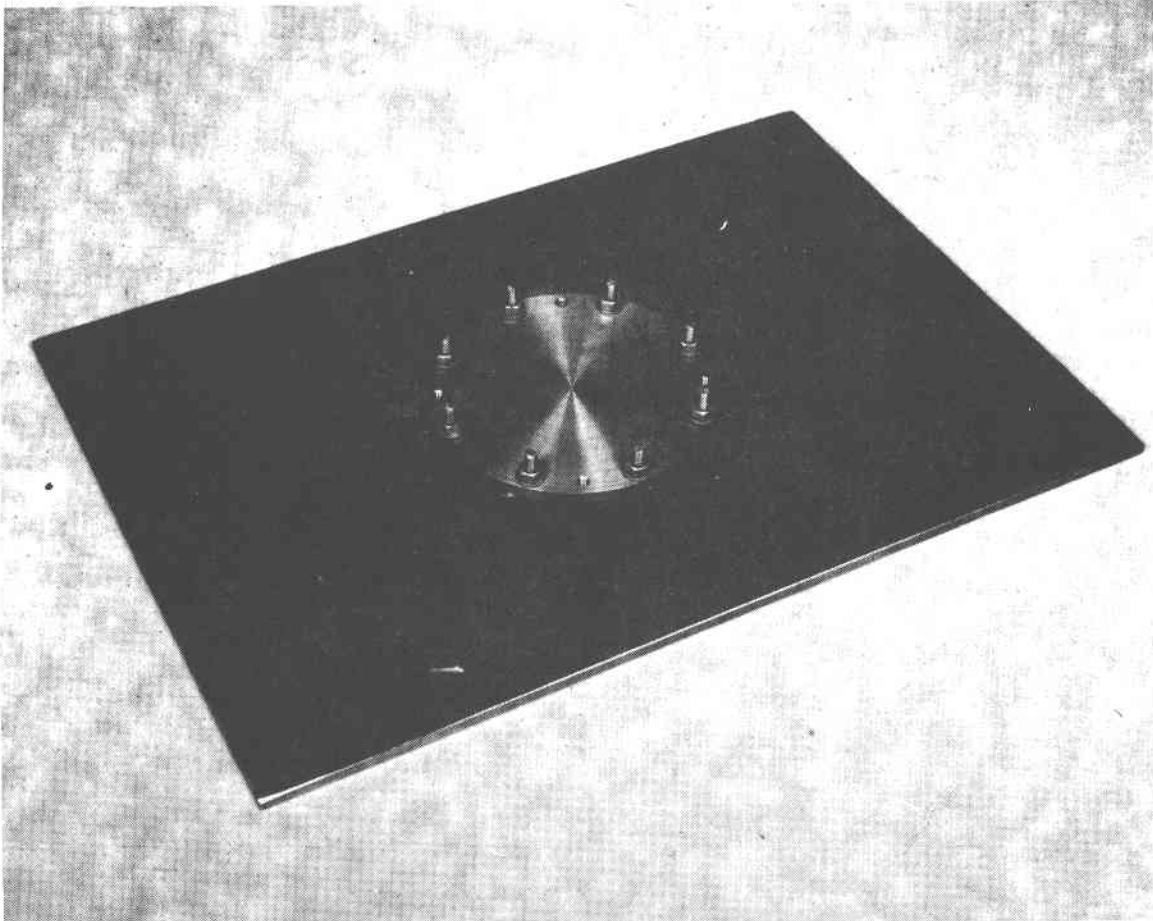


Figure 4-57. Flowby Module Cover with Viewing Port Flange

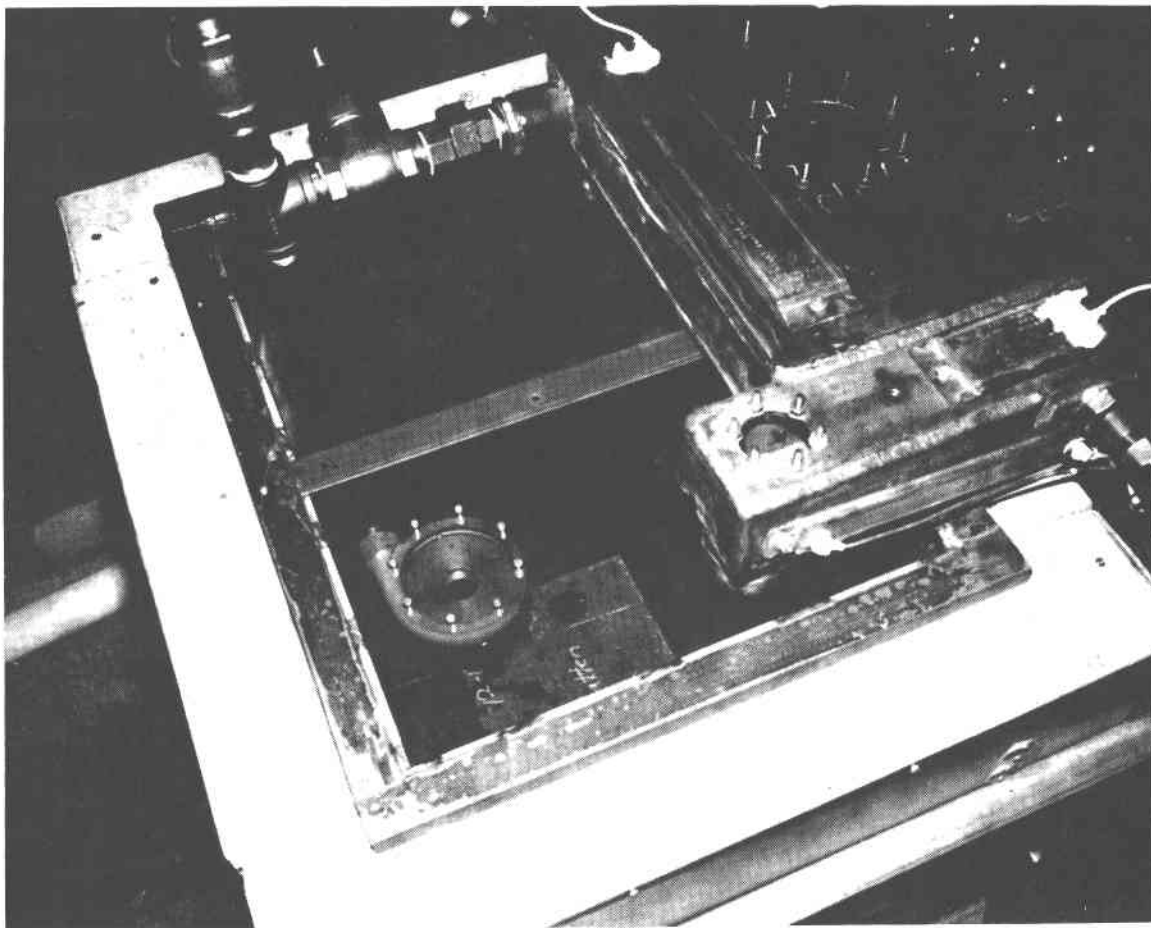


Figure 4-58. Flowby Module Installed Over Salt Storage Tank

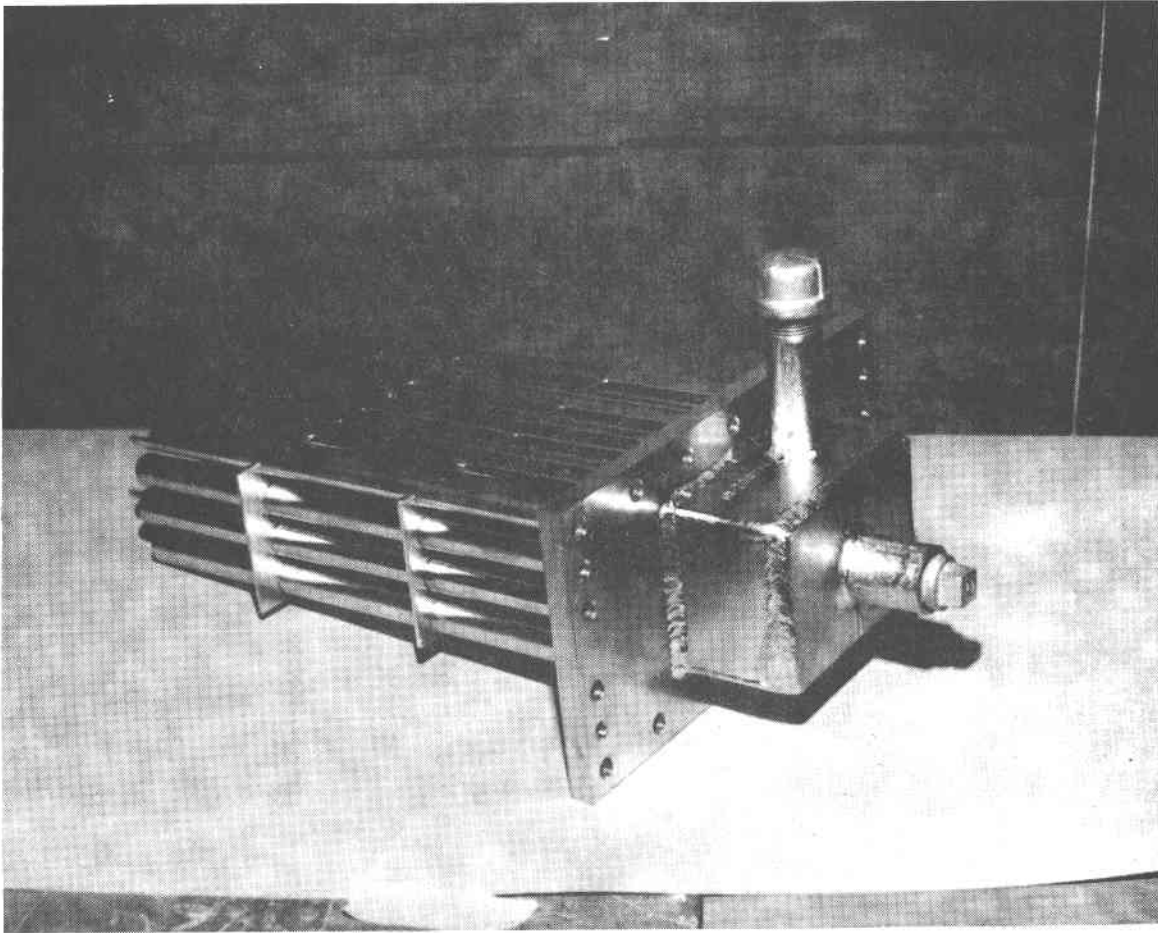


Figure 4-59. Nickel-plated Tube Manifold

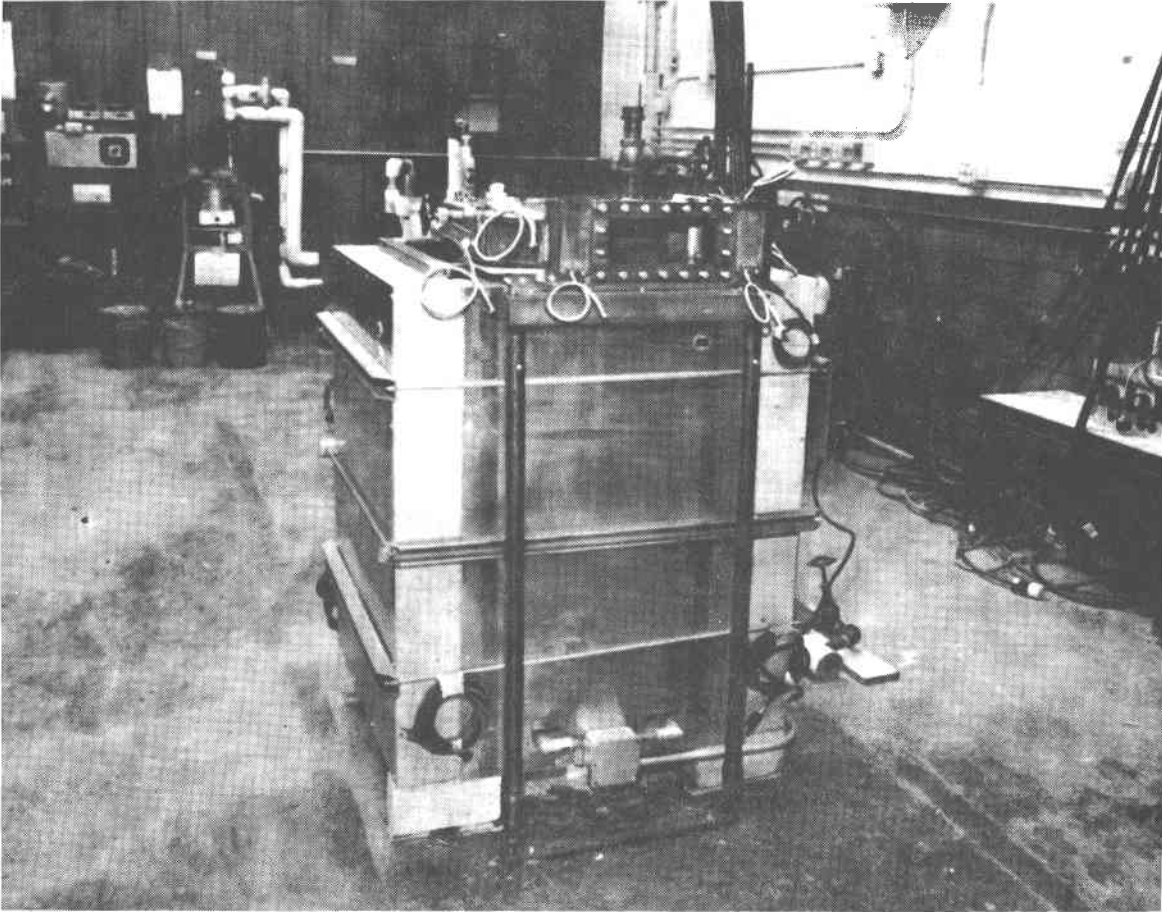


Figure 4-60. Side View of Salt Storage Tank with Flowby Module

## SECTION 5.0

## EXPERIMENTS TESTS, RESULTS AND DISCUSSION

## 5.1 TEST RESULTS AND DISCUSSION--REFLUX BOILER

Five tests were run with molten salt in the reflux boiler. These were basically centered around experimenting with various high pressure feedwater injectors and addressing water solubility and chemical compatibility issues. An evaluation of the test results indicates that a chemical degradation of the PCM was taking place due to a hydrolysis reaction of the injected water with the  $\text{NaNO}_3$ . This precluded the generation of sufficient quantities of steam to develop the expected saturation pressures corresponding to the PCM mixing temperatures. These tests and associated results are discussed below.

Test Run 127--The system was configured in this test for open-loop, pressure-demand, batch operations. The regulator at the water pumping unit was adjusted for 9.3 MPa (1350 psig) discharge from the water pump. This pressure corresponds to the saturation temperature of steam at the salt fusion temperature at 1350 psig, i.e.,  $307^\circ\text{C}$  ( $584^\circ\text{F}$ ). The water preheater was designed to receive high pressure feedwater and heat it to the saturation temperature for injection into the molten salt boiler. Ideally, the injected water would then be vaporized as it extracted the heat of fusion from the salt. Boiler pressure would rise to the feedwater pressure level, where a check valve would stop the flow. The generated steam then would be condensed by the oil flow and collected as high pressure water in the condensate receiver. Subsequent to the test, the high pressure water would be blown down through a water-cooled heat exchanger, and collected at atmospheric pressure in a holding tank.

Results from this run are shown in Figure 5-1. The injector was a long tube with 30 holes distributed along its length and was located above the molten salt level in the reflux boiler. The feedwater flow loop arrangement used in

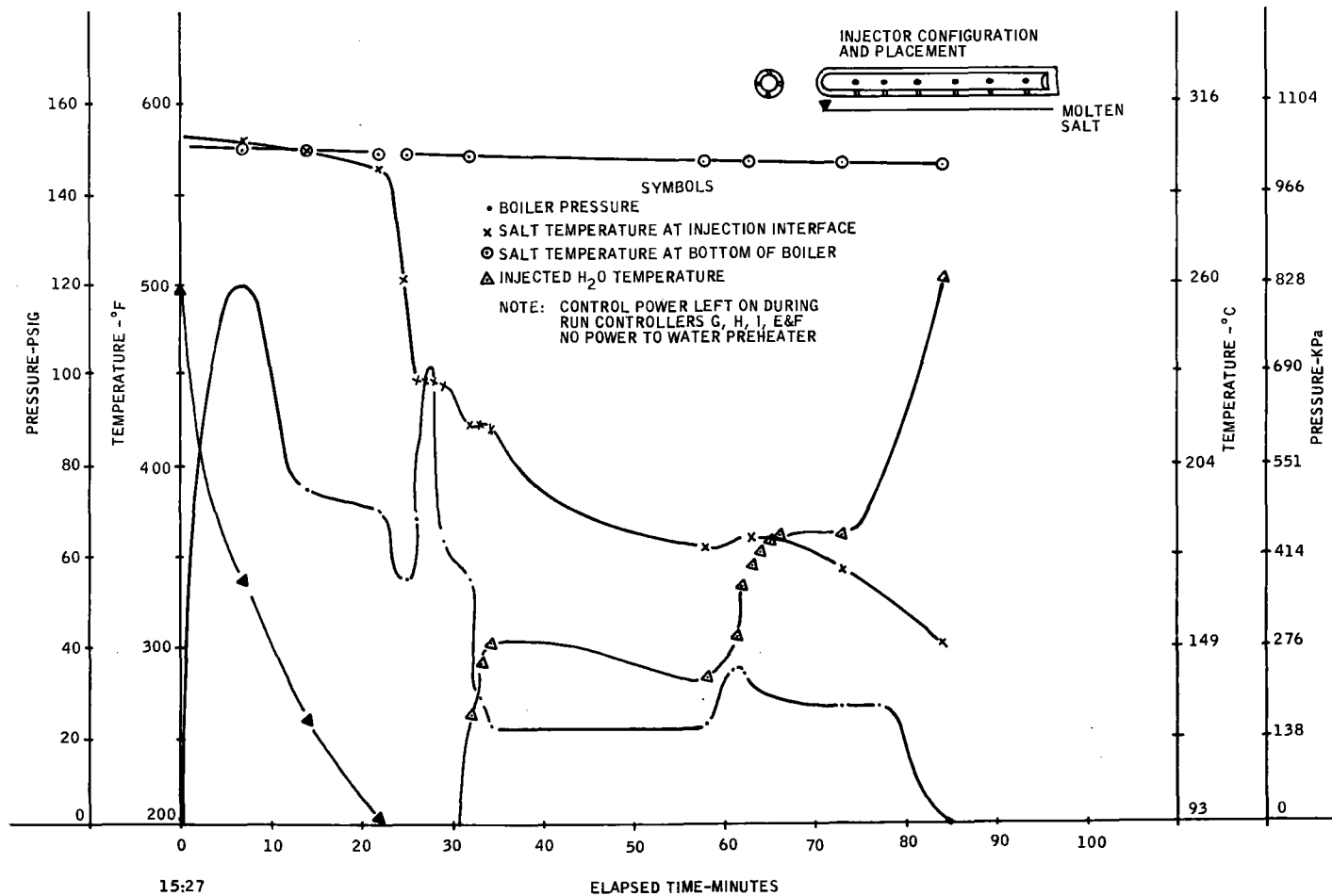


Figure 5-1. Reflux Boiler Experiment Time History Plot - Run 127



this test is shown in Figure 5-2. No heat was input to the water preheater as the unit had been recently repaired and conservative measures were being practiced. The plot shows the results from a series of cold water injections. The pressure increased from 0 to over 800 kPa in about 6 minutes. This was expected to be a rapid pressure response; instead it was quite sluggish. The amount of water injected was in excess of that required to fill the ullage at 9.3 MPa. High pressure subcooled feedwater was admitted to the boiler. At 30 minutes into the run (strip heaters located on the boiler tank were supplying heat to the salt--permitting the water injection experiment to be ongoing) additional high pressure-cold water was injected, and at this point the salt froze, crusted over, and the boiler was flooded with water. The boiler pressure fell to less than 276 kPa (40 psig) and the solid salt crusted at the interface was at 177°C (350°F).

Test Run 128--The results from this run are given in Figure 5-3. The basic purpose of this test was to determine if heated high pressure feedwater could be maintained to the boiler and if this would eliminate the crusting problem. It was anticipated that 9.3 MPa water at 308°C could be maintained if steam were generated at sufficient rates into the boiler ullage. The plot demonstrates the poor thermal response of the feedwater heater to feedwater flow. Notice that the feedwater was injected in a series of discrete spurts. This was done because it was feared that continuous injection of subcooled feedwater would cause freezeup and flooding. It was also clear that a metering valve was required downstream of the check valve as the standard gate valve was too coarse for accurate control.

Heat rates of 14.5 kW(t) at 5.5 MPa (800 psig) were achieved in this test, as shown in Figure 5-4. This compares with a design requirement of 10 kW at 9.3 MPa or 1350 psig. If the difference in heats of vaporization at the two pressures is taken into account, a heat rate capability of 1.7x design was demonstrated. The plot also demonstrates that the saturation temperature corresponding to the boiler pressure closely approximates the condenser tube

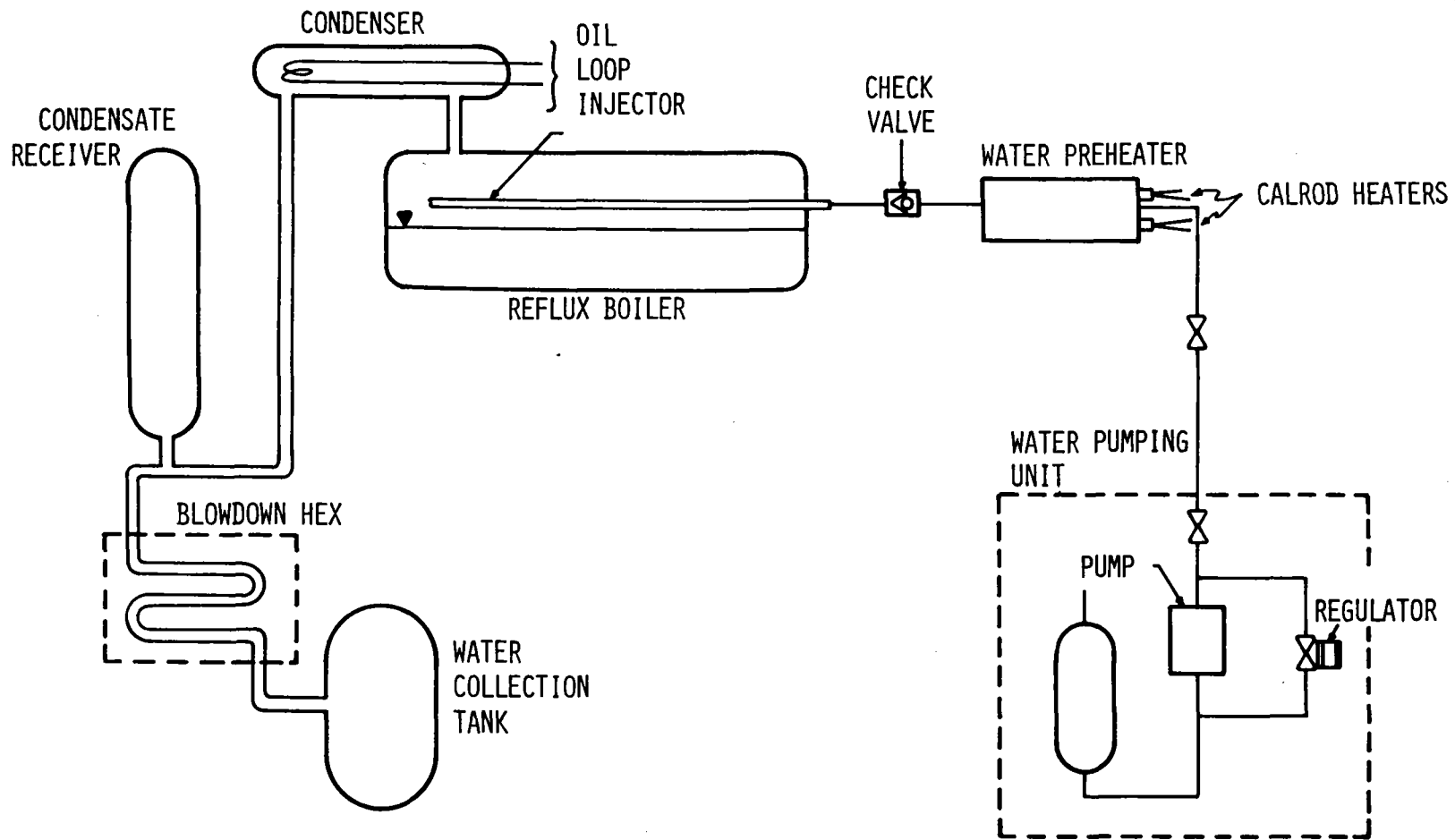


Figure 5-2. Feedwater Injection Flow Loop

RUN 128  
11/18/79

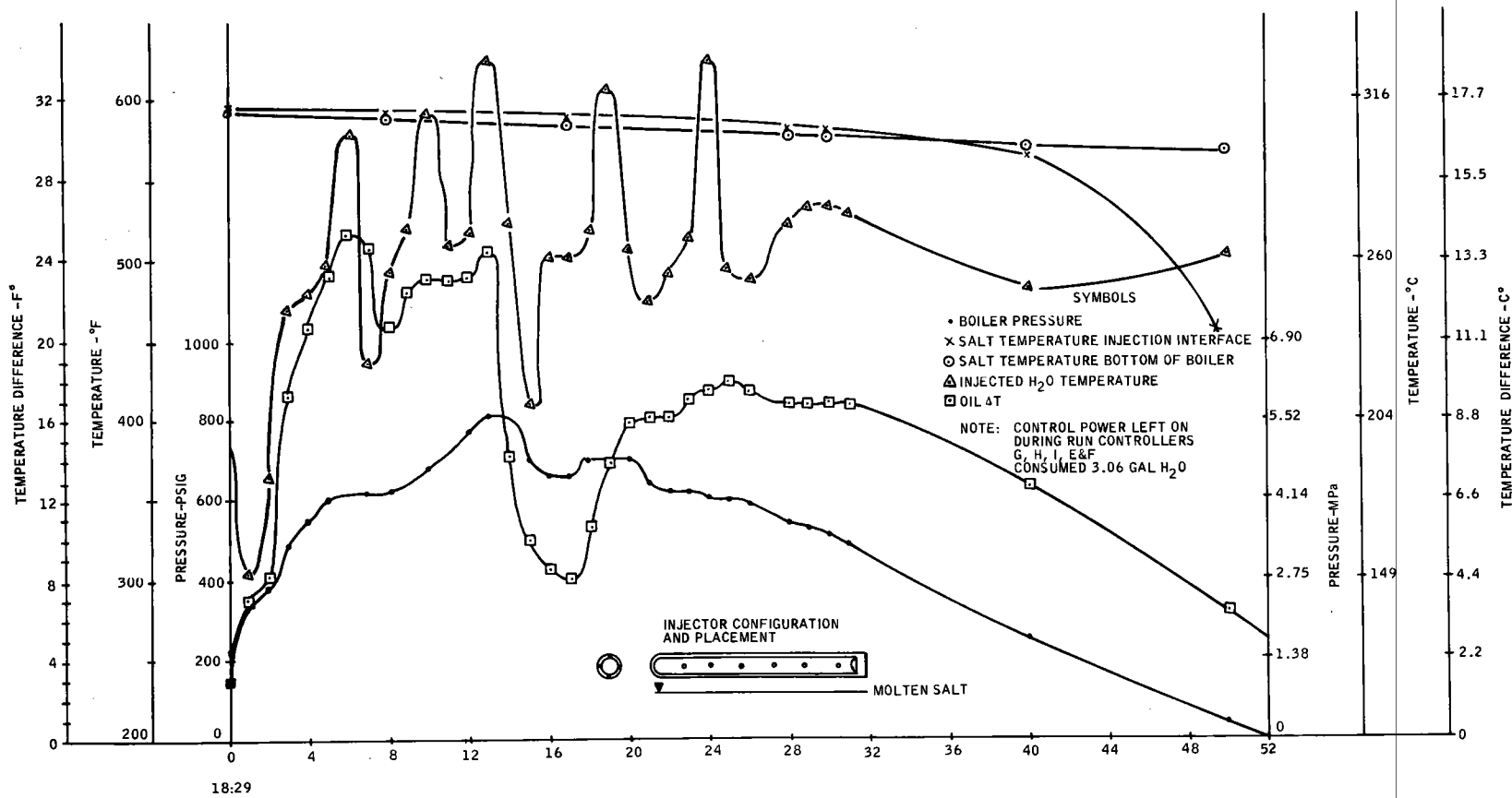
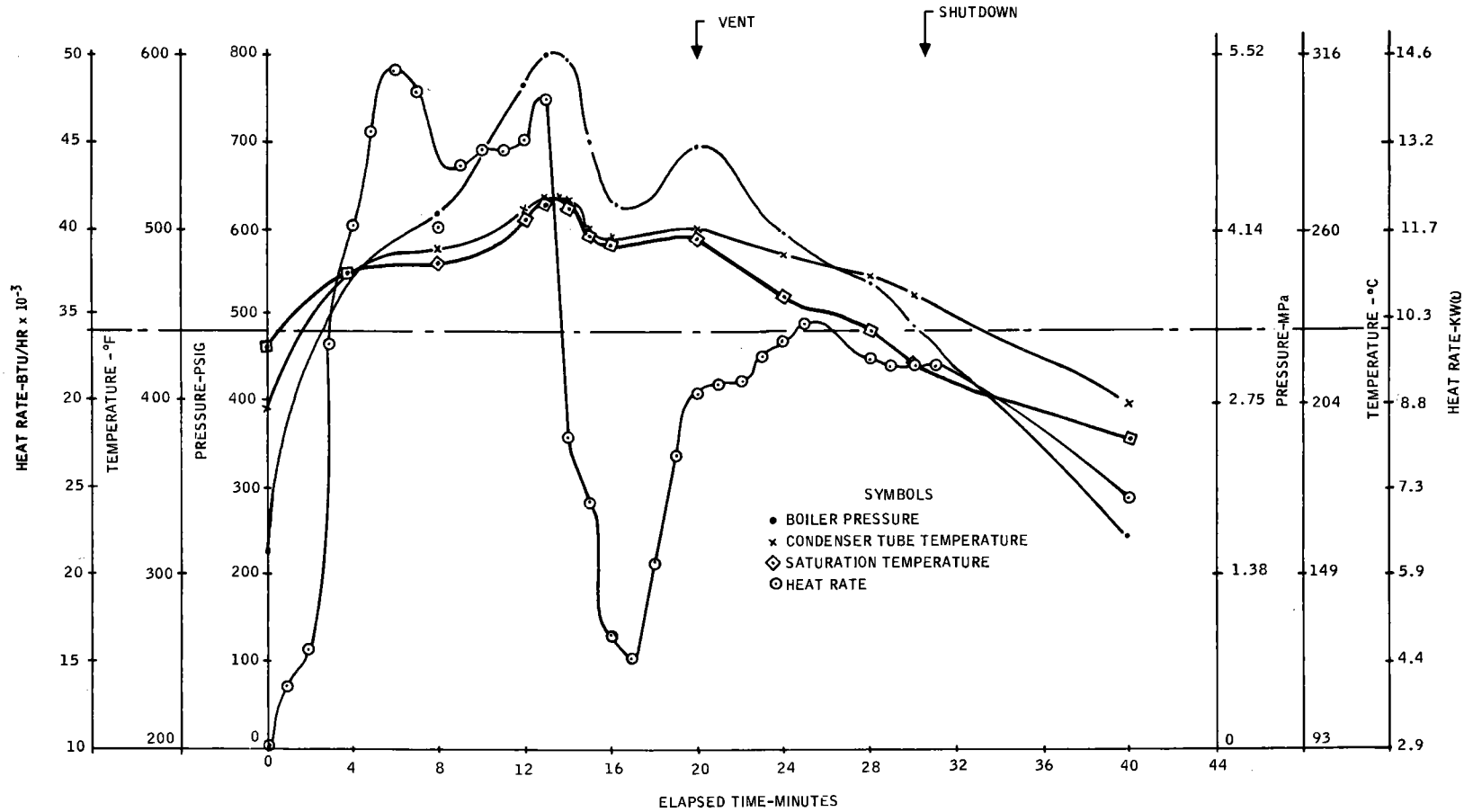


Figure 5-3. Reflux Boiler Experiment Time History Plot - Run 128

RUN 128  
11/18/79



9-5

Figure 5-4. Reflux Boiler Experiment Time History Plot - Run 128 (Continued)

temperature. It was concluded that the pressure did not build up to the expected 9.3 MPa level because the water was not being mixed with sufficient volume of molten salt. It requires 3x volume of salt per volume of saturated water at 9.3 MPa to effect proper heat exchange. (The possibility of a chemical reaction between the water and salt mixture was not suspected seriously at this time primarily due to information obtained on the operating experience of the Olin Chemicals  $\text{NaNO}_3$  Production Plant at Lake Charles, Louisiana.) In addition, from the plot it was reasoned that the low condenser tube temperature was allowing condensate to accumulate at a rate to preclude continued boiler pressure buildup. No attempt was made to evaluate the total energy discharge since operating pressure and injection technique were still indeterminate.

At completion of this run an attempt was made to remove the high pressure condensate and measure the weight for a heat balance. Inspection of the apparatus revealed that the vent line was plugged; later inspection revealed that sodium nitrate carryover from the boiler was causing the blockage. The carryover was in the form of dissolved solids in the water that flooded the boiler and condenser as a result of the boiler freezeup, which started at time = 40 minutes. It appeared that the freezeups were being caused by (1) admitting subcooled feedwater into the boiler, (2) admitting the water through a distributed spray type injector above the molten salt surface, and (3) lack of mixing at the interface. This led to certain modifications and the conduct of the next test run.

Test Run 026--A new injector was supplied for this run. The distributed spray tube was replaced by a two-orifice, downward oriented ( $45^\circ$  to molten surface) nozzle providing a high velocity jet action onto the molten salt surface. In addition, the boiler was pressurized to 9.7 MPa (1400 psig) at the onset of the run with  $\text{GN}_2$ . The results of the run are shown on Figure 5-5.

Notice that there was no tendency of the salt to freeze up. However, the rate of heat removed by the oil (oil  $\Delta T$ ) reached a maximum of about 5 kW at time = 36 minutes. The feedwater temperature fluctuations were lessened with improved

RUN 026  
11/26/79

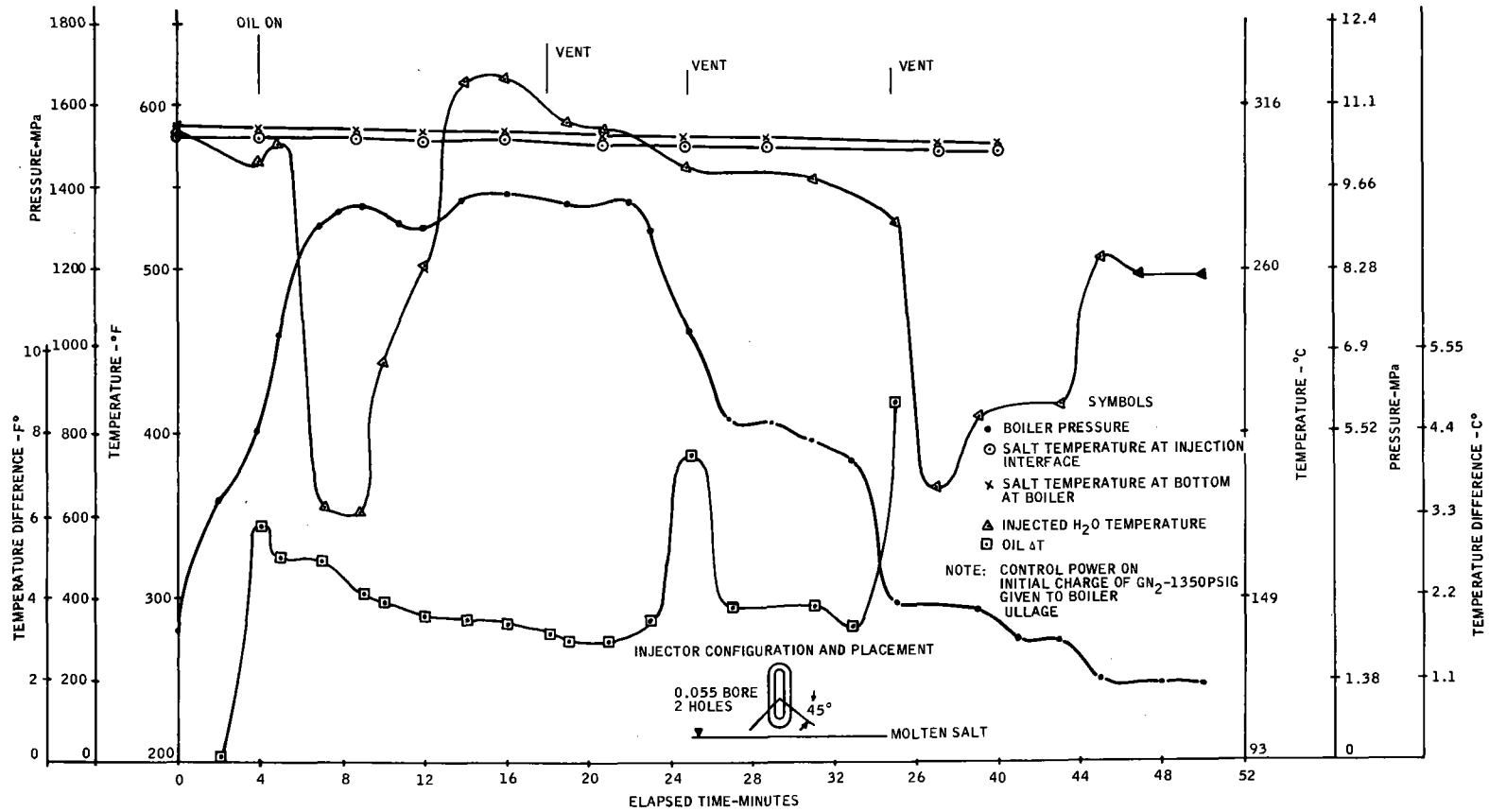


Figure 5-5. Reflux Boiler Experiment Time History Plot - Run 026

operating procedures. The partial pressure of water based on the condenser tube temperature (180 to 216°C) was between 1.1 and 2.3 MPa. This low temperature was caused by the loss of oil loop temperature during the run. The run was aborted.

Test Run 027--This run was an attempt to correct the operating deficiency on the oil loop temperature control and to start the run without the  $\text{GN}_2$  pre-charge, incorporate a control valve at the injector, and obtain more data on the new injector. The results of this run are shown in Figure 5-6. During the run a sluggish response of boiler pressure to injected feedwater became apparent. The series of injections during the first 20 minutes into the run produced less than 138 kPa of boiler pressure. Since only 0.7 to 1.5 kg of  $\text{H}_2\text{O}$  vapor at 260 to 304°C is required to produce an ullage pressure of between 4.8 and 9.3 MPa, the degree of chemical inertness of  $\text{NaNO}_3/\text{NaOH}$  and water mixtures at high temperatures and pressures began to be suspect. At 20 minutes into the run, with the injector valve open, the salt in the boiler began to freeze in response to the sudden decrease in feedwater temperature. It took approximately 10 minutes for the water preheater to provide temperature recovery. In the meantime, the boiler pressure increased to almost 2.5 MPa. Unfortunately, the characteristics of the control valve were poor beyond one-quarter turn, and approximately 2 l/m (0.5 gpm) of water was being pumped into the boiler. The preheater simply could not keep up at that rate. Essentially no heat was removed by the oil flowing in the condenser at the time. This was due to the condenser tube temperature being at a higher temperature than that of the saturated water vapor corresponding to the boiler pressure; this precluded condensation. Under these conditions the boiler pressure settled off at 2.75 MPa.

Test Run 011--The purpose of this run was to test the performance of the unit with a new jet injection placed below the salt level (about 7.6 cm). A new control valve was installed for better metering of the feedwater. It was planned to keep the condenser tube at a high temperature (about 300°C) to preclude con-

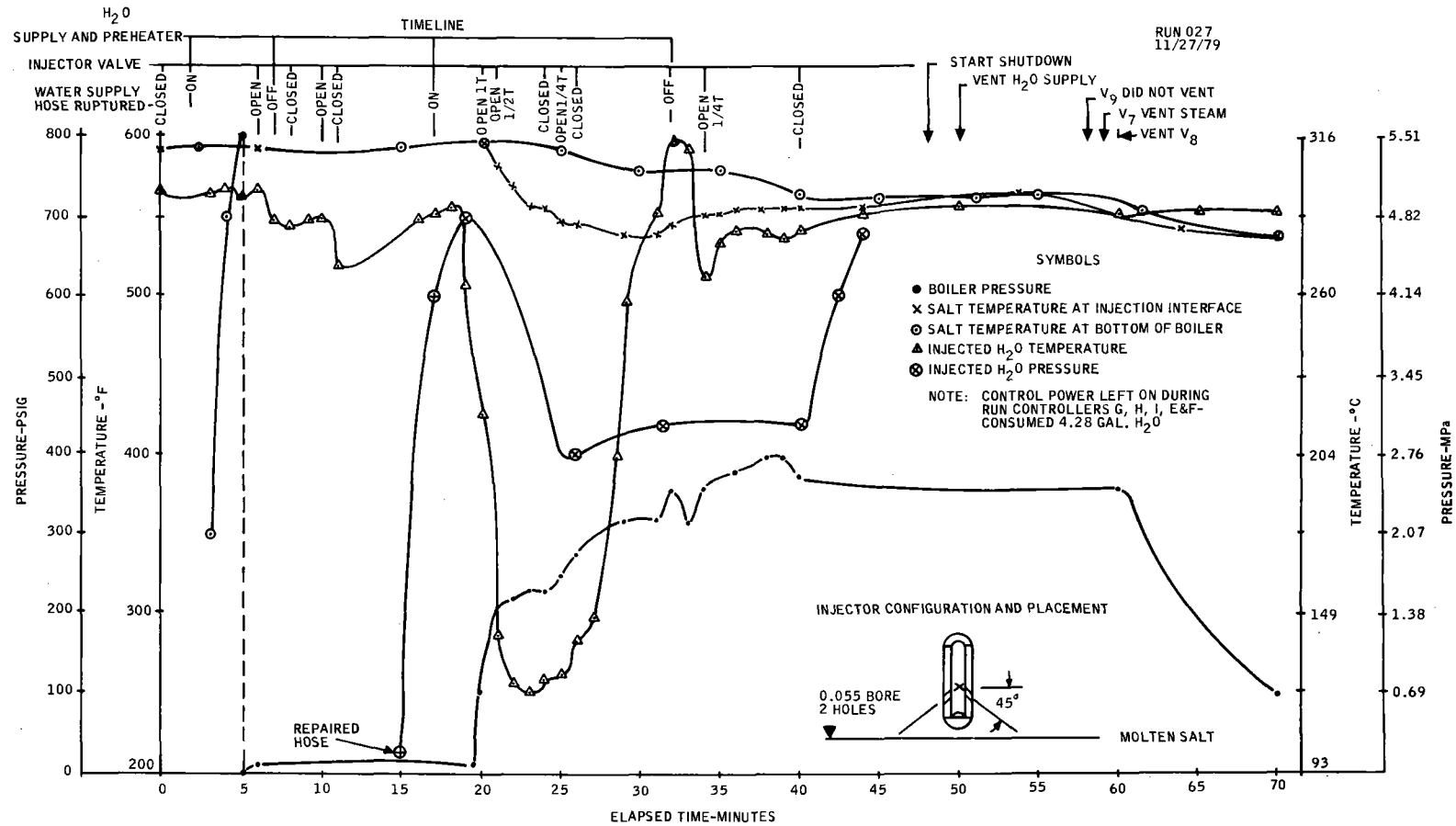
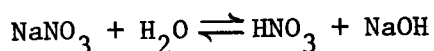


Figure 5-6. Reflux Boiler Experiment Time History Plot - Run 027



densation until the boiler pressure rose to 8.6 MPa to ensure a good "head of steam." Figure 5-7 is a plot of the significant parameters observed during the run. Again the sluggish reaction of boiler pressure to water injection was observed.

A series of 14 discrete injections were made over the operating period. The maximum pressure achieved was 2.6 MPa. The water injection pressure and temperature were oscillating, but the control band was improved. Notice that the condenser tube temperature was maintained at a high level to preclude steam condensation. This allowed the boiler and system ullage pressure to increase at the maximum rate based on the heat and mass transfer between the salt mixture, the feedwater, and its vapor. At the end of the run, 13.6 liters of distilled water (ambient temperature) had been consumed in the experiment. The system was shut down and sealed and allowed to cool to room temperature. An inventory of the water was made. Approximately 3.6 liters were contained in the water preheater and lines with 1.1 liters in the condensate receiver, and 0.9 liters in the internal lines. The net difference of 8 liters was contained in the boiler. Since 1.5 liters of water vapor is sufficient to generate an ullage pressure of 9.3 MPa at 304°C, it was concluded that the water either (1) hydrolyzed the salt mixture, i.e.,



(2) dissolved in the salt mixture, or (3) formed a chemical complex.

Subsequent chemical analysis indicated that the PCM in the boiler was 70 percent (weight) NaOH with mixtures of iron oxides,  $\text{NaNO}_3$  and water making up the remainder. A sample of this PCM was evaluated for chemical complex formation with negative results.

Therefore, the first two degradation mechanisms were investigated. First was the hydrolysis reaction of sodium nitrate with water to form nitric acid and

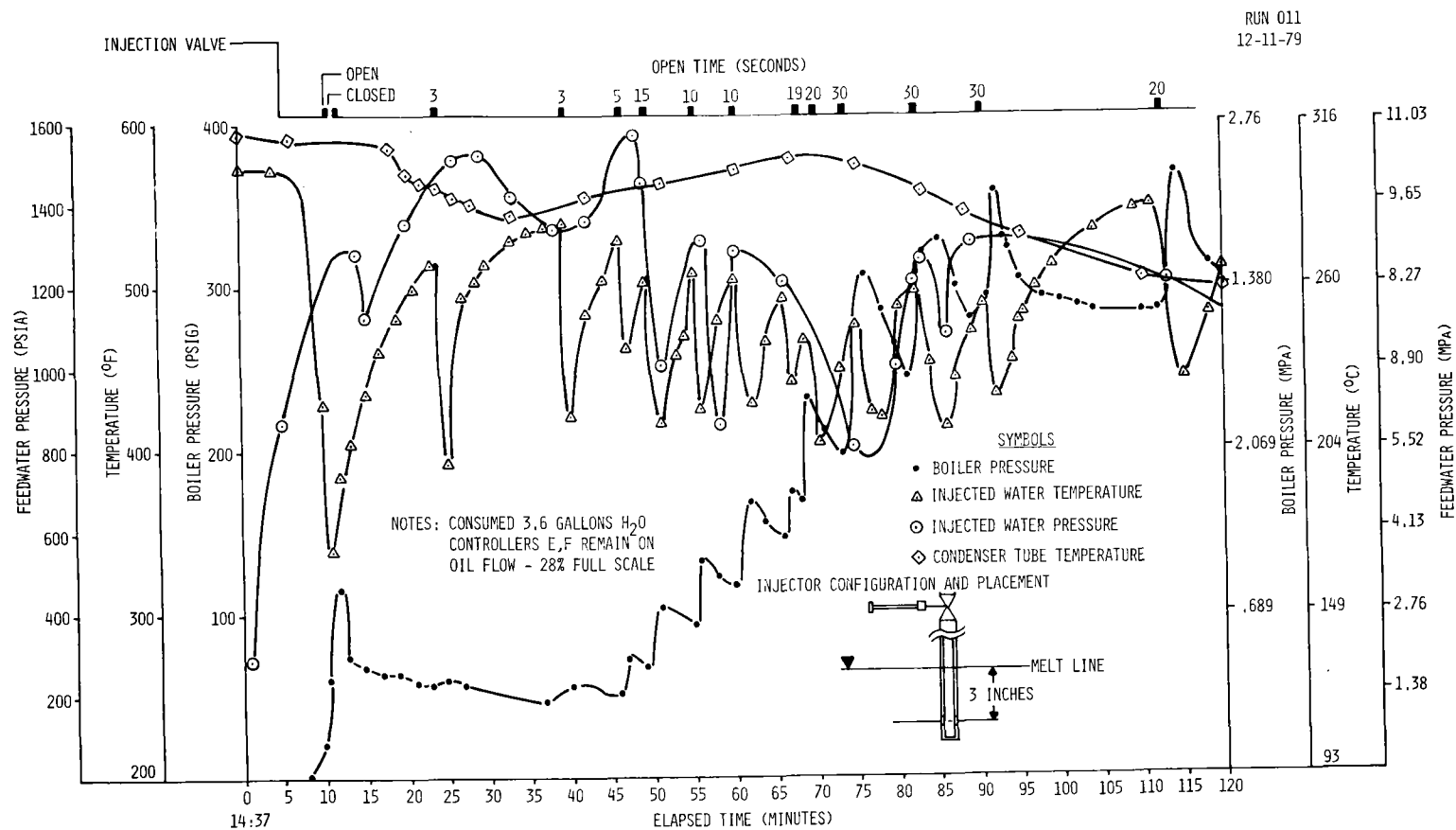
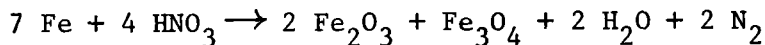


Figure 5-7. Reflux Boiler Experiment Time History Plot - Run 011

sodium hydroxide, followed by the reaction of the nitric acid with the container walls



Reaction (2) was postulated because iron oxides were present in the mixture. Based on the information obtained from reviewing the Sodium Nitrate Production Plant at Lake Charles, Louisiana, it was generally deduced that the Gibbs free energy of the hydrolysis reaction (1) was positive and by applying LeChatelier's Theorem, pressure should not influence the reaction. Therefore the removal of the nitric acid was necessary to cause reaction (1) to proceed to any appreciable extent.

The second mechanism consisted of a series of reactions involving the thermal decomposition of  $\text{NaNO}_3$  into  $\text{NaNO}_2$ ,  $\text{O}_2$ ,  $\text{Na}_2\text{O}$ ,  $\text{NO}_2$  and  $\text{NO}$ , followed by the reaction of  $\text{Na}_2\text{O}$  with water to form  $\text{NaOH}$ , i.e.,



It was realized that the thermal decomposition of  $\text{NaNO}_3$  was not normally significant until much higher temperatures were reached; however, the iron in the container walls might have been acting as a catalyst.

The change in Gibbs free energy for the reaction in which the products are sodium hydroxide liquid and nitric acid vapor was computed to be -4.7 Kcal, corresponding to an equilibrium constant of 59.

A thermodynamic analysis of the decomposition of sodium nitrate into sodium nitrite and oxygen indicated that this reaction was not an important mechanism in the degradation of the salt. The equilibrium constant for reaction (3) was  $7 \times 10^{-2}$  at  $550^{\circ}\text{C}$ .<sup>1</sup> Assuming that the heat of reaction was not a function of temperature, an equilibrium constant of  $2 \times 10^{-7}$  at  $310^{\circ}\text{C}$  was obtained.

This corresponded to a  $\Delta G_{\text{rxn}}$  of +17.7 Kcal. The equilibrium constant was small; therefore, the decomposition reaction was not considered an important factor in the degradation of the salt.

The equilibrium constant for the hydrolysis reaction was calculated to be 0.15 if the final state of nitric acid was assumed to be liquid. Even at this, a considerable degradation in salt properties could occur.

Therefore, the hydrolysis of the sodium nitrate and water to sodium hydroxide and nitric acid appears to be an inescapable result of operation in a system where the salt and water are in direct contact. The thermal decomposition of the sodium nitrate does not appear to contribute to the salt degradation. Additionally, a reduction in the pressure of the steam produced in the reflux boiler below that which corresponds to saturation conditions appears likely, although the exact magnitude of the reduction cannot be easily calculated. Because the hydrolysis reaction of water and sodium nitrate appears to be an inevitable result of their contact at high temperatures, further research into a system using sodium nitrate and water in direct contact would not be useful. However, it may be possible to find other materials combinations which are chemically compatible and capable of performing in direct contact in the reflux boiler.

---

<sup>1</sup>Silverman, M.D. and Engel, J.R., Survey of Technology for Storage of Thermal Energy in Heat Transfer Salt.

## 5.2 TEST RESULTS AND DISCUSSION--SHELL AND TUBE FLOWBY

Four tests were run with the Shell and Tube Flowby Module. As a prelude to these tests a series of experiments were conducted on candidate coatings to evaluate the most promising types. An electroless nickel coating was selected as the primary candidate with chrome metal and Teflon, Ryton plastic as alternates. However, all of the tests with the Flowby Module were conducted with the nickel-coated tubes. Tests planned with the other coatings were not conducted because of schedular and financial program constraints. The four tests conducted with the Flowby Module were made over a range of salt velocities and overall temperature differences. The salt flow to the heat exchanger was controlled manually. The temperature difference was varied by adjusting temperature controllers in the oil loop. Salt velocities of up to 1 m/s and temperature differences of 30 K<sup>o</sup> were achieved. An evaluation of the results indicated that the PCM adhered to the outside of the nickel-coated tubes under all conditions of salt velocity and  $\Delta T$  tested. The electroless nickel coating did not provide an antistick surface. The results from each test are discussed below.

Run 1--In this run the salt temperature was well above the freezing point. The oil temperature, which initially was at 304<sup>o</sup>C, was lowered to 271<sup>o</sup>C. Figure 5-8 shows a plot of heat rate, overall coefficient, and  $\Delta T$  versus time. Figure 5-9 shows a plot of the salt coefficient versus calculated temperature difference between the salt and the tube. The salt flow rate was estimated at 60 l/m, with a corresponding velocity of 0.6 m/s. Due to difficulty with the force gauge and the bubble tube for measuring salt flow, this value was estimated from the heat rate and temperature drop in the salt during sensible heat extraction. In the sensible heat region, the salt heat transfer coefficient ranged between 2128 and 3080 Wm<sup>2</sup>-<sup>o</sup>K. The higher coefficient was obtained when the tube temperature was above the freezing temperature of the salt. When the salt approached its initial freezing temperature, the salt coefficient decreased with increasing  $\Delta T$ . The heat rate, when the tube temperature is

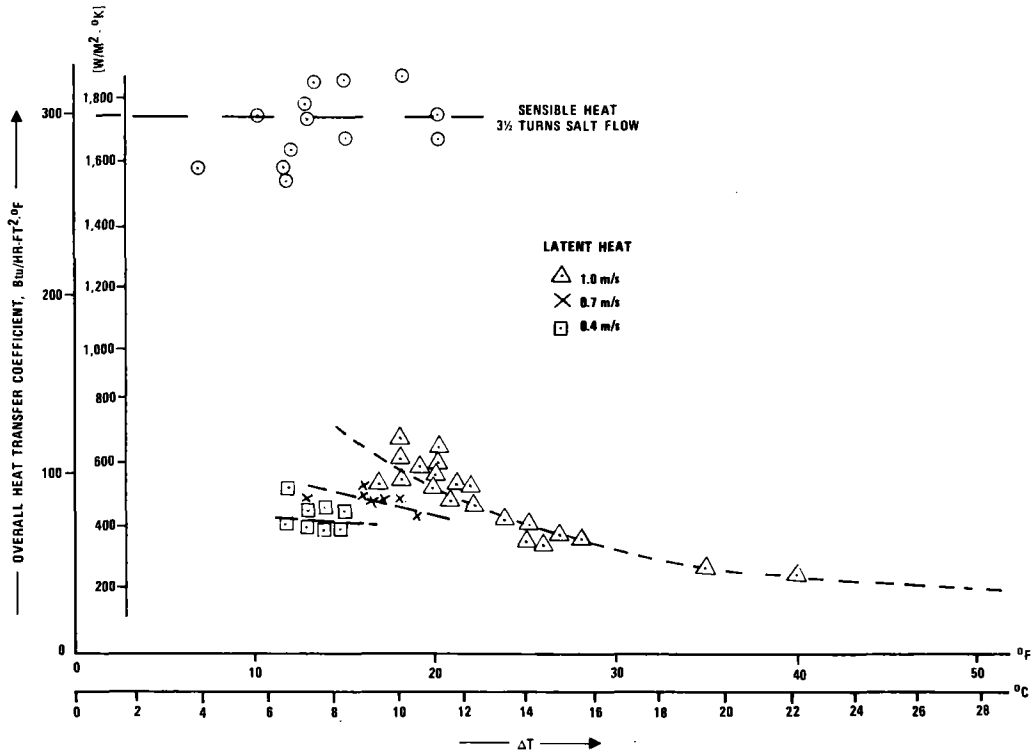


Figure 5-8. Flowby Experiment - Run 1, Overall Coefficient versus  $\Delta T$

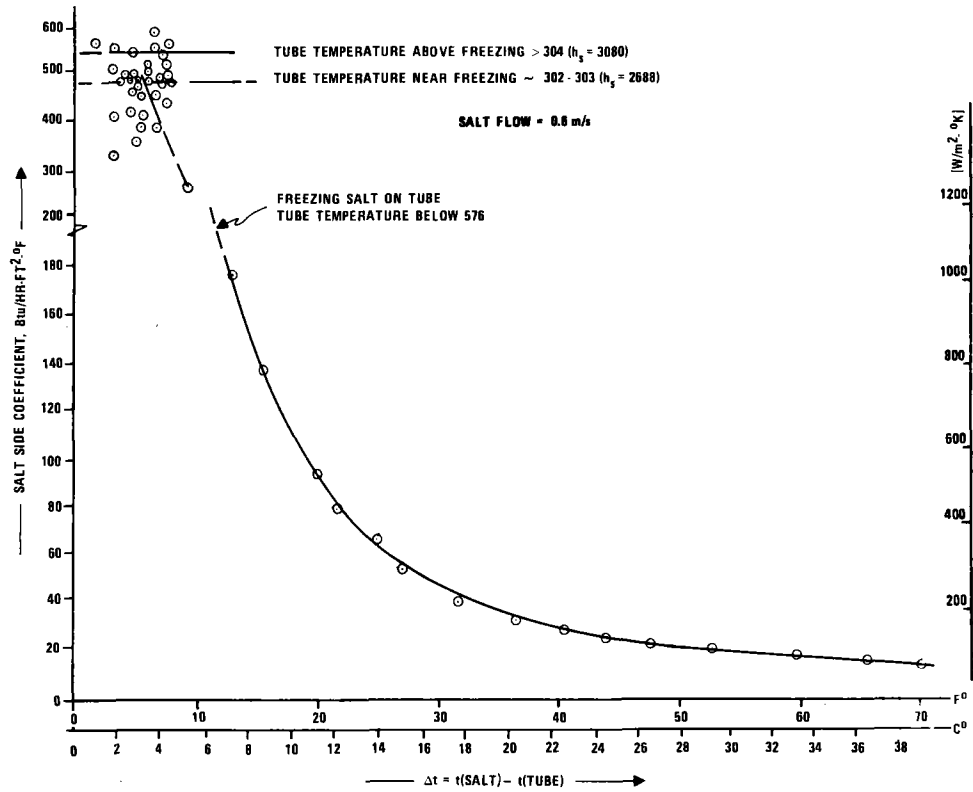


Figure 5-9. Flowby Experiment - Run 1, Salt Side Coefficient versus  $\Delta T$

below the salt freezing point, was approximately 1.17 kW. The salt heat transfer coefficient was  $380 \text{ Wm}^2\text{-}^\circ\text{K}$ , with an  $11 \text{ }^\circ\text{C}$   $\Delta T$  between the salt and the outside of the tube.

Run 2--The salt temperature at the start was  $312^\circ\text{C}$ . The salt flow rate was 76 l/m, with a 0.76 m/s salt flow velocity. The heat transfer coefficient in the sensible heat region was calculated to be  $4200 \text{ Wm}^2\text{-}^\circ\text{K}$ . There was uneven freezing on the tubes as indicated by the thermocoupler. Figure 5-10 shows the overall coefficient,  $\Delta T$ , and temperatures versus time.

Run 3--Figure 5-11 shows the  $q$ ,  $U$ ,  $\Delta T$  versus run time for Run 3. The initial salt temperature was  $307^\circ\text{C}$  ( $584^\circ\text{F}$ ), and the salt flow was the equivalent of 3-1/2 turns on the globe valve (estimated as 91 l/m and 0.91 m/s). The initial oil temperature was  $304^\circ\text{C}$  ( $579^\circ\text{F}$ ), which was above the freezing temperature of  $303^\circ\text{C}$  ( $577.5^\circ\text{F}$ ) for salt. Notice that with a decrease in oil temperature or an increase in overall temperature difference, the heat rate increased and the coefficient remained constant at about  $1250 \text{ Wm}^2\text{-}^\circ\text{K}$  ( $220 \text{ Btu/hr-ft}^2\text{-}^\circ\text{F}$ ). As the salt temperature decreased to near freezing, the heat rate and coefficient decreased, as at time = 50 minutes. With an increase in  $\Delta T$  from 10 to  $15^\circ\text{C}$  ( $18$  to  $27^\circ\text{F}$ ), between the time 50 to 200 minutes as shown in Figure 5-11, the overall coefficient decreased from  $540 \text{ Wm}^2\text{-}^\circ\text{K}$  ( $95 \text{ Btu/hr-ft}^2\text{-}^\circ\text{F}$ ) to  $340 \text{ Wm}^2\text{-}^\circ\text{K}$  ( $60 \text{ Btu/hr-ft}^2\text{-}^\circ\text{F}$ ) and the heat rate was approximately constant at 1465 W (5000 Btu/hr). After about 240 minutes of run time, the salt flow was decreased to 0.4 m/s. With the increase in  $\Delta T$  from 6 to  $8^\circ\text{C}$  ( $11$  to  $15^\circ\text{F}$ ), the overall coefficient decreased from about  $480 \text{ Wm}^2\text{-}^\circ\text{K}$  ( $85 \text{ Btu/hr-ft}^2\text{-}^\circ\text{F}$ ) to  $400 \text{ Wm}^2\text{-}^\circ\text{K}$  ( $70 \text{ Btu/hr-ft}^2\text{-}^\circ\text{F}$ ), but the heat rate was constant at about 880 W (3000 Btu/hr). With the salt flow at 0.7 m/s, the overall coefficient increased slightly. For a  $\Delta T$  from 8 to  $11^\circ\text{C}$  ( $15$  to  $20^\circ\text{F}$ ) the coefficient decreased from  $454 \text{ Wm}^2\text{-}^\circ\text{K}$  ( $70 \text{ Btu/hr-ft}^2\text{-}^\circ\text{F}$ ), while the heat rate was approximately constant at 1170 W (4000 Btu/hr).

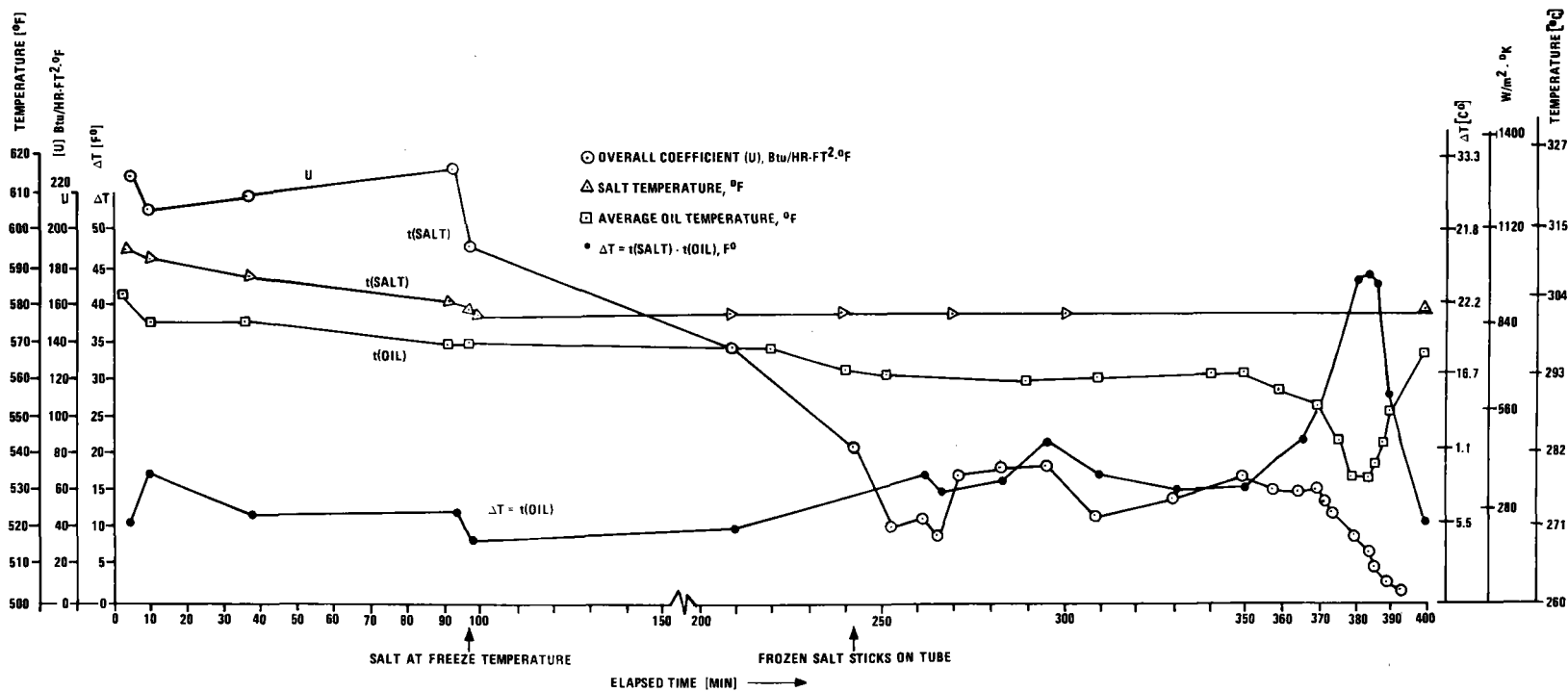


Figure 5-10. Flowby Experiment - Run 2, Time History Plot



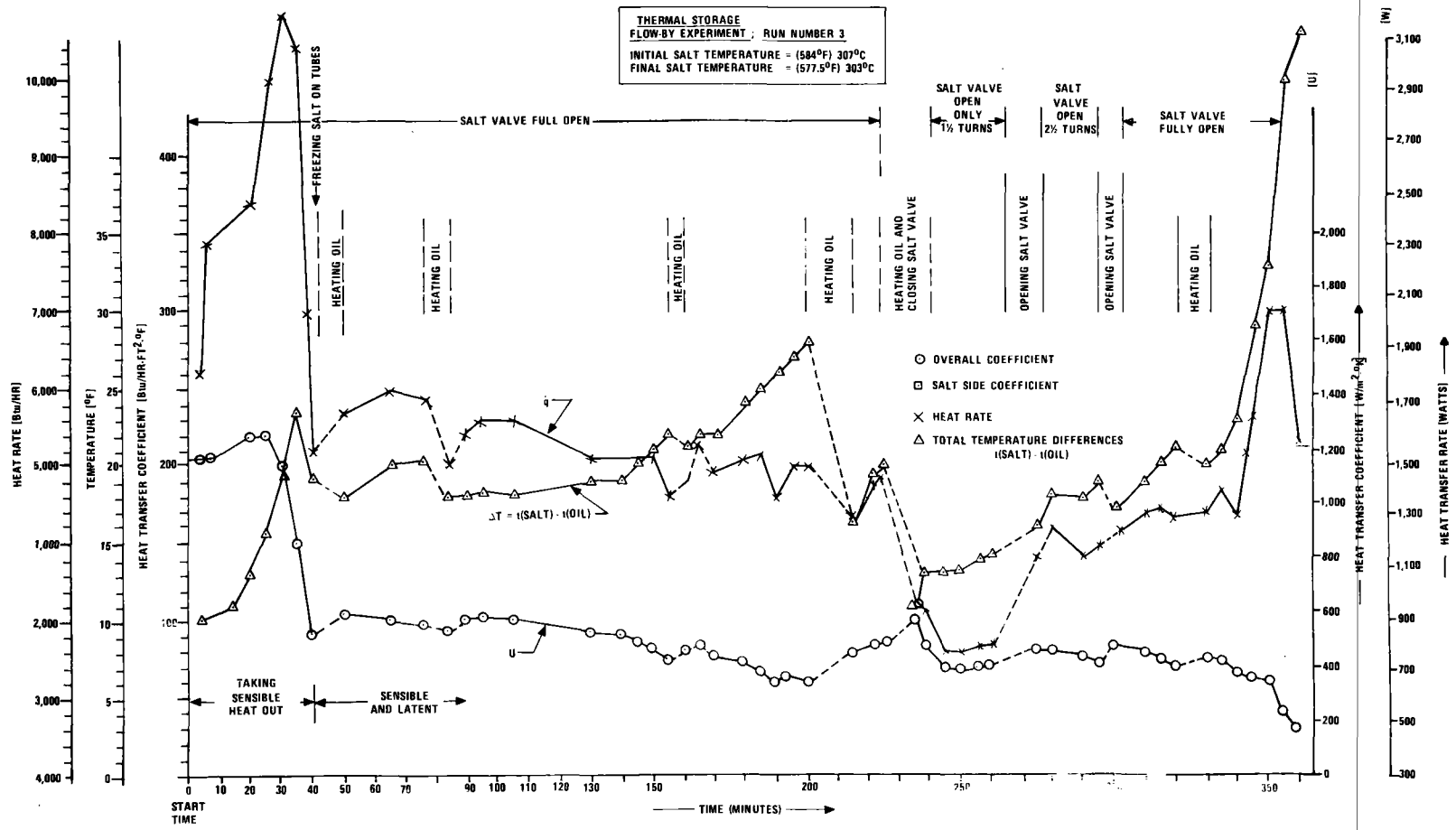


Figure 5-11. Flowby Experiment - Run 3, Time History Plot

Figure 5-12 shows a plot of heat rate versus  $\Delta T$  for three different salt flow rates, with salt near freezing temperature. Notice the heat rate is about constant for a given salt flow. Figure 5-11 shows a plot of overall coefficient versus  $\Delta T$ . The coefficient decreases with  $\Delta T$ . Figure 5-13 shows a plot of heat rate versus salt flow. The heat rate was about constant for a given salt flow rate. Figure 5-14 shows a plot of salt side heat transfer coefficient versus  $\Delta T$ .

With tube temperatures at or near freezing, the salt coefficient obtained at full flow of 1 m/s was  $3300 \text{ Wm}^2\text{-}^\circ\text{K}$  ( $575 \text{ Btu/hr-ft}^2\text{-}^\circ\text{F}$ ). With a salt velocity of 0.7 m/s the coefficient in the sensible heat region was from 2700 to 3100  $\text{Wm}^2\text{-}^\circ\text{K}$  ( $480\text{-}550 \text{ Btu/hr-ft}^2\text{-}^\circ\text{F}$ ). The lower coefficient occurred when the tube temperature was near freezing and the higher coefficient occurred when the tube temperature was well above freezing.

With the salt near freezing temperature, the low heat transfer coefficient was apparently due to the salt layer surrounding the tube. The salt layer thickness appears to be a function of salt velocity and  $\Delta T$ . Increased salt velocity and decreased  $\Delta T$  decreased the layer thickness. This suggests a possibility that at high salt velocities increased heat rates could be sustained.

However, increased salt velocity results in increased pump power. Due to the poor heat transfer coefficient across the module, the power required to pump salt through the heat exchanger was as much as the heat rate developed. At full flow, the pump power required was measured as 2080 W, while the heat rate was only 1500 W. At least 1250 W were added to the salt as heat as it was pumped through the heat exchanger. This high pump power requirement was specific to the experimental setup. On a large scale, the power requirements would be proportionately lower.

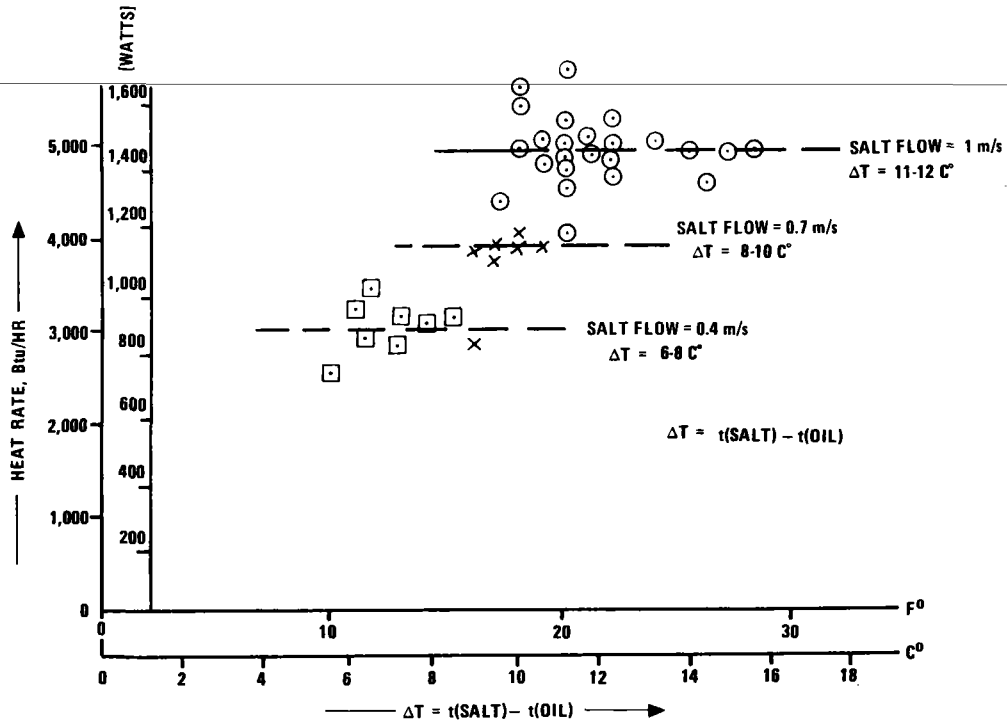


Figure 5-12. Flowby Experiment - Run 3, Heat Rate versus  $\Delta T$

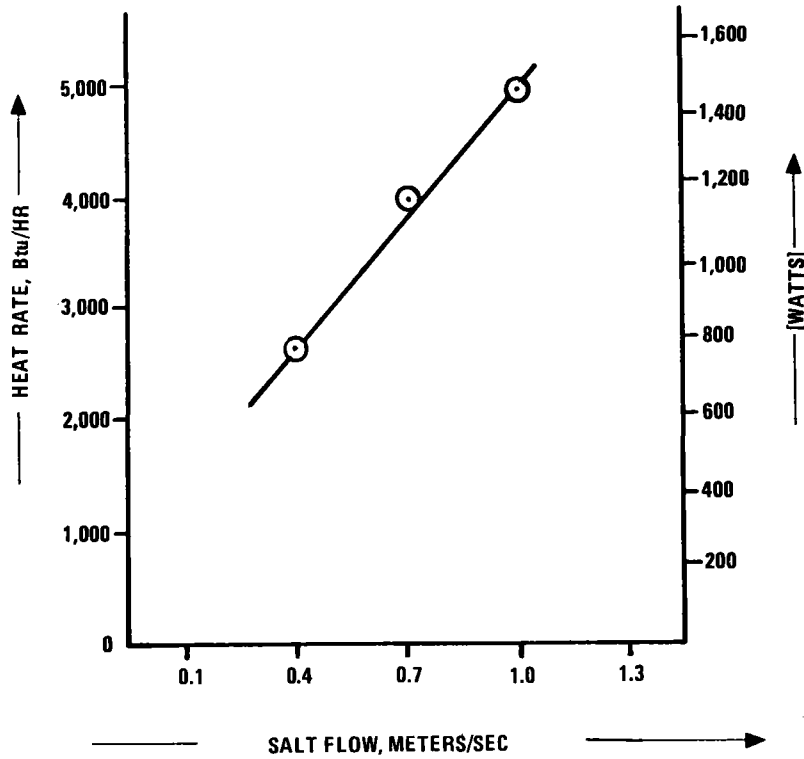


Figure 5-13. Flowby Experiment - Run 3, Heat Rate versus Salt Flow

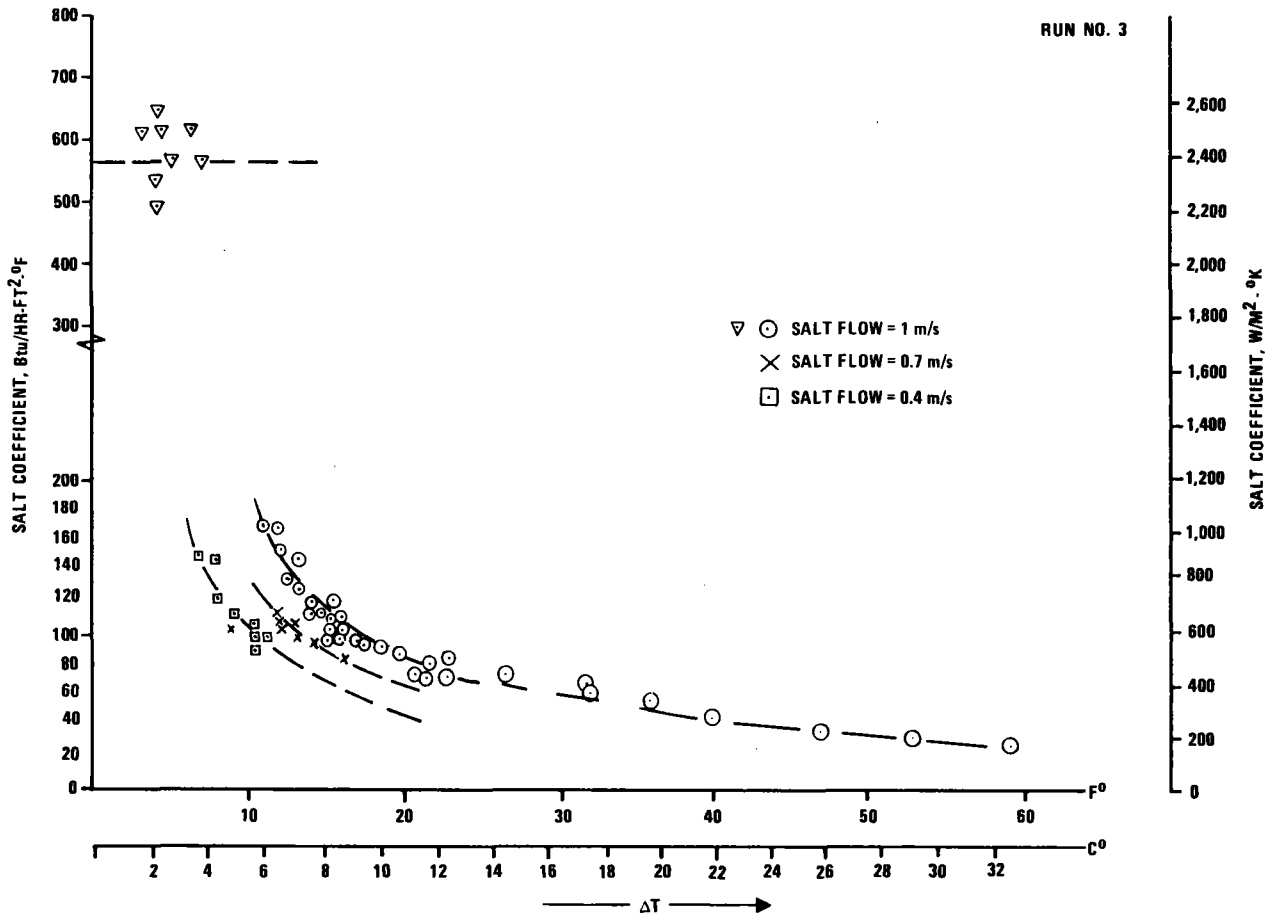


Figure 5-14. Flowby Experiment - Run 3, Salt Coefficient versus  $\Delta T$

Run 4--In the experiment it was possible to have the salt layer on the tubes build up to a thickness such that the temperature on the outside of the salt layer remained above the freezing point and the heat transferred was the sensible heat added by the pump. This suggested that salt was sticking to the coated heat transfer tubes. A further test to determine this was carried out in Run 4 by suddenly increasing the oil flow inside the tubes. The results are given in Figures 5-15 and 5-16. At low oil flow, the oil-side coefficient was controlling and increasing the oil rate, causing the outer tube temperature to decrease and the salt to freeze. If the salt did not stick to the tubes, the overall heat transfer coefficient and heat rate would increase. In Run 4

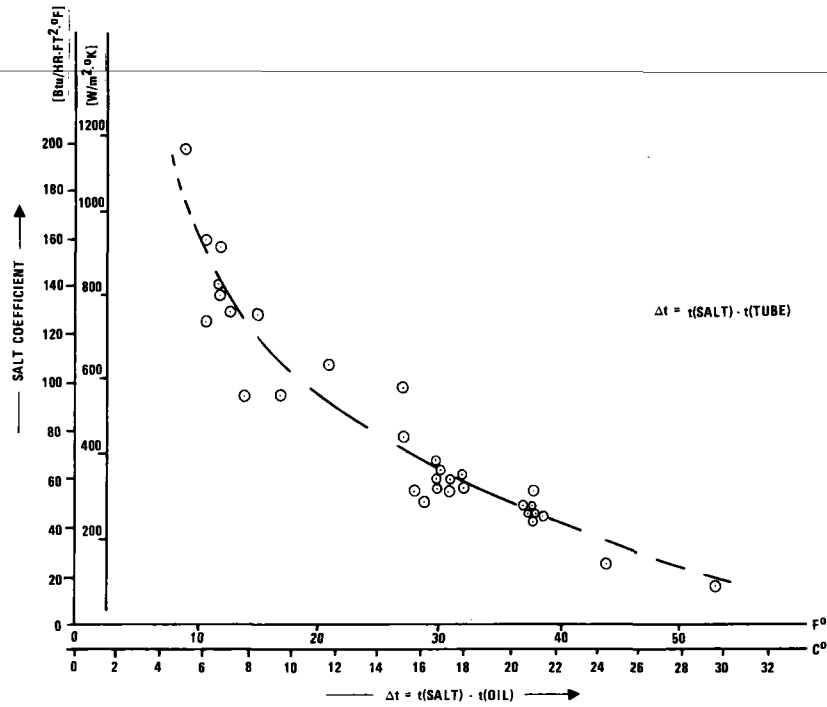


Figure 5-15. Flowby Experiment - Run 4, Salt Coefficient versus  $\Delta T$

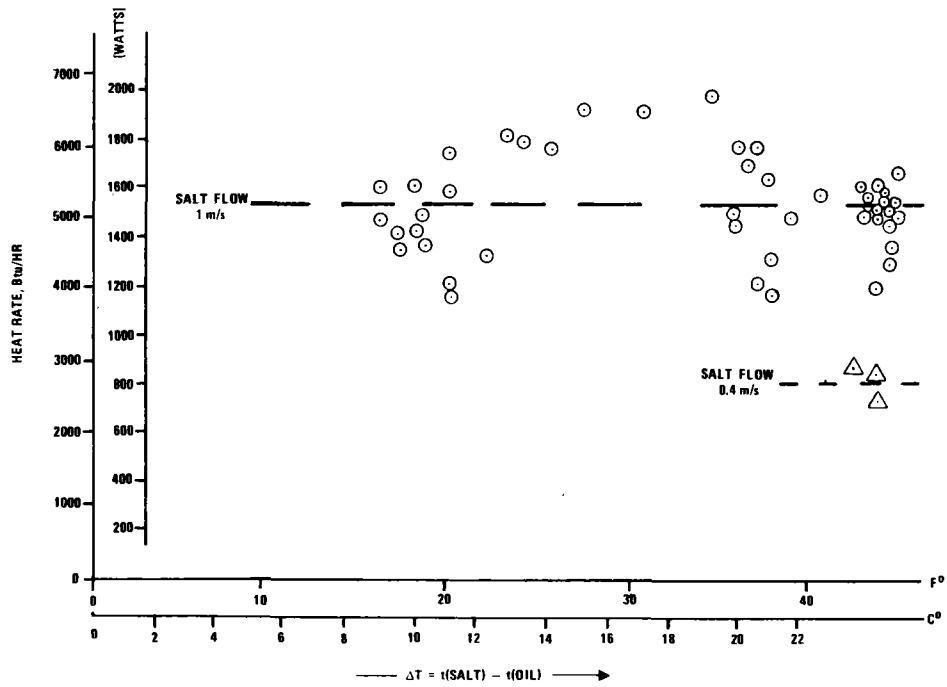


Figure 5-16. Flowby Experiment - Run 4, Heat Rate versus  $\Delta T$

at time = 128 minutes, with an increase in oil flow from 46 percent to 76 percent of full flow, the overall coefficient and the salt side coefficient decreased with the same overall temperature difference and the same salt flow rate. This decrease in heat rate indicated a salt buildup on the tubes.

SECTION 6.0  
RECOMMENDATIONS

6.1 SELECTED TES APPLICATION EVALUATION

The reflux boiler using continuous PCM flow was selected as the concept for large-scale 1000 MWh(t) commercial cost evaluation. The general concept mechanization given in Subsection 4.1 is recommended. However, based on the unsatisfactory results of the PCM in reflux boiler module tests, additional experimental work with other PCMs is necessary to establish proof of the Direct Contact Reflux Boiler Concept.

6.2 FOLLOW-ON TES PROGRAM PLAN CONCEPT

6.2.1 Reflux Boiler Concept

Experimentation is recommended with this concept to determine the extent of compatibility between water, other refluxing fluids and PCMs at high pressures and temperatures. Investigation of the physical chemistry of the mixtures should be included. The experimental modules should be designed to permit closed loop control for the water or fluid preheat, provide thermal tracing and heat loss control, positive level sensing technique for molten salts and provide comprehensive instrumentation.

If, as a result of additional experimentation, the reflux boiler qualifies for larger-scale development, then component development would be required in the following areas:

- High temperature hydraulic slurry turbines

- High pressure PCM pumps
- PCM boilers
- PCM flow measurement devices
- PCM pressure measurement devices
- PCM conductivity measurement devices
- PCM energy content measurement devices
- High temperature trace heating devices
- High temperature PCM valves

Of special concern is the development of the high pressure PCM pump and hydraulic turbine combination.

### 6.3 COATED TUBE AND SHELL FLOWBY CONCEPT

Continued experimentation is recommended with this concept due to its extreme attractiveness for large-scale mechanization. The additional testing should explore the following:

- The effect of higher salt velocities for a given  $\Delta T$  using nickel coated tubes.
- The evaluation of at least two other coatings with the  $\text{NaNO}_3/\text{NaOH}$  PCM; i.e., chrome plate and Ryton No. 164 (PPS/PTFE) coating.



- The influence of mechanical vibration and sonics on adherence of salt crystals to tubes.
- Analysis of the PCM supplier process producing sodium sulfate and its influence on the solidification of sodium nitrate from the melt.
- The effect of a magnetic field on the adherence of diamagnetic  $\text{NaNO}_3$  crystals to heat transfer surfaces.
- The effect of alternate heat of fusion phase change materials.

APPENDIX A  
COATED TUBE DATA

A letter of inquiry concerning antistick coatings, Figure A-1, was prepared and sent to the potential coatings suppliers listed in Table A-1. As a result of communications with several of these suppliers, samples of coatings were obtained. In most cases, a prepared substrate was furnished to the supplier over which the sample coating was applied.

The basic categories to be considered in a coating evaluation program include:

- Tube material and mill process
  - SA178-A
  - SA192-A
  
- Base condition
  - Mill run
  - Mechanical finish
  - Chemical finish
    - . Electro-polish
    - . Electro-etch
  
- Coating application
  - Metallic
  - Plastic
  - Ceramic
  - Other

The tubes considered included welded and seamless with mill run, special mechanical electropolish finishes. The coatings included metallic and plastic.

# Honeywell

January 3, 1979

E.I DuPont De Nemours & Co., Inc.  
Fabrics and Finishes Dept.  
308 East Lancaster Avenue  
Wynnewood, Penn. 19096

Attn: Mr. Rist

Dear Sir:

The Energy Resources Center of Honeywell, Inc. is developing thermal energy storage devices using the heat of fusion of molten salts in the temperature range of 550-600°F. Specifically we are seeking a coating to be applied to the outside of tubes which when immersed in a molten nitrate bath will inhibit the nitrate crystals from sticking to the tubular surfaces as they fractionally solidify from the melt during heat extraction.

The coating should provide a micro-smooth, thin, non-porous, non-reactive surface with a non-crystalline structure (or crystalline but dissimilar to the nucleating sodium nitrate crystal structure at 580°F). Also it appears that a low electrical conductivity is desirable if good release properties are to be assured. However, heat flow must not be limited by this film coating. Obviously this coating must be stable at the operating temperature under the influence of the molten salt for an "industrial" equipment lifetime. Finally, this coating must show promise of large scale use on tube and shell type heat exchangers at reasonable cost compared to tubular plating techniques.

Since your company is a recognized leader in anti-stick coatings your candidates and/or recommendations are solicited.

Sincerely,



R. T. LeFrois  
Energy Storage Systems  
612/378-4940  
Mail Station MN19-T540

RTL;cb

Figure A-1. Letter of Inquiry

Table A-1. Coatings and Finishes--Survey Status (Continued)

Industrial Source	Response and Comments
Ferro Company Cleveland, Ohio	No response.
SermeTel Inc. Limerick, Pennsylvania	No response.
Gen. Magnaplate Corp. Linden, New Jersey	Do not have anything at this time. Expect it will require extensive R&D.
International Polymer Co. Houston, Texas	Provided three sample plastic coatings including PPS, TFE, and Tyton.
Donwell Company Manchester, Connecticut	Provided two sample plastic coatings including PTFE and PFA teflon.
Morton Chemical Co. Woodstock, Illinois	Discontinued their line of HNS ceramic coatings.
Gulf Oil Co. Houston, Texas	Suggests use of BTDA and epoxy or polyimides. Contacted five formulators.
Allied Chemical Corp. Morristown, New Jersey	No materials they feature capable of with- standing environment. Suggest HALAR or ECTFE for lower temperature.
Phillips Chemical Co. Pasadena, Texas	PPS/PTFE coating called Ryton may work with NaNO <sub>3</sub> at 300°C. Provided samples.
Dow Chemical Co. Midland, Michigan	Provided information on Molykote 321R bonded lubricant spray. Good to 450°C.
ICI Americas Inc. Wilmington, Delaware	Nothing compatible at required temperature including PTFE. Suggest "Fluon" for lower temperatures. Would provide sample.
Pennwalt Corp. King of Prussia, Pennsylvania	No response.
Dixon Industries Corp. Bristol, Rhode Island	Recommended PD-2839, basically a fluoro- carbon. Good for temperatures to 371°C. Extremely interested in this program and results.
Union Carbide Corp. Indianapolis, Indiana	UCAR ceramic coatings. Plasma or Detonation Gun application; not economical for pipe. Suggests UCAR-LC-1H chrome carbide. Very expensive.
Cotronics Corp. Waterford, New York	Ceramic coatings - application problems for pipes.

Table A-1. Coatings and Finishes--Survey Status (Concluded)

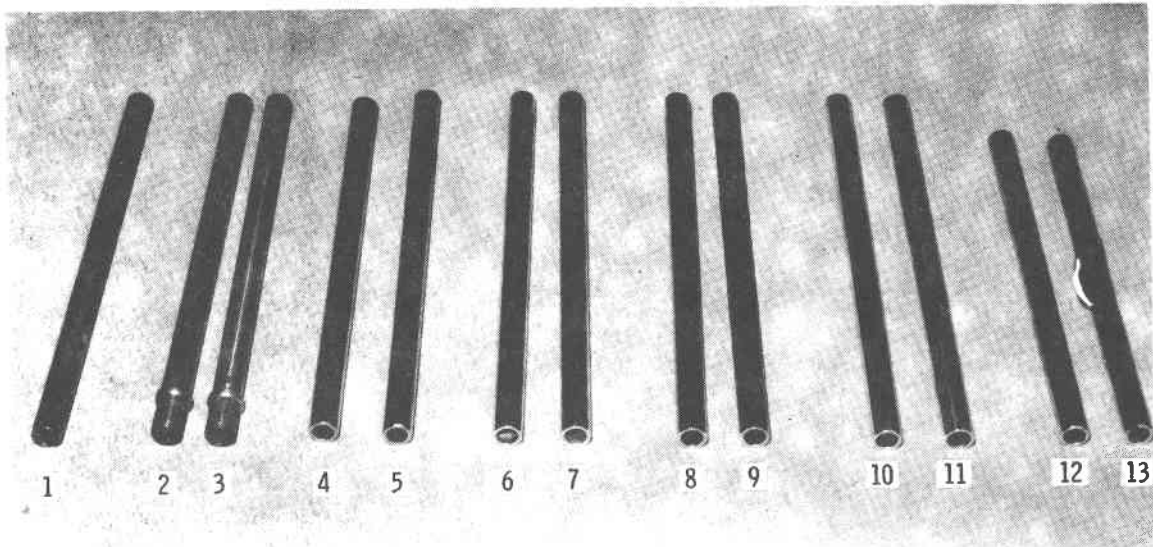
Industrial Source	Response and Comments
General Electric Co. Waterford, New York	Silicone release coatings good only to 260°C. Nothing to recommend.
Whitford Corp. West Chester, Pennsylvania	Will provide special formulation containing silicon resin to be cured at 700°F. Xylan series 8500 modified.
Corning Glass Works Corning, New York	No response.
Fluorocarbon Tribal Santa Ana, California	Provided samples of Milkon-600, a copolyester, and Tribolon PI-501, a polyimide.
Superior Plating Inc. Minneapolis, Minnesota	Provided eight samples including various electroless nickel and chrome platings.
Electro-Coatings Inc. Moraga, California	Provided Kanigan electroless nickel and hard chrome samples.
Boyd Coating Research Gleasondale, Massachusetts	Provided two samples of PFA teflon.
E.I DuPont Wynwood, Pennsylvania	They feel that the only possible plastic coatings capable of surviving in molten salts are PFA and PTFE teflon. Provided data on formulators of teflon.
Fiber Materials Inc. Biddleford, Maine	Did not work in this area. Suggest TFE or FEP teflon, H.T. silicone or H.T. polysulfone without graphite powder.
Electro-Glo Co. Chicago, Illinois	Provided five samples of electropolished tubes with varying mechanical finishing conditions.
Able Electropolishing Chicago, Illinois	Provided two samples of electropolished tubes.
Valspar Corp. Ft. Wayne, Indiana	No response.
Armstron Prod. Warsaw, Indiana	No response.
The Dexter Corp. Industry, California	No response.
P. D. George Co. St. Louis, Missouri	Highly recommends a Tritherm 98 Amide-Imide. Ability of material to withstand high temperatures and exposure to salts is outstanding according to this supplier.
Rust-Oleum Corporation Vernon Hills, Illinois	Have a large number of heat-resistant coatings: phenolics/silicones for temperatures to 650°C (dry heat condition).

Figure A-2 shows various metallic platings on welded/seamless tubes with different base preparations. Likewise Figure A-3 shows various plastic and other types of coatings.

A series of tests was conducted to determine the general compatibility of the tube coating with the molten salt. The first test was to dip the coating into the molten salt for about 20 seconds to verify that no chemical reaction or mechanical failure was apparent. The second test was to let the specimen soak in the molten salt for about 2 minutes. This was sufficient time for the tube temperature to rise to the salt temperature. At this point it was removed and wiped clean of the salt and examined. The results of these tests are given in Table A-2. These results narrowed the investigation to the following coatings:

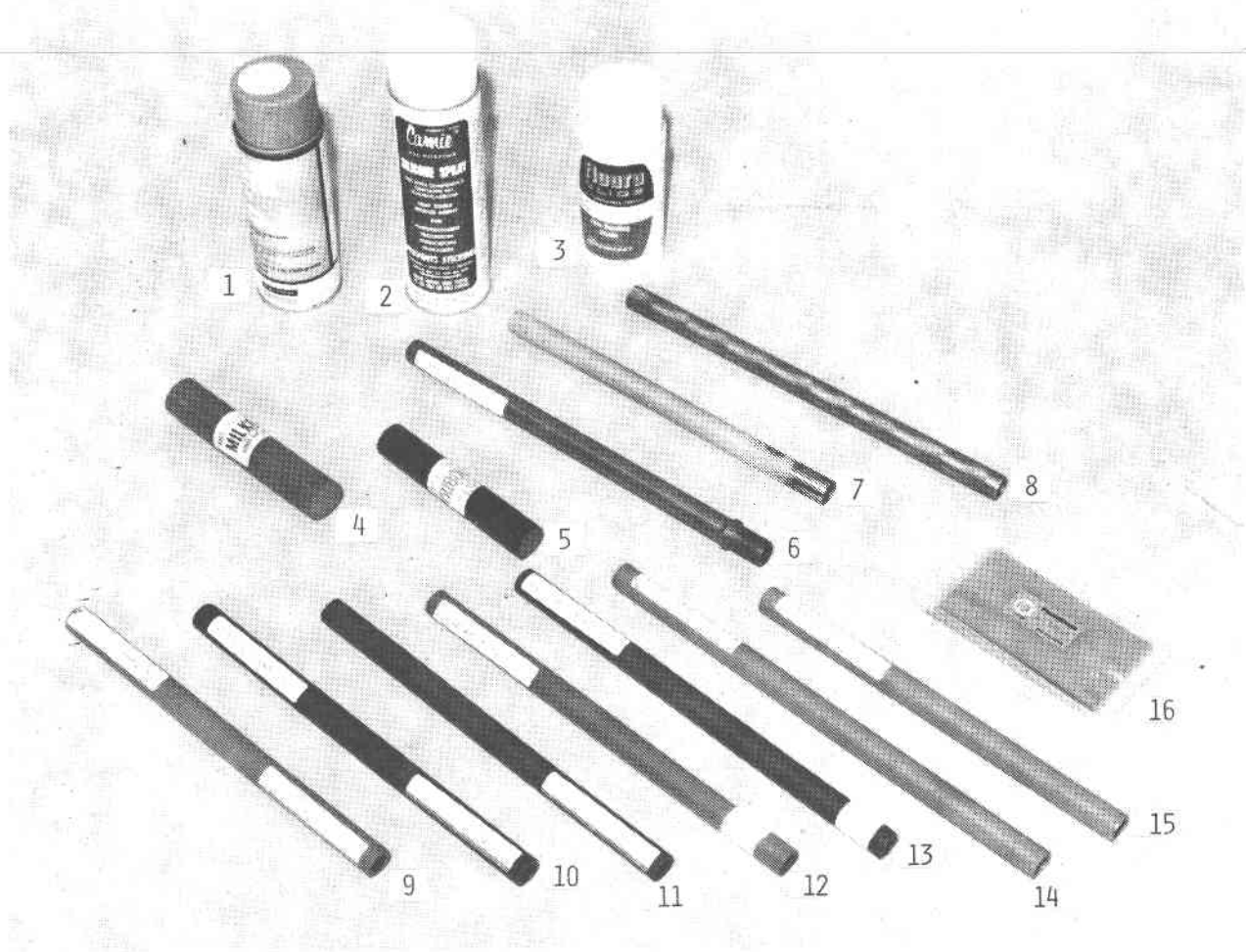
- Electroless nickel
- Chrome
- PTFE Teflon
- Ryton 164

A series of photomicrographs were prepared for selected specimens to aid in the evaluation of the coatings. These are shown in Figures A-4 through A-11.



1. SA 178-A tube with standard mill finish.
2. SA 178-A tube with 400-grit finish and MoS<sub>2</sub> dry film coating.
3. SA 178-A tube with 400-grit finish.
4. SA 178-A tube with standard mill finish and 1-mil electropolish.
5. SA 178-A tube with 400-grit finish and 1-mil electropolish.
6. SA 192-A tube with standard mill finish and 1-mil electroless nickel plate.
7. SA 192-A tube with 400-grit finish and 1-mil electroless nickel plate with color buff.
8. SA 192-A tube with standard mill finish and 1-mil hard-chrome plate.
9. SA 192-A tube with 400-grit finish and 2-mil hard-chrome with polish.
10. SA 178-A tube with mill finish and 1-mil electroless nickel plate.
11. SA 178-A tube with 400-grit finish and 1-mil electroless nickel plate.
12. SA 178-A tube with standard mill finish and 0.5-mil hard-chrome plate.
13. SA 178-A tube with 400-grit finish and 1-mil hard-chrome plate with polish.

Figure A-2. Tubes with Various Metallic Finishes



- |                                          |                                     |
|------------------------------------------|-------------------------------------|
| 1. Molykote Spray ( $\text{MoS}_2$ )     | 9. Ryton 164 Plastic coating - IPC  |
| 2. Silicone Spray                        | 10. Ryton 104 Plastic coating - IPC |
| 3. Fluoro-Glide Spray                    | 11. PPI System I                    |
| 4. Milkon 600                            | 12. PTFE Teflon                     |
| 5. Tribolon PI 501                       | 13. PFA Teflon                      |
| 6. SA-192-A tube with molykote spray     | 14. PFA Teflon                      |
| 7. SA-192-A tube with silicone spray     | 15. PFA Teflon                      |
| 8. SA-192-A tube with fluoro-glide spray |                                     |

Figure A-3. Tubes with Various Plastic and Other Types of Coatings



Table A-2. Test Results

SPECIMEN NO.

FIG. A-2 METALLIC	FIG. A-3 OTHER	DIP TEST	SOAK TEST	REMARKS
11		✓		TURNUED DARK, THEN BLACK
9		✓		TURNUED MOTTLED BROWN
5		✓		TURNUED BLUISH
	13	✓	X	10 MIN. SOAK AT 327°C, SOFT WHEN RUBBED
	12	✓	✓	2 MIN. SOAK AT 324°C
	10	✓	✓	8-10 MIN. AT 316°C, NON-WETTING - OK
	9	✓	✓	2 MIN. AT 316°C
	11	✓	X	2 MIN. AT 310°C - CHARRED WITH RESIDUE
	14	✓	✓	2 MIN. AT 310°C - OK
1		✓	X	TURNUED BROWNISH, SALT STICKS
	14	✓	✓	15 MIN., 310°C - OK
10		✓	✓	10 MIN. AT 316°C, TARNISHED
13		✓	✓	10 MIN. AT 321°C, TARNISHED
	7	✓	X	COATING PEELED OFF
	4	✓	X	CHARRED AND EVOLVED SMOKE
	5	✓	X	DECOMPOSED AND REACTED WITH SALT
	16	✓	-	SAMPLE NOT ADEQUATE
	9	✓	✓	23 MIN. AT 316°C - OK
	10	✓	X	20 MIN. AT 320°C, SOFTENING
	9	✓	✓	4 HOUR AT 321°C - OK
	12	✓	✓	4.5 HOUR AT 316°C, MOTTLED BUT OK

Before



After

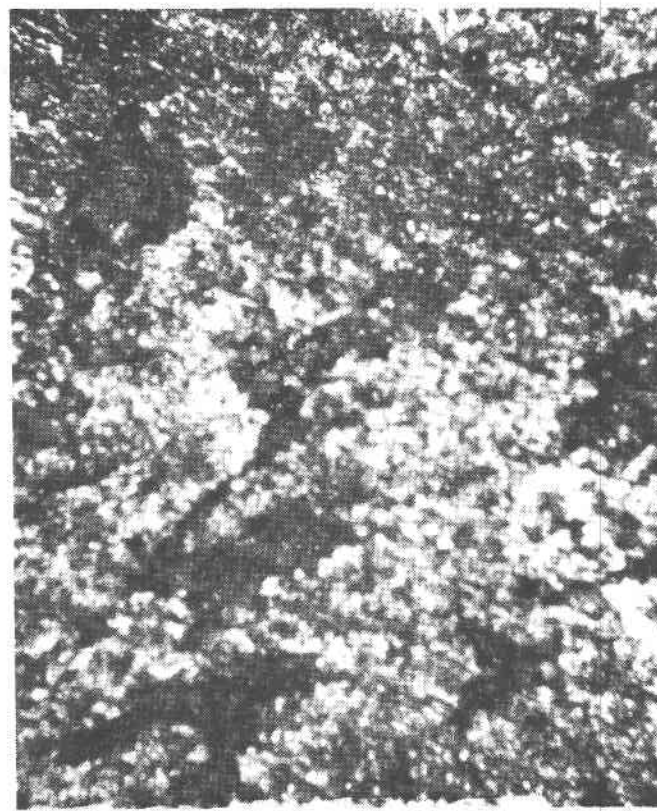
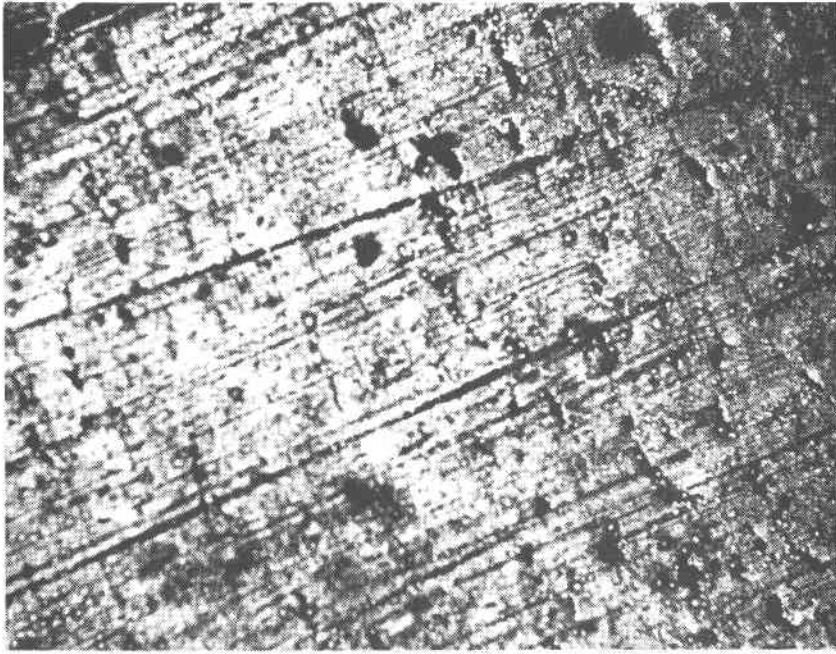


Figure A-4. Uncoated Mild Steel Tube, M = 167x

A-10

After



Before

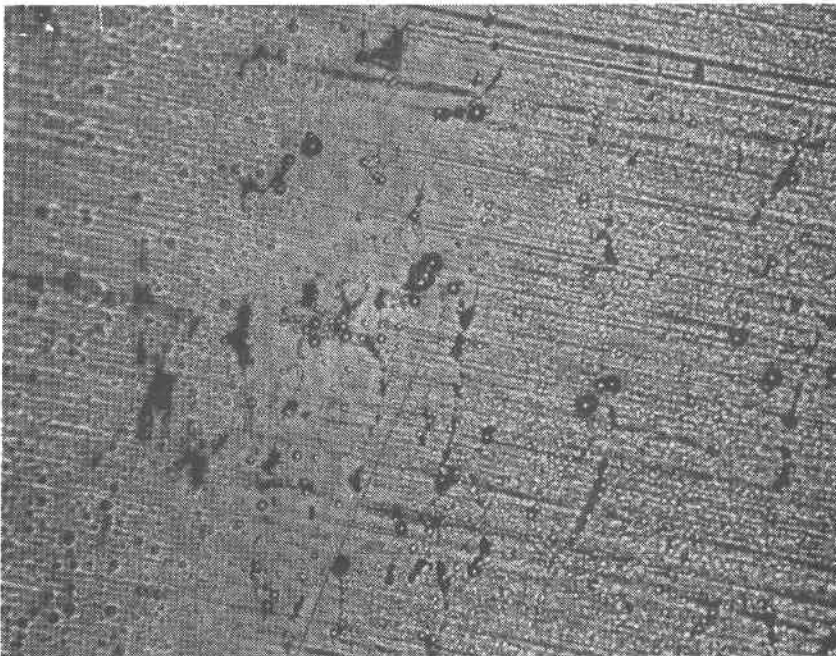
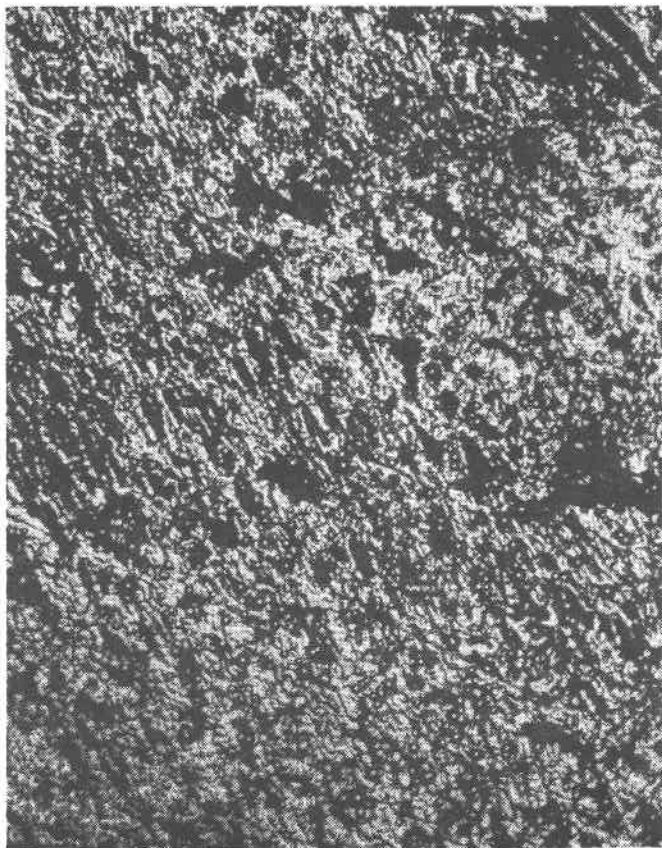


Figure A-5. Electroless Nickel Plate, M = 167x

Before



After

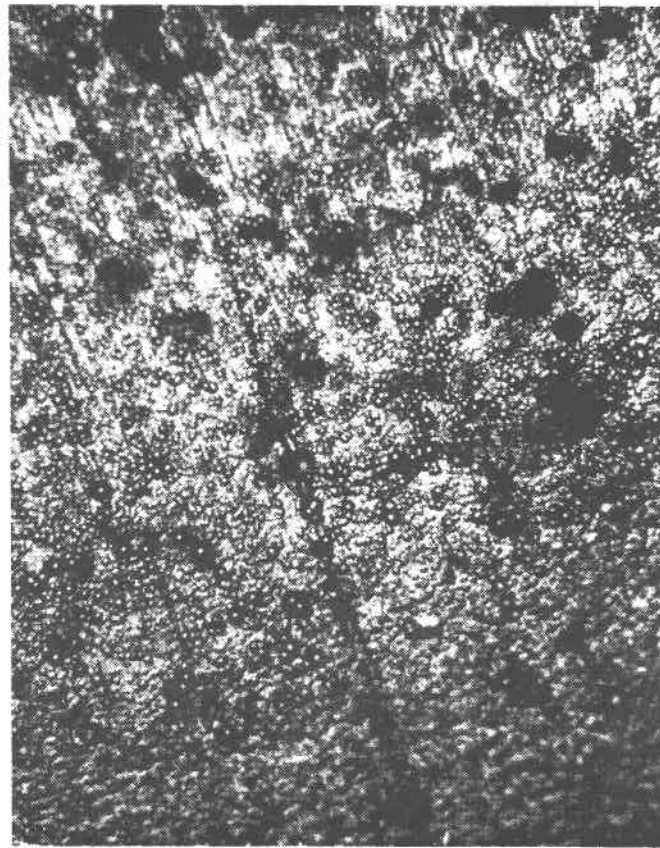
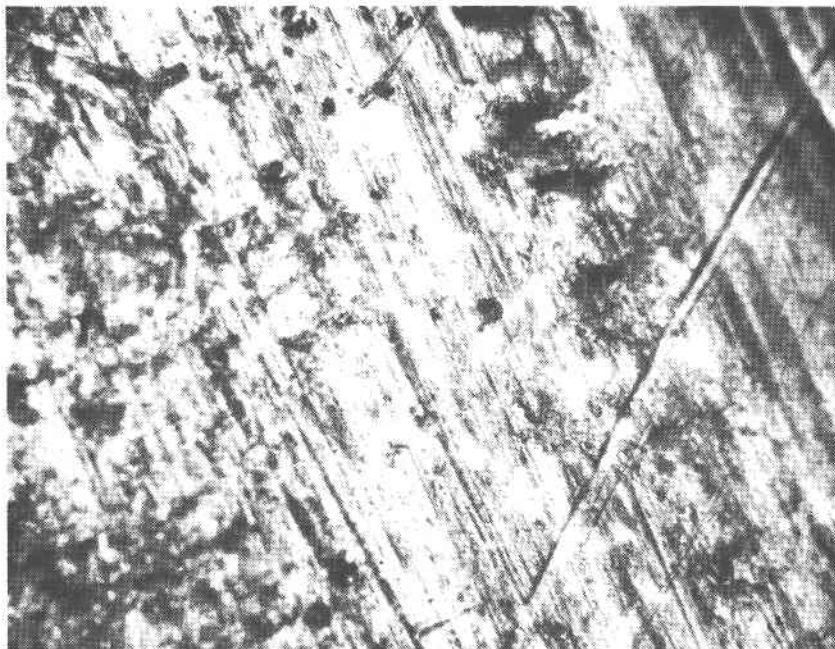


Figure A-6. Chrome Plate--Electro-Coatings, M = 167x

After



Before

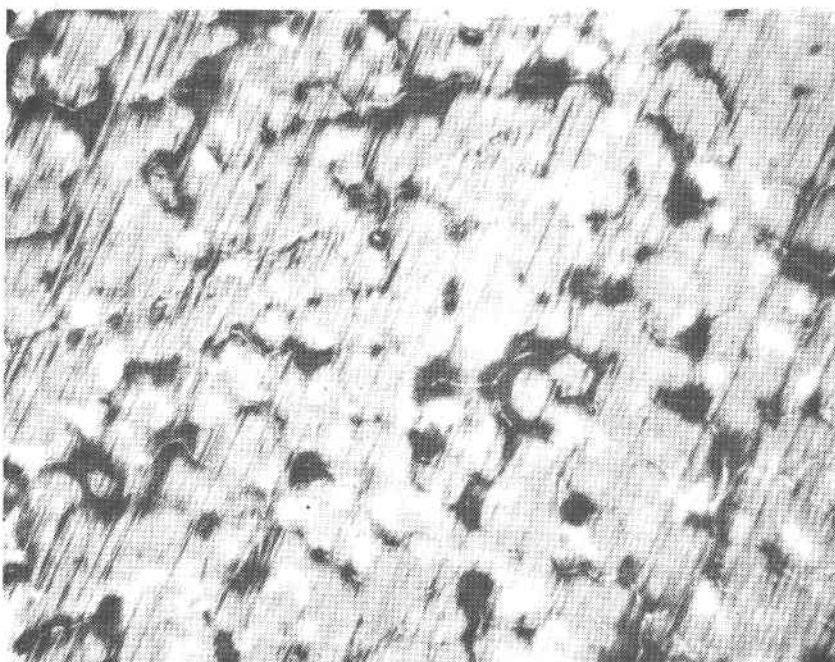


Figure A-7. Teflon PFA--Donwell Co., M = 167x

Before

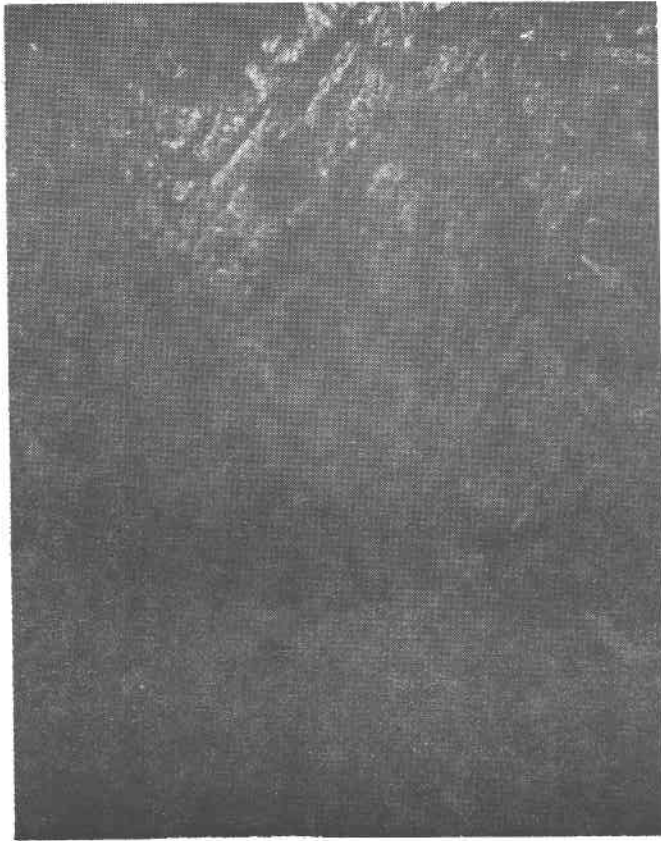


After

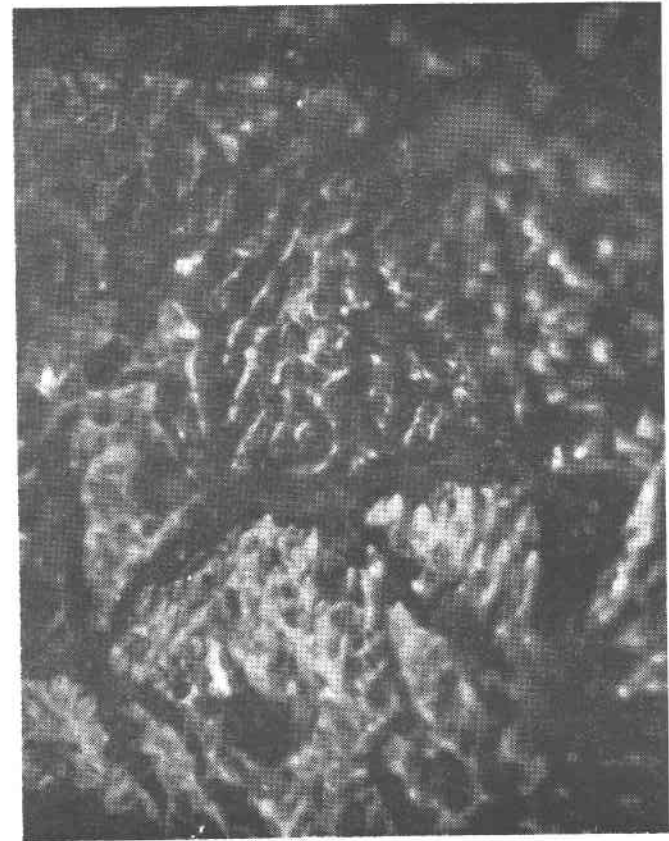


Figure A-8. Teflon PTFE--Donwell Co., M = 167x

After Dip



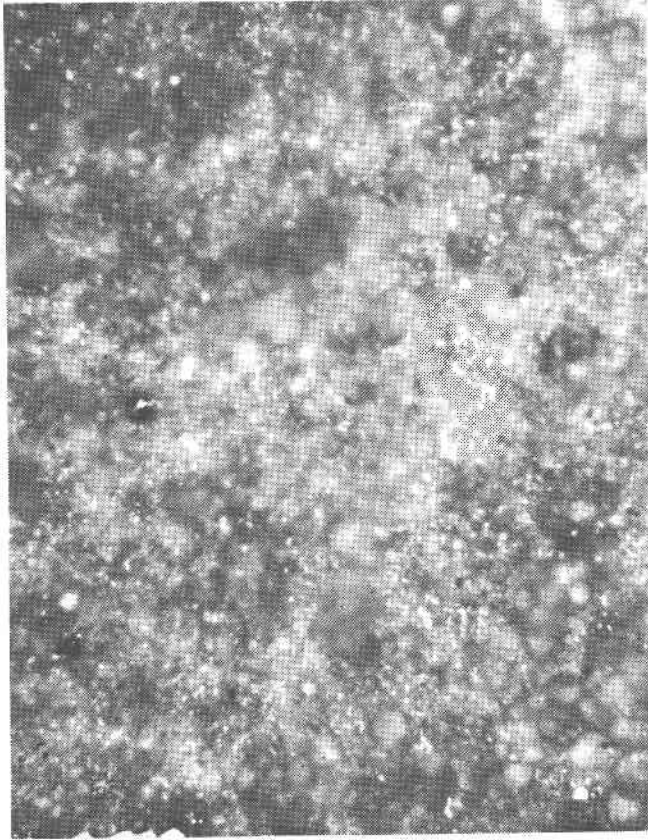
After Dip



A-14

Figure A-9. PPI System 1, Impreglon IPC-M = 167x (left) and IPC-M = 335x (right)

After



After

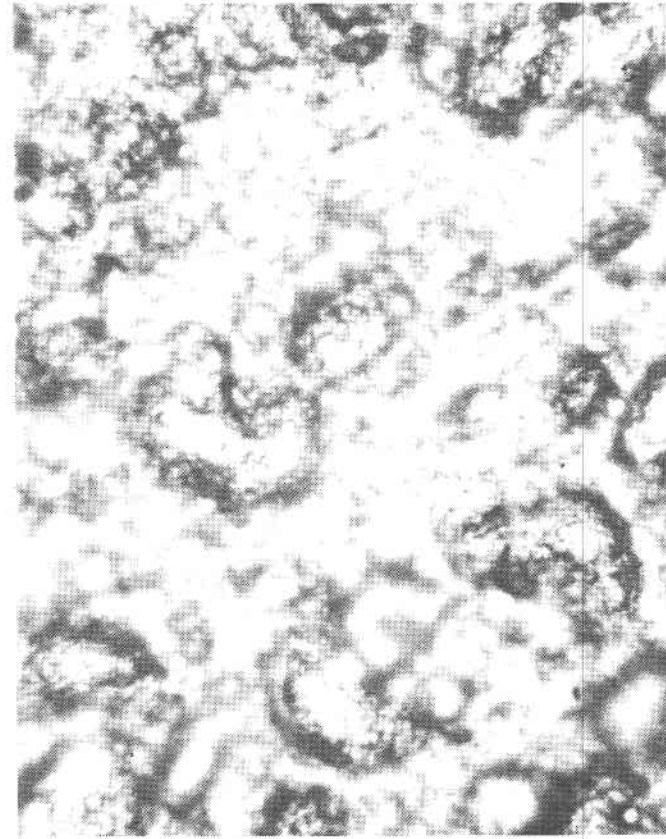
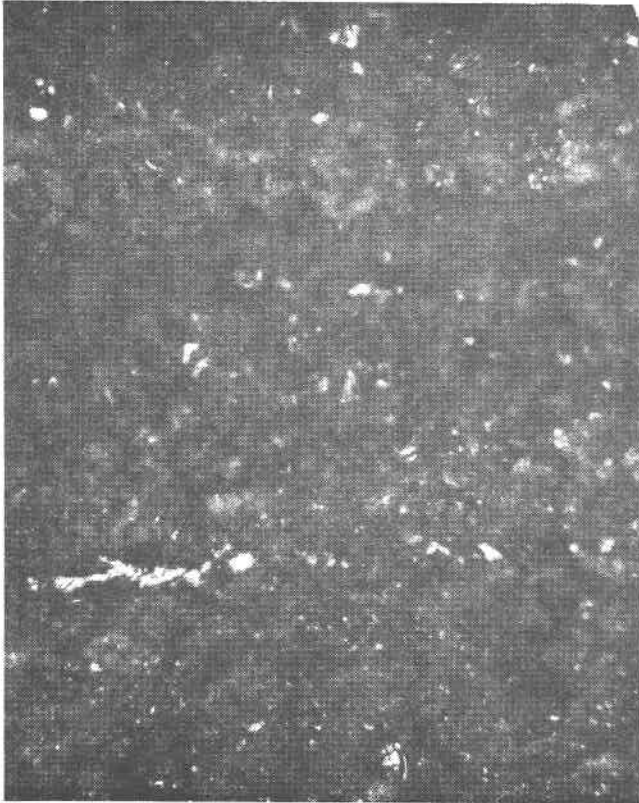


Figure A-10. Ryton 164, M = 167x (left) and Ryton 104, M = 335x (right)



Before



After

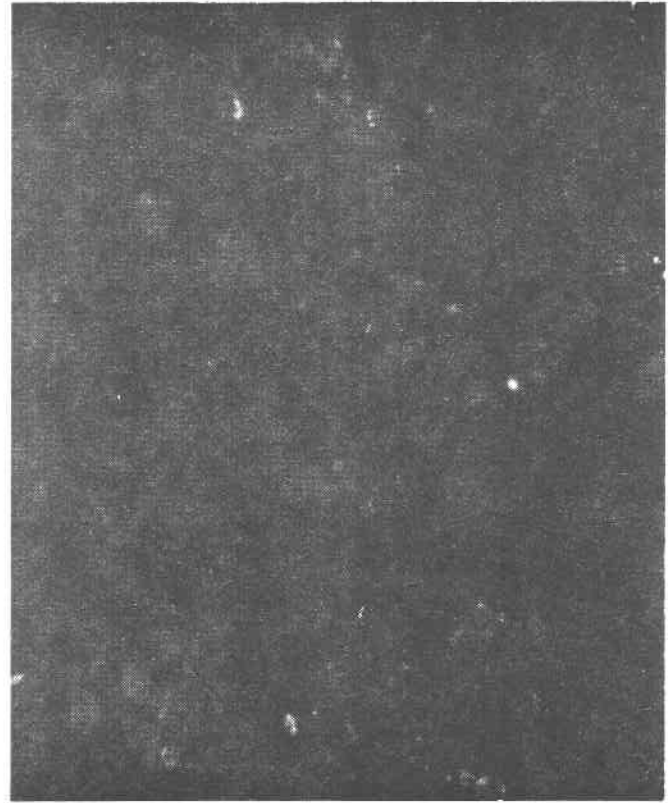


Figure A-11. M = 167x (left) and M = 167x (right)

## APPENDIX B

## PROPERTIES OF MOLTEN NITRATES AT HIGH PRESSURES

Fusion Temperature

The Clausius equation for variation of melting point with pressure is

$$\frac{dT}{dP} = T \left( \frac{v_l - v_s}{h_f} \right)$$

$v_l$  and  $v_s$  are specific volumes of liquid and solid.  $h_f$  is heat of fusion.

Now,

$$\rho_l = \frac{1}{v_l} = \rho_{LO} \exp \left[ -\beta_T (P - P_o) \right]$$

Substituting and integrating, we get

$$\ln \frac{T_{f2}}{T_{f1}} = \frac{1}{h_f} \left[ \frac{P - P_o}{\rho_s} + \frac{1}{\beta_T \rho_{LO}} \left( \exp(-\beta_T P) - \exp(\beta_T P_o) \right) \right]$$

or approximately,

$$\frac{T_{f2}}{T_{f1}} = \exp \left[ \frac{P}{h_f \rho_{LO}} \left( 1 - \frac{\rho_{LO}}{\rho_{so}} \right) \right]$$

For  $\text{NaNO}_3$  near melting point,

$$\rho_{LO} = 1910 \text{ kg/m}^3$$

$$\rho_{so} = 2114 \text{ kg/m}^3$$

$$h_f = 173.2 \text{ kJ/kg}$$

$$T_f = 580^\circ \text{ k}$$

At  $P = 1 \times 10^7 \text{ N/m}^2$  or 1500 psi

$$\frac{T_{f2}}{T_{f1}} = 1.0029 \text{ or } T_{f2} - T_{f1} = 1.7 \text{ C}^\circ \text{ or } \frac{dT}{dP} = 0.017 \text{ C}^\circ/\text{atm}$$

Electrical Conductance

Electrical conductance can be determined by

$$k_e = k_o \exp(-AP)$$

where,

$$k_o = 0.3018 \exp(0.00383t)$$

$$A = 4.58 \times 10^{-4} \exp(-5.84 \times 10^{-3}t)$$

$$k_o = \text{conductance at 1 atm in (ohm-cm)}^{-1}$$

t = temperature in °C

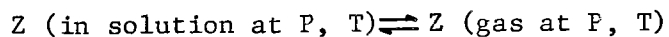
P = pressure in atm

For  $\text{NaNO}_3$  near m.pt,  $P = 100$  atm,  $k_o = 0.9522$ , and  $k = 0.9447$  (ohm-cm)<sup>-1</sup>.

Solubility

The solubility of water in molten sodium nitrate near melting point is given as  $S_o = 14.1 \times 10^{-4}$  moles  $\text{H}_2\text{O}$ /mole melt.

The solubility of a gas, Z, in a molten salt may be described by the equation



The free energy equation with products and reactants in arbitrary state is

$$\Delta F = RT \ln \frac{Q_p}{K_p}$$

$$Q_p = \frac{P_z}{a_z} \sim \frac{1}{s} \quad ; \quad K_p \approx \frac{1}{s_o}$$

$$\therefore \Delta F = RT \ln \left( \frac{S_o}{S} \right)$$

From thermodynamics, we have

$$dF = Vdp - SdT$$

At constant temperature,

$$dF = V dP$$

For gas,

$$\Delta F_g = F_g - F_g^{\circ} = RT \ln P$$

for pressure changing from 1 atm to P atm, and assuming ideal gas behavior.

For liquids,

$$\Delta F_l = F_l - F_l^{\circ} = \int_1^P V dP = \int_1^P \frac{M}{\rho} dP$$

Substituting for  $\rho = \rho_0 \exp(-\beta_T P)$ , integrating and simplifying, we get

$$F_l - F_l^{\circ} = -\frac{M}{\rho_0 \beta} \left[ \exp(-\beta_T P) - 1 \right] \approx \frac{MP}{\rho_0}$$

At 1 atm,

$$\Delta F^{\circ} = F_g^{\circ} - F_l^{\circ} = -RT \ln S_0$$

$$S_0 = 14.1 \times 10^{-4} \frac{\text{mole H}_2\text{O}}{\text{mole melt}}, \quad T = 580^{\circ} \text{K}$$

$$\Delta F^{\circ} = -7614 \text{ Cal/mole}$$

At P atm,

$$\Delta F = F_g - F_e = (F^{\circ} + RT \ln P) - \left( F_e^{\circ} + \frac{MP}{\rho_0} \right)$$

or

$$\Delta F = \Delta F^{\circ} + RT \ln P - \frac{MP}{\rho_0}$$

At P = 100 atm,

$$\Delta F = -7614 + 5242 - 106 = -2478 \frac{\text{Cal}}{\text{mole}}$$

i.e.,

$$RT \ln \frac{S_0}{S} = -2478$$

$$S = 8.5 S_0 = 1.2 \times 10^{-2} \frac{\text{mole H}_2\text{O}}{\text{mole melt}}$$

Solubility at 100 atm and near melting point is 0.012 mole H<sub>2</sub>O/mole melt.

Density

The variation of density as a function of pressure can be estimated from isothermal compressibility data or velocity of sound data. The data is given in Handbook of Molten Salts by G. J. Janz. The isothermal compressibility ( $\beta_T$ ) and velocity of sound ( $\mu_s$ ) are defined as:

$$\beta_T = \frac{1}{\rho} \left( \frac{\partial \rho}{\partial P} \right)_T$$

$$\mu_s = \sqrt{\left( \frac{\partial P}{\partial \rho} \right)_T} \cdot \gamma; \quad \gamma=1$$

P and  $\rho$  are pressure and density respectively.

Integration of the equations gives,

$$\rho(T, P) = \rho(T, P_o) \left[ \exp \left( \beta_T (P - P_o) \right) \right]$$

Either one of the equations can be used. The data for  $\rho$  and  $\mu_s$  as a function of temperature is given in the literature.

Viscosity

Based on the kinetic theory of liquids, an approximate equation for viscosity is given.

$$\mu = \frac{\tilde{N} h}{\tilde{V}} \cdot \exp \left( - \frac{0.408 \Delta U_{\text{vap}}}{RT} \right)$$

Where

$\tilde{N}$  = Avogadro's number

h = Planck's constant

$\tilde{V}$  = Molar volume, = M/ $\rho$

$\Delta U_{\text{vap}}$  = Internal energy for vaporization

R = Gas constant

T = Temperature, °K

M = Molecular weight

Now, at  $T = T_0$ ,  $\rho = \rho_0$ , and  $\mu = \mu_0$

$$\mu_0 = \frac{Nh}{M} \cdot \rho_0 \cdot \exp\left(\frac{0.408 \Delta U_{\text{vap}}}{RT}\right)$$

Dividing the two equations we get

$$\frac{\mu}{\mu_0} = \frac{\rho}{\rho_0}$$

but,

$$\rho = \rho_0 \left[ \exp(\beta_T P) - \exp(\beta_T P_0) \right]$$

$$\therefore \mu = \mu_0 \left[ \exp(\beta_T P) - \exp(\beta_T P_0) \right]$$

For  $\rho P \gg P_0$ ,  $\mu = \mu_0 \exp(\beta_T P)$

### Thermal Conductivity

From the kinetic theory of liquids, an approximate equation for thermal conductivity is given.

$$k = 2.80 \left( \frac{N}{V} \right)^{2/3} K \cdot u_s$$

Substituting equation 3 for  $u_s$ , we get

$$k/k_0 = \left( \frac{\rho}{\rho_0} \right)^{1/6}$$

or

$$k = k_o \left[ \exp \left( \frac{1}{6} \beta_T (P - P_o) \right) \right]$$

or  $P \gg P_o$ 

$$k = k_o \exp \left( \frac{1}{6} \beta_T P \right)$$

$k_o$  is thermal conductivity at  $P_o$ .

### Heat Capacity

From thermodynamic properties of fluids, we can write

$$\left( \frac{\partial H}{\partial P} \right)_T = - T \left( \frac{\partial \hat{V}}{\partial T} \right)_P + \hat{V}$$

Differentiating with respect to T gives

$$\frac{d}{dT} \left( \frac{\partial H}{\partial P} \right)_T = \frac{\partial^2 H}{\partial T \partial P} = \frac{\partial^2 H}{\partial P \partial T} = \left( \frac{\partial C_P}{\partial T} \right)_T$$

or

$$\left( \frac{\partial C_P}{\partial P} \right)_T = \frac{\partial}{\partial T} \left[ - T \left( \frac{\partial \hat{V}}{\partial T} \right)_P + \hat{V} \right]$$

Substituting for  $\hat{V} = \frac{1}{\rho}$  (specific volume), we get

$$\left( \frac{\partial C_P}{\partial P} \right)_T = -\frac{2}{3} \frac{T}{\rho^3} \left( \frac{d\rho}{dT} \right)^2$$

Now,

$$\rho = a - bT \quad \text{and} \quad \frac{d\rho}{dT} = -b$$

$$\therefore \left( \frac{\partial C}{\partial P} \right)_T = -\frac{2}{3} \left[ T b^2 \right] \frac{1}{\rho^3}$$

Substituting for  $\rho = \rho_{CP}$  and integrating, we get

$$C_P - C_{P_0} = \frac{2}{3} \frac{b^2 T}{\rho_0^3 \beta_T} \left[ \exp(-3\beta_T P) - \exp(-3\beta_T P_0) \right]$$

Using the other equation for density,  $\rho = \rho_0 + P - P_0 / u_s^2$ , we get

$$\left( C_P - C_{P_0} \right) = b^2 T U_s^6 \left[ \frac{1}{(\rho_0 u_s^2 + P)^2} - \frac{1}{(\rho_0 u_s^2 + P_0)^2} \right]$$

Both the expressions give the same result.

### Calculations

The properties for molten  $\text{NaNO}_3$  as a function of pressure and temperature are given in Table B-1.

The isothermal compressibility is

$$\begin{aligned} \beta_T &= 17.8 \times 10^{-12} \text{ CM}^2/\text{dyne} && \text{at } 300^\circ \text{ C} \\ &= 21.6 \times 10^{-12} \text{ CM}^2/\text{dyne} && \text{at } 400^\circ \text{ C} \\ &= 26.8 \times 10^{-12} \text{ CM}^2/\text{dyne} && \text{at } 500^\circ \text{ C} \end{aligned}$$



Table B-1. Properties of Molten  $\text{NaNO}_3$

Property	300° C		400° C		500° C	
	1 atm	100 atm	1 atm	100 atm	1 atm	100 atm
Density, $\text{kg}/\text{M}^3$	1910	1913.4	1839	1843.0	1767	1771.7
Viscosity, $\text{N}\cdot\text{s}/\text{M}^2$	3.062	3.068	1.964	1.968	1.414	1.418
Thermal conductivity, $\frac{\text{W}}{\text{M}\cdot\text{°k}}$	0.570	0.571	-	-	-	-
Heat capacity, $\frac{\text{Joules}}{\text{kg}\cdot\text{°k}}$	1840	1831.7	-	$\Delta C_p = 9.3$	-	$\Delta C_p=10.5$

A thermodynamic relationship between electrical conductance and pressure for molten  $\text{NaNO}_3$  has been developed. The relationship is expressed as  $\log_{10} K = A + BP$ , where K is the specific conductance, P is the pressure in atmospheres, and A and B are constants. This expression can be used to calculate conductivity of  $\text{NaNO}_3$  at any pressure and temperature.

Effect of pressure on the conductance of molten sodium nitrate and sodium nitrate containing 1 percent by weight of NaOH.

The fundamental relationship has been developed from the experimental data available in the literature.

$$\log_{10} K = A + BP$$

Where

K = specific conductance (ohm - cm)<sup>-1</sup>

P = pressure (atm)

A and B are constants

$$A = -0.447908 + 1.4556 \times 10^{-3}t$$

$$B = -6.618 \times 10^{-5} + 0.011 \times 10^{-5}t$$

Where t = temperature, °C.

This relationship is applicable from 1 to 1000 atm and 330° to 450°C with a maximum error of 3%.

The velocity of sound is

$$u_s = u_o - at = 2164 - 1.15 \times t \text{ (}^\circ\text{C)}; \text{ m/s}$$

The density is

$$\rho_o = 2320 - 0.715 \times T \text{ (}^\circ\text{K)}; \text{ Kg/m}^3$$

The viscosity is

$$\mu_o = 15.45 \times 10^{-5} \exp \left( \frac{3400}{RT} \right); \frac{\text{N}\cdot\text{s}}{\text{M}^2}$$

$$Cp_o = 1840 \text{ Joules/kg } ^\circ\text{K}$$

$$k_o = 0.570 \text{ W/M } ^\circ\text{K}$$

The above data is at atmospheric pressure.

From the table it can be seen that the effect of pressure on properties is insignificant for pressure up to 100 atm.

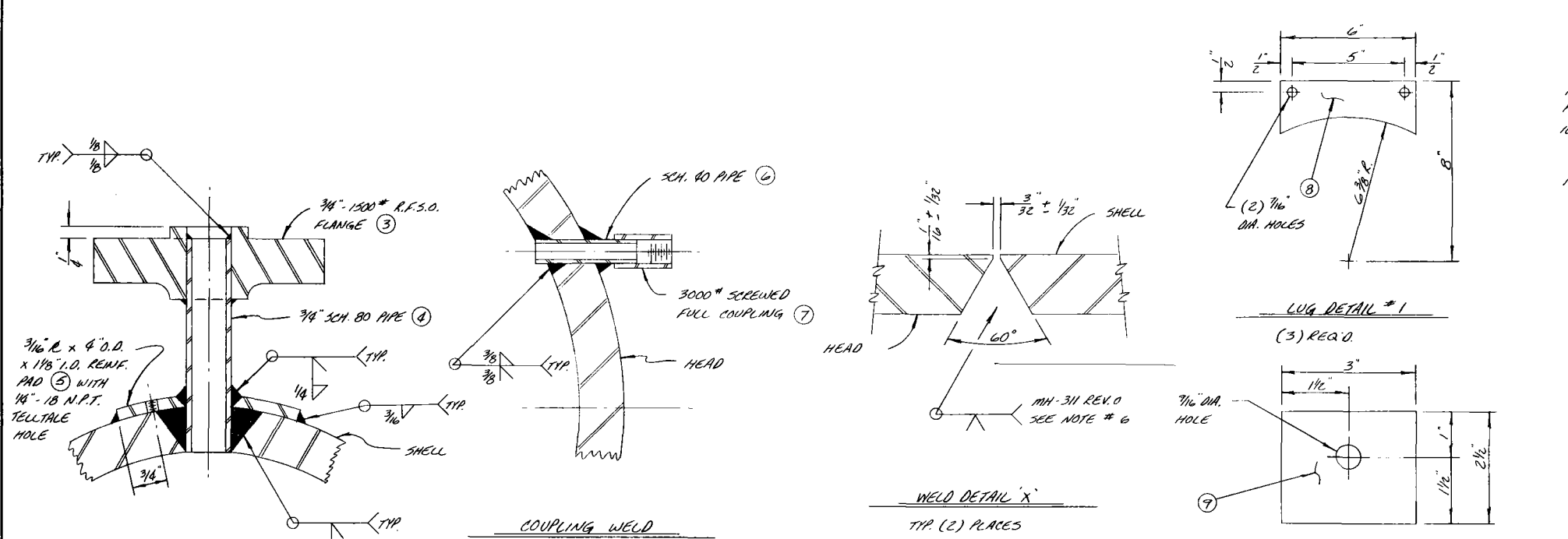
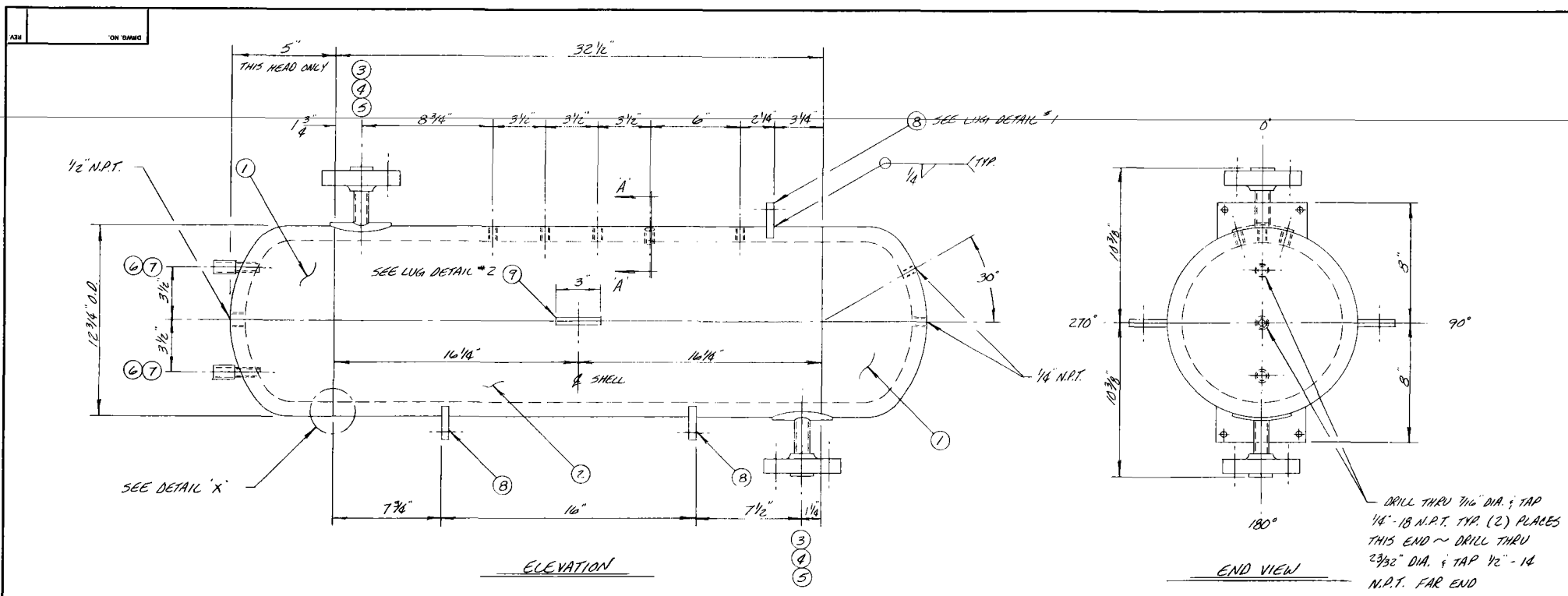
Pressure (atm)	$\log_{10} K$ (calculated)	$\log_{10} K$ (observed)
At 334°C, $\log_{10} K = 0.0382624 - 2.944 \times 10^{-5}P$		
1	0.0382	0.0343
294	0.0296	0.0253
666	0.0187	0.0160
1006	0.0086	0.0057
At 346°C, $\log_{10} K = 0.05573 - 2.812 \times 10^{-5}P$		
1	0.0557	0.0567
223	0.0495	0.0500
388	0.0448	0.0461
666	0.0370	0.0386
862	0.0315	0.0333
1006	0.0274	0.0295
At 364°C, $\log_{10} K = 0.08193 - 2.614 \times 10^{-5}P$		
1	0.0819	0.0845
294	0.0742	0.0776
705	0.0635	0.0681
980	0.0563	0.0613

APPENDIX C  
REFLUX BOILER MODULE  
DRAWING LIST

<u>DRAWING NO.</u>	<u>TITLE</u>
D-79015	General Arrangement Plan View of Reflux Boiler System
D-79016	General Arrangement Elevation of Reflux Boiler System
D-79017	Boiler
D-79018	Condensate Receiver
D-79019	Water Preheater
D-79020	Filler Tank
D-79021	Air Heater
D-79022	Condenser
D-79023	Boiler Coil and Tube Sheet Details
D-79024	Inner Coil Details
D-79060	Reflux Boiler System Frame
D-79061	Frame Details
D-79062	Piping Assemblies







NOTES					
ITEM NO.	QTY.	PART NO. & QTY.	DESCRIPTION	MATL.	WT. LB.
1	2		12" SCH. 120 PIPE WELDING CAP	238-WPAC	162 X
2	1		12" SCH. 120 PIPE x 2" B.V.	SA-106-B-C	340 X
3	2		3/4" - 1500# R.F.S.O. FLANGE	SA-105 C	18 X
4	2		3/4" SCH. 80 PIPE x 0" 4 3/4"	SA-106-B-C	1 X
5	2		3/16" x 4" O.D. x 1 1/8" I.D.	235-C	1 X
6	2		3/8" - 3000# SCREENED FULL COUPLG.	SA-105 C	1 X
7	2		3/8" SCH. 80 PIPE x 2 1/4" T.O.E.	SA-106-B-C	1 X
8	3		1/2" x 2 7/16" x 0"	A-36	2
9	2		1/2" x 2 1/2" x 3"	A-36	1

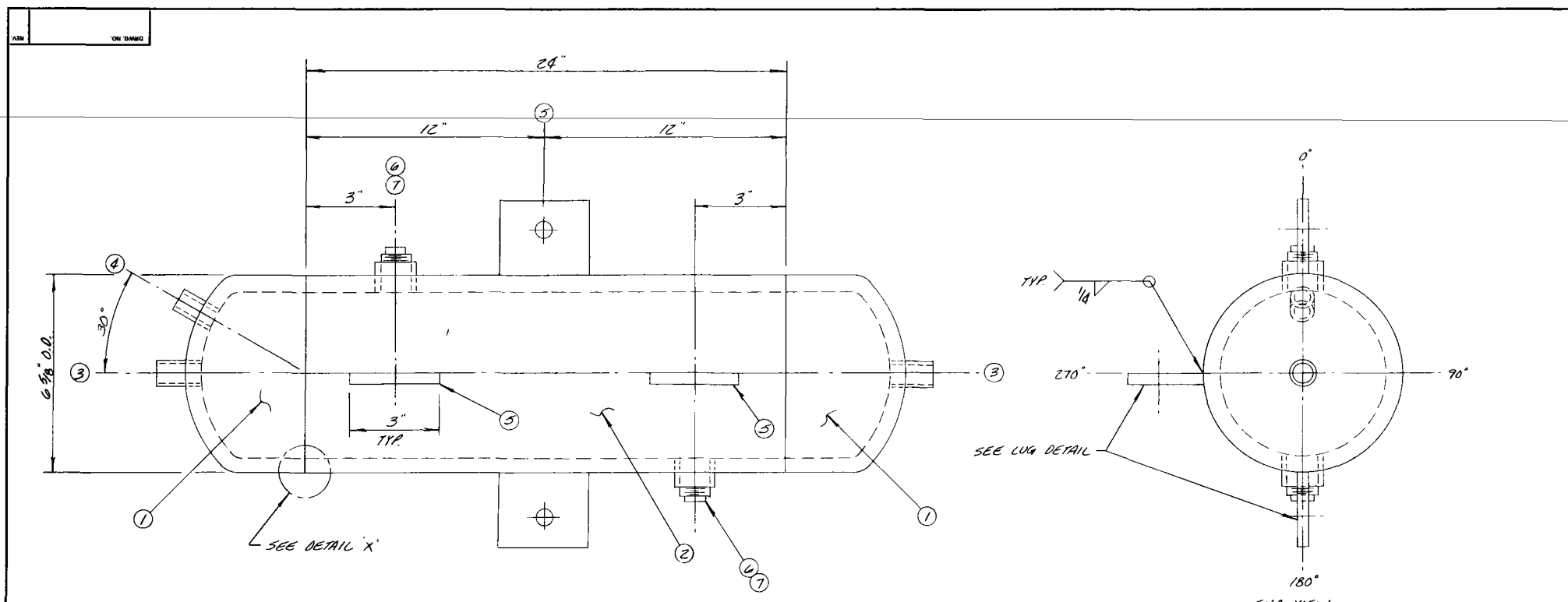
- \* - C - CODE MAT'L., NC - NON-CODE MAT'L.
- NOTE:
- DESIGN & CONSTRUCTION TO BE IN ACCORDANCE WITH THE LATEST EDITION OF SECTION III OF THE A.S.M.E. BOILER & PRESSURE VESSEL CODE.
  - A.S.M.E. & NATIONAL BOARD STAMPS REQ'D.
  - DESIGN CONDITIONS - 1837 PSI @ 625°F CORROSION ALLOW. = 1/16"
  - HYDROSTATIC TEST @ 2756 PSI (PER PROCEDURE MH-ND-PV-1 REV. 2)
  - USE MOOREHEAD MACH. & BLR. CO. WELD PROCEDURES MH-300 REV. 2, MH-311 REV. 0, MH-381 REV. 2, OR MH-REA REV. 2
  - GTAW ROOT USING PROCEDURE MH-311 REV. 0 MAY BE FOLLOWED BY SUB ARC WELDING PER PROCEDURE MH-381 REV. 2 IN LIEU OF SMAW AS CALLED FOR IN MH-311 REV. 0
  - INSPECTION HOLD POINTS SHALL BE AS SPECIFIED ON MM & B CHECKLIST TRAVELER
  - 100% RADIOGRAPHY IS REQ'D. ON CIRCUMFERENTIAL SHELL SEAMS. RADIOGRAPHY TO BE IN ACCORDANCE WITH MM & B PROCEDURE TS-RT-001 REV. C
  - ALL WELDS NOT RADIOGRAPHED TO BE INSPECTED BEFORE STRESS RELIEF AND ALL WELDS TO BE INSPECTED AFTER HYDROTEST BY THE WET FLUORESCENT MAGNETIC PARTICLE METHOD USING PROCEDURE TB-MT-MHZ REV. 0
  - ALL PIPE CONNECTIONS TO BE MADE USING ONLY NEVER - SEE 2 ANTI SEIZE LUBRICATING COMPOUND. DO NOT USE SUBSTITUTES, EVEN FOR TEMPORARY CONNS.
  - COMPLETED VESSEL TO BE STRESS RELIEVED IN ACCORDANCE WITH MM & B PROCEDURE MH-SR-PV2 REV. 0

12) PAINT VESSEL (1) PRIME COAT RUST-OLEUM HEAT RESISTANT RED PRIMER \* 4268 & (1) FINISH COAT RUST-OLEUM HEAT RESISTANT GRAY \* 4286

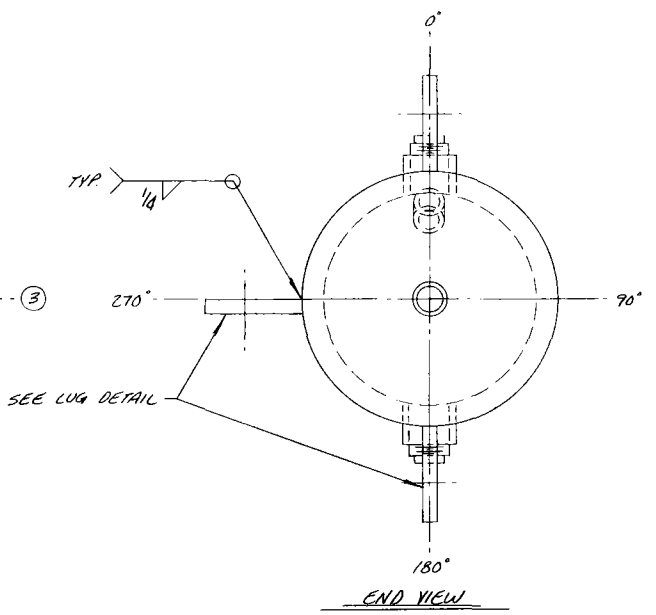
ENGR. APPR.	DATE	G.A. APPR.	DATE	REV.	DATE	DESCRIPTION OF REVISIONS
		A. J.S.	2-23-79			ADDED PAINY NOTE

Approved for Engr. Requirements by _____ Date _____	Approved for G.A. Requirements by _____ Date _____
<b>BOILER</b>	
MINNEAPOLIS, MINN.	
<b>MOORHEAD MACHINERY &amp; BOILER CO.</b>	
MINNEAPOLIS, MINNESOTA	
DRWN: HONEYWELL, MC.	DATE: 1-26-79
CHKD: J. SWANSON	DATE: 1-26-79
REV. NO. 1	REV. DATE
REV. NO. 1	REV. DATE

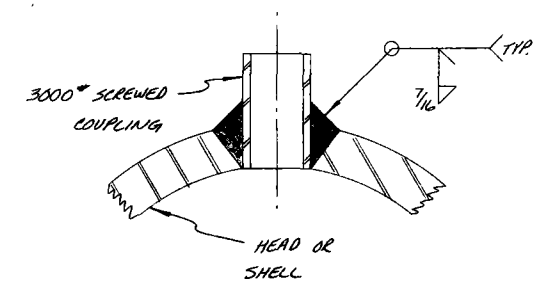




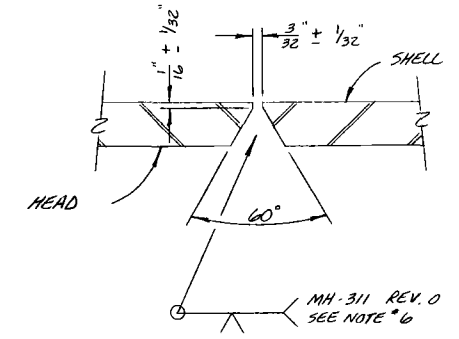
ELEVATION  
NO SCALE



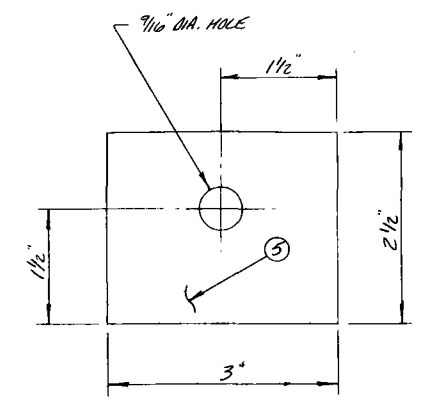
END VIEW



TYP. COUPLING WELD  
TYP. (5) PLACES




WELD DETAIL 'X'  
TYP. (2) PLACES



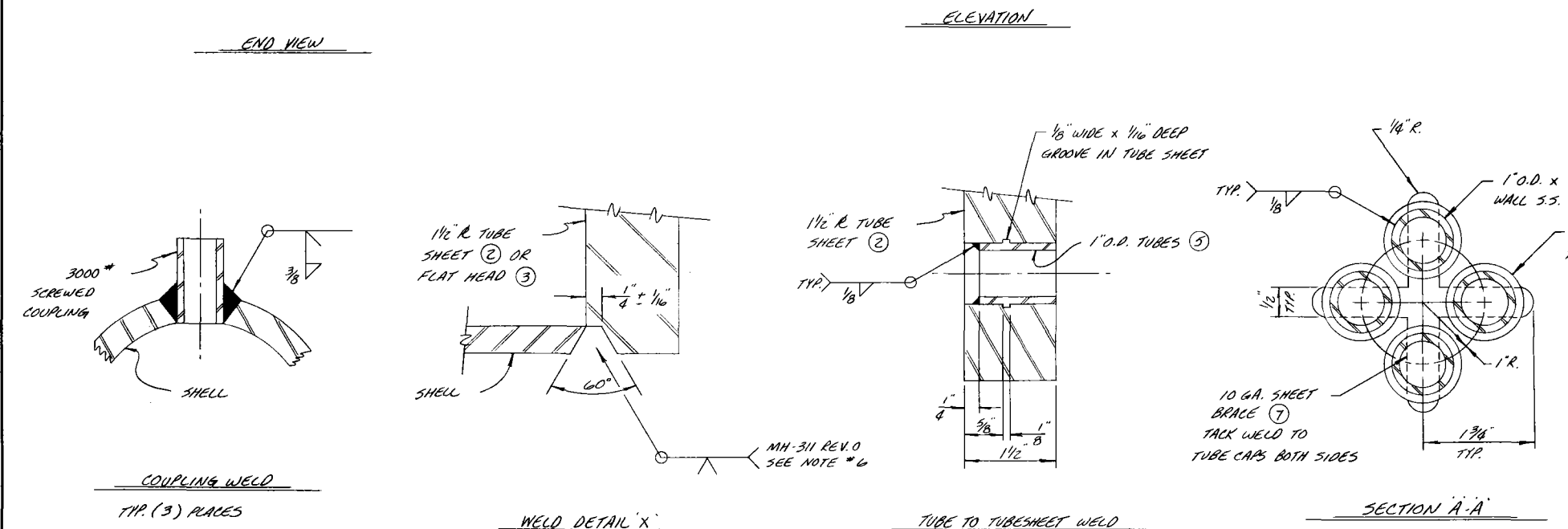
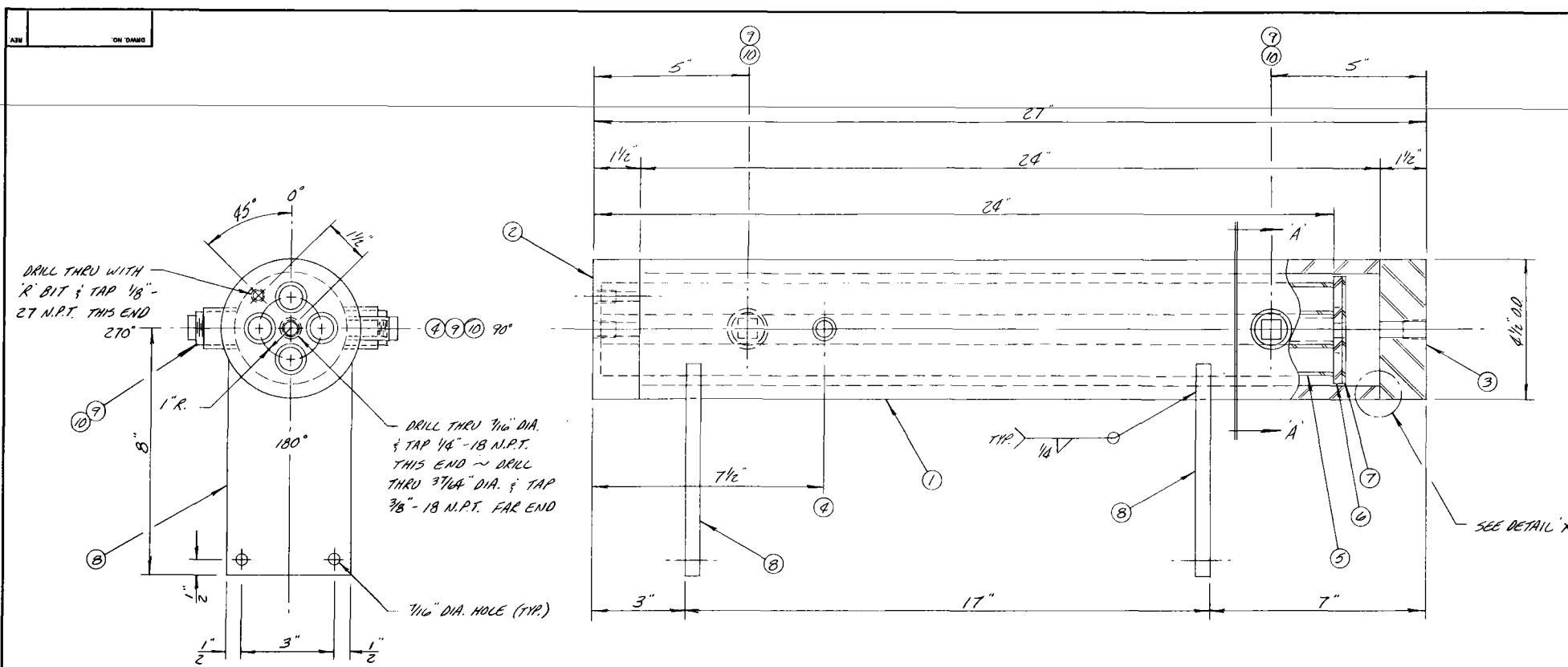
LUG DETAIL  
(4) REQ'D.

NOTES						
ITEM NO.	QTY.	PART NO.	DESCRIPTION	MAT'L.	WT.	PKT.
1	2		6" SCH. 120 PIPE WELDING CAP	SA-106B C	2.60	X
2	1		6" SCH. 120 PIPE x 2'-0" LG.	SA-106B C	7.3	X
3	2		3/4" 3000* SCREWED FULL COUPL.	SA-105 C	1	X
4	1		1/4" 3000* SCREWED FULL COUPL.	SA-105 C	1	X
5	4		3/8" x 2 1/2 x 3"	A-36	2	X
6	2		3/4" 3000* SCREWED HALF COUPL.	SA-105 C	1	X
7	2		3/4" 3000* 20 HEAD PIPE RUG	SA-105 C	1	X

- NOTE: \* - C - CODE MAT'L., N.C. - NON-CODE MAT'L.
- DESIGN & CONSTRUCTION TO BE IN ACCORDANCE WITH THE LATEST EDITION OF SECTION VIII OF THE A.S.M.E. BOILER & PRESSURE VESSEL CODE.
  - A.S.M.E. & NATIONAL BOARD STAMPS READ.
  - DESIGN CONDITIONS - 1837 PSI @ 625°F WITH 1/16" CORR. ALLOW.
  - HYDROSTATIC TEST @ 2756 PSI (PER PROCEDURE MH-ND-PV-1 REV. 2)
  - USE MOORHEAD MACH. & BLR. CO. WELD PROCEDURES MH-300 REV. C, MH-311 REV. O, MH-341 REV. C, OR MH-R2A REV. 2
  - GTAW ROOT USING PROCEDURE MH-311 REV. O MAY BE FOLLOWED BY SUB ARC WELDING PER PROCEDURE MH-341 REV. C IN LIEU OF SMAW AS CALLED FOR IN MH-311 REV. O
  - INSPECTION HOLD POINTS SHALL BE AS SPECIFIED ON MH-B CHECKLIST TRAVELER
  - 100% RADIOGRAPHY IS REQ'D ON CIRCUMFERENTIAL SHELL SEAMS. RADIOGRAPHY TO BE IN ACCORDANCE WITH MH-B PROCEDURE 75-RT-001 REV. C
  - ALL WELDS NOT RADIOGRAPHED TO BE INSPECTED BEFORE HYDROTEST AND ALL WELDS TO BE INSPECTED AFTER HYDROTEST BY THE WET FLUORESCENT MAGNETIC PARTICLE METHOD USING PROCEDURE 7B-MT-MH2 REV. O
  - ALL PIPE CONNECTIONS TO BE MADE USING ONLY NEVER-SEEZ ANTI-SIEZE LUBRICATING COMPOUND. DO NOT USE SUBSTITUTES, EVEN FOR TEMPORARY CONN.
  - PAINT (1) PRIME COAT RUST-OLEUM HEAT RESISTANT RED PRIMER # 426B & (1) FINISH COAT RUST-OLEUM HEAT RESISTANT GRAY # 428G

Approved for Engr. Requirements by _____ Date _____		Approved for Q.A. Requirements by _____ Date _____	
TITLE CONDENSATE RECEIVER		MOORHEAD MACHINERY & BOILER CO.	
MINNEAPOLIS, MINN.		 MINNEAPOLIS, MINNESOTA	
CUST. HONEYWELL INC.			
P.O. # 431586-AA-30W*10073-01		DRAWN SWANSON	DATE 1-23-79
ENGR. APPL. DATE		SCALE A-391	DRIVE NO. D-77018
Q.A. APPL. DATE		REV.	B

ENGR. APPL.	DATE	Q.A. APPL.	DATE	REV.	DESCRIPTION OF REVISIONS
B	J.S.	2-23-79			ADDED PAINT NOTE
A	J.S.	2-5-79			ADDED ITEMS # 6 & 7

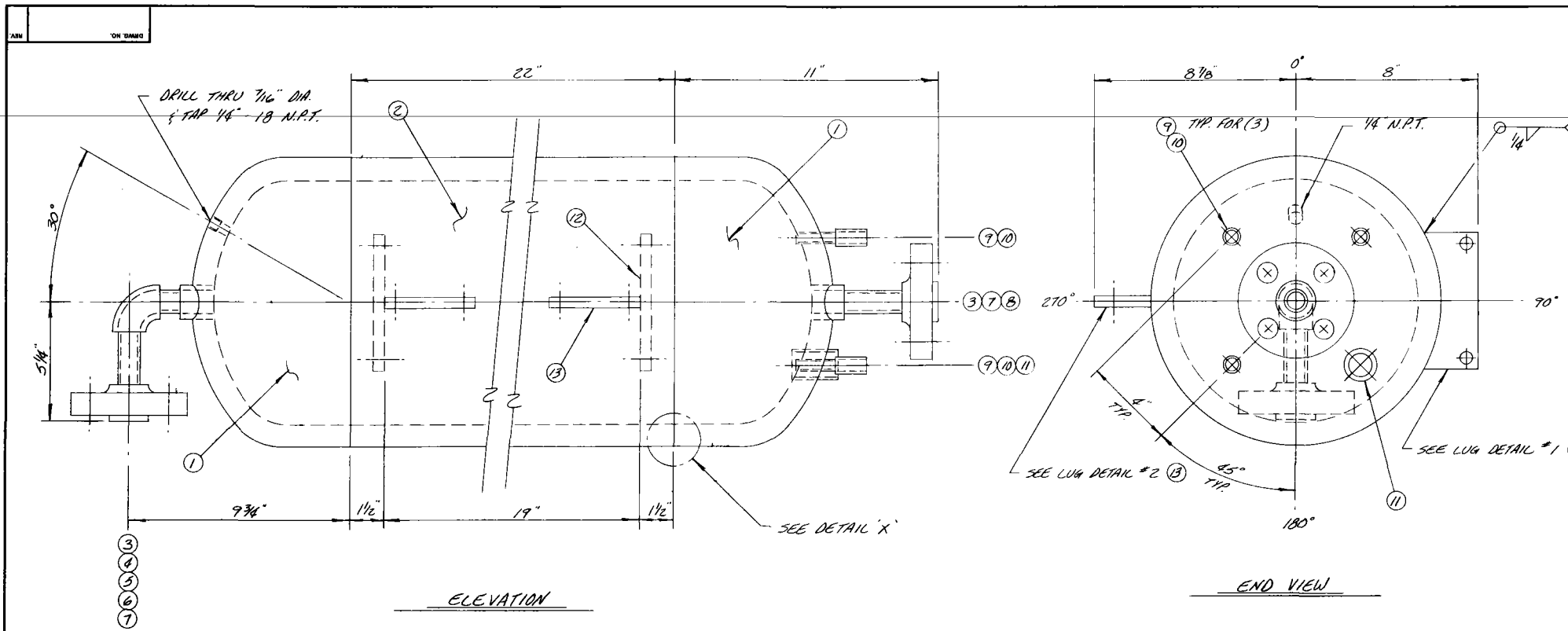


NOTES					
ITEM NO.	QTY	PART NO.	DESCRIPTION	MATL.	WT. LB.
1	1		4 SCH. 120 PIPE x 2'-0"	SA-106-B	30 X
2	1		1 1/2 R. TUBE SHEET x 4 1/2 O.D.	285-C	7
3	1		1 1/2 R. FLAT HEAD x 4 1/2 O.D.	285-C	7
4	1		1/4" 3000* SCREWED FULL CPLG.	SA-105	X
5	4		1" O.D. x .120" WALL TUBES x 1'-11 3/4"	SA-105	9 X
6	4		1/4" R x 1 1/4" O.D.	285-C	1
7	1		10 GA. SHEET x 3 1/2" SA.	A-36	NC
8	2		1/2" R x 4" x 7"	A-36	NC B
9	2		3/4" 3000* SCREWED MALE CPLG.	SA-105	X
10	2		3/4" 3000* SA HEAD PIPE PLUG	SA-105	X

- NOTE: \* - C CODE MAT'L., NC - NON-CODE MAT'L.
- DESIGN & CONSTRUCTION TO BE IN ACCORDANCE WITH THE LATEST EDITION OF SECTION VIII OF THE A.S.M.E. BOILER & PRESSURE VESSEL CODE.
  - A.S.M.E. & NATIONAL BOARD STAMPS REQ'D.
  - DESIGN CONDITIONS = 1837 PSI @ 625°F w/ 1/16" CORR. ALLOW.
  - HYDROSTATIC TEST @ 2750 PSI (PER PROCEDURE MH-ND-PV-1 REV. 2)
  - USE MOORHEAD MACH. & BLR. CO. WELD PROCEDURES MH-300 REV. 2, MH-311 REV. 0, MH-381 REV. 2, OR MH-R2A REV. 2
  - GTAW ROOT USING PROCEDURE MH-311 REV. 0 MAY BE FOLLOWED BY SUB ARC WELDING PER PROCEDURE MH-381 REV. 2 IN LIEU OF SMAW AS CALLED FOR IN MH-311 REV. 0
  - INSPECTION HOLD POINTS SHALL BE AS SPECIFIED ON MP & B CHECKLIST TRAVELER
  - ALL WELDS TO BE INSPECTED BEFORE AND AFTER HYDROTEST BY THE WET FLUORESCENT MAGNETIC PARTICLE METHOD USING PROCEDURE TB-MT-MHZ REV. 0
  - ALL PIPE CONNECTIONS TO BE MADE USING ONLY NEVER-SEEZ ANTI SEIZE LUBRICATING COMPOUND. DO NOT USE SUBSTITUTES, EVEN FOR TEMPORARY CONNS.
  - INSERT CUSTOMER SUPPLIED CAL-ROD HEATERS IN 1" O.D. 5S. TUBES TO INSURE PROPER FIT BEFORE WELDING TUBE SHEET TO SHELL.
  - PAINT VESSEL (1) PRIME COAT RUST-OLEUM HEAT RESISTANT RED PRIMER # 426B & (1) FINISH COAT RUST-OLEUM HEAT RESISTANT GRAY # 4286

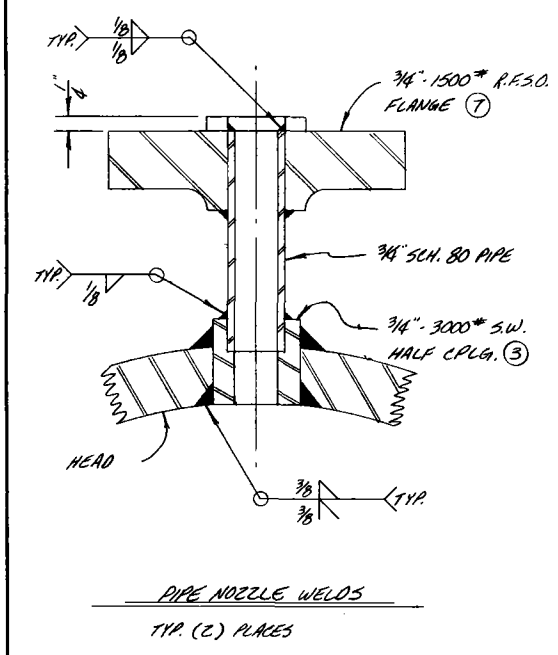
Approved for Engr. Requirements by _____ Date _____	Approved for Q.A. Requirements by _____ Date _____
TITLE <b>WATER PREHEATER</b>	
MINNEAPOLIS, MINN.	
CUST. MONEYWELL INC.	
P.D. # 431584-AA ~ S.A.W. # 10073-01	
DRAWN SWANSON	DATE 1-24-79
CHECKED	DATE
SCALE A-391	
DRWG. NO. D-79019	
REV. B	

ENGR. APPR.	DATE	Q.A. APPR.	DATE	REV.	DATE	DESCRIPTION OF REVISIONS
B	J.S.	2-23-79				ADDED PAINT NOTE
A	J.S.	2-5-79				ADDED ITEMS # 9 & 10

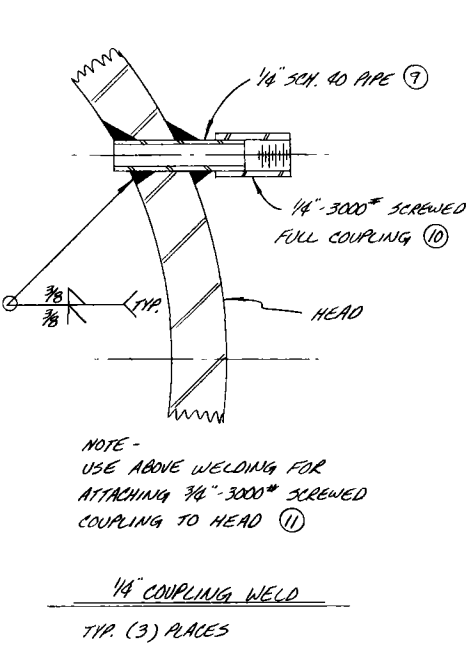


NOTES					
ITEM NO.	QTY.	PART NO. SHIP	DESCRIPTION	MAT'L.	* WT. LB.
1	2		12" SCH. 120 PIPE WELDING CAPS	234-WPB C	162 X
2	1		12" SCH. 120 PIPE x 1'-10"	SA-106 B C	230 X
3	2		3/4" 3000* S.W. HALF CPLG.	SA-105 C	1 X
4	1		3/4" SCH. 80 PIPE x CHECK HD. W/PTH	SA-106 B C	X
5	1		3/4" 3000* 90° S.W. ELBOW	SA-105 C	1 X
6	1		3/4" SCH. 80 PIPE x 4 1/4"	SA-106 B C	5 X
7	2		3/4" 1500* R.F.S.O. FLANGE	SA-105 C	18 X
8	1		3/4" SCH. 80 PIPE x CHECK HD. W/PTH	SA-106 B C	X
9	3		1/4" SCH. 40 PIPE x 2 1/4" T.O.E.	SA-106 B C	1 X
10	3		1/4" 3000* SCREWED FULL CPLG.	SA-105 C	1 X
11	1		3/4" 3000* SCREWED FULL CPLG.	SA-105 C	1
12	2		1/2" R x 2 1/4" x 6"	A-36	NC 4
13	2		1/2" R x 2 1/2" x 4"	A-36	NC 2

- \* - C = CODE MAT'L., NC = NON-CODE MAT'L.
- NOTE:
- DESIGN & CONSTRUCTION TO BE IN ACCORDANCE WITH THE LATEST EDITION OF SECTION VIII OF THE A.S.M.E. BOILER & PRESSURE VESSEL CODE.
  - A.S.M.E. & NATIONAL BOARD STAMPS REQ'D.
  - DESIGN CONDITIONS - 1837 PSI @ 625°F CORROSION ALLOWANCE - 1/16"
  - HYDROSTATIC TEST @ 2756 PSI (PER PROCEDURE MH-ND-PV-1 REV. 2)
  - USE MOORHEAD MACH. & BUL. CO. WELD PROCEDURES MH-300 REV. 2, MH-311 REV. 0, MH-341 REV. 2, OR MH-R2A REV. 2
  - GTAW ROOT USING PROCEDURE MH-311 REV. 0 MAY BE FOLLOWED BY SUB ARC WELDING PER PROCEDURE MH-341 REV. 2 IN LIEU OF SMAW AS CALLED FOR IN MH-311 REV. 0
  - INSPECTION HOLD POINTS SHALL BE AS SPECIFIED ON MM;B CHECKLIST TRAVELER
  - 100% RADIOGRAPHY IS REQ'D. ON CIRCUMFERENTIAL SHELL SEAMS. RADIOGRAPHY TO BE IN ACCORDANCE WITH MM;B PROCEDURE 75-R1 001 REV. C
  - ALL WELDS NOT RADIOGRAPHED TO BE INSPECTED BEFORE HYDROTEST AND ALL WELDS TO BE INSPECTED AFTER HYDROTEST BY THE WET FLUORESCENT MAGNETIC PARTICLE METHOD PER PROCEDURE TB-MT-MHZ REV. 0
  - ALL PIPE CONNECTIONS TO BE MADE USING ONLY NEVER-SEEZ ANTI SIEZE LUBRICATING COMPOUND. DO NOT USE SUBSTITUTES, EVEN FOR TEMPORARY CONNS.

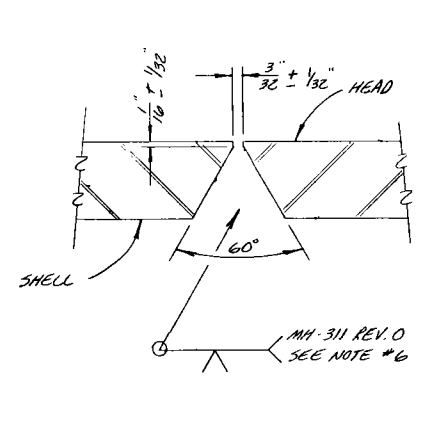


PIPE NOZZLE WELDS  
TYP. (2) PLACES

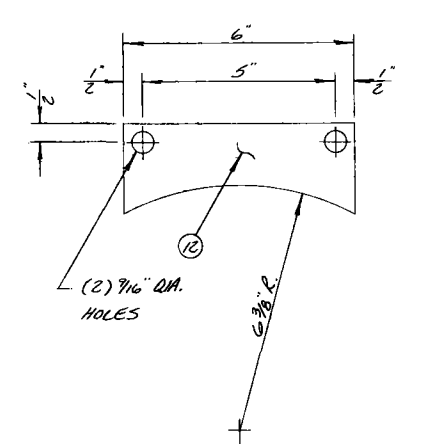


NOTE - USE ABOVE WELDING FOR ATTACHING 3/4\"/>

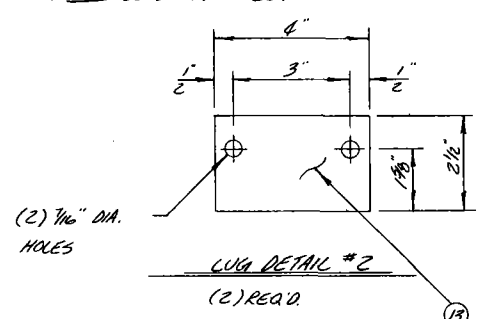
1/4" COUPLING WELD  
TYP. (3) PLACES



WELD DETAIL 'X'  
TYP. (2) PLACES



LUG DETAIL #1  
(2) REQ'D.

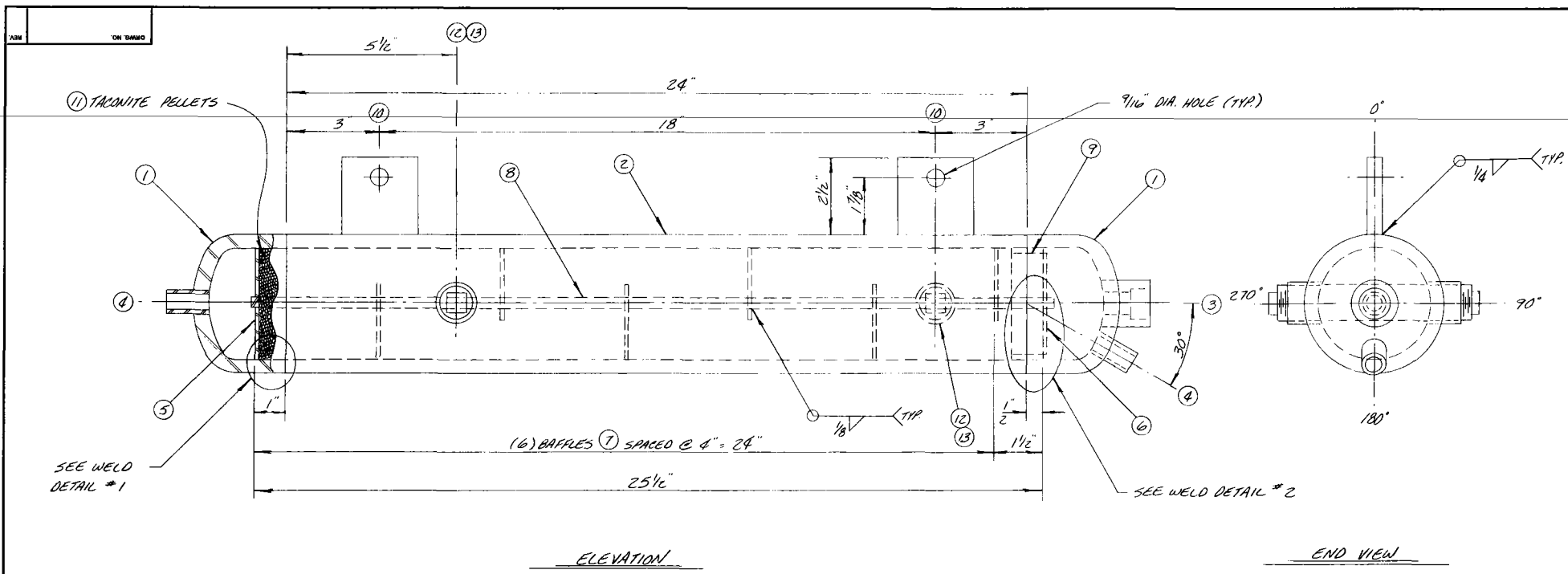


(2) 7/16" DIA. HOLES  
LUG DETAIL #2  
(2) REQ'D.

11) PAINT VESSEL (1) PRIME COAT RUST-OLEUM HEAT RESISTANT RED PRIMER #4268 & (1) FINISH COAT RUST OLEUM HEAT RESISTANT GRAY #8286

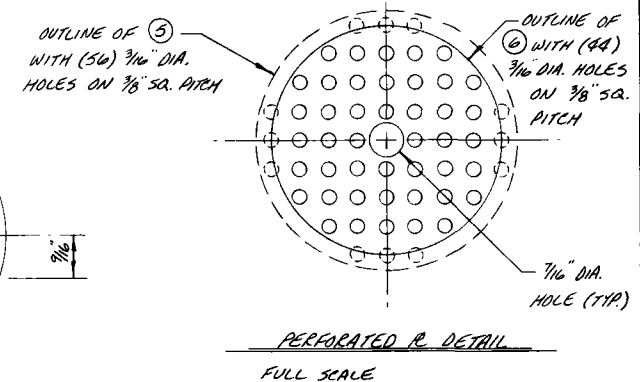
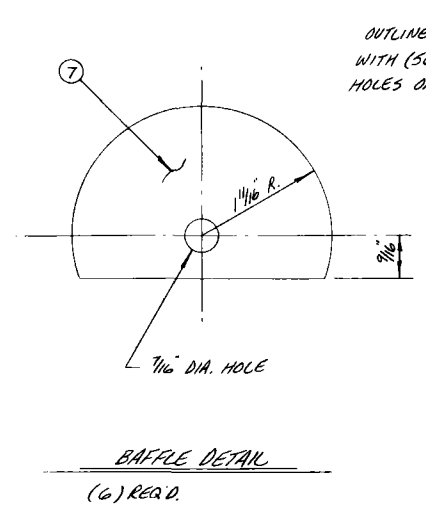
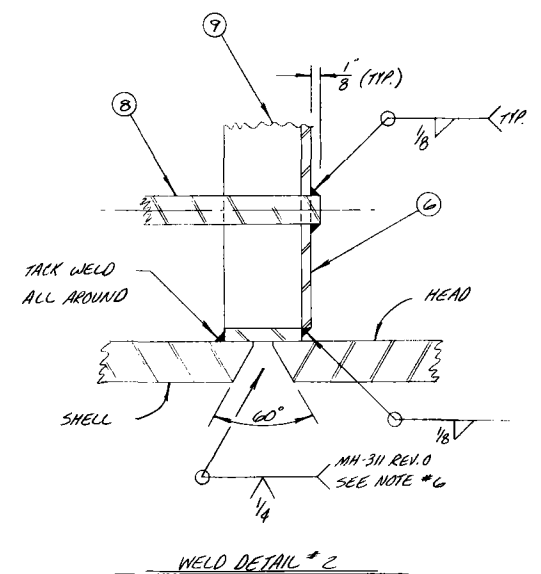
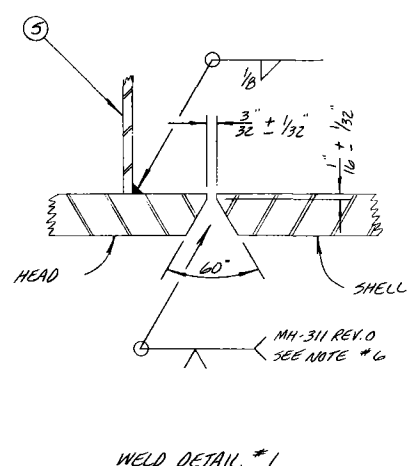
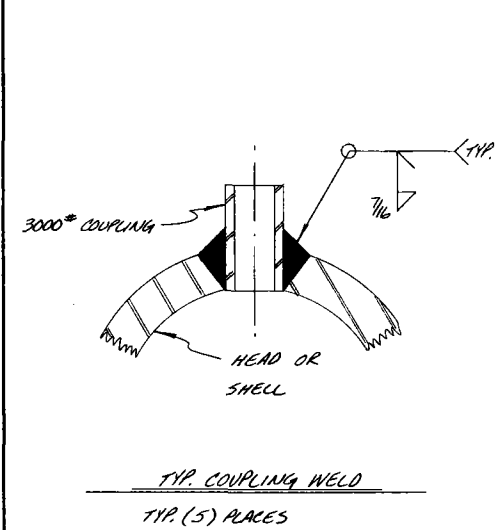
Approved for Engr. Requirements by _____ Date _____	Approved for Q.A. Requirements by _____ Date _____
TITLE <b>FILLER TANK</b>	
MINNEAPOLIS, MINN.	
DRAWN: <b>MOONEYWELL, INC.</b>	
NO. <b>431586-AA-5001-0073-01</b>	
DRAWN: <b>SWANSON</b>	DATE: <b>1-30-79</b>
CHECKED: _____	SCALE: <b>A-391</b>
	DRAW. NO. <b>D-79020</b>
	REV. <b>A</b>

ENGR. APPR.	DATE	Q.A. APPR.	DATE	REV.	DRAWN	DATE	DESCRIPTION OF REVISIONS
					A J.S.	1-23-79	ADDED PAINT NOTE



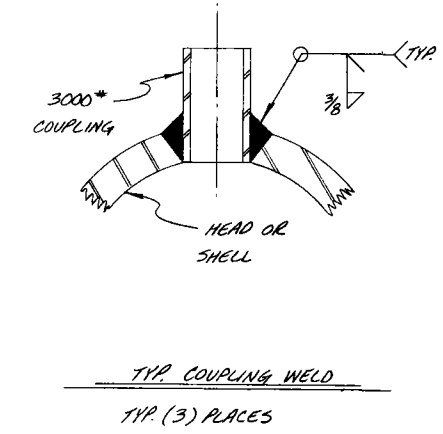
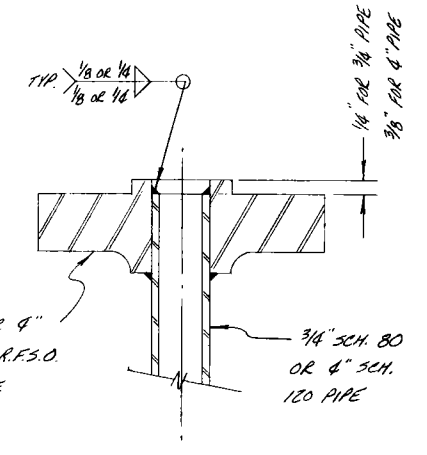
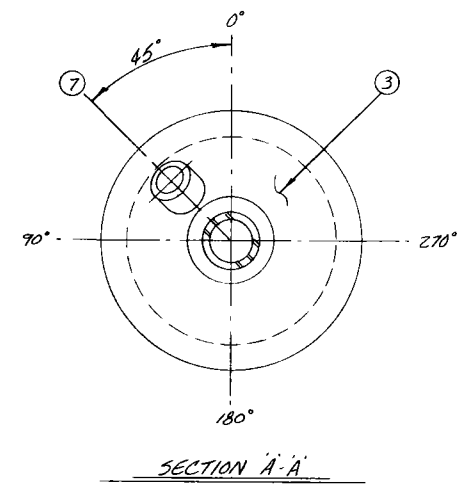
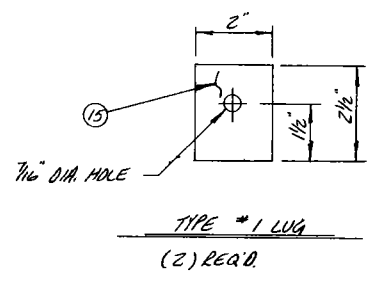
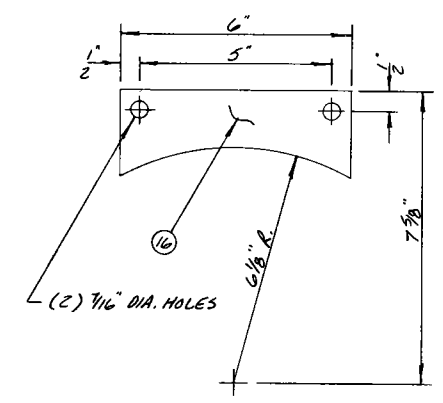
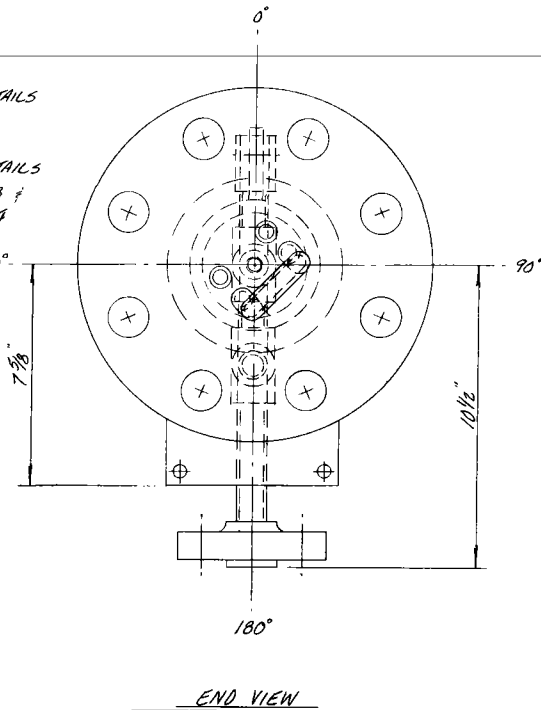
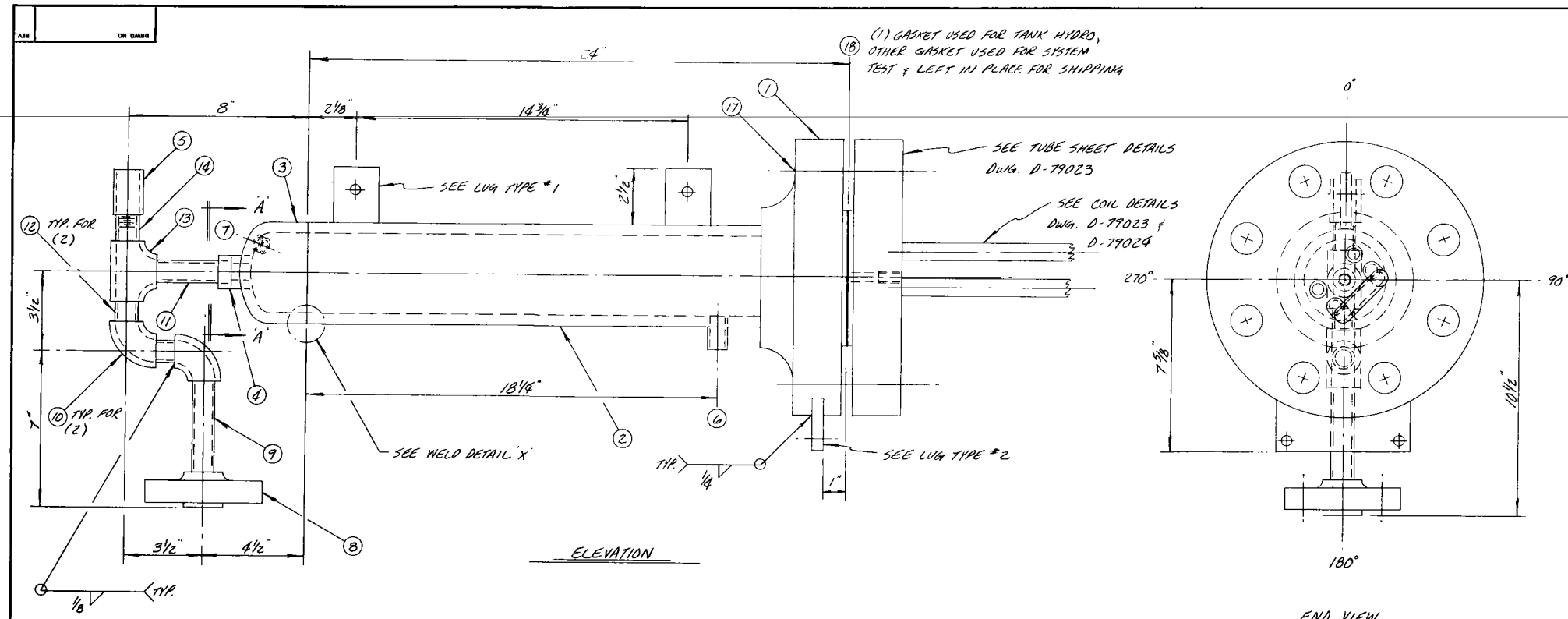
NOTES					
ITEM NO.	PART NO.	DESCRIPTION	MAT'L.	QTY.	REMARKS
1	2	4" SCH. 100 PIPE WELDING CAP	E34-WPB	C 14	X
2	1	4" SCH. 160 PIPE X 2'-0"	SA-106-B	C 65	X
3	1	3/4" 3000* S.W. HALF COUPL.	SA-105	C 1	X
4	2	1/4" 3000* SCREWED FULL COUPL.	SA-105	C 1	X
5	1	10 GA. PERF. SHEET X 3 3/8" O.D.	M1020	NC	
6	1	10 GA. PERF. SHEET X 3" O.D.	M1020	NC	
7	6	10 GA. SHEET X 2 1/4" X 3 3/8"	M1020	NC	
8	1	3/8" DIA. ROD X 2'-2"	M1020	NC	
9	1	3/16" X 1" F.F. X 10 3/16"	285-C	C	
10	2	1/2" R X 2 1/2" X 2 1/2"	A-36	NC	
11		APPROX. 250 CU. IN. OF 1/2" DIA. TACONITE PELLETS		NC	
12	2	3/4" 3000* SCREWED FULL COUPL.	SA-105	C	X
13	2	3/4" 3000* S.W. HEAD PIPE FLG.	SA-105	C	X

- NOTE: \* - C - CODE MAT'L., NC - NON - CODE MAT'L.
- DESIGN & CONSTRUCTION TO BE IN ACCORDANCE WITH THE LATEST EDITION OF SECTION VIII OF THE A.S.M.E. BOILER & PRESSURE VESSEL CODE
  - A.S.M.E. & NATIONAL BOARD STAMPS REQ'D.
  - DESIGN CONDITIONS - 1837 PSI @ 800°F  
CORROSION ALLOWANCE = 1/16"
  - HYDROSTATIC TEST @ 3827 PSI  
(PER PROCEDURE MH-ND-PV-1 REV. 2)
  - USE MOORHEAD MACH. & BCR. CO. WELD PROCEDURES MH-300 REV. 2, MH-311 REV. 0, MH-341 REV. 2, OR MH-RCA REV. 2
  - GTAW ROOT USING PROCEDURE MH-311 REV. 0 MAY BE FOLLOWED BY SUB ARC WELDING PER PROCEDURE MH-341 REV. 2 IN LIEU OF SMAW AS CALLED FOR IN MH-311 REV. 0
  - INSPECTION HOLD POINTS SHALL BE AS SPECIFIED ON MM-18 CHECKLIST TRAVELER
  - ALL WELDS TO BE INSPECTED BEFORE AND AFTER HYDROTEST BY THE WET FLUORESCENT MAGNETIC PARTICLE METHOD PER PROCEDURE TB-MT-MNZ REV. 2
  - ALL PIPE CONNECTIONS TO BE MADE USING ONLY NEVER - SEEZ ANTI SEIZE LUBRICATING COMPOUND. DO NOT USE SUBSTITUTES, EVEN FOR TEMPORARY CONNS.



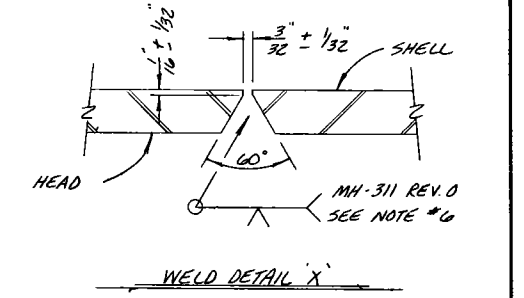
Approved for Engr. Requirements By: _____ Date: _____	Approved for Q.A. Requirements By: _____ Date: _____
TITLE AIR HEATER	<b>MOORHEAD</b> MACHINERY & BOILER CO.
MINNEAPOLIS, MINN.	
DRW. HONEYWELL INC.	MINNEAPOLIS, MINNESOTA
NO. *431584-AA ~ S.O.M. *I0073-01	
DRAWN SWANSON DATE 2-1-79	J.D. A-391
CHECKED _____ DATE _____	SCALE D-79021
REVISIONS	REV. A

ENGR. APPR.	DATE	D.A. APPR.	DATE	REV.	DATE	DESCRIPTION OF REVISIONS
A	J.S.	2-22-79				REVISED HYDROSTATIC TEST PRESSURE



NOTES					
ITEM NO.	QTY.	PART NO. SHIP	DESCRIPTION	MAT'L.	WT. LB.
1	1		4" 1500 R.F.S.O. FLANGE	SA-105 C	73 X
2	1		4" SCH. 120 PIPE X 11 7/8"	SA-105 C	38 X
3	1		4" SCH. 120 PIPE WELDING CAP	234 WAB C	5 X
4	1		3/4" 3000 S.W. HALF COUPLING	SA-105 C	X
5	1		3/4" 3000 S.W. FULL COUPLING	SA-105 C	X
6	1		3/4" 3000 S.W. FULL COUPLING	SA-105 C	X
7	1		1/4" 3000 S.W. FULL COUPLING	SA-105 C	X
8	1		3/4" 1500 R.F.S.O. FLANGE	SA-105 C	9 X
9	1		3/4" SCH. 80 PIPE X 0'6"	SA-105 C	1 X
10	2		3/4" 3000 90° S.W. ELBOW	SA-105 C	2 X
11	1		3/4" SCH. 80 PIPE X 0'3 3/4"	SA-105 C	X
12	2		3/4" SCH. 80 PIPE X 0'2"	SA-105 C	1 X
13	1		3/4" 3000 S.W. TEE	SA-105 C	1 X
14	1		3/4" SCH. 80 PIPE X 0'2 1/8" TOE	SA-105 C	X
15	2		1/2" R x 2" x 2 1/2"	A-36 NC	2
16	1		1/2" R x 2 1/4" x 6"	A-36	1
17	8		1 1/4" DIA. X 1 1/2" LG. BOLT W/ NUT	A-307 C	27 X
18	2		4" 1500 LAMONS SPIRAL SEAL	304 S.S. C	X
			GASKET STYLE WR		

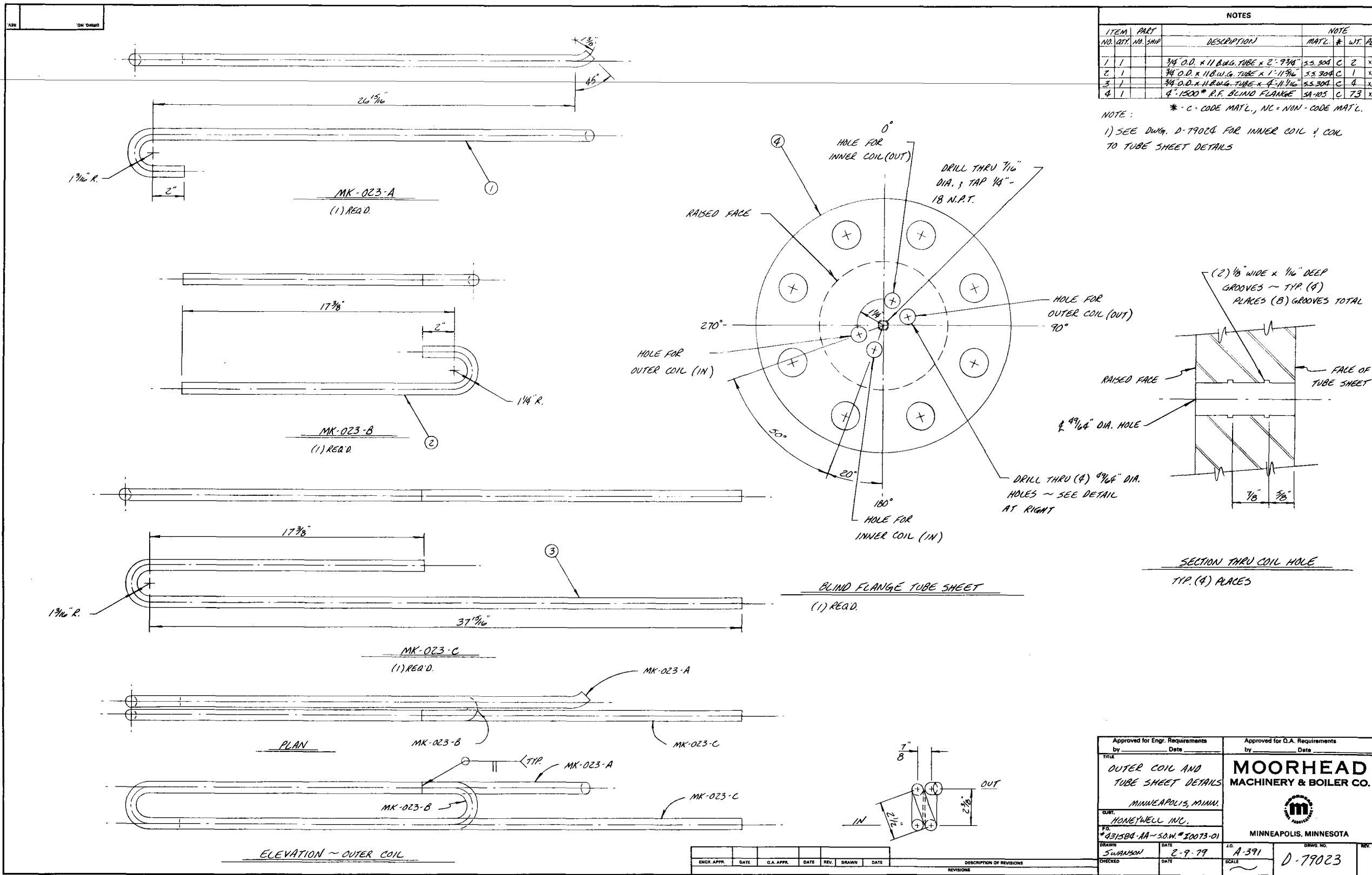
- \* - C = CODE MAT'L., NC = NON-CODE MAT'L.
- NOTE:
- DESIGN & CONSTRUCTION TO BE IN ACCORDANCE WITH THE LATEST EDITION OF SECTION VIII OF THE A.S.M.E. BOILER & PRESSURE VESSEL CODE
  - A.S.M.E. & NATIONAL BOARD STAMPS REQ'D.
  - DESIGN CONDITIONS - 1837 PSI @ 625°F CORROSION ALLOWANCE = 1/16"
  - HYDROSTATIC TEST @ 2756 PSI (PER PROCEDURE MH-ND-PV-1 REV. 2)
  - USE MOORHEAD MACH. & BLD. CO. WELD PROCEDURES MH-300 REV. 2, MH-311 REV. 0, MH-341 REV. 2 OR MH-R2A REV. 2
  - GTAW ROOT USING PROCEDURE MH-311 REV. 0 MAY BE FOLLOWED BY SUB ARC WELDING PER PROCEDURE MH-341 REV. 2 IN LIEU OF SMAW AS CALLED FOR IN MH-311 REV. 0
  - INSPECTION HOLD POINTS SHALL BE AS SPECIFIED ON MM & B CHECKLIST TRAVELER
  - ALL WELDS TO BE INSPECTED BEFORE AND AFTER HYDROTEST BY THE WET FLUORESCENT MAGNETIC PARTICLE METHOD PER PROCEDURE TB-MT-MH2 REV. 2
  - ALL PIPE CONNECTIONS TO BE MADE USING ONLY NEVER-SEEZ ANTI-SIEZE LUBRICATING COMPOUND. DO NOT USE SUBSTITUTES, EVEN FOR TEMPORARY CONNS.



Approved for Engr. Requirements by _____ Date _____	Approved for Q.A. Requirements by _____ Date _____
TITLE <b>CONDENSOR</b>	<b>MOORHEAD</b> MACHINERY & BOILER CO.
MINNEAPOLIS, MINN.	
CONTR. HONEYWELL INC.	MINNEAPOLIS, MINNESOTA
DRAWN SWANSON	DATE 2-8-79
SCALE A-391	REV. D-79022

10) PAINT VESSEL (1) PRIME COAT RUST-OLEUM HEAT RESISTANT RED PRIMER \*426B & (1) FINISH COAT RUST-OLEUM HEAT RESISTANT GRAY \*4286

ENGR. APPR.	DATE	Q.A. APPR.	DATE	REV.	DATE	DESCRIPTION OF REVISIONS
A J.S.	2-23-79					ADDED PAINT NOTE



NOTES						
ITEM NO.	PART NO.	QTY.	DESCRIPTION	MATL.	WT.	PO.
1			3/4" O.D. x 11 B.W.G. TUBE x 2'-9 3/4"	55-304 C	2	x
2			3/4" O.D. x 11 B.W.G. TUBE x 1'-11 3/4"	55-304 C	1	x
3			3/4" O.D. x 11 B.W.G. TUBE x 4'-11 1/2"	55-304 C	4	x
4			4" 1500 R.F. BLIND FLANGE	SA-105 C	73	x

NOTE:  
 \* - C - CODE MAT'L., NC - NON - CODE MAT'L.  
 1) SEE DWG. D-79024 FOR INNER COIL & COIL TO TUBE SHEET DETAILS


BLIND FLANGE TUBE SHEET  
 (1) REQ'D.

SECTION THRU COIL HOLE  
 TIP (4) PLACES

PLAN

ELEVATION ~ OUTER COIL

ENGR. APPR.	DATE	C.A. APPR.	DATE	REV.	DRAWN	DATE	DESCRIPTION OF REVISIONS

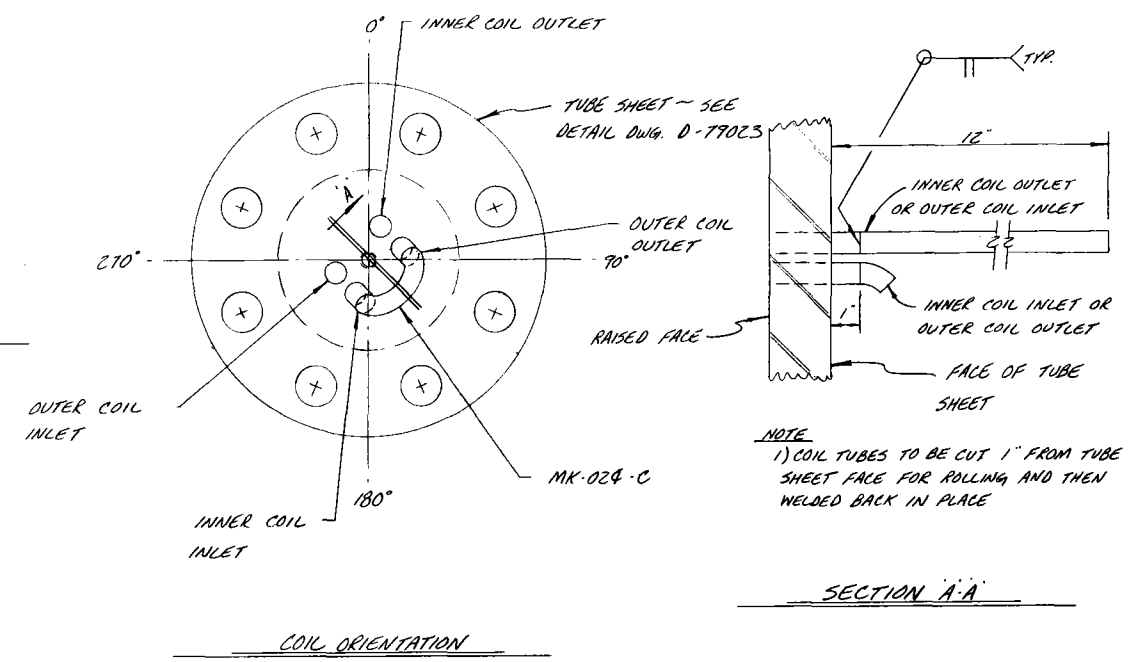
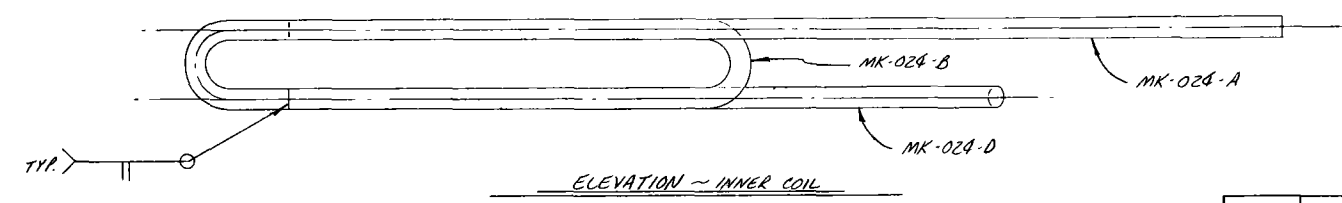
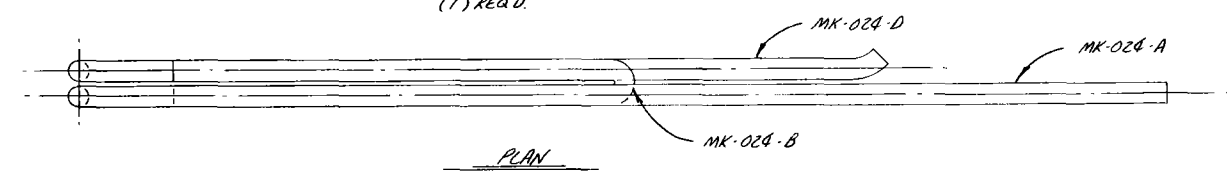
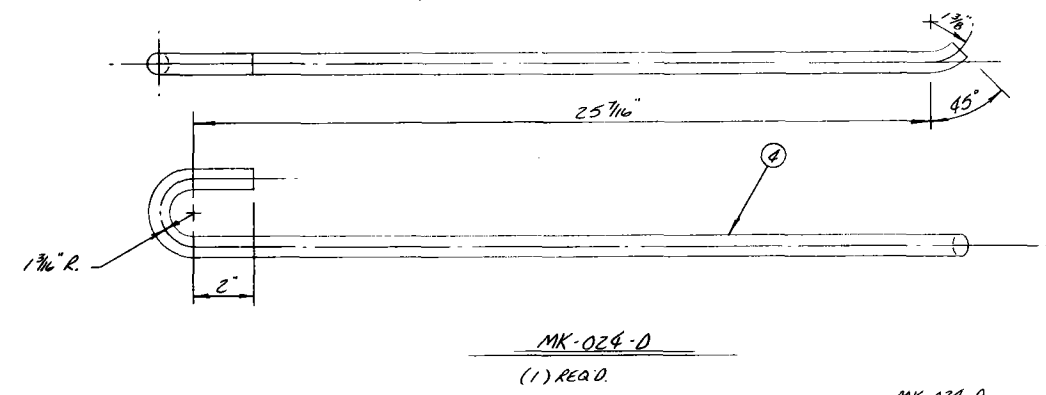
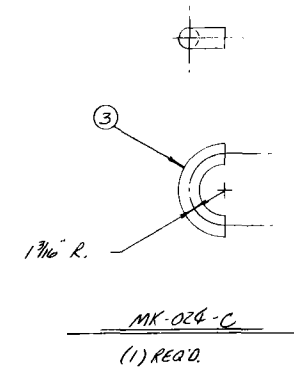
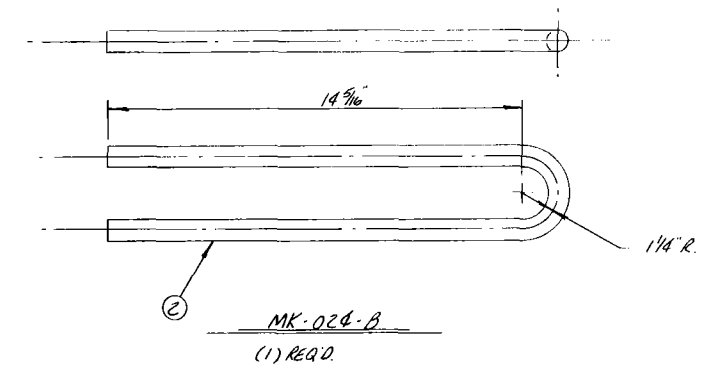
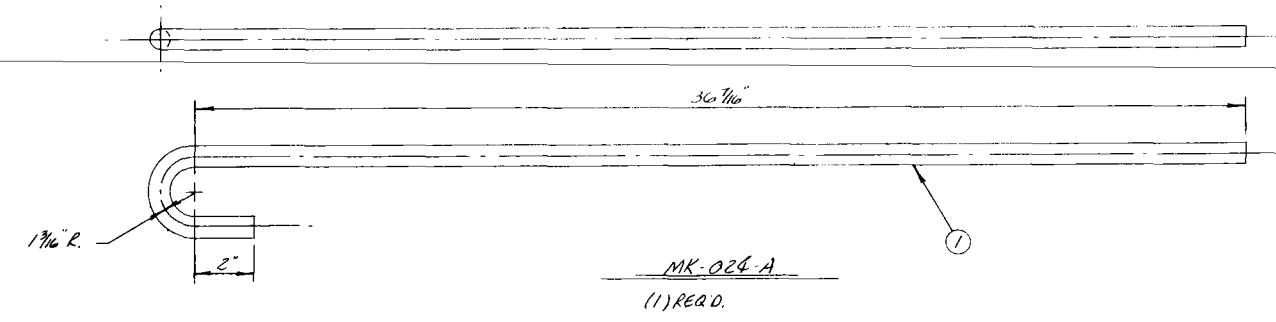
Approved for Engr. Requirements by _____ Date _____		Approved for O.A. Requirements by _____ Date _____	
TITLE OUTER COIL AND TUBE SHEET DETAILS MINNEAPOLIS, MINN.		MOORHEAD MACHINERY & BOILER CO.  MINNEAPOLIS, MINNESOTA	
DWT. HONEYWELL INC.			
P.O. # 831584-AA-S.O.W.# 10073-01			
DRAWN SWANSON	DATE 2-9-79	S.D. A-391	DRAWG. NO. D-79023
CHECKED	DATE	SCALE	REV.

ASB ON DWG

NOTES						
ITEM NO.	QTY.	PART NO. SHIP	DESCRIPTION	MATL.	WT.	PA.
1	1		3/4" O.D. x 11 B.W.G. TUBE x 3'-6 3/16"	SS-304 C	3	X
2	1		3/4" O.D. x 11 B.W.G. TUBE x 2'-8 7/16"	SS-304 C	2	X
3	1		3/4" O.D. x 11 B.W.G. TUBE x 2'-5 7/8"	SS-304 C	2	X
4	1		3/4" O.D. x 11 B.W.G. TUBE x 2'-8 7/16"	SS-304 C	2	X

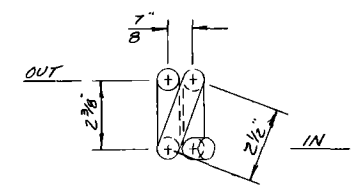
\* - C = CODE MATL., NC = NON-CODE MATL.

NOTE:  
1) SEE DWG. D-79023 FOR OUTER COIL & TUBE SHEET DETAILS



NOTE:  
1) COIL TUBES TO BE CUT 1" FROM TUBE SHEET FACE FOR ROLLING AND THEN WELDED BACK IN PLACE

SECTION A-A

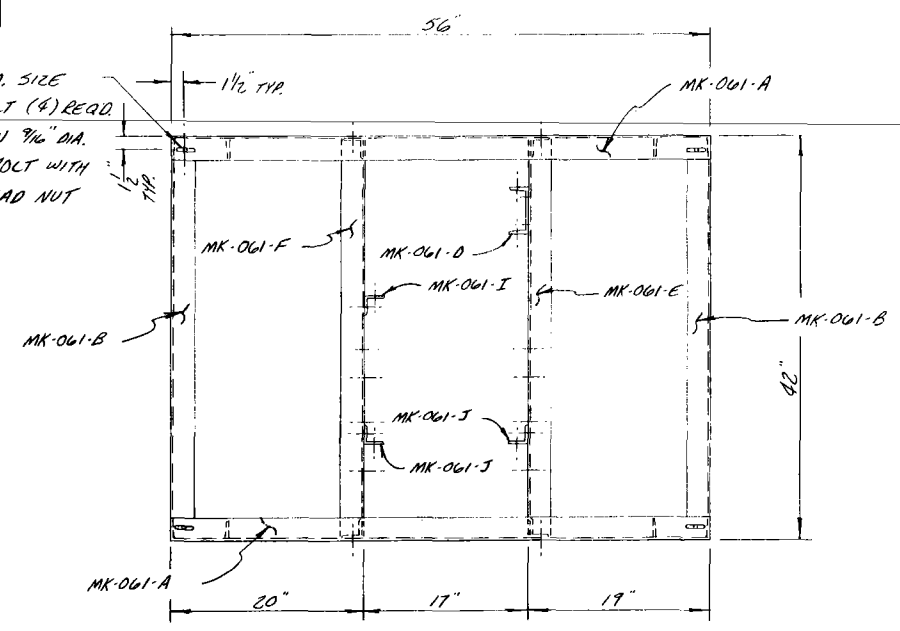


ENGR. APPR.	DATE	C.A. APPR.	DATE	REV.	DRAWN	DATE	DESCRIPTION OF REVISIONS

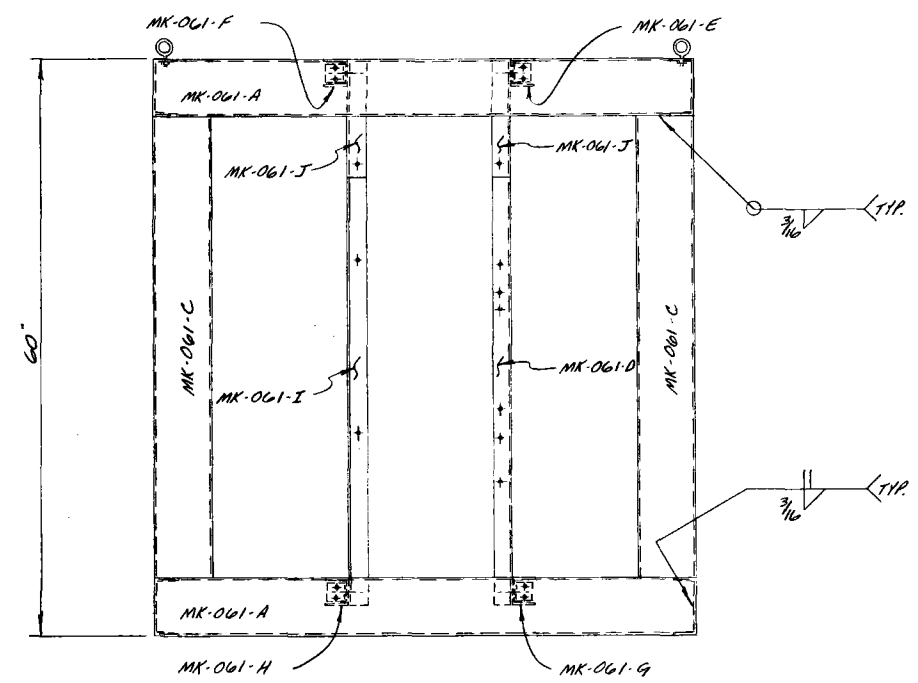
Approved for Engr. Requirements by _____ Date _____	Approved for C.A. Requirements by _____ Date _____
TITLE INNER COIL DETAILS	<b>MOORHEAD</b> MACHINERY & BOILER CO.
MINNEAPOLIS, MINN.	
CUSTOMER HONEYWELL INC.	MINNEAPOLIS, MINNESOTA
PROJECT NO. #431584-AA - S.O.W. #20073-01	
DRAWN SWANSON	DATE 2-12-79
CHECKED	DATE
J.D. A-391	SCALE
	DRAWING NO. D-79024

NOTES  
 1) SEE DRAWING D-79061 FOR PIECE DETAILS

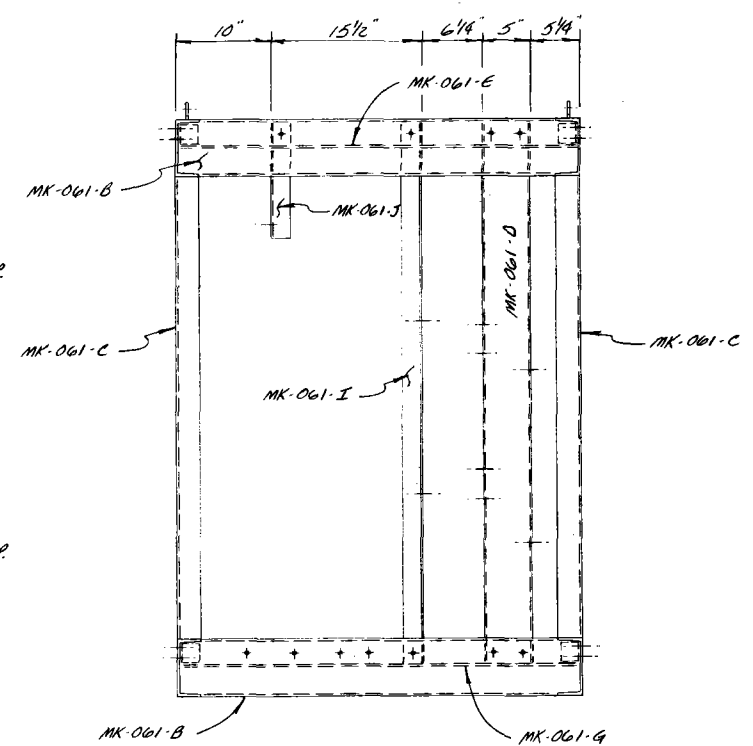
1/2" NOM. SIZE  
 EYE BOLT (4) REQ'D.  
 DRILL THRU 3/16" DIA.  
 HOLE & BOLT WITH  
 1/2" HEX HEAD NUT



PLAN




ELEVATION

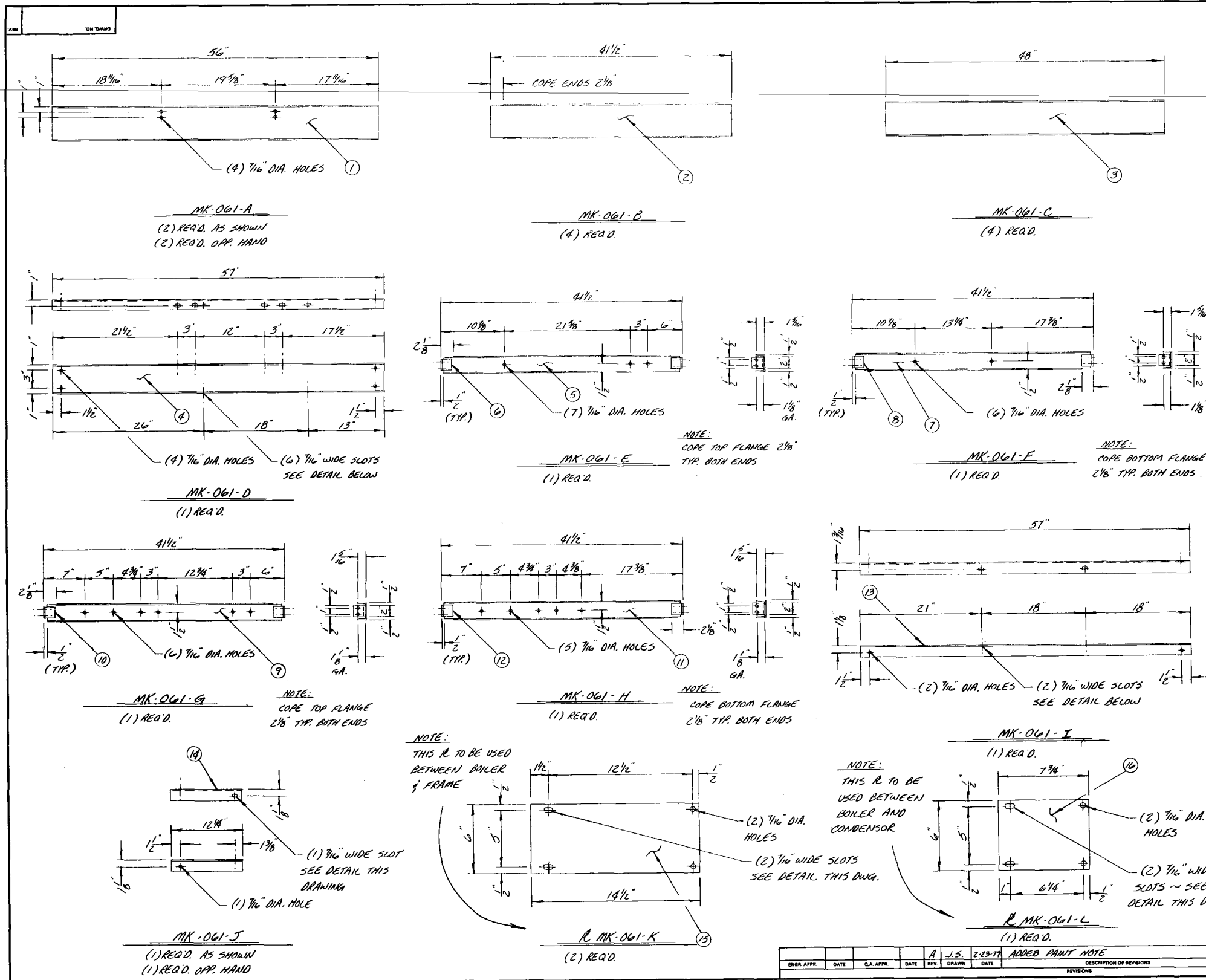


END ELEVATION

ENGR. APPR.	DATE	G.A. APPR.	DATE	REV.	DATE	DESCRIPTION OF REVISIONS	
				A	J.S.	3-2-79	ADDED EYEBOLT LIFTING LUGS

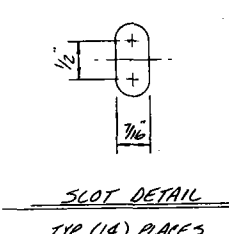
Approved for Engr. Requirements by _____ Date _____	Approved for G.A. Requirements by _____ Date _____
TITLE REFLUX BOILER SYSTEM FRAME MINNEAPOLIS, MINN.	<b>MOORHEAD</b> MACHINERY & BOILER CO.  MINNEAPOLIS, MINNESOTA
DRW. SWANSON DATE 2-14-79	J.O. A-391 DATE 2-14-79
DRIVE NO. D-79060	REV. A
SCALE 1/8" = 1"	





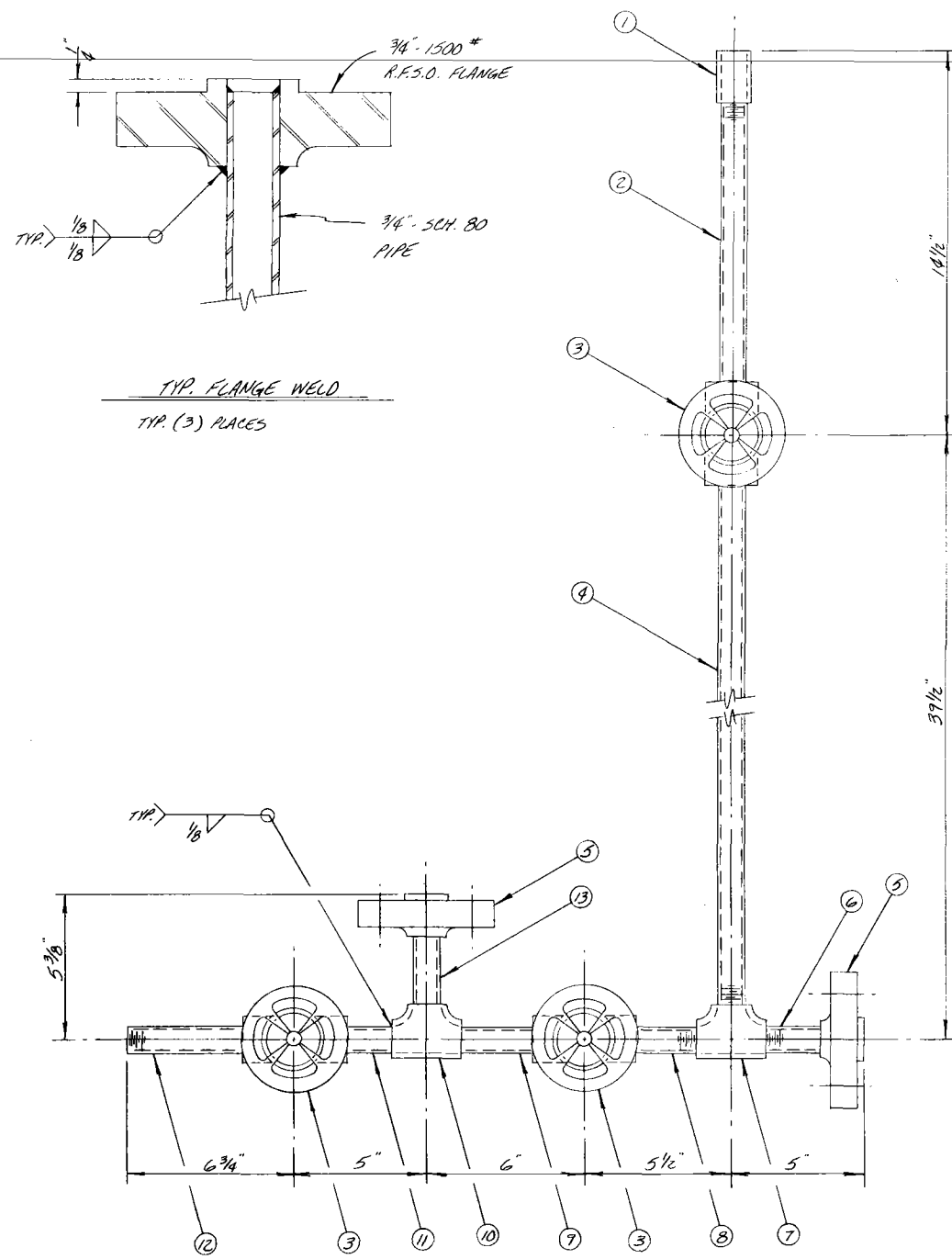
NOTES					
ITEM NO.	QTY.	PART NO.	DESCRIPTION	MATL.	WT. PO.
1	4	061-A	C6" x B.2" x 4.8"	A-36	153 X
2	4	061-B	C6" x B.2" x 3.5 1/2"	A-36	113 X
3	4	061-C	C6" x B.2" x 8.0"	A-36	131 X
4	1	061-D	C5" x 4.7" x 4.9"	A-36	32 X
5	1	061-E	C3" x 4.1" x 3.4 1/2"	A-36	14 X
6	2	061-F	C2" x 2" x 3/8" x 0.2"	A-36	2 X
7	1	061-G	C3" x 4.1" x 3.4 1/2"	A-36	14 X
8	2	061-H	C2" x 2" x 3/8" x 0.2"	A-36	2 X
9	1	061-I	C3" x 4.1" x 3.4 1/2"	A-36	14 X
10	2	061-J	C2" x 2" x 3/8" x 0.2"	A-36	2 X
11	1	061-K	C3" x 4.1" x 3.4 1/2"	A-36	14 X
12	2	061-L	C2" x 2" x 3/8" x 0.2"	A-36	2 X
13	1	061-M	C2" x 2" x 3/8" x 0.2"	A-36	22 X
14	2	061-N	C2" x 2" x 3/8" x 1.0 1/4"	A-36	10 X
15	2	061-O	1/2" R x 6" x 1 1/4"	A-36	21
16	1	061-P	1/2" R x 6" x 1 1/4"	A-36	7
17	50		7/8" DIA. x 1 1/2" LG. BOLT W/ NUT	A-307	4 X

NOTE:  
 1) SEE DRAWING D-79060 FOR FRAME ASSEMBLY DETAILS  
 2) WELD ANGLE CLIPS TO ITEMS MK-061-E THRU MK-061-H WITH 3/16" FILLET WELD ALL AROUND  
 3) PAINT FRAME PIECES (1) PRIME COAT RUST-OLEUM HEAT RESISTANT RED PRIMER # 426B (1) FINISH COAT RUST-OLEUM HEAT RESISTANT GRAY # 4286

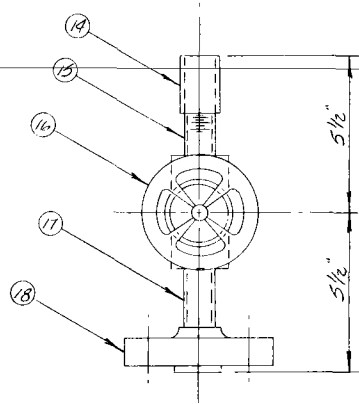


Approved for Engr. Requirements by _____ Date _____	Approved for C.A. Requirements by _____ Date _____
TITLE <b>FRAME DETAILS</b>	
MINNEAPOLIS, MINN.	
MOTORWELL INC.	
FR. 931584-AA~S.W. # 10073-01	
DRAWN SWANSON	DATE 2-16-79
CHECKED	DATE
SCALE 1/8" = 1"	
D-79061	
REV. A	

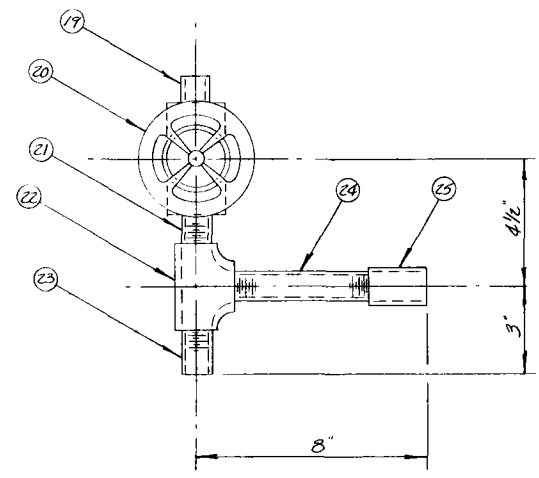
ENGR. APPR.	DATE	C.A. APPR.	DATE	REV.	DRAWN	DATE	DESCRIPTION OF REVISIONS
		A	J.S.	2-23-79			ADDED PAINT NOTE



PIPING ASSEMBLY MK-062-A  
(1) REA D.



MK-062-B  
(1) REA D.




MK-062-C  
(1) REA D.

NOTES						
ITEM NO.	QTY.	PART NO. SHIP	DESCRIPTION	ITEM MAT'L.	#	WT. RD.
1	1		3/4" 3000* SCREWED FULL CPLG.	SA-105	C	X
2	1		3/4" SCH. 80 PIPE x 0'-11 3/16" T.O.E.	SA-106-B	C	X
3	3		3/4" 1500* F.S. GATE VALVE		C	20 X
4	1		3/4" SCH. 80 PIPE x 3'-1 1/16" T.O.E.	SA-106-B	C	X
5	2		3/4" 1500* R.F.S.O. FLANGE	SA-105	C	18 X
6	1		3/4" SCH. 80 PIPE x 0'-3 3/16" T.O.E.	SA-106-B	C	X
7	1		3/4" 3000* SCREWED TEE	SA-105	C	2 X
8	1		3/4" SCH. 80 PIPE x 0'-3 3/16" T.O.E.	SA-106-B	C	X
9	1		3/4" SCH. 80 PIPE x 0'-0"	SA-106-B	C	X
10	1		3/4" 3000* S.W. TEE	SA-105	C	2 X
11	1		3/4" SCH. 80 PIPE x 0'-3"	SA-106-B	C	X
12	1		3/4" SCH. 80 PIPE x 0'-5 1/2" T.O.E.	SA-106-B	C	X
13	1		3/4" SCH. 80 PIPE x 0'-0 3/8"	SA-106-B	C	X
14	1		3/4" 3000* SCREWED FULL CPLG.	SA-105	C	X
15	1		3/4" SCH. 80 PIPE x 0'-0 3/16" T.O.E.	SA-106-B	C	X
16	1		3/4" 1500* F.S. GATE VALVE		C	7 X
17	1		3/4" SCH. 80 PIPE x 0'-0"	SA-106-B	C	X
18	1		3/4" 1500* R.F.S.O. FLANGE	SA-105	C	9 X
19	1		1/4" 6000* SCREWED FULL CPLG.	SA-105	C	X
20	1		3/4" 1500* F.S. GATE VALVE		C	7 X
21	1		3/4" SCH. 80 PIPE x 0'-2 3/16" T.O.E.	SA-106-B	C	X
22	1		3/4" 3000* SCREWED TEE	SA-105	C	2 X
23	1		3/4" SCH. 80 PIPE x 0'-2 1/16" T.O.E.	SA-106-B	C	X
24	1		3/4" SCH. 80 PIPE x 0'-5 3/8" T.O.E.	SA-106-B	C	X
25	1		3/4" 3000* SCREWED FULL CPLG.	SA-105	C	X

NOTE:  
1) SEE DRAWINGS D-79015 & D-79016 FOR LOCATION OF PIPING ASSEMBLIES  
2) ALL THREADED PIPE CONNECTIONS TO BE MADE USING ONLY NEVER-SEEC ANTI SEIZE LUBRICATING COMPOUND. DO NOT USE SUBSTITUTES, EVEN FOR TEMPORARY CONNECTIONS.

ENGR. APPR.	DATE	G.A. APPR.	DATE	REV.	DRAWN	DATE	DESCRIPTION OF REVISIONS

Approved for Engr. Requirements by _____ Date _____	Approved for O.A. Requirements by _____ Date _____
TITLE <b>PIPING ASSEMBLIES</b> MINNEAPOLIS, MINN.	<b>MOORHEAD MACHINERY &amp; BOILER CO.</b>  MINNEAPOLIS, MINNESOTA
CLIENT <b>HONEYWELL INC.</b>	
DRAWN SILVANOSON	DATE 2-16-79
CHECKED	SCALE A-391 D-79062

APPENDIX D  
INSTRUMENTATION

The basic instrumentation plan was centered around an automated data recording system, the Fluke Data Logger, and served both experiments. Data were organized as to type, quantity, purpose, and location, as shown in Table D-1.

The liquid sensors in the boiler and transfer tanks were located as described in paragraph 4.2.3.1 and calibrated for volume and area in accordance with the curves shown on Figures D-1 through D-4.

The boiler pressure transducer was converted from a 4 to 20 milliamperes to a 20 to 100 millivolt device, as shown in Figure D-5, and matched to the calibration curve shown in Figure D-6.



D-3

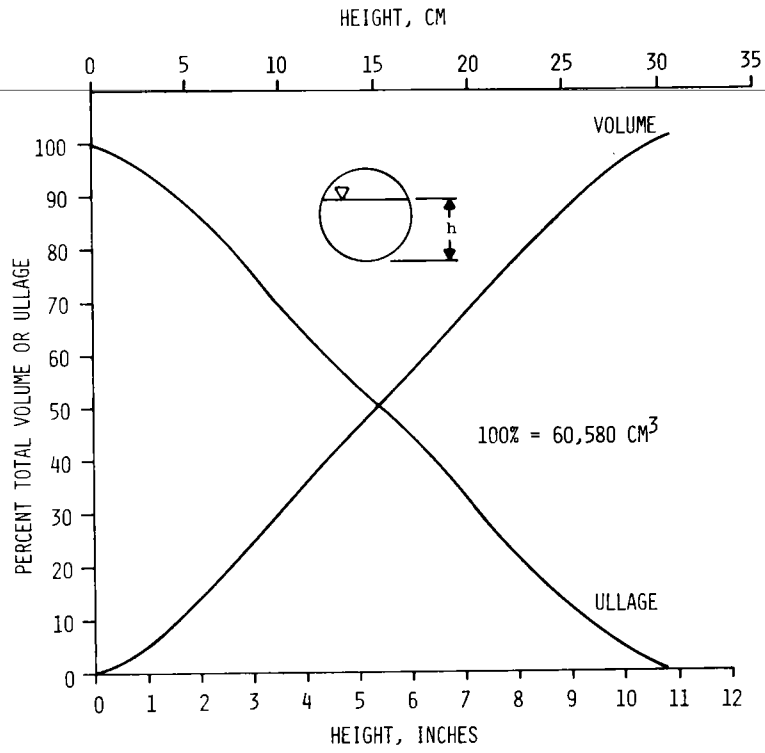


Figure D-1. Boiler Module Height versus Volume

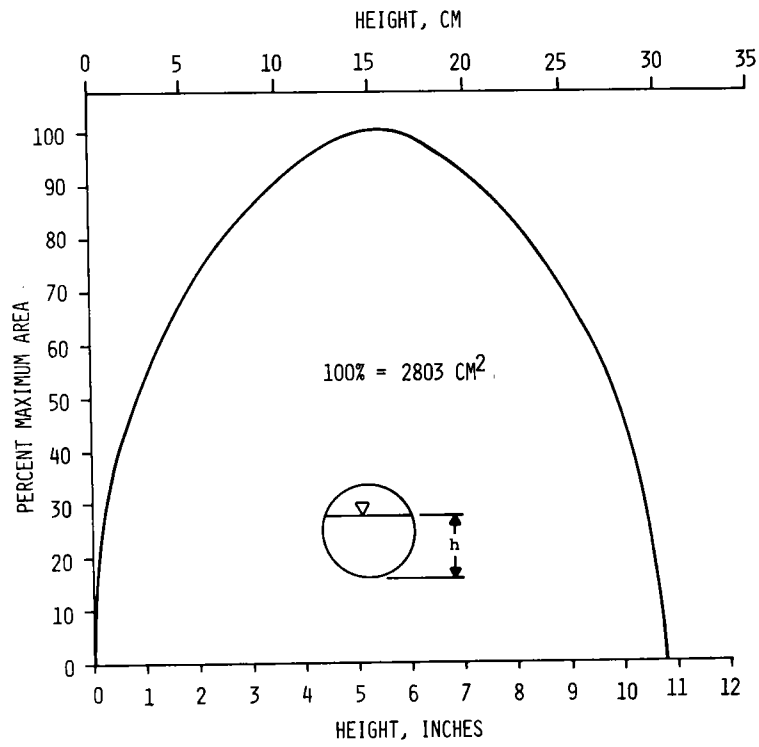


Figure D-2. Boiler Module Height versus Area

D-4

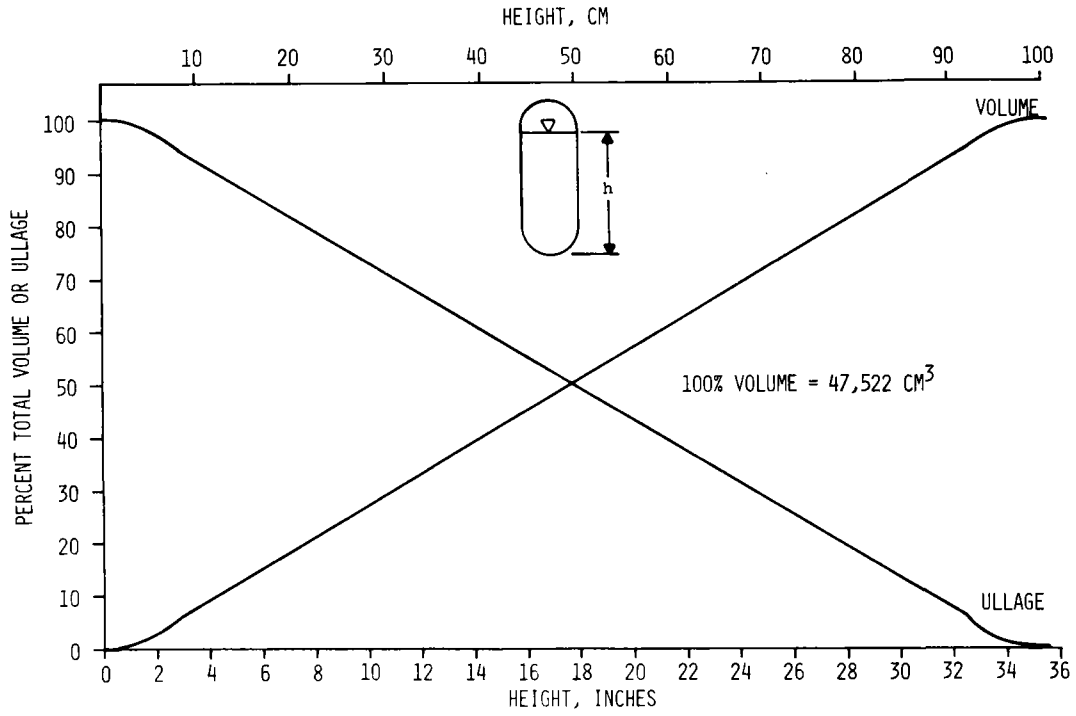


Figure D-3. Transfer Tank Height versus Volume

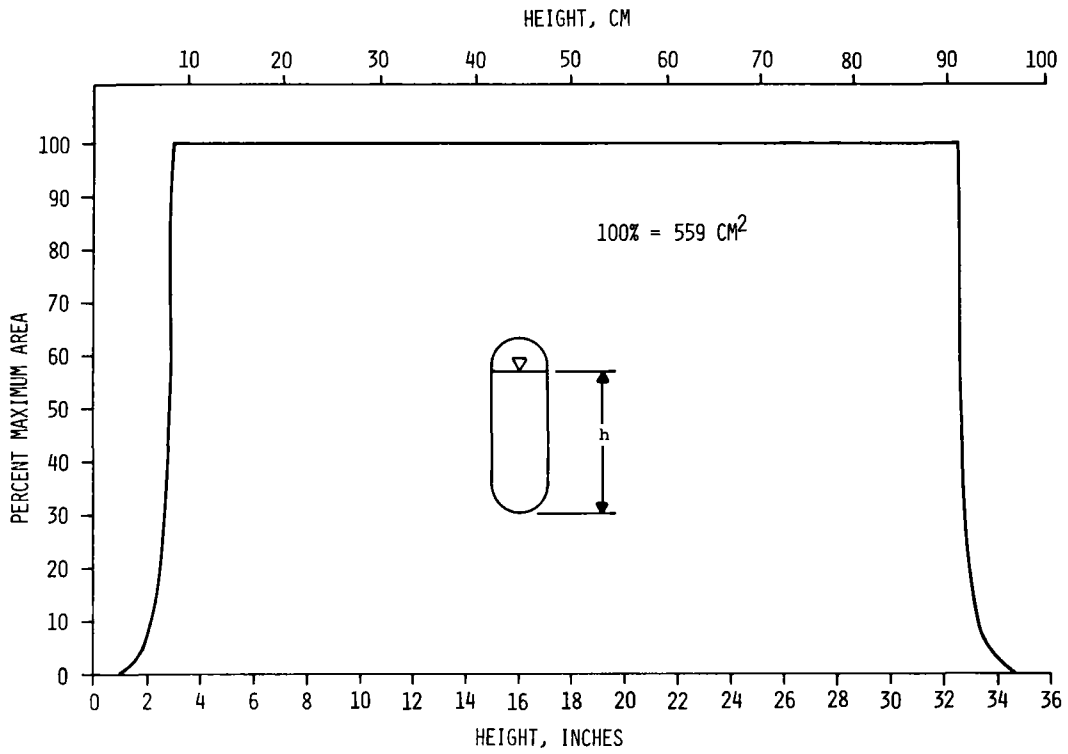


Figure D-4. Transfer Tank Height versus Area

D-5

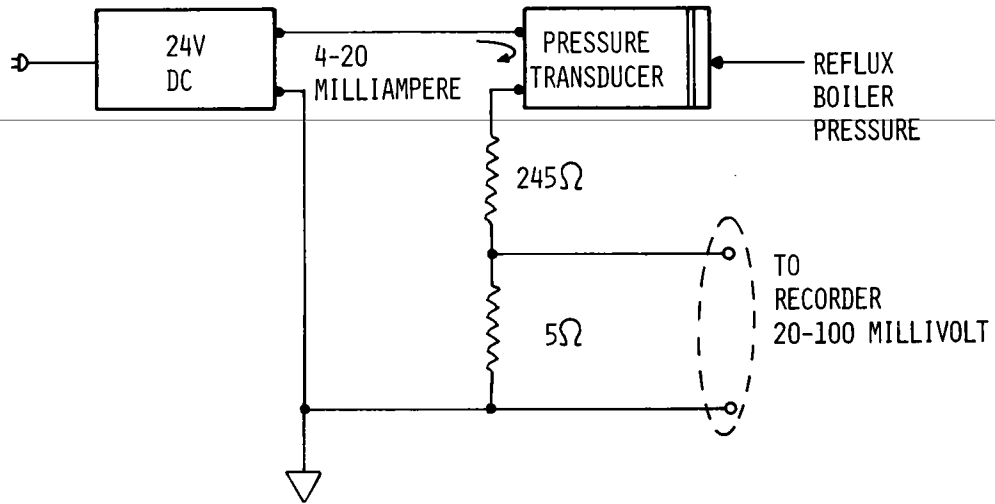


Figure D-5. Boiler Pressure Transducer Readout Schematic

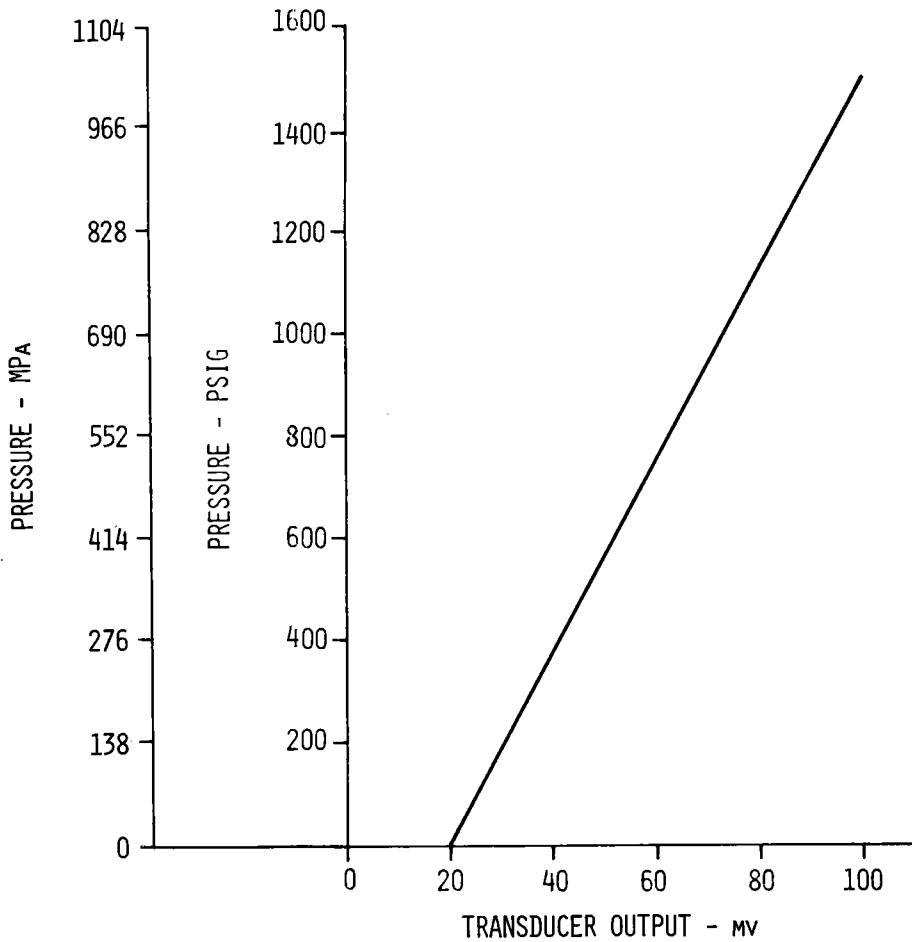


Figure D-6. Boiler Pressure Transducer Calibration Curve

1. Report No. NASA CR 159727		2. Government Accession No.		3. Recipient's Catalog No.	
4. Title and Subtitle ACTIVE HEAT EXCHANGE SYSTEM DEVELOPMENT FOR LATENT HEAT THERMAL ENERGY STORAGE				5. Report Date April 1980	
				6. Performing Organization Code	
7. Author(s) R.T. LeFrois				8. Performing Organization Report No. HI #79188	
9. Performing Organization Name and Address Honeywell Inc. Technology Strategy Center 2600 Ridgway Parkway Minneapolis, MN 55413				10. Work Unit No.	
				11. Contract or Grant No. DEN 3-38	
12. Sponsoring Agency Name and Address U.S. Department of Energy Division of Energy Storage Systems Washington, D.C. 20545				13. Type of Report and Period Covered Contractor Report	
				14. Sponsoring Agency Code DOE/NASA/0038-80/2	
15. Supplementary Notes Final Report. Prepared under Interagency Agreement EC-77-A-31-1034. Project Manager, James E. Calogeras, Power Generation and Storage Division, NASA Lewis Research Center, Cleveland, Ohio 44135					
16. Abstract This final report describes active heat exchange concepts for use with thermal energy storage systems in the temperature range of 250° to 350°C, using the heat of fusion of molten phase change materials for storing thermal energy. Over 25 novel techniques for active heat exchange thermal energy storage systems were identified. Salt mixtures that freeze and melt in appropriate ranges were selected and evaluated for physico-chemical, economic, corrosive and safety characteristics. Eight active heat exchange concepts for heat transfer during solidification were conceived and conceptually designed for use with selected storage media. The concepts were analyzed for their scalability, maintenance, safety, technological development and costs.  A model for estimating and scaling storage system costs was developed and used for economic evaluation of salt mixtures and heat exchange concepts for a large-scale application. The heat exchange concepts were sized and compared for 6.5 MPa/281°C steam conditions and a 1000 MW(t) heat rate for 6 hours. A cost sensitivity analysis for other design conditions was also carried out.  The study resulted in the selection of a shell and coated tube heat exchange concept and a direct contact reflux boiler heat exchange concept. For the storage medium, a dilute eutectic mixture of 99 percent (weight) NaNO <sub>3</sub> and 1 percent (weight) NaOH was selected for use in experimenting with the selected heat exchanger concepts.  Two 10 kW(t)/Hour capacity, 10 kW(t) rate Thermal Energy Storage (TES) modules, embodying the selected concepts, were designed, constructed and instrumented for testing.  Test results with nickel-coated tubes showed that the shell and coated tube heat exchanger could not generate the required heat rate due to the salt sticking to the tubes. The direct contact reflux boiler demonstrated high heat transfer rates, but also showed strong hydrolysis of the sodium nitrate.					
17. Key Words (Suggested by Author(s)) Thermal Energy Storage Active Heat Exchange Crystallization Process Heat of Fusion Material Direct Contact Heat Exchange				18. Distribution Statement UNCLASSIFIED - UNLIMITED STAR Category 44 DOE Category UC-94a	
19. Security Classif. (of this report) UNCLASSIFIED		20. Security Classif. (of this page) UNCLASSIFIED		21. No. of Pages 224	22. Price*

\* For sale by the National Technical Information Service, Springfield, Virginia 22161